Towards Multi-modal Sclera and Iris Biometric Recognition with Adaptive Liveness Detection

Mr. Abhijit Das

Master of Technology (Information Technology)

School of Information and Communication Technology

Griffith Sciences

Griffith University

Submitted in fulfilment of the requirements of the degree of
Doctor of Philosophy

May 2017

Abstract

Security breaches due to misidentification of an individual pose one of the greatest threats and challenges for today's world. The use of biometrics can be quite promising in minimising this threat. Biometrics refers to the automatic authentication of individuals based on their physiological and behavioural characteristics. To date, various biometric systems have been proposed in the literature, among them biometric traits such as the face, iris, fingerprints, retina, gait, and vocal patterns are found to be distinctive to each and every person and are considered to be most reliable biometric identifiers.

Regardless of the available biometrics traits, to date, no biometric system has been found to be a perfect, and which can be applied universally in a way that is robust/adaptive to change in different environmental conditions. Multimodal biometric systems were proposed in the late 1990's to extend the range of biometric applicability. In a multimodal biometric system, two or more biometric identifiers are fused by an information fusion technique, thereby providing robustness for changing in a greater range of environmental conditions and enhancing other properties that an ideal biometric system should possess. Another important property that a biometric system should possess is a capability to distinguish between real and fake data. Although both the robustness of the system and capability to distinguish between a real and fake data should be incorporated into a single system, there is a trade-off. Therefore, due to the aforementioned research problems, this thesis addresses advancements in multimodal ocular biometrics using iris and sclera and also investigates the trade-off between robustness/adaptability and anti-spoofing/liveness detection (which is one method to distinguish between real and fake data).

Biometrics traits that allow personal identification, eye traits offer a good choice of biometrics, as the eye offers a wide range of unique characteristics. The two common eye biometric identifiers that can be found in the literature are the iris and retina. Two more biometrics that are becoming popular nowadays are the sclera and the peri-ocular. The iris biometric is believed to be the most reliable eye biometric and that is why various commercial products based on this biometric are available; but the iris biometric used in an unconstrained scenario is still an open research area. The performance of iris biometrics with changes in the gaze angle of the eye can be affected highly. Therefore, due to this restriction, high user cooperation is required by persons with squinty eyes to get successfully identified in an iris biometric system. Identifying individuals with darker irises is another big challenge in iris recognition in the visible spectrum. To mitigate this problem, multi-modal eye biometrics was proposed by combining iris and sclera traits in the visible spectrum.

However, in order to establish the concept of multimodal eye biometrics using the iris and sclera, it is first necessary to assess if sufficient discriminatory information can be

gained from the sclera, further assessment in regards to its combination with the iris pattern and adaptiveness of the traits with respect to changes in environmental conditions, population, the data acquisition technique and time span. Multimodal biometrics using sclera and iris have not been extensively studied and little is known regarding their usefulness. So, the state-of-the-art related to it is not sufficiently mature and still in its infancy. This thesis concentrates on designing an image processing and pattern recognition module for evaluating the potential of the scleral biometric with regards to biometric accuracy. Thus, research is also carried out investigate usefulness of the sclera trait in combination with the iris pattern. Various, pre-processing techniques, segmentation, feature extraction, information fusion and classification techniques are employed to push the border of this multimodal biometrics.

The latter half of the thesis concentrates on bridging the anti-spoofing technique liveliness with adaptiveness of biometrics. Traditional biometric systems are not equipped to distinguish between fake and real data that has been scanned in front of the sensors. As a result, they adhere to forgery attacks by intruders who can take the privilege of a genuine user. With the rising demand of involuntary or unmanned biometric systems in border security, flight checking, and other restricted zones, the incorporation of the automatic detection of forgery attacks is becoming very obvious. Adaptability of the system with respect to the change in the trait is another important aspect that this biometric system should be enriched with. As mentioned previously both the forgery detection method (termed as liveness detection in the literature of biometrics) and adaptability of the trait is necessary for a trusted involuntary biometric system, but initial studies in the literature exhibit it as a trade-off. Therefore to fulfil the gap, this thesis aimed to propose a new framework for software-based liveness detection, which is also associated to the adaptability of the trait. To fulfil the above-highlighted aim in the proposed framework, intra-class level (i.e. user level) liveness detection is introduced employing image quality-based features. Furthermore, to incorporate the adaptability of the trait, online learning-based classifiers are used. Initial investigation and experimental results solicit the use of the proposed framework for trusted involuntary biometric systems. Two new multi-angle eye datasets were developed and published as a part of the current research. The thesis also consists of contributions to other fields of pattern recognition such as wrist vein biometrics, multiscript signature verification and script identification.

Statement of Originality

I hereby confirm that this work has not previously been submitted for fulfilment of a degree or diploma in any university/institute. To the best of my knowledge and belief, the thesis contains no material previously published or written by another person except where due reference is made in the thesis itself.

Abhijit Das
May 12, 2017

Acknowledgements

At the outset, I would like to express my gratitude to the almighty who has given me the chance, inspiration, and the mental, physical and economic strength to undertake my Ph. D. studies.

I am sincerely grateful to my principal supervisor Prof. (Dr.) Michael Blumenstein for his guidance and support during my Ph. D. candidature. His encouragement and all his contributions have made my experience during the tenure of Ph. D. a very productive. I wish to express my sincere gratitude to my external supervisor Prof. (Dr.) Umapada Pal, Indian Statistical Institute and Prof. (Dr.) Miguel Angel Ferrer, University de Las Palmas de Gran Canarias for his constant guidance, motivation, and support during my Ph. D. tenure. I would like to thank my associate supervisor, Asst. Prof. (Dr.) Alan Liew, Griffith University, for his support and insightful advice on during my Ph. D. candidature.

I will extend my special thanks to Asso. Prof. Jun Jo, Griffith University, for his support. I would like to thank Prof. Arun Ross, Michigan State University and Prof. Javier Ortega-Garcia, University Autonoma Madrid for their fruitful collaboration in a few of the works in this thesis.

I would like to thank the School of ICT, Griffith University, and all other staff members for their help and support. I am thankful to my colleagues, Dr. Srikanta Pal, Dr. Nabin Sharma, Adel Fazel, Rituraj Kunwar, Chandranath Adak, and Rupam Deb for their help, support, and inspiration.

My regards and respect to my parents, and all my family members for their constant inspiration, love, support and patience, without which it would not have been possible to complete my Ph. D. journey.

Contents

List of Figures

from printed eye where the original image was captured by Micromax camera.

List of Tables

Abbreviations

DCT	Discrete Cosine Transforms
KNN	K-Nearest Neighbours
SIFT	Scale-Invariant Feature Transform
DSIFT	Dense Scale-Invariant Feature Transform
SPM	Spatial Pyramid Matching
BoF	Bag of Feature
SVM	Support Vector Machine
FAR	False Acceptance Rate
FRR	False Rejection Rate
EER	Equal Error Rate
ROC	Receiver Operating Characteristic
CMC	Cumulative Match Characteristic
LBP	Local Binary Pattern
D-LBP	Dense Local Binary Pattern
GLCM	Grey Level Co-occurrence Matrix
DCT	Discrete Cosine Transform
OLBP	Orientated Local Binary Pattern
LDP	Local Directional Pattern
ICE	Iris Challenge Evaluation
BATH	University of Bath
IR	Infra-Red

WVU	West Virginia University
UPOL	University of Palack eho
MMU	Multimedia University
CASIA	Institute of Automation from the Chinese Academy of Sciences
MASD	Multi-Angle Sclera Dataset
ICB	International Conference on Biometrics
BTAS	International Conference on Biometrics: Theory Application and System
QF	Quality Features
AB	Adaptive Biometrics
SVM	Support Vector Machine
NN	Neural Network
DDD	Diversity for Dealing with Drifts
ASV	Automatic Signature Verification
HMM	Hidden Markov Model
SFS	Skilled Forged Signature
RFS	Random Forged Signature
BD	Bhattacharyya Distance
OCR	Optical Character Recognition
LDerP	Local Derivative Patterns

List of Publications during Candidature

Book chapters:

1. Abhijit Das, Rituraj Kunwer, Umapada Pal, Miguel Ferrer Ballaster and Michael Blumenstein, Book chapter entitled "An online learning technique for adaptive biometric system" pp. 73-96, in book of Adaptive Biometric Systems to be published by Springer.

Peer-reviewed journal publications:

2. Abhijit Das, Umapada Pal, Miguel Ferrer Ballester and Michael Blumenstein,"A Framework for Liveness Detection for Direct Attack in Visible Spectrum for Multimodal Ocular Biometrics". Pattern Recognition Letter, ISSN: 0167-8655, 2015.

3. Abhijit Das, Miguel Ferrer Ballester, Umapada Pal, Srikanta Pal, Moisis Diaz and Michael Blumenstein ,"Multi-script vs single-script scenarios in automatic off-line signature verification". IET biometrics.

3. Abhijit Das, Rituraj Kunwar, Umapada Pal , Miguel Ferrer Ballester and Michael Blumenstein ,"A more efficient and adaptive biometrics system using online learning". to be Communicated to Pattern Recognition.

4. Abhijit Das, Umapada Pal, Miguel Ferrer Ballester and Michael Blumenstein, "Sclera Information Fusion-Based Robust and Adaptive Iris Biometrics in Visible Spectrum". to be communicated Pattern Recognition Letter.

5. Abhijit Das, Umapada Pal, Miguel Ferrer Ballester and Michael Blumenstein "Sclera biometrics: state-of-the-art and a way forward".to be Communicated to ACM survey.

Peer-reviewed conference publication (oral presentations):

6. Abhijit Das, Umapada Pal, Miguel Ferrer Angel Ballester and, Michael Blumenstein, "A New Method for Sclera Vessel Recognition using OLBP", appeared in International Conference Chinese Conference on Biometric Recognition, LNCS 8232, pp. 370–377,2013.

7. Abhijit Das, Umapada Pal, Miguel Ferrer Ballester and Michael Blumenstein,' Sclera Recognition Using D-SIFT', Appeared In 13th International Conference on Intelligent Systems Design and Applications pp.74-79, 2013.

8. Abhijit Das, Umapada Pal, Miguel Ferrer Ballester and Michael Blumenstein,'Fuzey Logic based Sclera Recognition ', pp. 561-568, In IEEE World Congress on Computational Intelligence - IEEE International Conference on Fuzzy Systems 2014.

9. Abhijit Das, Umapada Pal, Miguel Ferrer Ballester and Michael Blumenstein,' Multi-angle Based Lively Sclera Biometrics at a Distance'. pp. 22-29, IEEE Symposium Series on Computational Intelligence, December 9-12, 2014, Orlando, USA.

10. Abhijit Das, Umapada Pal, Miguel Ferrer Ballaster and Michael Blumenstein, "A New Efficient and Adaptive Sclera Recognition System", pp.1-6, IEEE Symposium Series on Computational Intelligence, December 9-12, 2014, Orlando, USA.

11. Abhijit Das, Umapada Pal, Miguel Ferrer Ballaster and Michael Blumenstein, "A New Wrist Vein Biometric System", pp. 68-75, IEEE Symposium Series on Computational Intelligence, December 9-12, 2014, Orlando, USA.

Peer-reviewed conference publication (poster presentations):

12. Abhijit Das, Umapada Pal, Michael Blumenstein and Miguel Ferrer Ballester, "Sclera Recognition - A Survey" Appeared in Recent Advancement in Computer Vision and Pattern Recognition, pp. 917 -921, 2013.

13. Abhijit Das, Umapada Pal, Miguel Ferrer Ballester and Michael Blumenstein,"SSBC 2015: Sclera Segmentation Benchmarking Competition". pp. 1-6, at International Conference Biometrics Theory, Applications and Systems (BTAS), 2015.

14. Abhijit Das, Prabir Mondal, Umapada Pal, Michael Blumenstein and Miguel Angel Ferrer Sclera Pattern Synthesis Based on Non-parametric Texture Synthesis Technique, at Computer Vision and Image Processing (CVIP-2016).

15. Abhijit Das, Umapada Pal, Miguel Ferrer Ballester and Michael Blumenstein,"SSRBC 2015: Sclera Segmentation and Recognition Benchmarking Competition". at International Conference on Biometrics, 2016.

16. Abhijit Das, Prabir Mondal, Umapada Pal, Michael Blumenstein and Miguel Angel Ferrer, "Fast and Efficient Multimodal Eye Biometrics using Projective Dictionary Pair Learning", at IEEE World Congress on Computational Intelligence- IEEE CEC 2016.

Ethical Clearance

Granted Ethical Clearance GU Protocol Number: ICT/05/13/HREC

Dedicated to my parents, and all family members...

1

Introduction

Security failing due to misidentifying an individual is one of the greatest threats to today's world. Various techniques have been adopted to mitigate this threat, like utilising passwords, electronic cards, etc. But the risk of forging cannot be satisfactorily minimised. Biometrics is the technique that can be quite promising in this scenario. Biometrics refers to the automatic authentication of individuals based on their physiological and behavioural characteristics Jain et al. [130]. Biometrics has received significant attention by the researchers in industry, government, and academia. Over the last few decades, intensive research work has been performed in the field of biometrics to identify individuals as accurately as possible based on biological or physiological traits or both Zhou et al. [5]. Nowadays the need for biometric systems is increasing in day-to-day activities (e.g. attendance system for organisations, citizenship proof, door locks for high-security zones, etc.). Due to its ease of use by common people and organisations, financial sectors, government and reservation systems are also adopting biometric technologies for ensuring security in their own domains and to maintain signed log activity for every individual.

The earliest biometric cataloguing can be found in 1891 when Juan Vucetich started a collection of fingerprints of criminal identification in Argentina. The first automatic biometric system was proposed in the 1980's. An example of a typical biometric system and a few examples of different biometric traits are given below in Figure 1.1
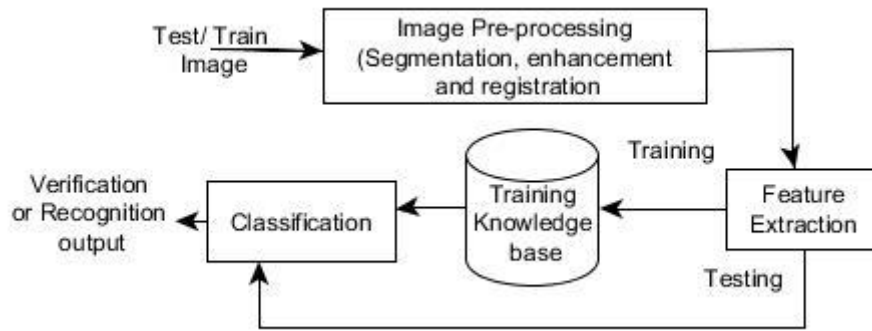
(a)

(b)

Figure 1.1: (a) Block diagram of a typical biometric system (b) Various biometric techniques available.

Biometric systems can be classified into two categories: behavioural biometric and physiological biometric. Some examples of this biometrics are given below.

1. **Behavioural:** The behavioural biometric system, biometric characteristics of an individual are employed for biometric authentication.

- **Voice recognition-** Voice recognition systems distinguish between various people's voices by frequency, pitch, and intensity of the voice. Voice biometrics is a growing technology in computer security. It uses a measurable, physical characteristic, or personal behavioural trait to verify and authenticate an individual. It uses what you are as a way to identify yourself. Further, it compares two samples of data and verifies if they match.

- **Types on a keyboard/ keystroke biometric-** A behavioural measurement aiming to identify users based on typing pattern/ rhythms or attributes. Typing rhythms is an idea whose origin lies in the observation (made in 1897) that telegraph operators have distinctive patterns of keying messages over telegraph lines.

- **Mouse movement dynamics-** The mouse biometric system uses continuous dynamic authentication by the movement of the mouse. No additional hardware is a requirement here. There are different approaches available to collect data for this biometrics.

- **Signature-** Signature verification is not only a popular research area in the field of image processing and pattern recognition, but also plays an important role in many applications

such as security, access control, contractual matters etc. A signature verification system can be divided into two classes: online and off-line based methods.

- **Gaits**- It aims to discriminate individuals by the way they walk. It is unobtrusive as it depends on how the silhouette shape of individual changes over time in an image sequence.

- **Lip movement**- Motion History Images (MHI) can be utilised for a biometric template of a spoken word for each speaker.

2. **Physiological:** The physiological characteristics of an individual are employed for biometric authentication for this type of biometric systems.

- **Fingerprint:** The lines that flow in various patterns across fingerprints are called ridges and the spaces between ridges are valleys. Fingerprint features (associated with some matching algorithm): Ridge pattern - global pattern matching technique is adapted for this biometric.

- **Hand geometry**- The shape of the hand of a human being can be used for biometric authentication by mathematical modelling of the hand shape.

- **Iris**- It is a ring of tissue on the eyeball that contains a pattern which is used in biometric.

- **Retina**- The retina is a thin layer of cells at the back of the eyeball of vertebrates. It is the part of the eye which converts light into nerve signals. The retina contains photoreceptor cells (rods and cones) which receive the light; the resulting neural signals then undergo complex processing by other neurones of the retina and are transformed into action potentials in retinal ganglion cells whose axons form the optic nerve which creates a pattern that can be utilised for biometrics.

- **Sclera**- The white region of the eye that contains blood vessels pattern that can be used in biometrics.

- **Peri-ocular**- The pattern around the eye is utilised here for biometrics

- **Face**- Central role in human interactions which can contribute to biometrics as each and every individual look alike by face.

- **Vein patterns** – The vein pattern at different parts of the body contain different ordination and pattern that is also used for biometrics.

Till date, many biometric systems have been proposed in the literature, such as a face in Das et al. [42,] iris in Das et al. [39, 40], etc. Still, no such system can be applied universally and can be robust to change in different environmental conditions or hold the properties of a perfect biometric system Zhou et al. [5]. In order to increase population coverage, extend

the range of environmental conditions, improve resilience to spoofing, and achieve higher recognition accuracy, further research on biometric traits was performed. In order to negate the above motion problem and to make the biometric system more universal multimodal biometric was proposed. So further research on a combination of various biometric agents is continuing on the popular biometrics with some biometrics (iris and sclera) or another popular biometric (iris and face) was carried out.

1.1. Overview

Eye biometric is believed to be one of the most popular and reliable biometrics Zhou et al. [5]. Among eye biometrics that can be found in the literature, the iris is the most popular and reliable one. Unfortunately, some disadvantages in the iris recognition have been found in the literature. For example robustness of iris biometrics with changes in gaze angle of the eye (off-angle eye), iris biometric in the visible spectrum for darker irises, are found to be tough. Moreover, the information of iris patterns reduces when images are captured in the visible spectrum rather than Infra Red (IR) band. As a solution, multimodal eye biometric using iris and sclera was proposed in the visible spectrum. The sclera is the white region in the eye that consists of blood vessels pattern. A label image of sclera and iris are shown in Figure 1.2.
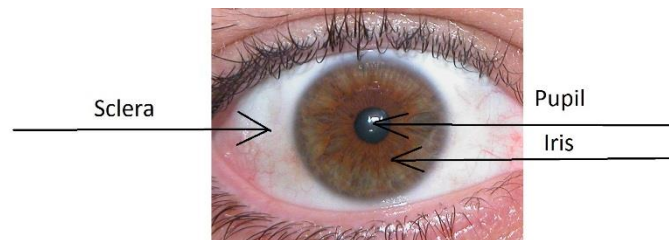
Figure. 1.2. Colour image of an eye consisting of pupil, iris and sclera area.

Iris and sclera-based multi-modal eye biometric in the visible spectrum can be easily spoofed by scanning a high-resolution image or high definition video. Therefore, to enrich the security and reliability of the discussed multimodal ocular biometric it is necessary to incorporate it with an antispoofing/ liveness detection technique, which can differentiate between the fake and the real data. Moreover, a review of the extant literature reveals that liveness detection and the robustness/ adaptability of the trait is a trade-off.

So in this thesis, an adaptive liveliness based multimodal eye biometric is proposed using the iris and sclera. The organisation of this section is as follows: Subsection 1.2 explains the aim of the proposed research: in subsection 1.3 problem description and the scope of the research is explained, and contributions of the thesis are explained: in subsection 1.4, and in subsection 1.5, the organisation of the report is summarised.

1.2 Motivation

Recent advancements in digital imaging technology have led to the development of sophisticated digital cameras, camcorders, and smartphones with cameras. These electronic 'gadgets' are not only low-priced and portable but also have tremendous scope to act as a biometric sensor. Due to the revolution in digital sensor technology and claim for a more secure world, biometric research and commercial products have received significant attention. This leads to the claim for more secure and trusted universal biometrics. Initial research found that no biometric trait can be universal in regards to its application. So, multimodal biometric was proposed.

Among all biometrics traits for people identification, eye traits offer a good choice of biometrics and also offer a wide range of traits. Moreover, the eye is a highly protected organ of a human being that cannot get changed by external activities. The traits are also stable and they are different even for identical twins Zhou et al. [5]. Major eye biometric identifiers that can be found in the literature are iris and retina. Two more biometrics that is becoming more popular nowadays is sclera and peri-ocular Oh et al, [41]. The iris contains a tissue structure (as labelled in Figure 1.2) which has a texture that is utilised for biometric identification of an individual. The retina consists of blood vessel patterns which can be utilised for human identification. The sclera is the white region of the eye (as labelled in Figure 1.2), which contains red blood vessels in different orientation and layers, which creates a pattern that is utilised for human authentication. Finally, the peri-ocular is the region around the eye which has been also used for biometric identification recently.

All of the eye traits are very rich in personal information, discriminative features, and stability. Regardless of its advantages, there are a few disadvantages which are also present in this biometrics. The major problem is the user acceptability, comfort, level of participation, and robustness to change in different environmental condition. Eye traits acquisition is another problem: iris, retina, and sclera vein pattern (includes cornea surface shape) and peri-ocular are not easy to acquire precisely. The iris is considered as one of the most reliable biometric measures Zhou et al. [5], but due to some pitfall of this biometric further research in this field is required. The biggest problem with iris systems occurs, with changes in the gaze angle of the eye (which is quite common for people with squint/ cock eye). Recognised becomes tough and hence the level of user participation required is high. Another scenario where iris recognition needs research attention is in the mobile environment. In this scenario, iris needs to be captured in the visible spectrum, but the performance of the iris biometrics in the visible spectrum reduces dramatically for darker irises. One salutation to these problems is combining other eye traits with iris biometrics. As a result, multimodal eye biometric was proposed. Iris and sclera-based multimodal eye biometrics can be found in the literature Zhou et al. [5].

However, in order to establish this concept, it is necessary to first assess if sufficient discriminatory information can be gained from the sclera and the accompanying iris pattern of the eye in a combination. It is also to an important investigation regarding it adaptively with respect to change in environmental conditions, population coverage, data accruing technique and time span. To date, this biometrics is relatively less studied and little is known regarding its usefulness. So, the state-of-the-art related to them are not mature enough and still in its infancy

The beginning of this research concentrates on designing an image processing and pattern recognition module for evaluating the potential of the scleral biometric in regards to accuracy and adaptability with changes in condition. Also, evaluation was carried out in combination with iris pattern. It will be also interesting to explore the field of sclera biometrics, as it is essential to consider different feature extraction and matching techniques in order to determine an effective method to characterise this biometric. But it will be more interesting to invade the paradigm of multimodal using ocular biometric in using sclera and iris due to their above-mentioned properties. Iris and sclera based multimodal eye biometric system in the visible spectrum can be easily spoofed by scanning a high-resolution image or high definition video in front of the sensor of the system.

With the recent demand for trusted involuntary biometrics system in international border checking, airport checking, etc., it are important to research on the aspect of liveness detection. Present biometric systems used in these security places are not equipped to distinguish between fake and real data. As a result, they are prone to forgery attacks by intruders who can take the privilege of a genuine user and can jeopardise the security. Adaptability of the system with respect to the change in the trait is another important aspect that this biometric system should be enriched with. As mentioned previously both the forgery detection method (termed as liveness detection in the literature of biometrics) and adaptability of the trait is necessary for a trusted involuntary biometric system, but initial studies exhibit it as a trade-off. Therefore to fulfil the gap, this part of the thesis is conceived

1.3. Problem Description and Scope of Research

In this thesis, the primary focus will be to identify individuals based on their physiological trait namely iris and sclera. Considering both the trait are captured as an image, the steps for biometric processing include the following steps:

- Segment the iris and the sclera trait individually

- Image enhancement of the trait after the image is segmented

- Feature extraction of the trait individually

- Combining the feature at different level of information fusion

- Classification of the trait after information fusion

The liveness detection of the input image is done by analysing

- Its image contrast property

- Image aspect property and frequency domain quality properties.

The adaptability of the input trait is done by using online learning based classifier

The objective of this research is to develop an adaptive liveness-based multimodal recognition system using the iris and sclera, and which will result in the reliable involuntary biometric system. Several shortcomings of the previously proposed approaches were identified and taken into consideration during this study. The following are the major shortcomings which were identified as needing to be addressed:

- Iris and sclera based multimodal biometrics were not extensively studied. Therefore, it is very important to investigate the biometric property of the sclera individually and in combination with the iris.

- The work proposed in the earlier work used multi-angle eye images from a few discrete angle, therefore a new dataset in multi-angle with more multi-angle of sclera and iris is proposed.

- Segmentation of sclera from the eye image was not studied intensively with modern segmentation techniques, this thesis fulfils the gap.

- Sclera image enhancement from the eye image was not studied intensively with modern enhancement techniques, this thesis covers the gap.

- Template matching techniques were mainly used in the literature for classification of the iris and sclera-based multimodal biometrics. The slow processing time of the template matching technique makes it inappropriate for real-life application. The thesis introduces the use of texture-based featuring techniques followed by probabilistic classification.

- The liveness detection was performed at the database level. The thesis introduces a framework which performed liveness detection at the user level, which it is not a trade-off with the adaptability of the system with respect to change in traits.
- Adaptability of the traits is also not investigated in the literature. An online learner based adaptive biometric system is proposed in the thesis to fulfil the gap.

1.4. Contributions

The proposed techniques described and introduced in this thesis are based on a number of research areas within biometrics. The following contributions are made in this thesis,

- Various pre-processing techniques for the sclera and the iris trait are investigated to find the best possible pre-processing approach.

- Introduces the use of a probabilistic classification technique and texture=based features to classify the iris and sclera-based multimodal ocular biometrics.

- The proposed pre-processing, feature extraction and classification techniques were also successfully applied to other biometric traits (wrist vein patterns and signatures) as well as other pattern classification tasks (script identification)

- Proposes a multi-angle eye dataset which is publicly available and used for three biometrics competitions organised in conjunction with BTAS 2015, ICB 2016 and IJCB 2017.

- A user level-based liveness detection framework is proposed which is not a trade-off with the adaptability of the system with respect to change in the trait.

- Introduces the use of an online learning-based classifier for adaptive biometrics.

- The thesis also contributes to other field of pattern recognition (multi-script signature, verification, wrist biometrics and script identification)

1.5. Organisation of the Thesis

The rest of this thesis is organised as follows.

- Chapter 2, includes the recent developments and approaches in the related area of the sclera, iris, and multimodal eye biometrics using sclera and iris. Followed by a review of the recent literature of the liveness detection and adaptive biometrics.

- Chapter 3, includes advancement carried out on the iris and sclera, and their combination.

- Chapter 4, includes proposed research methodology for liveness detection, followed by results, and discussion.

- Chapter 5, includes proposed research methodology for adaptiveness, followed by results, and discussed.

- Chapter 6, includes the contribution to other fields of biometrics and pattern recognition.

- Chapter 7, includes the conclusion and future scope of the thesis.

2

Literature Review

In this chapter first, the iris literature are summarised, followed by sclera biometrics anatomy, its challenges and literature. Next, the chapter summarised the literature on liveness detection and adaptability of biometrics. Section 2.1 reviews the iris biometric followed by Section 2.2 which highlights the sclera anatomy, challenges in characterising this biometrics and its literature till date. In Section 2.3 liveness detection literature is summarised. In Section 2.4 literature on adaptive biometrics is discussed.

2.1. Iris Literature

Iris literature is rich and vast, therefore only the major and the related works on the iris literature is focused in this survey. The possibility of using iris patterns as a basis for personal identification was first proposed by Herschel in 1858 followed by Bertillon [26] in 1885 by the French scientist. Science the 19th-century various automatic iris biometric systems have been proposed. The various stages involved in the iris biometric system, the initial stage deals with iris segmentation. This process consists of localising the iris inner (pupillary) and outer (scleric) borders, assuming either circular or elliptical shapes for both of the borders. In order to compensate for the variations in the pupil size and in the image capturing distances, it is common to translate the segmented iris region into a fixed length and dimensionless polar coordinate system for image registration. Regarding feature extraction, iris recognition approaches can be divided into three major categories: phase-based methods, zero-crossing methods and texture analysis based methods. Finally, the comparison between iris signatures is made, producing a numeric dissimilarity value. If this value is higher than a threshold, the system outputs a non-match meaning that each signature

belongs to different irises. Otherwise, the system outputs match, meaning that both signatures were extracted from the same iris. A block diagram of a typical iris biometric is as given below in Figure 2.1.
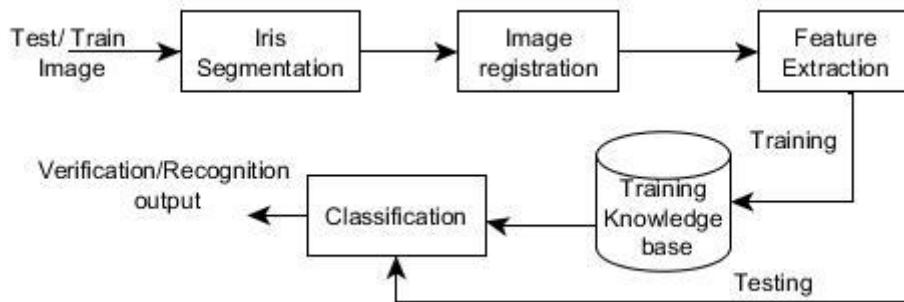
Figure 2.1. A block diagram of a typical iris biometric.

The rest of the section is divided into the following sub-sections. The sub-section 2.1.1 explains major work on the main stages of iris recognition; 2.1.2 highlights the pioneer works of iris literature, followed by sub-section 2.1.3 which focuses on the non-ideal iris recognition literature. In the last subsection 2.1.4, the available iris datasets are summarised

2.1.1 Seminal Work and Main Stages of Iris Recognition

The overviews of the most relevant works on the main stages of iris recognition that can be found in the literature are in the next sub-sections. The sub-subsections describe some usual approaches to performing each of the above-identified stages.

2.1.1.1. Iris Segmentation

In 1993, Daugman [16] presented one method for iris segmentation based on the majority of the functioning systems. Regarding the segmentation stage, Daugman introduced an integrodifferential operator to find the inner and outer borders of the iris. This operator remains efficient and was proposed in 2004 with minor differences developed by Nishino and Nayar [23].

Camus and Wildes [24] and Martin-Roche et al [24] proposed integrodifferential operators that finds the N^3 space, with the objective of maximising the process which identifies the iris borders. Wildes [50] proposed an iris segmentation method through a gradient-based binary edge map construction coupled by a circular Hough transform. This method has been proposed with minor variants by Cui et al. [16], Huang et al. [51], Kong and Zhang [52], Ma et al.[54], [55] and [56]. Liam et al. [53] proposed another interesting method, this method is based on thresholding and maximising a simple function to obtain two ring parameters that correspond to the iris inner and outer borders.

Du et al. [57] proposed an iris detection method-based on the prior pupil segmentation. The iris outer border is detected as the largest horizontal edge resultant from Sobel Filtering, further, the image is transformed into polar coordinates. However, this approach may fail in scenarios of non-concentric iris and pupil and for very dark irises. In a following work, a morphologic operators were applied by Mira and Mayer [58] to obtain iris borders. Authors detected the pupillary and scleric borders by using thresholding, image opening and closing. Kim et al. [59] proposed the use of the Expectation Maximisation algorithm to estimate the respective distribution parameters, based on the assumption that the pixels' intensity of the captured image can be well represented by a mixture of three Gaussian distributions.

2.1.1.2. Image Registration or Iris Normalization

Because of the varying size of the pupil, distance and angle of the image capturing, the size of the irises captured can have high variations, thereby increasing the complexity of the recognition. Robustness of the system is highly affected by this factors. The invariance to all of these factors can be achieved through the translation of the captured data into a double dimensionless polar coordinate system as proposed by Daugman in [16]. Figure 2.2 illustrates, this translation process-based both in polar (θ) and radial (r).
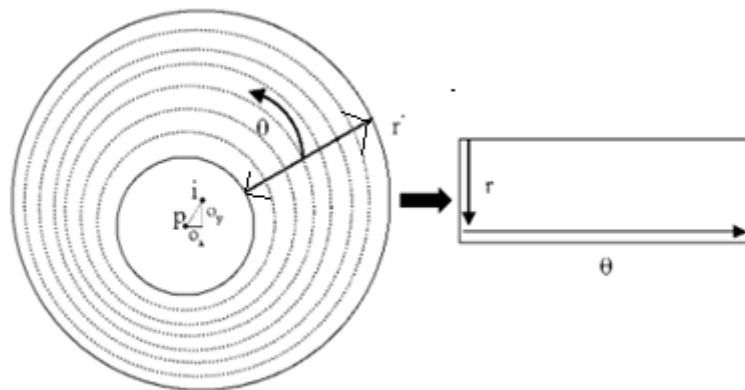
Figure 2.2 Illustrates of the translation process of iris-based on polar (θ) and radial (r).

A rubber sheet model was assigned to the each point of the iris. Despite its size and pupillary dilation, the iris can be expressed as a pair of real coordinates(r, θ), where r is in the unit interval of [0, 1] and θ is an angle in the range of [0,2π]. The mapping of an iris image I (x, y) from raw Cartesian coordinates (x, y) to the dimensionless non-concentric polar coordinate system (r, θ) can be represented as:

$$I(x(r,\theta), y(r,\theta)) \rightarrow I(r,\theta) \qquad (2.1)$$

Where x(r, θ) and y(r, θ) are linear combinations of both the set of the pupillary boundary points $(x_p(\theta), y_p(\theta))$ and set of limbus boundary points in the outer perimeter of the iris $(x_s(\theta), y_s(\theta))$ bordering the sclera, which were detected in the iris segmentation stage:

$$\begin{cases} x(r, \theta) = (1 - r) * x_p(\theta) + r * x_s(\theta) \\ y(r, \theta) = (1 - r) * y_p(\theta) + r * y_s(\theta) \end{cases}$$
(2.2)

2.1.1.3 Feature Extraction
Feature extraction and recognition approaches can be grouped into three major categories:

1. Phase-based methods used in Daugman [16],

2. Zero-crossing methods as proposed in Boles and Boashash [60], and Roche et al.[61],

3. Texture analysis based methods used in Wildes [62], Kim et al. [59] and Ma et al. [54].

Daugman [18] employed multiscale quadrature wavelets to extract texture phase information and obtain an iris signature of 2048 binary components. Similar to segmentation this proposal acted as a seminal work for others, with minor modification proposed in Ma et al. [65].

To feature the iris texture, Boles and Boashash [60] used the zero-crossing representation of a 1-D wavelet at different resolutions in concentric circles.

Wildes [62] proposed the featuring of the iris texture through a Laplacian pyramid. Using 4 different levels or scales. Most common approaches were found in the wavelet decomposition, using Haar, Mallat or other basic wavelets. This similar proposal can be found in Ali and Hassanien [63], Ma et al. [55] and Lim et al. [64],

Another approach can be found in Huang et al. [68] that employed the independent coefficient analysis to characterise the iris texture. Muron et al. [65] proposed the use of the power of the Fourier spectrum for featuring iris. Du et al. [57] proposed iris featuring technique through the computation of invariant local texture patterns. Nam et al. [66] proposed directional properties of the image to create a binary signature, by the analysis of the image second derivatives.

2.1.1.4. Classification
The use of distance metrics is proposed for iris feature classification in the literature:

1. Hamming distance in Daugman [18] and Tissue et al. [67],

2. Euclidean in Huang et al. [68] and

3. Weighted Euclidean in Zhu et al. [69] and Ma et al. [54].

Methods-based on signal correlation for iris feature classification was proposed in Wildes [62]. The specific proposal was proposed by Lim et al. [64], by the utilisation of a competitive learning neural network. In another work Ma et al. [55], modified nearest neighbour to compare the acquired and enrolled samples to assign recognition.

2.1.2. Some Pioneer Iris Recognition Methods

The following sub-subsections describe with the detail of some pioneering work of iris recognition methods. Apart from the Daugman's method, that acts as seminal works for other proposals, were the methods proposed by Wildes [62] and Li et al. [70].

2.1.2.1. Daugman's Method

The Daugman's recognition method proposed in [18] is as following:

- **Iris segmentation:** Author proposed an integrodifferential operator that finds the maximal difference between the average intensity of circumferences with consecutive radius values of the iris.

- **Normalisation:** To normalise for the dissimilarity in the size of the pupil, maps iris images to a dimensionless polar coordinate system through a process known as the Daugman Rubber Sheet [18].

- **Feature Extraction:** The iris featuring was performed through the use of 2D Gabor filters.

- **Feature Comparison:** Binarization process of the 2D Gabor filter is performed and the Hamming distance was used as similarity measure.

2.1.2.2. Wildes' Method

In [62], Wildes proposed a machine vision system for non-invasive iris biometric. The proposed system is divided following parts:

- **Image Acquisition:** The small dimension of the iris is considered as the major challenge by the author for the image acquisition. The author also discussed the role sufficient resolution, sharpness, good contrast, level of illumination as the detail challenges. The captured images must in the centred of the image and noises like specular reflections and optical aberrations should be minimised. Based on these, the author describes a framework for the iris acquiring from a distance of 20 cm. using an 80 mm. lens.

- **Iris Localization:** The author performs localization in two steps.

  1. The image is converted into a binary edge map.

  2. The edge points vote for instantiating particular contour parameter values. The edge map was reconstructed through a gradient-based edge detection, which consists of thresholding the magnitude of the image intensity gradient convolved with a two-dimensional Gaussian Kernel.

- **Pattern Matching:** The author decomposes this task in four parts: alignment, representation, comparison and decision.

2.1.2.3. Ma et al.'s Method

Ma et al. [64] proposed an iris recognition-based on the key local variations. It is composed of following stages:

- **Iris Localization:** The authors estimated both the pupillary and scleric borders as circles. The procedure initiates by roughly finding the iris region followed by the exact finding of the parameters correspondent to iris borders, similar to the procedure proposed in Wildes' [62].

- **Iris Normalization:** In order to minimize the effect of the variations in pupil size and image capturing distance, authors used the normalisation process described by Daugman [18].

- **Image Enhancement:** due to non-uniform brightness and low contrast of the iris images, the authors performed image enhancement-based on the subtraction of the estimated background illumination using small blocks of 32×32. Such pre-processing normalised the effect of non-uniform illumination.

- **Feature Extraction:** Authors proposed a set of 1-D intensity signals for iris featuring.

- **Matching:** The feature vector is converted into binary form, then the similarity is computed through the XOR function.

2.1.3. Non-Cooperative Iris Recognition

In the latter half of the iris, literature concentrates on non-cooperative iris recognition, which occurs due to automatic recognise of individuals, using their iris images captured at a distance and without any active participation.

This type of motivations has increased the researcher's interests and was the subject of several studies proposed by Du et al. [57]. In [71] the authors investigated the performance of partial iris for recognition. They analysed 3 different types of partial iris images: "left-to-right" that is left middle part of the iris,"outside-to-inside" and" inside-to-outside". The authors found a distinguishable and unique signal while analysing the inner parts of the iris and hence concluded that it is possible to employ a portion of the iris for biometrics.

Dorairaj et al. [72] proposed an iris recognition system that can handle off-angle images. The author's estimates of the gaze direction by the Hamming distance between the Independent Component Analysis of a frontal view image. Nest, they applied a projective transformation that maps the captured iris image to frontal view. Besides images of the CASIA database, the authors also used dataset captured in their institute to confirm the proposal. In Sung et al. [73] identified the potential problems that must be overcome in non-ideal iris recognition. The authors considered the problem of lighting conditions as hard to overcome unless a special lighting method is introduced. A slightly uncommon segmentation method by the initial inner eye corner detection followed by a least square elliptical fit to the limbic edge pixels was proposed form off-angle iris. The authors proposed a method-based on wavelet packet maximum by Shannon entropy for iris information reconstruction measuring due to off-angle. The feature extraction used a classical convolution with a bank of complex-valued 2D Gabor filters. A feature comparison by means of correlation and classification through the nearest neighbour was used for classification. Fancourt et al. [74] claim the use of human iris recognition up to 10 meters distance. An imaging framework composed by a telescope and an infra-red camera was proposed. A local correlation matcher was used by authors, which reported minor performance degradation with distance, off-angle images and eyewear. As in [75], fair results were obtained when the captured images do not contain significant portions of noise, specifically due to lighting. The works claim the possibility to capture images with enough quality in less cooperative modes and achieve accurate human recognition in these situations. Based on observations made in [227] following types of noise be found: the iris obstruction by eyelids (NEO) or eyelashes (NLO), specular (NSR) or lighting reflections (NLR), poor focused images (NPF), partial (NPI) or out of iris images (NOI), off-angle iris (NOA), motion blurred irises (NMB) and pupil (NPS) or sclera (NSS) portions wrongly considered as belonging to the iris. This type of noise can affect the iris recognition system and few methods to handle such scenario are prosed in [227]. In this next subsection, the main characteristics of the public and freely available iris image databases for biometrics purposes are described.

2.1.4. Iris Databases

The biometrics research and development need analysis on real data, although, a fair comparison between recognition methods depends on input data. Therefore, to test the

recognition methods standard biometric databases are of high relevance and become mandatory for the development process. Public and freely available iris image databases for biometrics purposes are highly anticipated and are described next.

2.1.4.1. BATH Database

The University of Bath (BATH) iris image database contains iris images taken from 800 eyes of 400 subjects [77]. The database comprises images taken from students and staff of the University of Bath. The images are of very high quality, taken with a professional machine vision camera, mounted on a height-adjustable camera-stand. The illumination was provided through a number of infrared LEDs, positioned below the camera and set at an angle such that reflections were aimed to the pupil. Next, an infrared pass filter was employed in order to negate the effect of the daylight and other environmental light reflections on the irises region. Images from the BATH database contain almost all noise factors of iris obstructions (due to eyelids and eyelashes).Along with ideal images, some non-ideal iris images are also including in the dataset incorporating variation in the dataset.

2.1.4.2. CASIA Database

Iris recognition has been an active research topic of the Institute of Automation from the Chinese Academy of Sciences. This database is clearly the most known and widely used by the majority of the researchers.

CASIA version 1: CASIA iris image database [78] (version 1.0, the only one that had access to) includes 756 iris images from 108 eyes, hence 108 classes. For each eye, 7 images are captured in two sessions, where three samples are collected in the first and four in the second session. In this dataset, images were captured within a highly constrained capturing environment. They have homogeneous characteristics and their noise factors are exclusively related   with   iris   obstructions   by   eyelids   and   eyelashes. *CASIA version 2:* In CASIA Version 2.0 (CASIA-IrisV2) includes two subsets captured with two different devices: Iris pass-h developed by OKI and self-developed device of CASIA, CASIA-IrisCamV2). Each subset includes 1200 images from 60 classes. *CASIA version 3:* CASIA-IrisV3 includes three subsets which are labelled as CASIA-Iris-Interval, CASIA-Iris-Lamp, CASIA-Iris-Twins. CASIA-IrisV3 contains a total of 22,034 iris images from more than 700 subjects. All iris images are 8-bit grey-level JPEG files, collected under near infrared illumination. Almost all subjects are Chinese except a few in CASIA-Iris-Interval. Because the three data sets were collected at different times, only CASIA-Iris-Interval and CASIA-Iris-Lamp have a small overlap in subjects. *CASIA version 4:* CASIA-IrisV4 contains a total of 54,601 iris images from more than 1,800 genuine subjects and 1,000 virtual subjects. All iris images are 8-bit grey level JPEG files, collected under near infrared illumination or synthesised. The six datasets were collected or synthesised at different times and CASIA-Iris-Interval, CASIA-Iris-Lamp,

CASIA-Iris-Distance; CASIA-Iris-Thousand may have a small inter-subset overlap in subjects.

2.1.4.3. ICE Database

The Iris Challenge Evaluation (ICE) is a competition designed to measure the accuracy of the underlying technology that makes iris recognition possible. Its goals are to promote the development and advancement of iris recognition and assess the technology's current level of performance. It is divided into two stages: first, it was asked to researchers and developers to participate in iris recognition challenge problems that might improve their recognition algorithms. Later, an opportunity to participate in a large-scale and independent evaluation will be given, through a new iris data set and a proper evaluation framework. Regarding the first stage of ICE, to facilitate the evaluation of different iris recognition proposals, an iris image database has been released for the researchers and entities that manifest the desire to participate in this competition. The ICE [79] database is comprised of 2954 images, with a variable number of images per subject. Similarly to the remaining public iris databases, its images were captured having quality as the main concern and clearly simulate the users' cooperation in the image capturing. Therefore, the noise factors that the ICE database contains are almost exclusively related to iris obstructions and poorly focused images.

2.1.4.4. MMU Database

The Multimedia University has developed a small data set of 450 iris images (MMU) [80]. They were captured through one of the most common iris recognition cameras presently functioning (LG Iris Access R© 2200). This is a semi-automated camera that operates at the range of 7-25 cm. Further, a new data set (MMU2) comprised of 995 iris images has been released and another common iris recognition camera (Panasonic BM-ET100US Authentic cam) was used. The iris images are from 100 volunteers with different ages and nationalities. They come from Asia, Middle East, Africa and Europe and each of them contributed with five iris images from each eye. Obviously, the images are highly homogeneous and their noise factors are exclusively related with small iris obstructions by eyelids and eyelashes.

2.1.4.5. UPOL Database

The UPOL [81] iris image database was built within the University of Palack eho and Olomouc. Its images have been captured through an optometric framework (TOPCON TRC50IA) and so images of extremely high quality are produced. The database contains 384 images from both eyes of 64 subjects.

2.1.4.6. WVU Database

The West Virginia University developed an iris image database (WVU) [82] comprised of 1852 images from 380 different eyes. The number of acquisitions from each eye ranges between three and six and an OKI Iris Pass-H hand-held device was used.

2.1.4.7. UBIRIS

The UBIRIS version 1 [21] database consists of 1877 RGB images taken in two distinct sessions (1205 images in session 1 and 672 images in session 2) from 241 identities. Both high-resolution images (800 x 600) and low-resolution images (200 x 150) are provided in the database. In UBIRIS version-2 the images were actually captured on non-constrained conditions at-a-distance, on-the-move and on them visible wavelength. Here 261 subjects of sclera 522 are present in this version. From these subjects, a total of 11,102 eye images is present in two sessions. Few subjects are there in the database, where the volunteers are wearing glasses.

2.1.4.8 Notre Dame Database

This dataset was Dept. of Computer Science and Engineering, University of Notre Dame, Notre Dame, United States of America. An Iridian LG EOU2200 64,980 camera was used to iris images from 356 subjects.

2.1.4.9. IIT Delhi Database

This dataset was collected at the Biometrics Research Laboratory in the Indian Institute of Technology Delhi (IITD). It was collected using JIRIS, JPC1000, digital CMOS camera. This dataset contains 1120 iris images from 224 users. Iris images are in bitmap format with 240*320 resolution.

2.1.4.10. MBGC

This database consists of 59,558 images collected from 240 users, using LG EOU 2200 Iris Camera near-infrared 8-bit intensity level, having 480*640. The images are stored in BMP image format.

2.1.4.11. Mobile Iris Challenge Evaluation

This challenge was organised in two-phase on two dataset MICHE I and II. MICHE-I is an iris biometric dataset captured under uncontrolled settings using mobile devices. The key features of the MICHE-I dataset are a wide and diverse population of subjects, the use of different mobile devices for iris acquisition, realistic simulation of the acquisition process (including noise), several data capture sessions separated in time, and image annotation using metadata. MICHE-II is to represent the starting core of a wider dataset to be collected with aforementioned unconstrained conditions.

2.1.5. Recent Works on Iris After 2010

Few recent works on iris segmentation are summarized as below.

1. Tan et al. [228] used UBIRIS v1 in their work. Clustering based coarse iris localization followed by Localization of pupillary and limbic boundaries and localization of eyelids is performed in this work.

2. Zhang et al. [229] employed ICE 2005, CASIA v3 in their work. A robust gradient map is used for iris localization. SIMC generated using spatial information and coarse iris location. Segmentation achieved by a level set method was used.

3. Roy et al. used [230] ICE 2005, CASIA v3, UBIRIS v1for their work. Game-theoretic decision making procedure to segment irises was used. Further, integrates region based segmentation and gradient-based boundary localization was performed.

4. Pundlik et al. [231] used WVU Non-Ideal and WVU Off-Angle datasets in their work. Images were modelled as MRF. Energy minimization is achieved via graph cuts was performed. Further, model iris as an ellipse to refine segmentation region.

5. In Zuo and Schmid [232] CASIA v3, ICE, WVU was used. A combined scheme for pre-processing, pupil segmentation, iris segmentation, and occlusion detection was reported

6. De Marisco et al. [233] used CASIA v3, UBIRIS v1 Pre-process using pasteurization filter. Canny filtering is applied to locate pupil boundary. The image is transformed to polar coordinates to identify the boundary between iris and sclera.

7. Proença [234] used UBIRIS v2 in this work. Sclera and iris are segmented and classified. By Polynomial fitting.

8. Koh et al. [235] used CASIA v3 in their work. Center of the pupil is estimated based on histograms. The pupillary boundary is computed using Hough transform. Applied Hough transform again to localize limbic boundary

9. Tan and Kumar [236] used UBIRIS v2 for the work. Iris features extracted using localized Zernike moments and sclera features are extracted using colour features. A robust approach is proposed for post-processing classified iris pixels

10. Tan and Kumar [237] used UBIRIS v2, FRGC v1 and CASIA v4 in the work. Multiple higher order local pixel dependencies are used to robustly classify eye region pixels into iris or non-iris regions. Post-processing operations effectively tackle noisy pixels

11. Sutra et al. [238] used ICE 2005, CASIA v3, North Dame IRIS-0405 in their work. Pre-processing is performed using anisotropic diffusion. Gradients are computed using the Sobel filter and Viterbi algorithm is applied to find contour.

12. Li et al. [239] CASIA v4 was used. Locate edge points on iris boundary. Boundary detectors for pupillary, limbic, eyelid boundaries are learned and iris boundaries are localized. Further eyelid edge points are modelled as parabolas.

13. Tan and Kumar [240] used UBIRIS v2 and CASIA v4 in their work. Iris segmentation approach based on cellular automata using grow-cut algorithm is proposed. Further, reduces computational complexity while increasing recognition was performance

14. Uhl and Wild [241] used CASIA Iris, North Dame dataset in their work. Adaptive Hough transforms estimates iris centre. Polar transform detects the first elliptic pupillary boundary. Ellipso-polar transform is used to find the second boundary

15. Li et al. [242] used CASIA v4 in their work. Assembled pupillary contour segments are fitted as an ellipse. Limbic boundary points detected by LBD. Unseen boundary points are extrapolated in eyelid occluded regions.

16. Alonso-Fernandez and Bigun [243] used CASIA v3 in their work. Pupil boundary is searched for and sclera is detected. Eyelid occlusion is computed and the iris is localized

17. Tan and Kumar [244] used UBIRIS v2, FRGC, CASIA v4 dataset in their work. The image is segmented using random walker algorithm. Coarsely segmented iris is refined and modelled as a graph

18. Hu et al. [245] used UBIRIS v2. FRGC l1-norm induces sparsity allowing coarse iris localization, limbic and pupillary boundary segmentation. Eyelid fitting and post-processing are performed

Some advanced pieces of work on iris featuring are as following:

1. Zhou and Kumar [246] used IITD v1 and CASIA v3 dataset in their work. LRT exploits the orientation information from the local features. Dominant orientation is used to generate feature representation. The similarity is computed using matching distances.
2. In Roy et al. [247] UBIRIS v1, ICE 2005, WVU dataset was employed. An Active contour model is deployed to segment non-ideal iris. A Modified Contribution-Selection Algorithm select informative features without affecting recognition performance

3. Zhang et al. [248] CASIA v4 was employed. DAISY descriptors are extracted from iris. Iris key points are localized on feature map. Extracted key points are matched for classification.

4. In Bastys et al. [249] CASIA v2, ICE v1, dataset were used. A fusion of multi-scale Taylor expansion phase information and its local extrema is proposed as a hybrid descriptor in this work.

5. Proença and Santos [250] NICE v2 Segment iris into coherent regions. Colour and shape information is extracted as a feature.

6. Kumar et al. [251] used UBIRIS v2, FRGC, CASIA v4 dataset in their work. Recognition of distantly acquired irises using LRT based orientation features. Iris is modelled as sparse coding solution based on computationally efficient LRT dictionary

7. Li and Wu [252] UBIRIS v2, CASIA v3 Iris boundaries and eyelids are localized. Log-Euclidean Co-variance Matrices are used to model correlation of spatial coordinates, intensities, further a 1st and 2nd-order image derivatives was used as feature

8. Rahulkar and Holambe [253] used UBIRIS, CASIA v3, IITD dataset in their work. Iris Features are extracted based on Triplet Half-Band Filter Bank. Post-classifier system achieves robustness against intra-class iris variations

9. Zhang et al. [254] employed CASIA v4, ICE 2005 dataset, propose Perturbation-enhanced Feature Correlation Filter for robust iris matching. Correlation filters are utilized for Gabor images matching.

10. Liu and Li [255] used UBIRIS v2, CASIA v4 dataset in the work. Normalized iris image is divided into patches, next represented by SIFT descriptors. The low-dimensional features are encoded to binary codes. Matching is performed by counting binary codes in the agreement was performed.

11. Kumar and Chan [256] UBIRIS v2 is employed. Hyper-complex sparse representation is used. The orientation of iris texture is extracted using a dictionary of oriented atoms. Iris representation as quaternion sparse coding problem is solved using convex optimization strategy

12. Zhang et al. [257] used UBIRIS v1, UBIRIS v2, NICE v2 dataset is used. Colour Texton is combined with the pixel value in multiple colour spaces. The image is represented by the histogram of the learnt Textron vocabulary for featuring.

13. Wang et al. [258] used CASIA v4. A large margin loss function is adapted to learn the robust model. Information from each feature is considered to remove noise. The model is solved using Simplex algorithm.

14. Sun et al. [259] employed CASIA. Hierarchical Visual Codebook integrates Vocabulary Tree and Locality-constrained Linear Coding was used for featuring followed by adopts coarse-to-fine visual coding strategy

15. Sun et al. used [260] CASIA v4 dataset in their work. Perform ordinal feature selection; objective function considers misclassification error of intra-class and inter-class matches. Multi-lobe Ordinal Filter is proposed to analyses ordinal measures of images

16. Tan and Kumar [261] used UBIRIS v2, FRGC, CASIA v4 for their work. Propose a non-linear approach to capture local consistency of iris bits and overall quality of weight map for recognition. Zernike moment based phase encoding of iris features is employed.

17. Tan and Kumar [262] used UBIRIS v2, FRGC, CASIA v4 dataset. Propose a strategy for accurate iris recognition from distantly acquired images. The algorithm generates a geometric key - set of coordinate-pairs assigned to each individual.

2.2. Sclera Literature

The first recognised work on sclera biometrics using blood vessels of sclera is recorded in Derakhshani et al., [1]. All the contributions of the different works found in sclera literature can be clustered into four basic categories. They are sclera segmentation, sclera vessel enhancement and image registration, feature extraction and classification. The various techniques that are employed for the above-mentioned steps are explained in the following sub-sections. Figure 2.3 is a block diagram of a typical sclera biometric system.
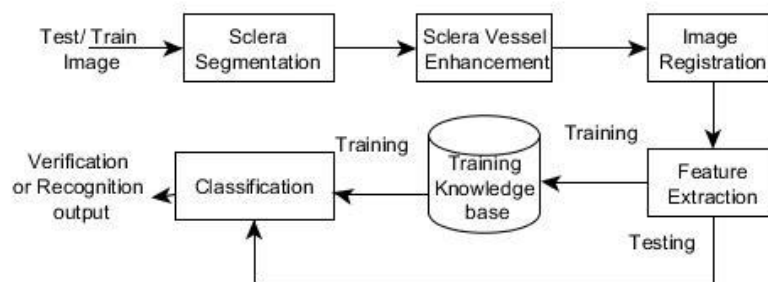
Figure 2.3. A block diagram of a typical sclera biometric

The rest of the section is divided into the following sub-sections. The sub-section 2.1.1. discusses the sclera anatomy; followed by sub-section 2.1.2 which highlights the several challenges in different stages of sclera biometrics, and in subsection 2.2.3 the available works in the literature and sclera datasets are discussed.

2.2.1 Sclera Anatomy

Investigating the characteristics of the human organ that is employed for a biometric trait is a very important step before using it. Therefore, in this section will discuss the properties of eye anatomy and will point out the biological richness of sclera as a biometric trait.

The eye is one of the most complex organs in human body. It is constituted of the following parts as described in Joussen et al. [85] and Kobayashi et al. [86]:

- Cornea/sclera the white portion of the eye i.e. the clear front surface of the eye. Light is focused primarily by the sclera. It contains the blood vessels which create a pattern.

- The iris of the eye functions like the diaphragm of a camera, controlling the amount of light reaching the back of the eye.

- The eye's crystalline lens is located directly behind the pupil (a small hole through which light enters into the eye) and further focuses light.

- Light is focused by the cornea and crystalline lens (and limited by the iris and pupil) then reaches the retina — the light-sensitive inner lining of the back of the eye.

- Other parts of the human eye play a supporting role in the main activity of sight: Some carry fluids (such as tears and blood) to lubricate or nourish the eye.
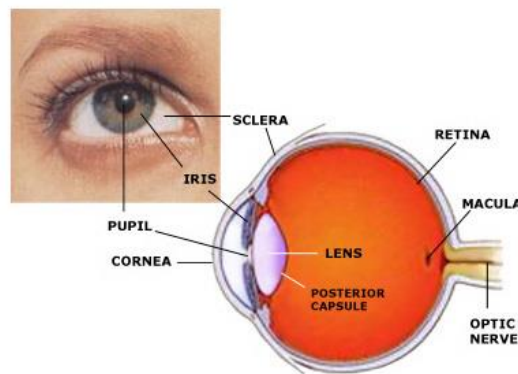
Figure 2.4: Different parts of the human eye [1].

Embryonal eye formation begins in the third week of the embryonic development and continues till the tenth week as mentioned in Ort et al. [87], Sadler [88], Keller [89], and Fuhrmann et al, [90]. The middle portion of the optic cup develops into the ciliary body and iris (Eiraku [91]). Further differentiation and mechanical rearrangement of cells in and

---

[1] http://www.vision-and-eye-health.com/eye-anatomy.html

around the optic cup gives rise to the fully developed eye which also includes the scleral part. Therefore, these facts prove that the sclera vessel patterns are present since birth.

As this article is focused on the sclera biometric trait, in the next subsection will provide further insight into sclera anatomy. It is interesting to note that humans are the only mammals with extensively exposed sclera, which is amenable to imaging (Kobayashi et al. [86]).This is another advantage of using sclera for human identification. It is formed randomly for each person due to the orientation of the blood vessels. The blood vessel patterns are also unique with both genetic and developmental components determining their structure. The structure of the blood vessels is visible and found to be stable over time. Even though with increasing age, collagen and elastic fibers deteriorate, glycosaminoglycan loss and sclera dehydration occur, and lipids and calcium salts accumulate, but the blood vessels do not deteriorate. Therefore, sclera's embryonal and biological properties prove and advocate the stability of the pattern.

As discussed, the sclera is a white opaque area around the iris, containing blood vessel pattern in different layers. The sclera as explained in Trier [92] and Kanski, [93], is a firm dense surface composed of collagen and elastic fibers, with thickness varying from 0.8 mm to 0.3 mm and organised in four layers: episclera, stroma, lamina fiscal and endothelium. The conjunctiva is a clear mucous membrane, made up of epithelial tissue, and consists of cells and underlying basement membrane that covers the sclera and lines the inside of the eyelids; the conjunctival vascular is hard to see with the naked eye at a distance.

- The episclera is the outermost layer and the endothelium is the innermost one. The sclera is avascular, except in its outermost surface. The episclera which contains the blood vessel patterns is employed for biometric applications.

- The anterior part of the sclera, up to the edge of the cornea (the sclerocorneal junction) and the inside of the eyelids, are covered by the conjunctival membrane, a thin layer containing secretory epithelium that helps lubricate the eye for eyelid closure, and protects the ocular surface from bacterial and viral infections.

- The part of the conjunctiva that covers the inner lining of the eyelids is called palpebral conjunctiva. The outer surface of the eyeball is covered by the bulbar conjunctiva, and the junction of the palpebral conjunctiva and the bulbar conjunctiva is called the conjunctival fornix. Bulbar conjunctiva is semi-transparent and colourless and contains blood vessels.

- Anatomically, the blood vessels in bulbar conjunctiva can be differentiated from those of episclera; while conjunctival vessels may slightly move because of the conjunctival membrane, those in episclera will not as mentioned in Heath [94].

The rich vasculature patterns revealed in the episclera and conjunctival membrane are together referred to as conjunctival vasculature/sclera in this article. Therefore, it can be concluded from the aforementioned discussion that the orientation of the blood vessels creates a pattern. It can also be concluded that their biological properties solicit their stability and ease for use as a biometric trait.

2.2.2. Challenges and Research Problems in Sclera Biometrics

A sclera biometric system is comprised of different stages. Which are: image acquiring, segmentation, image enhancement, feature extraction and classification. Each of these stages poses different challenges and research problems. Challenges and research issues of each of these stages are discussed below.

2.2.2.1 Image Acquisition

Image capture is the first and very crucial stage for any image processing related system. Likewise, for sclera biometric systems, image acquiring plays a vital role. Accurate and best quality information capturing is the main aim of this stage. However, there are several challenges that can resist this information gathering stage, this includes.

- The external lighting conditions (Figure 2.5), bulge structure of the sclera and specular reflections due to the water content of the eye are the general challenges. These noise issues can be minimised in controlled environments using indoor lighting conditions.
- Sclera patterns are more prominently visible in indoor lighting conditions. Although in indoor uncontrolled environments, specular reflection can get introduced in the eye image (Figure 2.6 a, b).

- The sclera patterns are less prominently visible in controlled and uncontrolled outdoor lighting conditions (Figure 2.6 c, d).
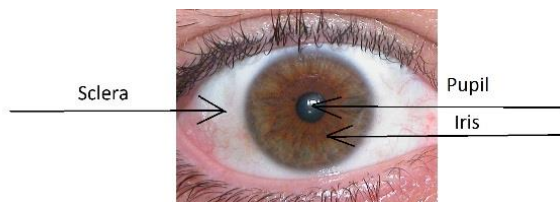
Figure 2.5: An eye image acquired in the visible spectrum with lighting in the visible spectrum (taken from UBIRIS version 1)

Moreover, capturing sclera patterns whilst also preserving the iris pattern is very important. Visibility of the sclera pattern is prominent for most of the eye angles (Figure 2.6), except when a person is looking downwards, as, during this scenario, the eye portion is mostly covered by the eyelid and lashes.

(a)   (b)

(b)   (d)
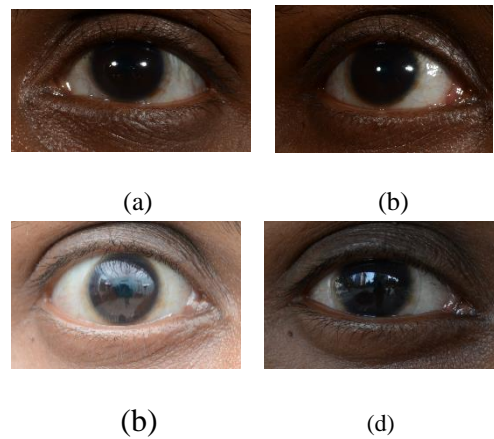
Figure 2.5: Eye image of an individual acquired in different lighting conditions taken from MASD (a) indoor controlled, (b) indoor uncontrolled, (c) outdoor controlled, (d) outdoor lighting uncontrolled.

The fineness of vascular patterns (medical condition) and age of the individual can also affect the quality of the sclera pattern acquired in different ways, such as:

- The sclera pattern of children is less visible as they are blueish in nature and the sclera region is less exposed

- Sometimes the sclera pattern can also be affected by medical conditions. A person suffering from an eye allergy will tend to have a less exposed sclera region. The prominence of patterns can be reduced for the patient suffering from the diabetic medical condition (Figure 2.7b).

(a)   (b)

(b)   (d)

(e)
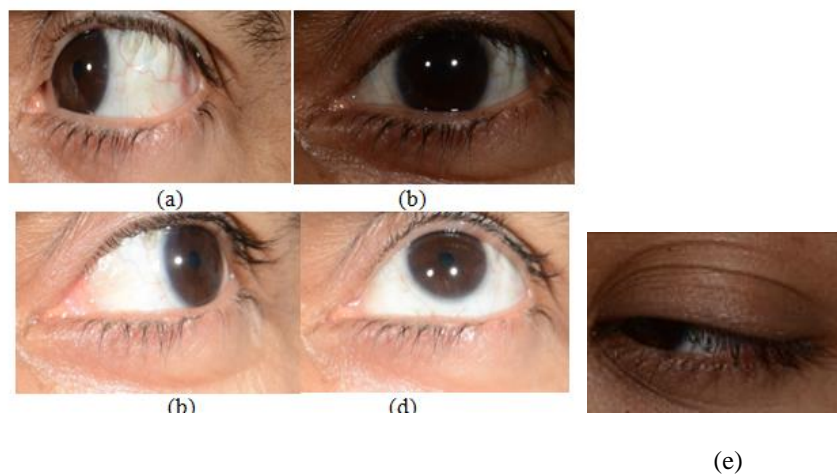
Figure 2.6: Eye image of an individual looking at different angles taken from MASD (a) looking right, (b) looking straight, (c) looking left, (d) looking up and (e) looking downwards.

- Movement of the eyeball can also affect the sclera pattern acquired; blur and other noises can get introduced in the pattern. Occlusions and other noisy factors are also a few of the challenges that need to be addressed during this step (Figure 2.7 c, d) ta.

<table>
<tr><td>(a)</td><td>(b)</td></tr>
<tr><td>(c)</td><td>(d)</td></tr>
</table>
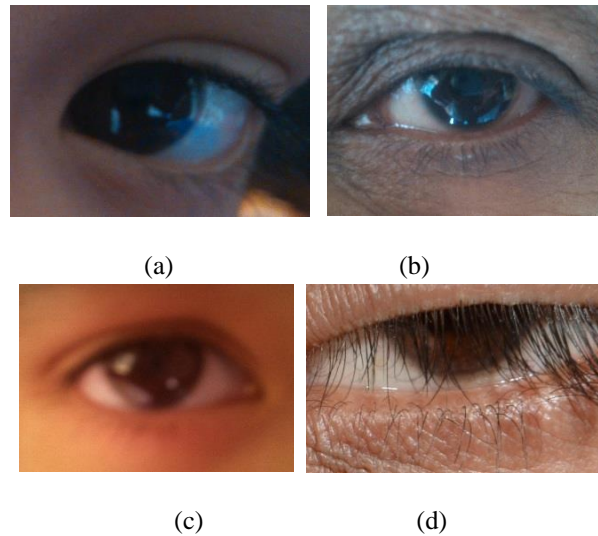
Figure 2.7: Examples of eye image (from MASD dataset) of a (a) child, (b) diabetic person, (c) with motion blur and (d) closed eye.

Another important aspect that needs to be addressed in the sclera acquiring stage, is the light spectrum in which the images will be captured. In general, the iris images are captured in the NIR spectrum, but the sclera vessels are hardly visible in the NIR image of the sclera (Figure 2.8 b), mainly due to the thin diameter of the veins in the eye (reflection and transmission in NIR band are the same).In contrast, both the sclera and the iris patterns are visible in the visible spectrum, which can be used for acquiring both patterns. More precisely, sclera patterns are more prominently visible in the green band of the visible spectrum and the iris in the red band. Therefore, one solution to obtain the iris and sclera pattern at best quality can be captured in the multi-spectrum band. Figure 2.8 (c-f) examples of images captured in multi-spectral bands. Eye images acquired with multispectral and hyperspectral cameras. Looking for a discriminative camera for the sclera or iris could be a better solution but the high cost of these cameras deters their use.

2.2.2.2. Segmentation

Segmentation is the first necessary step for most biometric related research. The main aim of segmentation is to identify the region of interest as accurately as possible. Similarly, in
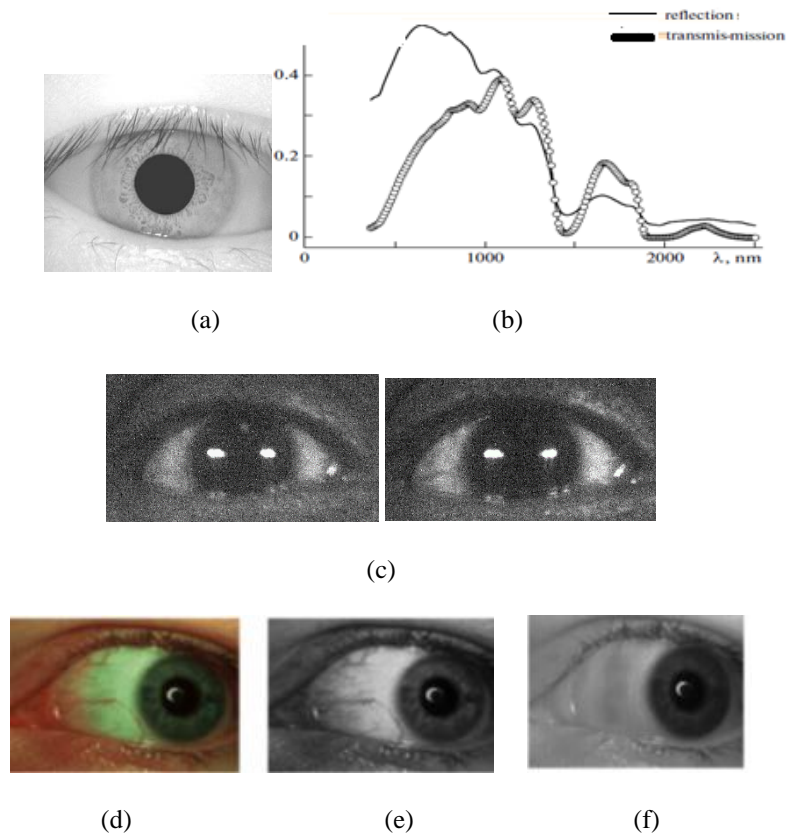
Figure 2.8: Eye image captured in (a) NIR taken from CASIA version 1 [78], (b) the plot of the transmission vs reflection for different spectra [85], (c) eye images in the hyperspectral band, (d) in the visible spectrum, (e) green band of visible spectrum and (f) red band of the visible spectrum. (d-f) are taken from Crihalmeanu and Ross [8].

sclera biometrics a precise segmentation is important otherwise, an incorrect segmentation can not only reduce the pattern available but also can introduce other patterns such as eyelashes and eyelids. In addition, there are also several other specific challenges of the sclera segmentation which are as follows:

- One main problem is the low contrast of the sclera region i.e. the foreground and its surroundings i.e. the background. Therefore it is difficult to apply traditional binarization methods for segmentation.

- Another significant challenge that affects sclera segmentation is highly bundled vessel patterns, mainly near the tear gland. These bundled patterns sometimes can be misclassified with the skin colour during segmentation and can be classified as the skin or non-sclera area.

- Lighting shades and specular reflections on the sclera region are the other few challenges that need to be tackled during sclera segmentation.[2]

- The variations in the specular reflections may be accentuated by the rapid movement of the eyeball. Based on the angle of the incoming ray of light, some specular highlights may have intensities closer to the background intensity values; hence isolating the specular reflections can be an additional difficulty.

2.2.2.3. Enhancement

The vessel pattern in the sclera is not prominently visible. So in order to make them clearly visible, image enhancement is required. The following are the challenges in the sclera vessel enhancement task.

- Low contrast between the sclera vessels i.e. the foreground and the white region (non-vascular part) i.e. the background are the main challenges for sclera vessel enhancement.

- The vessel patterns are of varying intensity. Moreover, the randomness in the intensity of the pattern varies from one individual to another.

- Reflection, shade and lighting conditions (that are introduced during image acquisition) can also affect the enhancement.

- The presence of fluid in the eye can introduce specular reflection, which can also affect the vessel pattern enhancement.

- Medical conditions can reduce vessel pattern intensity e.g., a person suffering from diabetes may get loose the capillaries present in the sclera.

- Other conditions such as the presence of artificial lenses/glasses, after a long period of near vision work (Figure 2.9a), irritation or rubbing of eyes, can introduce reddishness which affects sclera pattern enhancement.

- Ageing is another factor that affects the pattern enhancement i.e. the vessel pattern is less prominent in children and the sclera region is smaller as compared to the adult.

---

[2] The reason for the introduction of this specular reflection is because in order to image the scleral surface with its blood vessel patterns, a sufficient amount of light needs to be directed into the eye. This light will be prominent on the spherical surface of the sclera after passing through the conjunctiva. Optical processes such as reflection and refraction are difficult to fully control and these results in specular reflections with a variety of different intensity values, topologies, shapes, sizes and locations.

Moreover, eyes in kids are generally bluish so the contrast of the blood vessels and sclera is less prominent that of adults.

- Due to ageing, a brown ring and pattern can also be introduced in the sclera area that can be challenging to discriminate from blood vessels during enhancement due to their close intensity.

- The blood vessels can stretch and get loosened from the underlying sclera leading to the formation of vessel folds with ageing. The white portion of the eye becomes yellowish and an increase in melanin in the sclera region can also appear with ageing as mentioned in [Heath, 2006], which affects enhancement process (Figure 2.9b).

- The nonlinear blood vessel movement can also affect enhancement process.

(a)   (b)
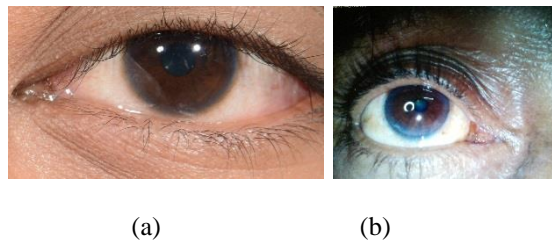
Figure 2.9: (a) Images of the sclera after stressful work. (b) Eye image of an old person with less prominent sclera visibility (taken from MASD).

Another vital factor that needs to be considered during enhancement of this trait, is the layers of the sclera to be considered for authentication. In the literature, both conjunctival vasculature and the sclera are used parallelly. Conjunctival vasculature considers only the episclera, while in the sclera the vessel patterns of the bulber layer are also present.

2.2.2.3. Feature Extraction

Feature extraction of a sclera involves a building of an appropriate mathematical model of the abstract sclera pattern to reliably identify persons for authentication and identification purposes. Following are the challenges that can be faced in feature extraction.

- Upon rubbing the eye, the conjunctiva can slightly move which can change the pattern.

- Even large changes in gaze can affect the feature as the vein pattern changes significantly with the orientation of the eyeball (e.g. looking left vs. right so on. Figure 2.10).

- Medical conditions can also influence the performance of the feature extraction algorithms. Owen et al., [95-96] mentioned diabetes is associated with the loss of capillaries, macro-vessel dilation and changes in tortuosity in vessel intensity.

- Hyperemia, conjunctivitis and haemorrhage influence a number of blood vessels seen on the sclera surface, and affect the contrast between the blood vessels and the background i.e. white part of the eye (the eye becomes reddish due to infections) Heath, [94].

Figure 2.10. An example of sclera pattern of the same individual left eye looking in different directions/ gaze (taken from MASD).

- Medical conditions can also influence the performance of the feature extraction algorithms. Diabetes is associated with the loss of capillaries, macro-vessel dilation and changes in tortuosity in vessel intensity as mentioned in Owen et al., [95, 96].

- Hyperemia, conjunctivitis and haemorrhage influence a number of blood vessels seen on the sclera surface, and affect the contrast between the blood vessels and the background i.e. white part of the eye (the eye becomes reddish due to infections) Heath, [94].

- Age is another factor that influences the appearance of the sclera surface. As mentioned previously, vessels can stretch and loosen from the underlying sclera, leading to the formation of conjunctival folds. The white region of the eye becomes yellowish and along with increment in melanin in the conjunctiva can also appear.

- In younger people, blood vessels may be less visible. With age, the conjunctival vasculature becomes thicker and more visible, hence appropriate techniques are required in order to determine and characterise this biometric to adjust this development.

2.2.2.4. Classification

Biometric algorithms generally aim to provide a score of the membership of the input trait by a given identity and hence classification plays an important role. The importance of classification method is also reflected in the sclera literature. The main challenge is how to best classify a trait on basis of the features extracted. In addition to general image classification challenges few other challenges are as following:

- Adaptation with respect to changes in lighting conditions, medical conditions, ageing and changes in orientation of the eyeball/gaze angle are the other challenges that make the classification task complex.

- Moreover, as referred to previously, upon rubbing the eye, the blood vessels can slightly move relative to the sclera surface, generating small deformations of its blood vessels as mentioned Heath, [94]. . Matching images of the conjunctival vasculature is greatly impacted by these deformations.

- Classification for larger samples and populations is another highlighted challenge that will be necessary to take into account at this stage.

2.2.2.5. Fusion with Other Traits

Multimodal biometrics use more than one means of biometric identification to achieve higher recognition accuracy. It was introduced to combine multiple biometrics to perform positive human identification proposed in Ross and Jain. [97]. Like other multimodal biometrics, such as iris and fingerprints, or iris and face, iris and sclera information can also be used easily. As sclera and iris pattern can be obtained at one camera short. Focusing on one-shot biometrics, for user convenience and transparency, the most reliable combination is iris and sclera traits. Regardless of these advantages, several challenges that can be faced in this stage are:

- Selecting the best level of fusion is a big challenge in the course of multimodal eye biometrics using iris and sclera.

- Keeping the complexity of the algorithm low is another big challenge.

- Studying the statistical independence of the traits is also required to build a more reliable system.
- Quality assessment of the traits is very important for assisting decision-making in the matching process.

- Adaptiveness of the quality assessment with a variance to lighting conditions, ageing and gaze angle of the eye are a few additional challenges that are also faced with the uni-modal scenario but can become more complex in a fusion scenario.

2.2.2.6. Performance Measures

In real life scenarios, it is required to know how well the system performs and what factors affect its performance so that proper system selection or setup adjustments can be made.

The only way to acquire such knowledge is through evaluation, which is the procedure that involves testing of a system on a database and/or in a specific setup for the purpose of obtaining measurable statistics that can be used for comparison. Several such measures have been proposed in the literature and several challenges are being identified at different stages of biometric data processing described in Snelick et al [98]. BEAT Biometrics Evaluation and Testing (http://www.beat-eu.org/) is a standard that has also been proposed in recent times.

A sclera biometric system also includes several stages of signal processing, image processing and pattern recognition tasks. Therefore, performance evaluation of each of these stages is required to be carried out individually. The identified challenges are as follows:

- Performance evaluation of a sclera segmentation is one of the greatest challenges because it requires good quality baseline (manually segmented masks or ground truth). Moreover, the sclera region may be occluded by eyelashes which additional challenge to segment and prepare baseline.

- For sclera vein pattern enhancement, developing a standard baseline and performance measure for it is challenging.

- An appropriate quantitative analysis method to evaluate the performance of the features employed and the classification process on a larger range of the population are also some of the main challenges faced.

In addition to the general challenges of biometric performance evaluation, the quality assessment of biometric raw data is receiving more and more attention since it is considered one of the main factors affecting the overall performance of biometric systems, as found by El-Abed et al [99]. These challenges are enlisted as below:

- Acquisition artefacts such as illumination and acquisition environments are difficult to maintain. Therefore, controlling the quality of the biometric raw data is absolutely necessary before undertaking performance evaluation of the trait.

- In general, to maintain standard using quality information can be performed, poor quality samples can be removed during the enrolment phase or rejected during the identification stage, followed by asking the user for a new sample. This scenario is also true for sclera biometrics.

- Contrast effects and their impact on the quality of the performance also need to be evaluated.

2.2.2.7. Anti-spoofing

Ratha et al. [100] mentions that with the potential growth of biometrics application, biometric systems need to be equipped with countermeasures against spoofing attacks. Toth [100] defines liveness/anti-spoofing detection refers to the different techniques that are employed to countermeasures spoofing attack. The liveness detection methods may scrutinise the physical properties of a living body (in terms of density, elasticity, electrical capacitance, etc.) or of spectral reflection, absorbance, visual properties (colour, etc.), involuntary signals of a living body (such as the pulse, blood pressure, etc.), or bodily responses to external stimuli, (for instance smiling or the blinking of an eye) are employed to detect liveness.

The potential types of approaches for forging that can be adapted in ocular biometric systems are as follows [Daugman, [16], [29]:

1. Eye image/video: Scanning an image/video from a portable screen can be a potential way of attacking the system (Figure 2.11b).

2. Printed images: Scanning a high resolution printed image as an artificial eye in front of the scanner (Figure 2.11c).

3. Lens: Glass/plastic lens and 3D print of an eye.

Similar to other biometric the sclera biometric system should also be equipped with anti-spoofing technique. Several challenges reside in designing anti-spoofing methods in sclera based biometrics systems:

• In general ocular biometrics in the visible spectrum, can face more threats of spoofing as addressed in Galbally et al. [102].

• Asking for responses to different stimuli could be effective, but also reduce the user transparency of the scheme.

• On the other hand, for software-based anti-spoofing methods, signal processing and image processing tools are employed to established liveness, these establishments can be tough to handle if 3D printing of an eye image is used to spoof.

• Besides the general challenges of anti-spoofing attacks, there are few additional challenges that exist for liveness detection. Liveness and adaptiveness of biometric traits both are necessary to be incorporated in a biometric system. However, liveness and adaptiveness of biometric traits have been found to be a trade-off in the literature.

(a)   (e)   (f)
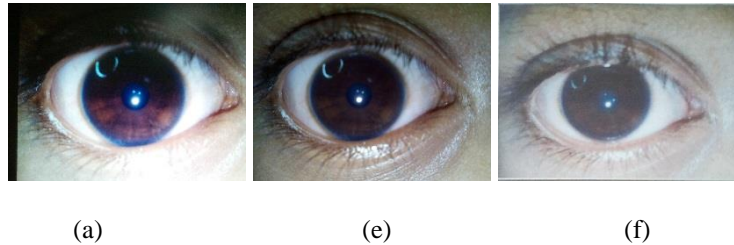
Figure 2.11: Example of (a) an eye image (b) fake generated by scanning the eye image from a digital screen and (c)) fake generated by scanning the eye image from a printed image (taken from Liveness dataset developed) [275].

2.2.3. Critical Review of the Sclera Literature

Various efforts have been made in the literature to solve the problems and challenges of sclera biometrics. The first recognised work on sclera biometrics using blood vessels of the sclera is recorded in Derakhshani et al. [1]. All the contributions of the different works found in the sclera literature can be clustered into four tasks: sclera segmentation, sclera vessel enhancement, sclera features, and classification. Although most of the works in the literature have not worked on each of these stages individually, rather they have proposed whole systems which consist of each of these stages. This section attempts for a critical analysis of the performed work. The various techniques proposed on the above-mentioned stages are reviewed in the following sub-sections.

2.2.3.1. Image Acquisition

Data acquisition or the sensor-level stage is one of the most important for any pattern recognition task. Therefore, data acquisition is equally important for biometrics. Hence, in the area of sclera biometrics, special attention and research have been carried out at this stage. The data acquiring setups proposed in the various works of the literature are summarised in Table 2.1. It can be concluded from the above Table 2.1, that varying sensor, spectral bands and artefacts are employed to acquired sclera data as precisely as possible. Moreover, most of the image acquisition processes adopted in the sclera literature are acquired in mostly controlled indoor environments. Moreover, the presence of illumination to the eye is also required to acquire the trait. Therefore, it will be beneficial to carry out research in this particular context of the research to implement sclera biometrics under more uncontrolled environments and illuminations, in order to push the border of sclera biometrics. Another, an avenue of research that should also be explore is using the different advance sensor to acquire sclera. Moreover, it will be also appealing to cultivate the interoperability of the trait with respect to acquiring sensor. Perhaps researchers can also start working with acquiring images with mobile cameras in unconstrained conditions.

Table 2.1: Different sensor level technique proposed in literature to acquire sclera

Work	Wavelength	Hardware used	Environment
Derakhshani et al. [1]	Visible	5 MP Sony digital camera	Indoor controlled
Derakhshani and Ross [2]	Visible	Canon 20D camera EFS 60mm f/2.8 Macro and EF 70-200 mm f/4L USM telephoto lenses	Indoor controlled
Zhou et al. [3, 5]	Multi-wavelength (purple (420 nm), blue (470 nm), green (525 nm), yellow (590 nm), orange (610 nm), red (630 nm), deep red (660 nm), infrared (820 nm))		
Crihalmeanu et al. [14]	Visible	SONY CyberShot DSC F717(5 megapixels)	Indoor controlled
Crihalmeanu and Ross [8]	Multiple spectral bands range from 350 to 1700 nm	Redlake (Duncan Tech) MS3100 multispectral camera (three array sensors based on CCD)	Ophthalmolog ist's slit-lamp mount and a light source
Tankasala et al. [9]	Visible	Canon 20D DSLR camera mounted on a tripod	Regular office environment using ambient lighting & no flash
Gottemukkula et al. [11]	Visible	NikonD3S FX-format camera with 12.1 effective megapixels and a micro Nikkor 105mm lens	Blocked ambient light
UBIRIS version 1 & 2 Proença and Alexandre [21]	Visible	Nikon E5700	Darkroom indoor lighting and outdoor light

2.2.3.2. Segmentation

As indicated in section 2.2.2.2 that sclera segmentation poses a huge amount of challenges, therefore special research attention is required to be paid. Sclera segmentation has evolved from manual segmentation to various intensity based and contour-based segmentation technique. In the initial works of the sclera biometric literature such as in Derakhshani et al. [1].and Derakhshani et al. [2], manual segmentation was used. Possibly Tan and Kumar [237] followed by Khosravi and Safabakhsh. [7] was the first works that proposed automated sclera detection in the visible spectrum. Rest of the works on sclera segmentation are summarised in the below Table 2.2.

Table 2.2: Different segmentation technique used in literature.

Work	Technique	Limitation	Database
Khosravi and Safabakhsh. [7]	TASOM (Time Adaptive Self-Organizing Map)-method detailed in [Shah-Hosseini 2003 a, b]	Some of the vein patterns in the sclera region are quite bright and bundled, especially in the edges that create hindrance to segment region growing.	In-house
Crihalmeanu et al. [14]	Semi-automated using k-means	Sclera region misclassified to skin region	In-house
Tankasala et al. [9]	K-means clustering and considering three clusters, sclera pixel cluster was determined as the cluster which has the largest Euclidean distance from the origin of the coordinate system to its centroid.	Vein patterns in the sclera region which are quite bright and bundled classified into skin cluster The performance also depends on the illumination of the image.	In-house
Zhou et al. [4]	Downsampling, to the HSV colour space, followed by eyelid and iris boundary refinement, mask creation and mask up-sampling	Performance depends on the illumination of the image.	UBIRIS version 1
Zhou et al.[5].	For grey image: Otsu's threshold method, refinement by Fourier active contour method [17]. Colour image estimation the best representation between two colour based techniques	Blur images cannot be handled	
Oh and Toh [10]	HSV colour model based segmentation	Illumination change can effect	
Gottemukkula et al. [11]	Tiled based	Blur images cannot be handled	In-house
Crihalmeanu and Ross [8]	The sclera-eyelids contour: (Land + Satellite), Pupil region segmentation, the sclera-iris boundary	Improper illumination or the presence of plenty of mascara leads to low segmentation performance	In-house

Sclera segmentation is a significantly important part of sclera biometrics. However, sclera segmentation has not been extensively investigated as a separate topic, but mainly summarised as a component of a broader task. It can be inferred from recent developments in the aforementioned literature reported in Table 2.2, that there has been a number of independent research efforts made by researchers to establish sclera segmentation. It can be inferred from the above discussions that, two strategies for sclera segmentation have been adopted in the literature. These categories of techniques are based on sclera pixel thresholding and sclera shape contour. Each of techniques is having their advantages and

disadvantages. Although from the observation made, active contour based is perhaps a better approach as it has less effect in presence of noise. Therefore, more research attention is required to establish the best technique for both low and high-resolution images. Another important concern that should also be raised is evaluating the segmentation biometric performance of the trait, depending on the perfectness of the trait. The goal is to obtain high biometric performance rather than to attend ideal sclera segmentation, which might not be attended on an unconstrained scenario.

2.2.3.3. Sclera Vessel Pattern Enhancement

Sclera vessel pattern is very important for proper featuring of the trait. Enhancement technique has got mature from basic pre-processing using tonal correction used in Derakhshani et al. [1] to wavelet enchantment used in Zhou et al. [5]. The different techniques proposed for the same are in Table 2.3.

Table 2.3: Different sclera vein enhancement technique used in literature.

Work	Technique	Database
Derakhshani et al. [1]	Contrast limited adaptive histogram equalisation (CLAHE) on the green channel of the RGB image of sclera to get better contrast Followed by selective line enhancement technique the region growing algorithm is applied before binarization	In-house
Derakhshani and Ross [2]	Green layer of the RGB image is pre-processed by a contrast-limited adaptive histogram equalisation by 8×8 tiles 256-bin histograms.	In-house
Crihalmeanu et al. [8, 14]	Histogram equalisation, a low pass filtering was employed. Image registration a local affine and a global smooth transformation were applied.	In-house
Gottemukkula et al. [11]	An image mapping method used followed by sclera, followed by CLAHE	In-house
Tankasala et al. [9]	CLAHE with parameters: 8×8 tiles, contrast enhancement limit of 0.01, and uniform distribution of the histogram.	In-house
Zhou et al.[3-5]	Bank of directional Gabor filters threshold for binarization, morphological thinning	UBIRIS version 1

Efforts have been made by researchers to resolve the problem of sclera vessel enhancement as accurately as possible. It can be concluded from the above Table 2.3 that mainly CLAHE and wavelet filters are used on the green channel of the sclera image to achieve prominent sclera pattern. Various algorithms have been proposed for sclera enhancement in subsequent independent research work. Still, sclera enhancement is an unsolved challenge and remains an open research area, as performance analysis of this particular area has not at all been investigated. Establishing performance measures for sclera vein enhancement can be a

notable approach to research. Furthermore, vein enhancement is a significantly important part of sclera biometrics, however, sclera enhancement has not been extensively investigated as a separate topic. Several other issues such as invariance of the algorithm with the individual ethnicity (individual with dark skin colour and white skin), cross sensor and medical issues (dark brown ring around the iris, brown patches around sclera region, red eyes, etc. as shown in Figure 2.12) have not been investigated yet.
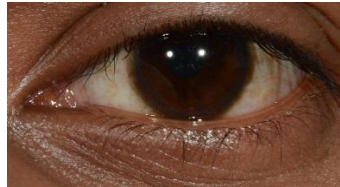
Figure 2.12: An eye image showing a sclera with dark brown ring and brown patches on the sclera region.

2.2.3.4. Feature Analysis

Sclera vessels patterns are rich in texture features. Considering this assumption, different texture feature-based extraction techniques are employed to model the pattern created by sclera vessel patterns. The most relevant features proposed in the literature are summarised in Table 2.4.

Table 2.4: Different feature extraction techniques used in the literature.

Work	Technique	Database
Derakhshani [1]	Minutia point-based feature extraction	In-house
Derakhshani [2]	Discrete Cohen-Daubechies-Feauveau 9/7 Wavelet transform, the resulting CDF 9/7 wavelet feature matrix ($16\times32=512$ features) * 8 levels.	
Crihalmeanu et al. [8, 14]	SURF (Speeded Up Robust Features), minutiae-based extraction, followed by direct correlation matching (by pixel to pixel matching) and finally, for fusing the features of the different poses, a minutia score and direct correlation scores were used. Models a local affine and a global smooth transformation.	
Gottemukkula et al. [11]	A tile-based feature extraction method (mean and variance)	
Tankasala et al. [9]	Statistical features of GLCM (Grey Level Co-occurrence Matrix, such as contrast, correlation, energy and homogeneity, were used in conjunction with Fisher linear discriminant analysis.	
Zhou et al. [4]	Average, min, max and quality based average score for combining multi-angle images.	UBIRIS version 1
Oh and Toh [10]	LBP (Local Binary Pattern)	

It can be inferred from the above Table 2.4 that typically, sclera features are assumed to be texture features, although the sclera vessel pattern is also rich in shape feature. Moreover, most of the work has been done on independent dataset so a fair comparison of their reported performance is impossible. Therefore, it is very important to benchmark them with a single dataset.

Regardless of the investigation made to date, several research areas such as the invariant feature extraction of the sclera pattern in the presence of noise, medical condition, stress condition and other external agents (eyelash or makeup introduced), need to be further investigated. The effect of acquiring images in uncontrolled conditions, medical conditions and cross sensor environments are also required to be further investigation.

Fresh ideas like, to produce view invariant feature are also required to research, to enrich the subject of research. Moreover, attending higher performance will remain always to be appealing, therefore designing more accurate featuring always remain an open research area.

2.2.3.5. Classification Techniques

Classification of the sclera vein pattern has been studied in most of the work in the literature on sclera biometrics. Classification techniques in sclera biometrics got advanced from basic classifiers as used in Derakhshani et al. [1]. The classification techniques used for classification are summarised in the below Table 2.5.

Table 2.5: Different classification technique used in sclera literature.

Work	Technique	Database
Derakhshani et al. [1]	First a coarse level procedure then a detailed matching.	In-house
Derakhshani and Ross [2]	Single hidden layer feed-forward NN (Neural Network)	In-house
Crihalmeanu et al. [8,14]	Score matching	In-house
Gottemukkula et al. [11]	Correlation coefficient	In-house
Tankasala et al. [9]	Neural networks (match score average method)	In-house
Zhou et al.[3-5]	Template matching	UBIRIS version 1
Oh and Toh [10]	A normalised Hamming distance	

An appreciable recognition result was attained in this above-mentioned work. However, matching speed was slow for techniques based on template matching, which could curb the utility of template matching for real-time applications. Although the best efforts have been

made by researchers to classify the traits, but in this studies the classification techniques have been investigated as a system not individually. Moreover, as all these works have used different classifiers, and even the feature inputs are different, therefore a fair comparison is impossible. Future effort should be made to make a fair comparison. Adaptability of the system with respect to changes (noise, medical condition, stress condition and other external agents) is still an open research area that needs to be thoroughly investigated. Especially, in regards to medical condition and cross-sensor environment needs extensive research attention. Fresh ideas for classification, score optimisation and matching are also required to be explored. Moreover, similar to featuring classification will always remain to be an open research area as it is directly related to the performance of the system. Robust user template registration and an efficient matching procedure also required being research.

2.2.3.6. Multimodal Approaches in the Sclera Literature

In Gottemukkula et al. [11], the concept of combining the sclera and iris pattern was proposed for the first time in the literature. Rest of the work proposed in the literature are summarised in Table 2.6. The performance of the work proposed in Zhou et al. [6], Tankasala et al. [9] and Gottemukkula et al. [12] depends on the Quality of the traits, which was further explored by the work of Zhou et al. [4]. Although, appreciable recognition accuracy was attained in the work of Zhou et al. [4], but multisession experimental scenarios were not explored in the study.

Table 2.6: Different multimodal biometric used in sclera literature.

Work	Modality	Fusion Technique	Database
Zhou et al.[4]	Iris and sclera	Score fusion based on GMM kernel	UBIRIS version 1
Gottemukkula et al. [12]	Iris and sclera	Weighted score fusion	In-house
Zhou et al. [6]	Iris and sclera	Quality assessment-based score fusion technique	UBIRIS version 1
Tankasala et al [9]	Iris and sclera	Match score level fusion	
Oh and Toh [10]	Periocular and sclera	Score level (TERELM)	

Techniques available for information fusion are available. Hence the challenging to find the optimal solution for fusing the sclera with other traits. In multi-biometric systems, the information acquired from different sources can be processed either in sequence or parallel. Hence it is important to decide about the processing architecture. The sensor should be fast in collecting quality images from a distance and should also have low cost with optimal failures to enrol. In sclera multi-biometrics, it is also very important to find this optimality

which is hardly addressed in the literature. Moreover, as the information are the best present at the sensor level, and it is possible to fuse the traits with sclera at the sensor level. Therefore, efforts should be made to research on sensor level-based sclera multi-biometrics.

2.3.3.7. Performance Analysis and Quality Assessment

Research on performance analysis for the sclera biometrics is not researched in the literature. Only the existing performance analysis measures for recognition and verification like FAR (False Acceptance Rate), FRR (False Rejection Rate) and EER (Equal Error Rate) are employed). In Zhou et al [4] a quality measure is proposed, which was able to detect 72 out of 78 blurred and distorted images present from session 1 of UBIRIS version 1 dataset. In another work Zhou et al [5] proposed a comprehensive approach to the sclera image quality measure. The work includes quality filter and quantitative quality assessment unit, segmentation evaluation unit, feature evaluation unit, and score fusion unit. The experimental results show that the combination score is highly correlated with the sclera recognition accuracy and can be used to improve and predict the performance of sclera recognition systems.

2.2.4. Available Datasets and Overall Performance

One of the main problems that can be found in the development, testing and performance evaluation of biometric recognition systems is the lack of publicly available large databases acquired under real life conditions. The availability of biometric features corresponding to a large population of individuals, together with the desirable presence of biometric intra-class variability, Scenarios like acquiring artefacts, cross-sensor, quality, etc. can introduce intra-class variability. There are various datasets proposed in the literature of sclera biometric. Some of them are available publicly and some are in-house datasets. These datasets and performance of the proposed systems employing them are summarised in the Tables 2.7 and 2.8. It is quite clear from the Table 2.7 that several works have been carried out in the literature on sclera biometric. Many of the identified challenges discussed in section 2.2.3 are address and best efforts were made to solve these challenges. Although it should be mentioned that all these works were performed on independent datasets, which defers in acquiring artefacts. Moreover, the methods used in the segmentation, enhancement, featuring and classification of sclera are discreet. Therefore, regardless of satisfactory performances, these works are not comparable in an unbiased way. Hence, it is clear that the literature should be more enriched with publicly available datasets. Public datasets are an important component of active research. They provide strong advantages in algorithmic development, provide a platform for performance evaluation of the trait, and also introduce new challenges to the research community. The availability of datasets associated with competitions is also required to

Table 2.7. Various in-house datasets proposed in the sclera biometric literature and their performance achieved

Data Set in Reference	Number of subjects and gaze	No. of images /subjects	Segment-ation technique	Enhancement technique	Feature	Classifier	Accuracy in %
Derakhshani et al. [1]	6 (Both left and right eye)+	6	Manual	CLAHE and region growing	Hu moment and minutia	Multi-level classification	100
Derakhshani and Ross. [2]	50 (Session 1) and 17 (Session 2 taken after 4 months)+	2 per gaze		CLAHE	CDF	ANN	4.3 (1 ft), 8.8 (5ft),9.2 (9 ft) 1 training (6.5%,7.4%, 11%)
Crihalmeanu et al. [14]	50 (Session 1); 17(Session 2) + (left looking left were only)	2 image per angle at distance of 1, 9 and 12 ft	K-means (Semi-automated)	CLAHE, selective enchantment filter	Key point-descriptor, affine transform.	Score matching	25
Tankasala [9]	50 (Session 1 and 47 (Session 2) #	Distance 254; 152 & 30cm.	K-means	CLAHE	GLCM	ANN	13.82
Gottemukkul-a et al. [12] *	50 (Session 1) and 47 (Session 2) 4-30 days apart	2 Varying gender and age	Tiled based	CLAHE	Tile-based feature	Correlation coefficient	4.29
Crihalmeanu and Ross [8]	103 #	3280 (8 per angle)	Contour:	CLAHE	Key point, affine transform.	Score matching	0.37
Crihalmeanu & Ross [22]					Hessian matrix	Cross correlation	0.6 average
Zhou et al. [4]	88, 44 subjects 4 different eye, 2	1 1ft distance	Otsu & HSV	Gabor & thinning	Score	TM (Template Matching)	11.89 8.49(manu-al segmentati-on)

* Multimodal sclera fusion with iris

+ looking left, right, straight and up

looking left and right

Table 2.8. UBIRIS version 1 publicly available datasets proposed in the sclera biometric literature and performance on them by various proposed work in the literature.

No. of subjects	No. of images per subjects	Work	Segme-Ntation	Enhan-cement	Feature	Classifier	Accuracy in %/EER S1/S2/S12/S21
241 in 2 discreet sessions	5 per session 1877 RGB images taken in two distinct sessions (1205 images in session 1 and 672 images in session 2) from 241 identities. Both high resolution images (800 x 600) and low resolution images (200 x 150)	Zhou et [3]*	Otsu and HSV	Gabor & thinning	Score	TM (Template Matching)	2.73/-/-/-
		Zhou et al. [6]					1.34/-/-/-
		Zhou et al. [6] *					96.42FAR(0.1)/94.92(0.01)/-/-/-
		Oh and Toh [10]	HSV,	CLAHE,	LBP		0.47/-/-/-

* Multimodal sclera fusion with iris

+Multimodal sclera fusion with peri-ocular

S1= UBIRIS version 1 session 1 images as training and testing

S2= UBIRIS version 1 session 2 images as training and testing

S12= UBIRIS version 1 session 1 images as training and session 2 images as testing

S12= UBIRIS version 1 session 2 images as training and session 1 images as testing

motivate researchers and benchmark dataset with the common experimental protocol. Moreover, the common framework also helps in gauging the performance of a new algorithm and can be compared with prior state-of-the-art approaches in an unbiased way.

As a reason in the second half of sclera literature, many researchers have started working on the publicly available dataset. They are summarised in the next Tables 2.8. It quite clear from Table 2.8 that several independent works were performed on UBIRIS version 1 dataset and appreciable results were achieved in most of the work. Although all these works have used a discrete technique in different stages and therefore it will be unfair to make a comparison in between them.

Moreover, the dataset partition i.e. the testing and the training sequence used, the performance measure used in these works were also different. Therefore only an overall conclusion can be drawn as a whole. From the critical analysis, it can conclude that performance of these systems on the single session experiment (employing images from the same session for testing and training) seems to be impressive. Furthermore, in all these work the result of the session 1 is of UBIRIS version 1 is found to better that session 2. Whereas, in multisession experiments (employing images from one session for testing and with images from the other session for training) the results falls quite a lot. The poor performance of inter-session can be assumed to be the change in the acquiring artefact. It is also notable that the difference is higher for iris trait, it illustrates the importance of illumination for capturing good quality eye images in the visible spectrum and as well as the effect of the illumination on iris pigment. Dark irises require NIR illumination or more intense diffused illumination in the visible spectrum with minimal specular reflection. The performances on few other publicly available datasets are summarised in the next Table 2.8.

In addition, from the Tables 2.7 and 2.8 it can also note that different segmentation, enhancement, featuring and classification present in the literature are explored in the sclera biometrics till date. As mention previously that many pieces of work are performed on independent datasets, therefore a fair comparison between them is not possible. Furthermore, the work proposed on the publicly available datasets have used discrete segmentation, enhancement, featuring and classification techniques, and experimental protocol which makes it hard to make an unbiased comparison between them. Therefore, it flags an alert to the scientific community to make a structured research on this subject of research. So, that it can prove the potentiality of sclera as a trait and future researchers can easily identify the state-of-the-art, and from where they should start.

In biometric data labels associated with individual samples, subject identity and possibly some demographic attributes e.g. gender, age, and race are necessary for inclusion. Most of the available datasets are lacking in these details. New datasets need to incorporate these details.

It can be inferred after reviewing the sclera literature that several works which have been carried out by different research groups to establish sclera biometrics for personal identification. Many of the identified challenges are also explored and addressed. Therefore, proposed works and the studied anatomy of the sclera establishes the preliminary viability of the trait. Although the initial viability of the trait is experimented in a laboratory environment, there are several issues remain unsolved and unaddressed. Especially, the main concern that should be undertaken is to push its boundary of applicability in real life scenario and to move out from its infant stage. To best of author's knowledge applicability of the sclera biometrics in a real life, the scenario is not explored at all. Moreover, as address previously the highest concern that this field of research should receive is systematic and structure research.

2.3. Liveness Detection Literature

Traditional biometric authentication systems are not equipped to discriminate impostors those who can illegally duplicate genuine traits and use the privileges to access a system as a genuine user. Therefore, in order to increase the security and reliability of the biometric system, anti-spoofing/ liveness detection is a necessary step to prevent threats from intruders.

Liveness detection refers to the different techniques employed as a countermeasure to overcome the threat of physical spoofing of biometric samples. The liveness detection methods may examine physical properties of a living body in terms of density, elasticity, electrical capacitance, etc. or spectral reflection and absorbance, visual (colour, etc.) or may analyse body fluids (DNA, etc.), involuntary signals of a living body such as the pulse, blood pressure, etc. Also bodily responses to external stimuli, for instance, smiling or the blinking of an eye can also employed to establish liveness.

In this context it worth of mentioning that, most of the eye liveness detection work and the associated databases that were developed in the literature were aimed at incorporating iris liveness. In those datasets, iris images in the infra-red spectrum were captured. Although, for multimodal eye biometrics, the acquisition of iris and sclera traits is required in the visible spectrum (as mentioned previously the sclera vessel patterns are not prominent in Infra-red images). Furthermore, in the well-known existing databases like, Biosec (Fierrez et al, [118]), Clarkson (Schuckers et al., [119]), NotreDame (Doyle, and Bowyer, [120]), Warsaw (Czajka, [121]) and MobBIO (Sequeira et al., [122]), the sclera vessel patterns are not visible due to the image acquisition approach adopted. Moreover, the fake images developed in these databases were produced from printed eye images and artificial lens patterns. Whereas, nowadays several other sophisticated techniques such as portable screens and mobiles can be used by intruders to forge the highlighted multimodal ocular system in the visible spectrum. These highlights for development of a new dataset for liveness detection.

Many approaches for identifying forgeries and establishing liveness have been investigated in the biometrics literature. In Ratha et al., [100], the authors identified two types of attacks that can be adopted by intruders while attacking a biometric system: Direct and Indirect.

a. Direct attack: Direct attacks are performed at the sensor level. It relates to the generation of synthetic biometric traits (for instance, iris, face images or videos) in order to fraudulently access a system.

b. Indirect attacks: Indirect attacks are performed at the digital level forging the data flow as explained in Ratha et al., [100], these attacks targets the feature extractor, the matcher or the weak points in the communication channels.

The proposed solutions and specific anti-spoofing method proposed in the literature can be categorised into two groups of techniques as mentioned in Ratha et al., [100], they are as follows.

a. Software-based techniques: In these techniques, fake biometric traits are detected once the sample has been acquired with a standard sensor. Subsequently, image quality features, body movement features, motion features, and physical properties are employed to realise liveness.

b. Hardware-based techniques: In these techniques, specific devices are added to the sensor in order to detect particular properties. As an example, this may include the detection of live fingers in a fingerprint recognition system via blood pressure.

Furthermore, it can be noted in the literature that the methods of liveness detection can be classified into four groups. This categorization is based on the approach adapted for featuring the biometric trait and liveness as well as the timing of measurement as mentioned in Une and Tamura [116].

As mentioned previously, among the ocular biometrics, the iris is the most promising trait. So, various examples of research for liveness detection of iris biometrics can be found in the literature. The potential approaches for forging iris-based systems that are highlighted in the literature are as followings:

 Eye image/video: Scanning an image/video from a probable screen.

Printed images: Scanning a high resolution printed image of an artificial eye.

Lens: Glass/plastic artificial lenses etc.

The feasibility of these attacks has been investigated and reported that it is actually possible to spoof iris recognition systems with printed iris images and well-made colour iris lenses as mentioned in Daugman, [28], Lee et al., [117], Daugman, [29].

In the literature of iris liveness detection, the potential of quality assessment to identify genuine and fake iris samples acquired from a high quality printed images has been explored as a way to detect spoofing attacks in Galbally et al., [101]. In this work, a strategy based on the combination of several quality-related features has also been used for anti-spoofing measure. This work also proposed a framework of image quality based feature selection. Another approach for quality-based features assessment has been used for liveness detection in Kanematsu et al., [125]. One more example for assessing the iris image quality for liveness measures, such as occlusion, contrast, focus and angular deformation can be found in Abhyankar and Schuckers, [126].

The use of texture analysis of the iris liveness can be found in He et al., [127]. The analysis of frequency distribution rates of some specific regions of the iris can be found in Ma et al., [128] used as an measure of liveness detection. Some significant developments in iris liveness detection can be found in the competition series of iris Livedet, organised to record the recent developments. Some well-established texture assessment-based measures were used by the participants to establish liveness detection.

In the context of previous research of liveness, manual segmentation was adopted to find the region of interest, which is quite unrealistic. A very recent work of Sequeira et al., [129] investigated and concluded that automatic segmentation does not affect the liveness detection measure. In the literature, most of the seminal and recent works concerning liveness detection Alonso-Fernandez et al., [123] in fingerprint-based recognition systems and Galbally et al., [101] in iris have employed image quality features for liveness detection.

Another approach for software-based liveness detection of direct attacks, by challenge-response framework embedded into the visual or audio-visual signal, is reported in Kollreider et al., [124]. Several properties of a living body such as bodily responses to external stimuli are reported in Kollreider et al., [124] for real-time face detection and motion analysis.

It can be evident for the above review of the literature that liveness detection for ocular biometrics can be more resilient to spoof attack and it is an open research area. Different image quality based feature, response to stimuli like asking blinking left eye, opening mouth, rotating head, etc. in an unknown sequence can be used to establish liveness.

Therefore, this thesis will concentrate to propose a framework for liveness detection of ocular biometric in the visible spectrum.

2.4. Adaptive Biometrics Literature

Adaptiveness of the biometric system with change or variation in the trait that may happen due to ageing, acquiring conditions or variation in the position of the trait while acquiring. Identifying correctly while handling these changes is a significant challenge and which gives growth to the new field of research i.e. Adaptive Biometrics (AB).

In the last decade, adaptive biometric systems have been a subject of great interested to the researchers from the biometric community. Various research techniques have been proposed by different researchers. Best of author's knowledge, the first adaptive biometric approach was introduced in Rattani et al. [103]. Literature of AB systems can be grouped by the key attributes of machine intelligence methods proposed. Supervised training used in Rattani et al. [105-107], Poh et al, [108], and Uludag et al, [109] against semi-supervised training in Rattani et al. [106], Poh et al, [108], and [113], Self-train Jiang and Ser [110], Rye et al. [111], Liu. et al, [112] or co-train Rattani et al. [106], Roli et al, [113], and Online Jiang and Ser [110], Rye et al. [111] and offline Rattani et al. [107], Roli et al, [114], Rattani et al. [115]. In the recent past, a general study has been done in regard to AB in Poh et al, [104] to address some general questions like:

• Whether supervised adaptation better than semi-supervised?

• Whether co-training can outperform self-training?

• Whether offline adaptation is better than online?

Further, an analysis was conducted to validate the hypothesis in Rattani et al, [103]. In work of Rattani et al, [105] the author proposes a two-stage classifier technique for automatically updating the biometric templates. In the work, a labelling scheme based on probabilistic semi-supervised learning was employed. Soft probabilistic labels were marked to each batch of input samples by calculating the minimum energy function on a graphical representation. A harmonic function was used for uniqueness representation of the samples. Also to ensure that labels assigned to input sample employing are performed both the enrolled and closely related input data. Further, the genuinely classified samples undergo a selection process designed on risk minimization. The experiment was perform to validate on DIEE fingerprint dataset, an appreciable result was achieved.

In research of Rattani et al, [106], the effect of different threshold settings was used to template update.

A novel method was proposed by passing the threshold selection step. This work also analysed that template update method could be better for group specific updating. This is due to the presence of different type of population. Attempts have been also made to give a preliminary guideline on the type of update procedures. That could be undertaken for a specific group of the population. Further, set of rules for simulating real world situation has been proposed for the unbiased validation of update methods. However, liveness and adaptiveness of biometric traits have been found to be a trade-off in the literature.

2.5. Summary

For the literature survey documented in this chapter, it is evident from the iris literature surveys that present works focus the non-ideal iris recognition and it can also be concluded that more research work on this topic is required to make it more accurate as much as possible.

The chapter further discusses the viability of the sclera biometric, list and, identify challenges that exist in the different stages of its processing and propose a whole set of future research line. The viability of the sclera biometrics is reviewed analysing its anatomy and existing work. Furthermore, a variety of databases proposed and their performances reported in the literature are also highlighted.

Very surprisingly the main gap that was found in this subject of research is that many discrete works have been proposed in the literature, perhaps which leads to haphazard research. Consequently, in thesis research will be performed using this particular trait to pursue systematic research.

It is also evident from the survey to date, the sclera biometrics both independently and as well in multi-modal has not been extensively studied and little is known regarding its usefulness. So, the state-of-art related to it is not mature enough and still in its infancy. Therefore more research should be performed for evaluating the potential of the sclera biometric in regards to accuracy and adaptability with changes in condition and also evaluation should be carried out for its combination with iris pattern to increase the biometric applicability of iris biometrics. Even the liveliness of the data for eye biometrics is not enlightened in the literature. Therefore the proposed research is conceived to solve the above-identified gaps identified in the literature.

In the next half of the chapter, the literature of liveness detection and adaptive biometric is surveyed. It can be concluded for the survey that liveness and adaptiveness of biometric traits have been found to be a trade-off in the literature.

Therefore, the second half of the thesis will concentrate on bridging the gap of liveness and adaptability in multimodal ocular biometric using iris and sclera.

3

Advancement in Multimodal Iris and Sclera Biometrics

In this chapter, the proposed advancement on sclera and iris segmentation process, pattern enhancement techniques, and feature extraction techniques are explained. Next, the classification techniques are discussed in detail. A block diagram of the proposed system is given in Figure 3.1.

The rest of this chapter is organised into the following Sections: 3.1 explain the proposed sclera segmentation processes; 3.2 explain the proposed iris segmentation process: section 3.3 and 3.4 sclera and iris image enhancement techniques are explained. In Section 3.5 the various proposed feature extraction processes are highlighted, while in Section 3.6 the various classification techniques are also explained. The experimental setup and the results of the proposed work are explained in rest of the chapter. Section 3.7 illustrates the different datasets used, followed by results, discussion and state-of-the-art comparison with the proposed works are described in Section 3.8

Major parts of the chapter have been published in the articles Das et al. [263-265, 267, 273].

3.1. Sclera Segmentation

Segmentation is the first step for most biometric systems. The aim of segmentation is to determine the appropriate region of interest or the region which has the information for biometric authentication. As sclera literature is very new, several segmentation techniques

have been employed to analyse the most stable and efficient segmentation technique, which are described in the sub-sections below.

3.1.1. Active Contour-based Region Growing Segmentation

The sclera is a white region of connective tissue and blood vessels surrounding the iris. This portion of blood vessels inside the sclera region is randomly-oriented which creates a pattern, that can be utilised for biometric identification. Segmentation is the first step for most biometric-related research. Similarly, in sclera biometrics a perfect segmentation is
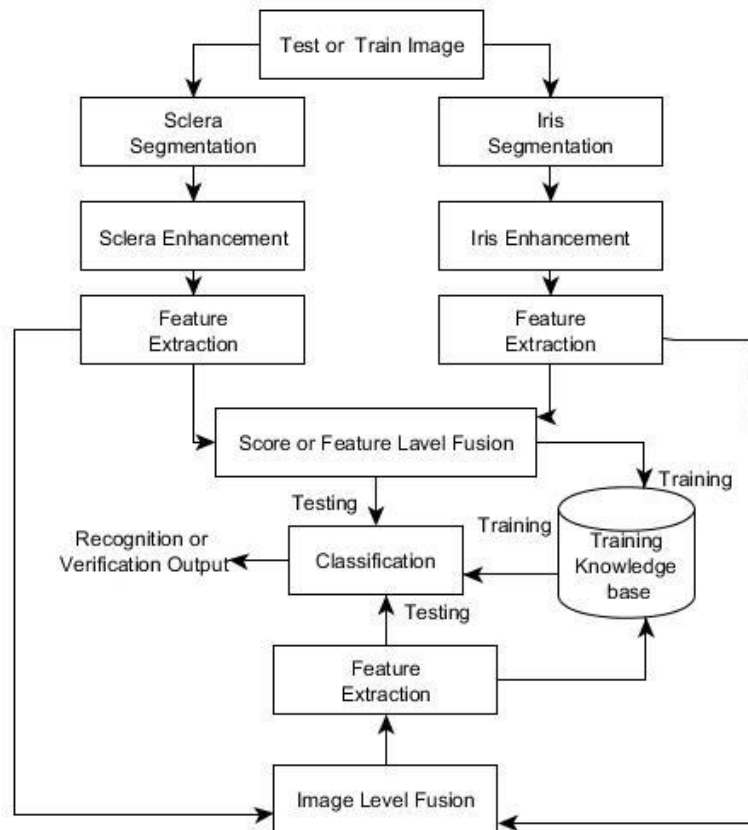
Figure 3.1. A block diagram of the proposed system.

important, otherwise an incorrect segmentation can reduce the scope of the pattern available and it can also introduce other patterns such as eyelashes and eyelids, which will bias the recognition result. As the blood vessels inside the sclera region are oriented in different layers, the intensity of the vessels varies highly. Some of them are quite bright and bundled, creating a hindrance to standard region growing. In order to minimise this hindrance, the red channel of the image has been selected for segmentation, as the blood vessels are less prominent in the red channel, as shown in Figure (b). A representation for each colour channel is indicated in Figure 3.2.

(a)   (b)

(c)   (d)
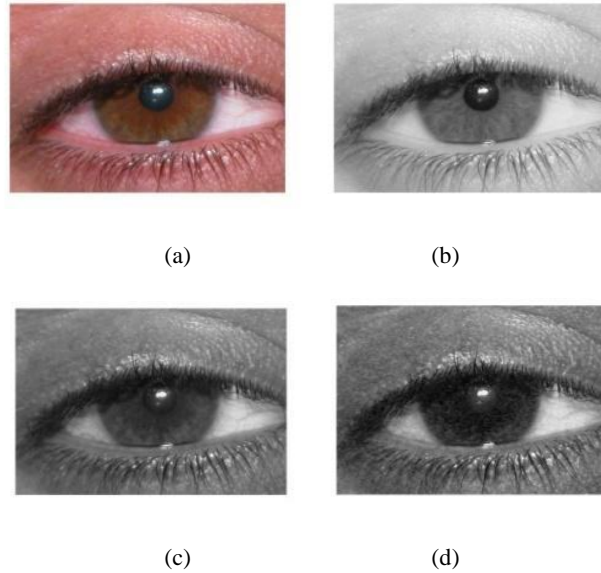
Figure.3.2. (a) The image of the original RGB image, (b) The red channel component of (a), (c) The Green channel component of 1(a), and (d) blue channel component of (a) [263].

Adaptive histogram equalisation was performed with a small window of 2x2 to reduce the vessel content. Next, a bank of low pass Haar reconstruction filters as described in Mallat [31] with a high cut-off was used to achieve a clear white sclera without the patterns of the blood vessel. Analysing different results the cutoff value was selected and the value that produces the best result was used for experimentation. Figure 3.3 (a) shows the histogram-equalized image and 3.3 (b) is the Haar filtered image of 3.3 (a).

(a)   (b)
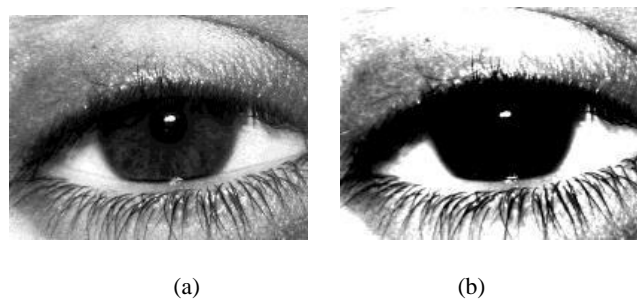
Figure. 3.3. (a) Is the histogram equalized image and (b) the Haar filtered image of 3.2(b) [263].

This pre-processed image can be used for segmentation by a time-adaptive active contour-based region growing segmentation method discussed in Chan and Vese [15]. The right and the left sclera are segmented separately. For region growing-based segmentation, a seed point was required. In order to get the seed point Daugmans integrodifferential operator in Daugman [16, 27] was used, to calculate the centre and radius of the iris. From the centre of the iris at a distance of 1.1 of the radius length of the iris and a deviation of 45 degrees with the horizontal, the seed point for region growing is set on both sides of the sclera as explained in Figure 3.4.
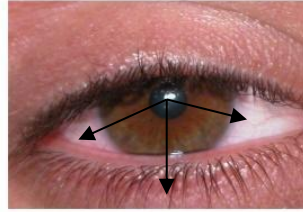
Figure.3.4. Seed point for sclera segmentation [263].

Now the seed point as shown in below Figure 3.5 (b and f), grows to provide the total sclera region as explained in Figure 3.5.
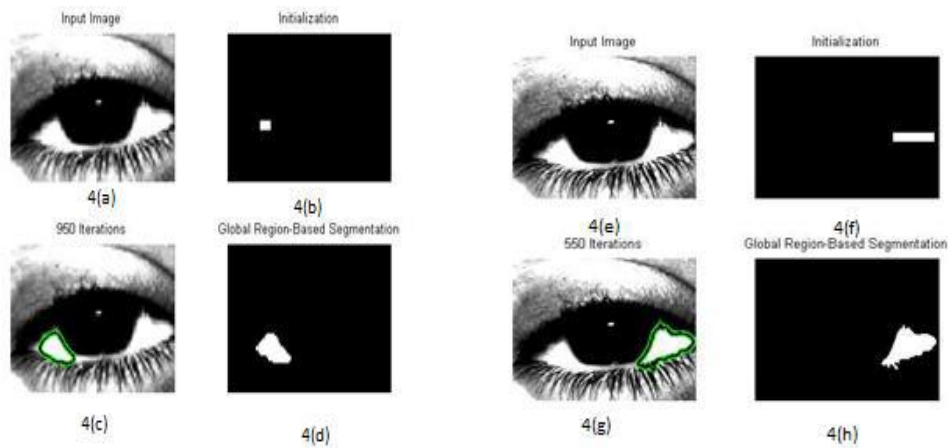
Figure. 3.5. Region growing segmentation method of left and right sclera. (a) The Histogram equalized and filtered image of red component of (a),,,(b) Initial size of the seed for right sclera,(c) Segmented image of (a),(d) Segmented mask developed for right sclera, (e)The Histogram equalized and filtered image of red component of (a),(f) Initial size of the seed for left sclera,(g) Segmented image of (e), (h) Segmented mask developed for left sclera [263].

3.1.2. K-means Based Segmentation

Among the different segmentation methods available in the computer vision area, a model -based segmentation algorithm based on k-means [32] has been chosen. The eye image was segmented into three clusters using a k-means algorithm, as shown in the Figure. 3.6.

(a)   (b)
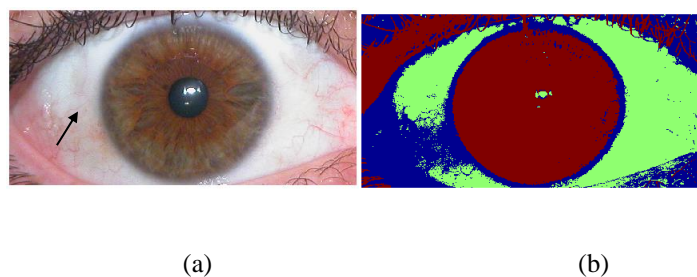
Figure. 3.6. (a) Iris image; (b) k-means clusters.

3.1.3. C-means based segmentation

In this scenario, sclera segmentation was performed by a Fuzzy C-means clustering-based segmentation proposed in Li et al. [35]. Fuzzy C-means is a method of clustering which allows one piece of data to belong to two or more clusters [33-34]. It is based on the minimization of the following objective function which appears in the equation below 3.1.

$$J_m = \sum_{i=1}^{N} \sum_{j=1}^{C} u_{ij}^m \left\| x_i - c_j \right\|^2 \quad \text{where } 1 \leq m < \infty \tag{3.1}$$

where m is any real number greater than 1, u_{ij} is the degree of membership of x_i in the cluster j, x_i is the ith of d-dimensional measured data, c_j is the d-dimension centre of the cluster, and $\|*\|$ is any norm expressing the similarity between any measured data and the centre. Fuzzy partitioning is carried out through an iterative optimisation of the objective function shown above, with the update of membership u_{ij} and the cluster centres c_j.

$$u_{ij} = \frac{1}{\sum_{k=1}^{C} \left(\dfrac{\left\| x_i - c_j \right\|}{\left\| x_i - c_k \right\|} \right)^{\frac{2}{m-1}}} \tag{3.2}$$

$$c_j = \frac{\sum_{i=1}^{N} u_{ij}^m \cdot x_i}{\sum_{i=1}^{N} u_{ij}^m} \tag{3.3}$$

This iteration will stop when $\max_{ij}\left\{ \left| u_{ij}^{(k+1)} - u_{ij}^{(k)} \right| \right\} < \varepsilon$, where s is a termination criterion between 0 and 1, and k are the iteration steps. This procedure converges to a local minimum or a saddle point of J_m. The performance of the level set segmentation is subject to appropriate initialization and optimal configuration of controlling parameters, which require substantial manual intervention. A new fuzzy level set algorithm was used to facilitate sclera segmentation. It is able to directly evolve from the initial segmentation by spatial fuzzy clustering. The controlling parameters of the level set evolution are also estimated from the results of the fuzzy clustering. Moreover, the fuzzy level set algorithm was enhanced with locally regularized evolution. Such improvements facilitate level set manipulation and lead to a more robust segmentation.

The parameters that are affecting the level set segmentation are:

    a.   Controlling the spread of the Gaussian smoothing function

b. Controlling the gradient strength of the initial level set function

c. Regulating or direct function

d. Weighted coefficient of penalty term

e. Coefficient of Counter length for smoothing

f. Artificial balloon force

g. Time set for level set initialization

h. Maximum iteration for level set evolution

A performance evaluation of the proposed algorithm was carried out on sclera images from the different index. The results confirm the effectiveness of the technique for sclera image segmentation. The number of clusters considered here was three and with index three. The segmentation was performed on grey image images Figure 3.7 (c) shows the Fuzzy C means-based sclera segmentation of (a) index 1. Figure 3.7 (d) shows the Fuzzy C means-based sclera segmentation of 3.7(a) index 2 and Figure 3.7(f) shows the Fuzzy C means-based sclera segmentation of 3.7(a) index 3 and 3.7(b) grey image of 3.7(a).

(a)   (b)   (c)

(d)   (e)
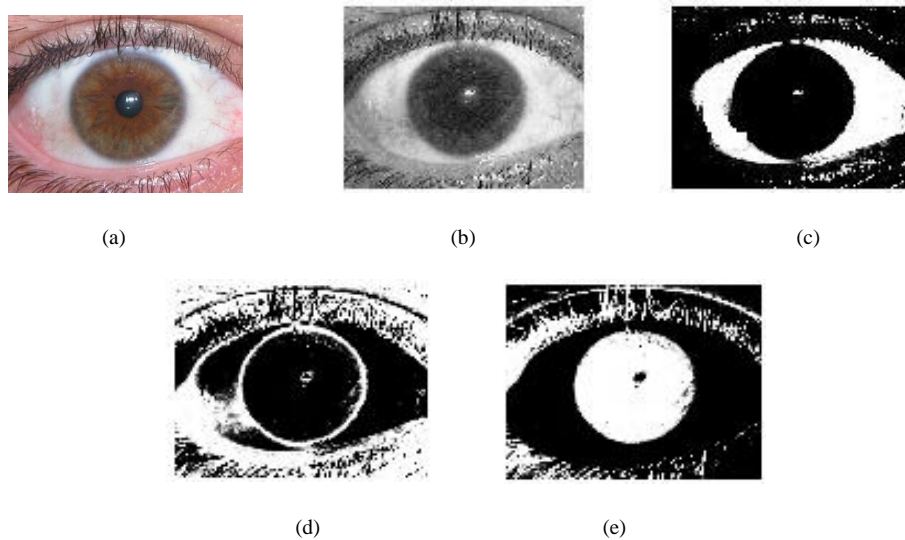
Figure 3.7: (a)original image, (b) grey image of (a).(c) shows the Fuzzy C means-based sclera segmentation of (a) index 1.Figure 1(d) shows the Fuzzy C means-based sclera segmentation of (a) index 2 and (e) shows the Fuzzy C means-based sclera segmentation of (a) index 3 [265].

Here the Fuzzy C means-based sclera segmentation of index 1 is used as the segmented mask for further experimentation.

3.2. Iris Segmentation

In order to get the segmented iris Daugman's integrodifferential operator proposed in [16] was used to calculate the centre of the iris. The iris image was cropped automatically along the iris centre as shown in Figure 3.8.

Figure 3.8: Segmented iris image

3.4. Sclera Vessel Structure Enhancement

The vessels in the sclera are not prominent, so in order to make them clearly visible, image enhancement was required. The various enhancement techniques employed are in the next sub-sections.

3.3.1. Adaptive Histogram Equalisation and Haar Wavelet-based Enhancement

Adaptive histogram equalisation was performed with a window size of 42x42 on the green channel of the sclera image (as the sclera vessel patterns are most prominent in the green channel), to make the vessel structure more prominent as shown in Figure 3.9.
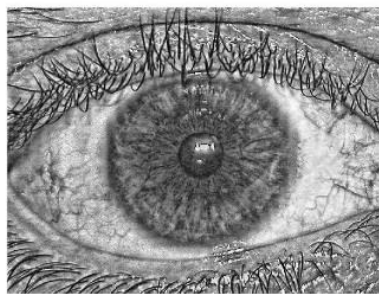
Figure 3.9: Adaptive histogram equalisation of sclera image [263].

A bank of 2D decomposition Haar wavelet multi-resolution filters was used to enhance the vessel patterns. Figure 3.10 shows the vessel enhanced image.
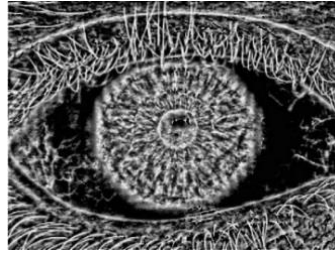
Figure 3.10: The vessel enhanced image [264].

3.3.2. Fuzzy logic-based Brightness Preserving Dynamic Fuzzy Histogram Equalisation and Discrete Meyer wavelet Based Enhancement

Adaptive histogram equalization [36] was performed with a window size of 42x42 on the green channel of the sclera image (as the sclera vessel patterns are most prominent in the green channel as shown in Figure 3.11(c)) to make the vessel structure more prominent as shown in Figure (a). Next Fuzzy logic-based Brightness Preserving Dynamic Fuzzy Histogram Equalisation proposed in Sheet et al.[43] was used to make the pattern clearer using Gaussian-based Fuzzy Membership function and a window size of 42 x 42 as shown in Figure 3.12(c).

(a)   (b)   (c)   (d)
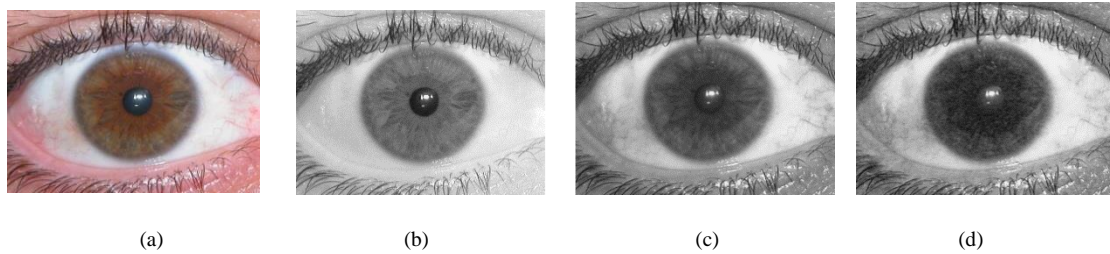
Figure 3.11 (a) The original RGB image, (b) The red channel component of (a), (c) The green channel component of (a), and (d) blue channel component of (a) [263],

Furthermore, the Discrete Meyer wavelet [37] was used to enhance the vessel patterns. A low pass reconstruction of the above-mentioned filter was used to enhance the Figure 3,12 (b) shows the vessel enhanced image after applying the filter.

(a)   (b)   (c)
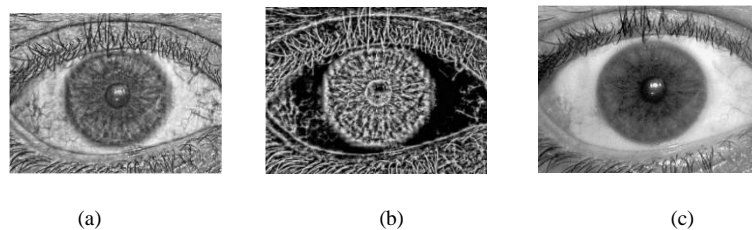
Figure 3.12: (a) Adaptive histogram equalisation of the sclera image. (b) the vessel enhanced image.(c) fuzzy logic based Brightness Preserving Dynamic Fuzzy Histogram Equalization on the green channel of the sclera image [265].

3.4. Iris Pattern Enhancement

The pattern in the iris is not prominent, so in order to make the pattern clearly visible, image enhancement was required. Adaptive histogram equalisation was performed with a window size of 2 x 2 on the red channel of the iris image (as the iris patterns are most prominent in the red channel as shown in Figure 3.13), to make the vessel structure more prominent as shown in Figure 3.14.
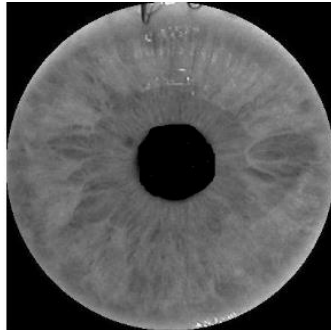
Figure 3.13: Red channel of the iris image
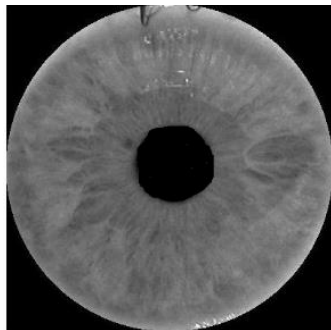
Figure 3.14: Adaptive histogram equalisation iris image.

3.5. Feature Extraction Method

The feature extraction of a biometric recognition system involves building a reliable mathematical model of the abstract sclera pattern to reliably identify persons for authentication and identification purposes. Only a few works related to sclera biometric were found in the literature, so analysing the performance of different features extraction technique is very important. The following sub-section the various features that were used for feature extraction are discussed.

3.5.1. Orientated Local Binary Pattern-based Feature Extraction

The local feature, such as LBP (Local Binary Patterns) proposed in Maenpaa and Pietikainen [44], can be seen as a unifying approach to the traditionally statistical and structural approaches to texture analysis. Applied to black and white images, an LBP can be considered as the concatenation of the binary gradient directions. This contains micro-

pattern information about the distribution of the edges, spots, and other local Figures in an image which can be used as features for sclera recognition. The original LBP operator labels the pixel of an image by thresholding the 3×3 neighbourhood of each pixel and concatenating the results binomially to form a number. Assume that a given image is defined as $I(Z) = I(x, y)$. The LBP operator transforms the input image to (Z) as follows:

$$LBP(Z_c) = \sum_{p=0}^{7} s\left(I(Z_p) - I(Z_c)\right) \cdot 2^p, \qquad (3.4)$$

Where $s(l) = \begin{cases} 1 & l \geq 0 \\ 0 & l < 0 \end{cases}$ is the unit step function and $I(Z_p)$ is the 8-neighborhood around $I(Z_c)$. The feature representation method called Orientated Local Binary Pattern (OLBP) proposed in Bu et al.[45] is an extension of the local binary pattern (LBP). OLBP can represent more explicitly the orientation information of the contours which is an important characteristic of the sclera. The $OLBP$ of a given pixel Z_c is computed as follows:

1.   Compute the sequence $s\left(I(Z_p) - I(Z_c)\right), p = 0, \dots, 7$.

2.   Find the starting index $(Start)$ and ending index (End) of the longest continuous 0 substring looking cyclically in the sequence of the previous step. $Start = $argmax($(StringLength))$, $End = Start + StringLength(StartOri)-1$,

3. The index of the zeros substring centre is the $OLBP$, i.e.

$$OLBP(Z_c) = round((Start + End)/2)mod8, \qquad (3.5)$$

Where *round*() rounds a number to the nearest integer, and the *mod* is the arithmetic complement operation. An example of OLBP images of the vessel structure is presented in Figure 3.15.
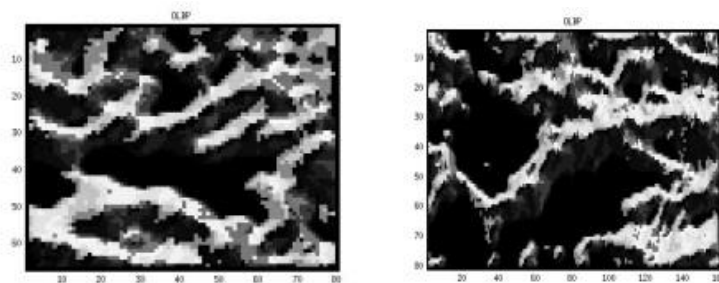
Figure. 3.15. OLBP of the vein images [263].

In order to make image translation independent, have registered the iris centre to the centre of the image for each of the OLBP images produced in the earlier section. Registration is performed by using the following equations.

$$\text{rowdiff} = \text{Imgx} - \text{Ix} \qquad (3.6)$$
$$\text{columndiff} = \text{Imgy} - \text{Iy} \qquad (3.7)$$

where (*Ix, Iy*) represents the iris centre location, (*Imgx, Imgy)* is the image centre, and (*rowdiff, columndiff*)denotes the relative distance of the iris centre from the image centre. Next, the relative amount of shift in the row direction and column direction was applied to the OLBP image to register it against the image centre.

3.5.2. SIFT-Based Feature Extraction

The SIFT was originally proposed in Lowe [46] and was used for biometrics such as palm print [47] and iris [48], among others. The method is divided into three main steps:

- **Key point location:** A detailed model is fitted to determine the location and scale of each candidate location at different scales. The candidate locations are potential interest points that are invariant to scale and orientation.

- **Descriptors generation:** Around each key-point, the local gradients are measured at the selected scale. The orientation of the region around the key point was introduced to increase the rotation invariance.

- **Matching:** The descriptors of the query pattern are compared with each of the descriptors extracted from the corresponding pattern in the gallery set. The score generation from the candidate matches was based on the Euclidean distance between the descriptor vectors. The final similarity score was the number of matches between query and gallery samples.

One of the advantages of this method is that it can be applied to both sclera and iris patterns and therefore, their combination is simple and efficient.

3.5.3. Patch-Based Descriptor for Feature Extraction

In recent years, the local patch-based descriptors have emerged as a way to improve feature extraction methods. It also worked efficiently in the presence of distortions such as of scale, rotation, translation and occlusion. It's high discriminative capability and robustness attracted researchers in the area of biometrics.

The variance of the position of eyelids produces occlusions which are difficult to manage with traditional texture feature methods. The robustness against occlusion is one of the most interesting factors in the application of sclera and iris recognition. The sclera and iris feature extraction based on Dense Scale Invariant Feature Transform (D-SIFT), Dense Local Binary Pattern (D-LBP) and Dense Local Directional Pattern (D-LDP) were performed here. The various patch based descriptors are described below.

3.5.3.1. Dense-SIFT

D-SIFT patches based descriptors for each training images are used to form a bag of the feature. Here, a 128-dimensional based SIFT keypoint was extracted which stores the gradients of 4×4 locations around a pixel in a histogram bin of 8 directions. The gradients of each key point were aligned to the main direction, which makes D-SIFT a rotation invariant descriptor. Different Gaussian scale spaces were considered for the computation of vector which makes it scale invariant.

(a)

(b)

(c)

(d)
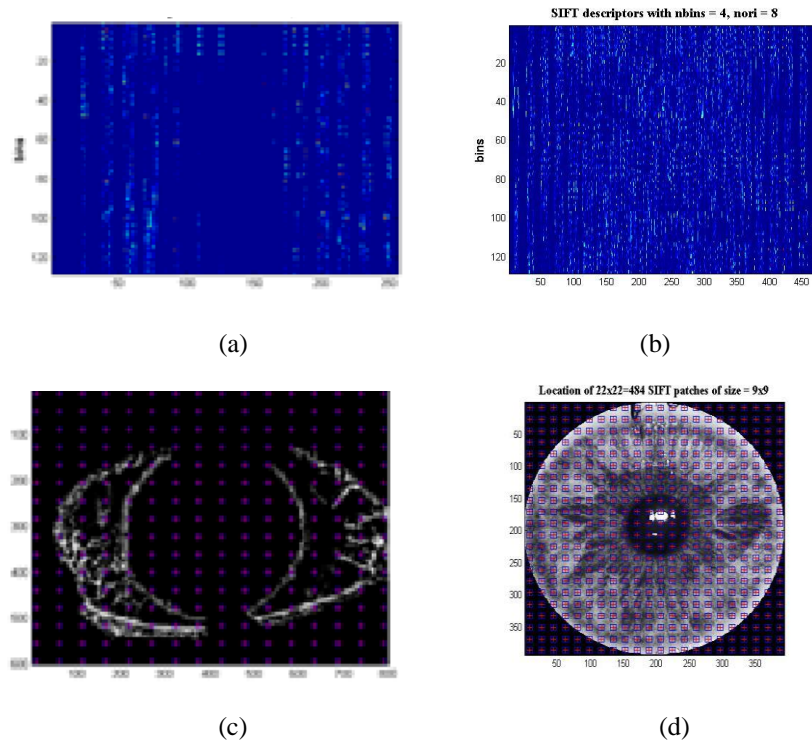
Figure 3.16: (a & b) The image is divided into a 22x22 location of a 9x9 patch size for the dense SIFT descriptor. (c and d) SIFT descriptor with a number of 4 bins and 8 orientations [264].

The blue cross in the Figure.3.16 (c and d) represent the 16×16 SIFT patches and Figure. 3.16 shows a graphical representation of SIFT descriptors of 4 bins and 8 orientations.

Next, all these patch based descriptors were processed through a feature extraction chain by K-means and Spatial Pyramid matching (SPM) [20]. In order to do so, the Bag-of-Features (BoF) histograms are computed within each of the 2^i segments of each of the patches to develop a k-means cluster, and all the histograms are finally merged to form a vector representation of the image by using a spatial pyramid matching technique. The spatial pyramid matching (SPM) is an extended version of the BoF model and is simple and computationally efficient. In the BoF model, the spatial order of local descriptors is not considered, so it restricts the descriptive power of the image representation. The limitation

of the BoF is overridden in the SPM [20] approach, and is successfully applied on image recognition tasks. An image is partitioned into $2^i x 2^i$ segments where $i=$ 0; 1; 2, each represent the different resolutions.

SPM reduces to BoF when the value of the scale is $i=$ 0. Here, the pyramid matching is performed in a two-dimensional image space and uses a traditional clustering technique in the feature space. The number of matches at level i was given by the histogram intersection function:

$$I(gX; gY) = \sum_{k=i}^{n} min(gX(i); gY(i)) \qquad (3.9)$$

Finally, the representation of the image for classification is the total number of matches from all the histograms, which is given by the definition of a pyramid match kernel:

$$K(X; Y) = \sum_{i=1}^{l} 0.5^i (Ii - Ii\text{-}1) \qquad (3.10)$$

All total 21 (16+4+1) BoF histograms are computed from these three levels, and all the histograms are concatenated to get the final vector representation of an image. The equation below represents the pyramid match kernel for three scales:

$$K\Delta = I2 + 0.5(I1 - I2) + 0.25(I0 - I1) \qquad (3.11)$$

3.5.3.2. Dense-LBP

Dense Multi-Block LBP (Dense-LBP) was proposed for feature extraction. They are based on a spatial pyramidal architecture of multi-block LBP (MBLBP) histograms. More precisely, the image I to be features, of n_x rows and n_y columns is divided, at each level $l = 1,2, ... , L$ into N_l^x by N_l^y patches of size h_l by w_l uniformly distributed in the image. For each patch the histogram of MBLBP descriptors at s different scales are worked out.

The scale is applied to every 9 blocks their LBP is computed. The final feature is calculated by concatinating the histogram of all the blocks, so it will be $\sum_{l=1}^{L} 256 s N_l^x N_l^y$ dimensional. In this scenario as in Figure 3.17, it is defined heuristically $L = 2$ and $s = 4$. At first level, $N_1^x = 1, N_1^y = 1, h_1 = n_x$ and $w_1 = n_y$, at the second level $N_2^x = 3, N_2^y = 3, h_2 = n_x/2$ and $w_2 = n_x/2$, so the 9 patches are 25% overlapped. Then, the feature vector dimension is 10240.

(a)   (b)
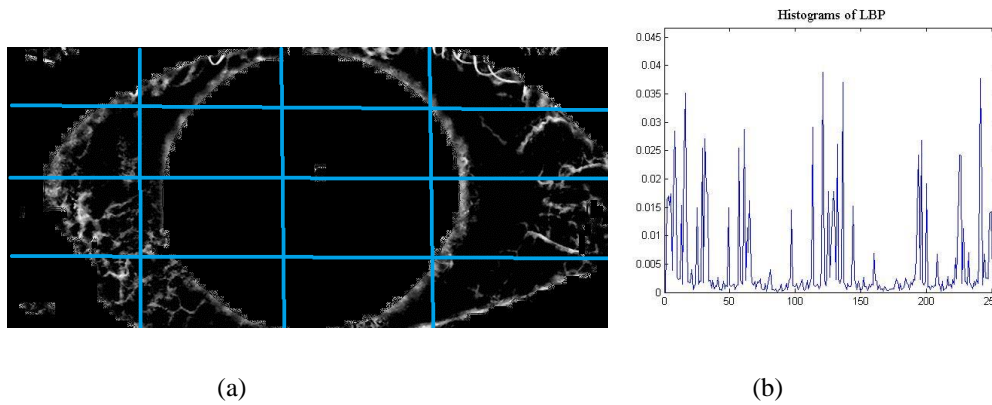
Figure 3.17: (a) Patch division of the image for D-LBP, (b) Histogram of LBP [265].

3.5.3.3. Dense LDP

The Local Directional Pattern (LDP) proposed in Kabir et al, [49], computes the edge response values in different directions and uses these to encode the image texture. Considering the relative edge response values in different directions by using eight filters (shown in Figure 3.18), the LDP feature encodes the local neighbourhood property of image pixels with a binary bit sequence. Feature extraction based on the Dense Local Directional Pattern (D-LDP) was performed by employing Multi-scale of a higher order of the LDP. Ten different spatial planes are considered for featuring. Each histogram distribution of bin size of 256 is calculated for each plane, order and spatial plane and concatenated to get the total feature of dimension 30720. This can be calculated as: FD= Ns * No* 256* Nsp Where, FD= feature dimension; Ns= number of scale, No= number of order, Nsp= number of spatial plane. The Spatial plane division of the image which divides the image into dense sampling plane is explained in the following Figure 7. The various level of the spatial division incorporates the local and the global feature of the traits.

$$\begin{bmatrix} -3 & -3 & 5 \\ -3 & 0 & 5 \\ -3 & -3 & 5 \end{bmatrix} \quad \begin{bmatrix} -3 & 5 & 5 \\ -3 & 0 & 5 \\ -3 & -3 & -3 \end{bmatrix} \quad \begin{bmatrix} 5 & 5 & 5 \\ -3 & 0 & -3 \\ -3 & -3 & -3 \end{bmatrix} \quad \begin{bmatrix} 5 & 5 & -3 \\ 5 & 0 & -3 \\ -3 & -3 & -3 \end{bmatrix}$$

East M_0 North East M_1 North M_2 North West M_3

$$\begin{bmatrix} 5 & -3 & -3 \\ 5 & 0 & -3 \\ 5 & -3 & -3 \end{bmatrix} \quad \begin{bmatrix} -3 & -3 & -3 \\ 5 & 0 & -3 \\ 5 & 5 & -3 \end{bmatrix} \quad \begin{bmatrix} -3 & -3 & -3 \\ -3 & 0 & -3 \\ 5 & 5 & 5 \end{bmatrix} \quad \begin{bmatrix} -3 & -3 & -3 \\ -3 & 0 & 5 \\ -3 & 5 & 5 \end{bmatrix}$$

West M_4 South West M_5 South M_6 South East M_7
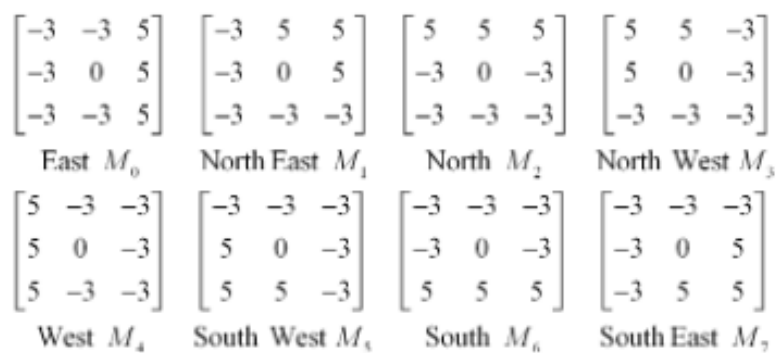
Figure 3.18: Filters used for LDP [49].

The blue cross in Figure 3.19 (a) represents the 22×22 D-LDP patches and Figure 3.19(b) shows a histogram representation of D-LDP descriptors of 3 different scales. Histogram of the 3 different histogram blocks is given below in Figure 3.19.
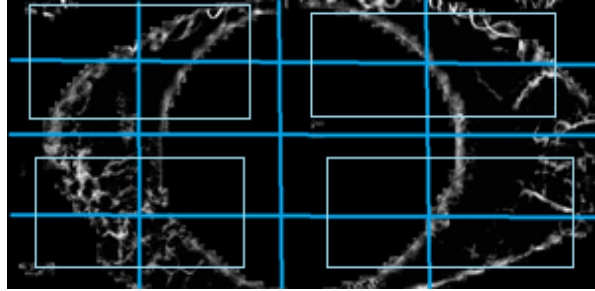
Figure 3.19: Patch division of the image to calculate D-LDP [267]

3.6. Classification

Biometric algorithms generally aim to provide a reasonable binary answer for all possible inputs and so classification plays an important role. Therefore the techniques used in the proposed method are highlighted here in the next sub-sections.

3.6.1. Template-based matching Based Classification

Template-based matching was used for classification. The gallery of query image was overlapped over the template of each class. The OLBP regions were binaries to get a binary template. Subsequently, identification was performed by template matching over the OLBP region by computing the Hamming Distance between the query image and templates, the matching which creates the minimum Hamming Distance is considered as the class of the query image. The Hamming Distance was calculated as below.

$$\text{HD} = \sum \frac{(\text{template} \oplus \text{query}) \cap (\text{mask} \cup \text{query mask})}{\text{template} - {\sim}(\text{mask} \cup \text{query mask})} \qquad (3.12)$$

Mask and query mask were the masks of the template and query image. The symbol $\oplus$ signifies the XOR operation, the symbol $\cap$ signifies the AND operation, the symbol $\cup$ signifies the OR operation, - signifies subtraction operator and the symbol $\sim$ signifies the NOT operation.

3.6.2. SVM-based Classification

The Support Vector Machines (SVMs) [38] are used for classification of the local descriptors. The SVMs are a popular supervised machine learning technique which performs implicit mapping into a higher dimensional feature space. This is also known as a kernel trick. After the mapping is completed it finds a linear separating hyperplane with a maximal margin to separate data from this higher dimensional space. The Library for Support Vector Machines (LIBSVM), was used for the SVM implementation.

Though new kernels are available, the most frequently used kernel functions are linear, polynomial, and Radial Basis Function (RBF). This study uses the RBF kernel. SVM or LIB-SVM makes binary decisions and multi-class classifications for personal identification which have been used in this study by adopting the one-against-all techniques.

3.6.3. Projective Pairwise Discriminative Dictionary

It is evident from the literature that most of the individual work on the sclera and multimodal eye recognition techniques using the sclera and iris employs a template matching-based technique for pattern classification, which is quite time-consuming. In subsequent work of this thesis sophisticated classifier techniques such as Support Vector Machines are employed, however, the time complexity of the feature extraction process is quite high.   To deal with the aforementioned problems of complexity and efficient pattern classification, namely Projective Pairwise Discriminative Dictionary learning (PPDD) is studied. The aims for most of the conventional DL methods are to learn a synthesis dictionary to represent the input signal while the representation coefficients, represent the residual to be discriminative. Adopting the "l0-norm" and "l1-norm" sparsity constraint on the representation coefficient, the time complexity for the training and testing phases places a major disadvantage on them. The discriminative DL framework, namely projective dictionary pair learning (DPL), has been used to deal with pattern classification problems with an optimised time complexity. The DPL learns a synthesis dictionary as well as an analysis dictionary together for signal representation and discrimination. DPL does not only reduce the time complexity in the training and testing phases but also leads a very effective and high accuracy in a variety of visual classification tasks. Inspired by the method proposed in [13], have hypothesised to explore DPL on multimodal eye recognition for better accuracy and reduced computational time complexity.

In the recent literature, Dictionary Learning (DL)-based feature extraction has evolved to be one of the most promising features extraction techniques. These techniques can also be explored for efficient biometric pattern recognition. Studies on sparse representation with a synthesis dictionary have had a significant impact in the recent years of study in Wright et al, [131], Mairal et al, [132] and Jiang et al. [133]. The "*lp-norm*" (*p<=1*) sparse coding which is computationally more expensive than analytical dictionary-based representation is used to obtain the representation coefficients of a pattern for the synthesis dictionary. Complex local image structures are modelled better by synthesis-based representation. This representation has led to many state-of-the-art results for image recognition. Allowing us to easily learn a desired dictionary from the training data is another important advantage of the synthesis-based sparse representation.

The seminal work of KSVD Aharon et al. [134] tells us that an over-complete dictionary can be learned from example natural images, and it can lead to much better image reconstruction results than the analytically designed off-the-shelf dictionaries. Many dictionary learning (DL) methods have been proposed and state-of-the-art performance in the image recognition task has been achieved by utilising KSVD. Regardless of these advantages, this synthesis DL poses high time complexity due to the use of l0 or l1-norm sparsity constraints. Therefore, a blend of the synthesis and analytical-based DL can be assumed to overcome the aforementioned pitfall, preserving the pattern recognition accuracy. Because of this, in this work, aim to explore such a dictionary-based learning for a multimodal eye pattern recognition task. Hypothesise to explore a projective dictionary pair learning for a biometric pattern recognition task. In the next subsection, discriminative dictionary learning, the projective dictionary pair learning model and the classification scheme is explained.

Discriminative dictionary learning- Let $X= [X1p, X2p,....., XKp]$ be the training samples set having p dimensionality from k classes. Where, Xk is a p-by-n matrix or a training sample set of class k, considering n is the number of samples of each class. An effective data representation model from X is learned by the discriminative DL methods for the classification tasks by exploiting the class label information in the training phase. The discriminative DL methods can be expressed as follows:

$$min_{D,A} || X - DA ||_F^2 + \lambda || A ||_p + \psi(D, A, Y), \quad (3.13)$$

Here Y represents the class label matrix of samples in X, λ is a scalar constant ($>=0$), D is the synthesis dictionary that has to be learned and A is the coding coefficient matrix of X on D. Therefore in the training model, $||X - DA||_F^2$ ensures representation efficiency of D, $||A||_p$ represents the *'lp-norm''* regularise on A and $\psi(D, A, Y)$ represents the discriminative function. Discriminative Learning works in two ways: some of them used in Ramirez et al, [136], Yang et al, [137] and Wang et al, [138] learn a structured dictionary for the discrimination of classes, whereas others in Mairal et al, [132], Jiang et al. [133], Mairal et al, [135] shared a dictionary for all classes and a classifier on the coding coefficients simultaneously. The "*l0-norm*" and "*l1-norm*" sparsity are regularise on the coding coefficients and are applied by all the DL methods. So there is some inefficiency in the training phase and the consequent testing phase.

The formula in (1) is for the conventional DL model. It learns a discriminative synthesis dictionary. In the DPL method, have used the DL which was extended to a novel DPL model that learns both synthesis and analysis dictionaries. It shows time computational efficiency as "*l0-norm*" or "*l1-norm*" and the sparsity regularise is not required for the coding coefficients rather it can be explicitly learned by linear projection.

Projective dictionary pair learning model- Learning a synthesis dictionary D to sparsely represent the signal X is the main objective of the conventional discriminative model in equation (3.14). To resolve the code A, the costly "*l1-norm*" sparse coding process is required. The representation of X would be very efficient if an analysis dictionary (P) can found which could satisfy $A=PX$. To do this, an analysis dictionary is learnt with the synthesis dictionary D and the model obtained can be formulated as follows,

$$\{P^*, D^*\} = arg \, {}^{min}_{P,D} \| X - DPX \|_F^2 + \psi(D, P, X, Y) \qquad (3.14)$$

Here to analytically code X, the analysis dictionary P is implemented and the synthesis dictionary D is used to reconstruct X. Where, $\psi(D, P, X, Y)$ is some discrimination function.

So the structured synthesis dictionary $D= [D1, D2,…, DK]$ and a structured analysis dictionary $P=[P1,P2,…, PK]$ is learned. Here Dk and Pk take part to produce a sub-dictionary pair corresponding to class k. The efficiency of the DPL model depends on the design of the discrimination function. Now the sparse subspace clustering [139] has proved that if signals satisfy certain incoherence conditions then the sample can be represented by its corresponding dictionary. It is desired that Pk should project the samples from class i (where i not equal to k) towards a null space with the structured analysis dictionary P. It can be formulated as follows,

$$P_k X_i \approx 0, \forall k \neq i. \qquad (3.15)$$

Similarly, the structured synthesis dictionary D can reconstruct the data matrix X. The data matrix Xk can be reconstructed efficiently by the sub-directory Dk from the projective code matrix $PkXk$. Hence the dictionary pair is used to minimise the reconstruction error. So,

$$min_{P,D} \sum_{k=1}^{k} \| X_k - D_k P_k X_k \|_F^2 \qquad (3.16)$$

and according to the above discussion, the DPL model can be formulated as,

$$\{P^*, D^*\} = arg \, {}^{min}_{P,D} \sum_{k=1}^{k} \| X_k - D_k P_k X_k \|_F^2 + \lambda \left\| P_k \overline{X}_k \right\|_F^2 ,$$

$$s.t. \, \| d_i \|_2^2 \leq 1. \qquad (3.17)$$

Here, $\overline{X}_k$ is the complement of Xk; in the whole training set X; the ith atom of synthesis dictionary D is di whose energy is constrained to avoid the trivial solution $Pk=0$ to make the DPL stable. λ is a scalar constant which is greater than 0.

It is argued that sparse coding may not be crucial in classification [140, 141]. However, the DPL model is much faster, and it has very competitive classification performance. Therefore, for the classification scheme, the following approach is used.

For optimisation purposes, the following methodology proposed in Gu et al, [142] is used. The objective function in (3.18) is generally non-convex. A variable matrix A is introduced and relaxed (3.18) to the following problem:

$$\{P^*, A, D^*\} = arg \min_{P,A,D} \sum_{k=1}^{k} ||X_k - D_k A_k||_F^2$$

$$= ||P_k X_k - A_k||_F^2 + \lambda ||P_k \overline{X}_k||_F^2,$$

$$s.t. \; || d_i ||_2^2 \leq 1. \tag{3.18}$$

where τ is a scalar constant. All terms in the above objective function are characterised by the Frobenius norm, and (6) can be easily solved. The analysis dictionary P and synthesis dictionary D is initialized as random matrices with the unit Frobenius norm, and then alternatively update A and $\{D, P\}$. The minimization can be alternated between the following two steps.

Fix D and P, update A

$$A^* = arg \min_{A} \sum_{k=1}^{k} ||X_k - D_k A_k||_F^2 + \tau ||P_k X_k - A_k||_F^2 \tag{3.19}$$

This is a standard least squares problem and has the closed-form solution:

$$A_k^* = (D_k^T D_k + \tau I)^{-1}(\tau P_k X_k + D_k^T X_k) \tag{3.20}$$

Fix A, update D and P:

$$\begin{cases} P^* = arg \min_{p} \sum_{k=1}^{k} ||P_k X_k - A_k||_F^2 + \lambda ||P_k \overline{X}_k||_F^2 \\ D^* = arg \min_{D} \sum_{k=1}^{k} ||X_k - D_k A_k||_F^2 \end{cases} \tag{3.21}$$

$$s.t. \; || d_i ||_2^2 \leq 1.$$

The closed-form solutions of *P* can be obtained as:

$$P_k^* = \tau A_k X_k^T (\tau X_k X_i^T + \lambda \overline{X}_k X_k^T + \gamma I) \tag{3.22}$$

where,

$\gamma = 10e - 4$ is a small number.

The *D* problem can be optimised by introducing a variable *S*:

$$min_{D,s} \sum_{k=1}^{k} ||X_k - D_k A_k||_F^2 \tag{3.23}$$

$$s.t. \ D = S, \quad || S_i ||_2^2 \leq 1.$$

The optimal solution of (3.25) can be obtained by the ADMM algorithm:

$$
\begin{cases}
D^{(r+1)} = arg \, \underset{D}{min} \sum_{k=1}^{k} ||X_k - D_k A_k||_F^2 + \\
\qquad p \, \left||D_k - S_k^{(r)} + T_k^{(r)}\right||_F^2 \\
S^{(r+1)} = arg \, \underset{S}{min} \sum_{k=1}^{k} p \, \left||D_k^{(r+1)} - S_k^{(r)} + T_k^{(r)}\right||_F^2 \\
\qquad s.t. \ D = || S_i ||_2^2 \leq 1 \\
T^{(r+1)} = T^{(r)} + D_k^{(r+1)} - S_k^{(r+1)},
\end{cases}
\tag{3.25}
$$

update *p* if appropriate

In each step of optimisation, closed-form solutions for variables *A* and *P*, and the ADMM-based optimisation of *D* converges rapidly. The training of the proposed DPL model is much faster than most previous discriminative DL methods. When the difference between the energy in two adjacent iterations is less than 0.01, the iteration stops. The analysis dictionary *P* and the synthesis dictionary *D* are then output for classification. One can see that the first sub-objective function in (3.23) is a discriminative analysis dictionary learner, focusing on promoting the discriminative power of *P*; the second sub-objective function in (3.23) is a representative synthesis dictionary learner, aiming to minimize the reconstruction error of the input signal with the coding coefficients generated by the analysis dictionary *P*. When

the minimization process converges, a balance between the discrimination and representation power of the model can be achieved.

Classification scheme- Classification is performed based on the residual value over the samples for a class. $P_k(*)$ is the analysis sub-directory trained to produce small coefficients for samples from classes other than k while the $Dk(*)$ is the synthesis sub-directory trained to reconstruct the samples of class k. Then the residual $||X_k - D_k^* P_k^* X_k||_F^2$ will be smaller than the residual $||X_i - D_k^* P_k^* X_i||_F^2$ when $i \neq k$. In the testing phase, a query sample y of an unknown class is considered a query image and its residual are calculated for every class. The class having the minimum residual is the class of the testing sample. The testing is formulated as follows,

$$identity(y) = arg_{\min i} || y - D_i P_i y ||_2 \qquad (3.26)$$

Here Di and Pi are the synthesis sub-directory and the analysis sub-directory respectively for class i. So according to (3.26), a sample from saying class i, would be the class of the sample y if the minimum residual is obtained from (3.26) for class i. As sclera literature is very new, several segmentation techniques have been employed to in this proposed approach to analyse the most Table and efficient segmentation technique, image enhancement technique, feature representation technique and classification technique. Proposed methodology also focuses on the combination of iris feature with sclera feature to build a robust multi-modal eye recognition system. The experimental result in support for the proposed technique is in the next subsection.

3.7. Data Set

In order to evaluate the performance of the proposed method, a public dataset (UBIRIS) and an in-house dataset were employed. The descriptions of the above-mentioned datasets are given in the sub-sections below.

3.7.1. UBIRIS

The UBIRIS version 1 is a public database [21] that was utilised in this experiment. This database consists of 1877 RGB images taken in two distinct sessions (1205 images in session 1 and 672 images in session 2) from 241 identities where each channel of RGB colour space is represented in grey-scale. The database contains blurred images and images with closed eyes. Both high-resolution images (800×600) and low-resolution images (200×150) are provided in the database and all the images are in JPEG format.

Different quality images have been used in the experiments, in which some of the sample images are shown in Figure 3.20. Some of them are not occluded having a good quality of

sclera regions visible, some of them are of medium quality and the third types were of poor quality with respect to sclera region visibility. In the experiments some closed eye images were also used, examples of such images are provided in Figure 3.21.

The first session images were taken in a dark room so that the noise factors such as reflection, luminosity, and contrast were minimised.

In the second session, the images were taken under natural illumination conditions with spontaneous user participation in order to introduce natural luminosity and add more noise factors than the first session.

(a)   (b)   (c)

(d)   (e)   (f)
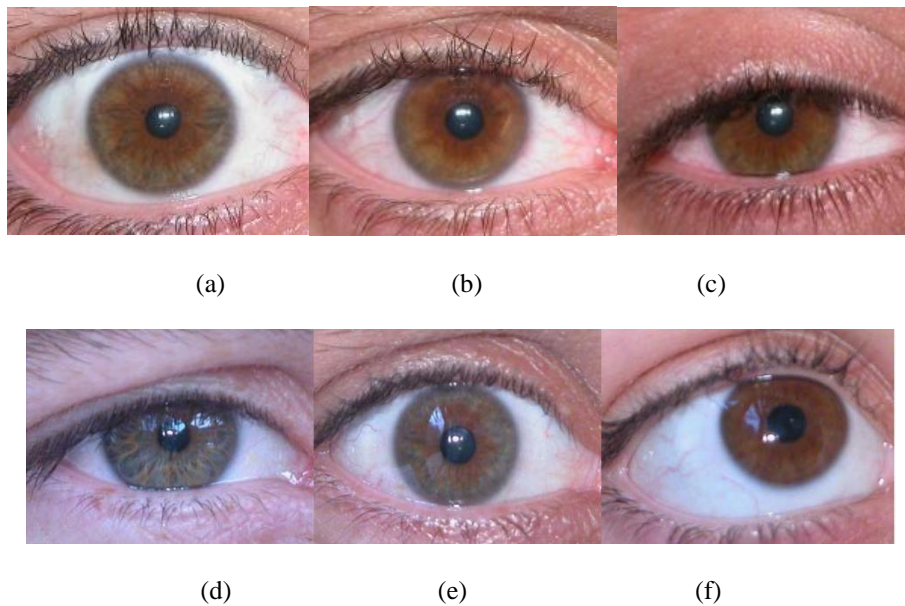
Figure 3.20: Different quality of eye images used in the experiment (a) is the type of best quality image of Session 1, (b)) is the type of medium quality of Session 1 (c) is the type of Poor quality of Session 1, (d) is the type of below average quality image of Session 2, (e) is the type of average quality of Session 2 (f) is the type of best quality in of Session 2.

The database contains blurred images and occluded images of eyes as shown in Figure 3.21.
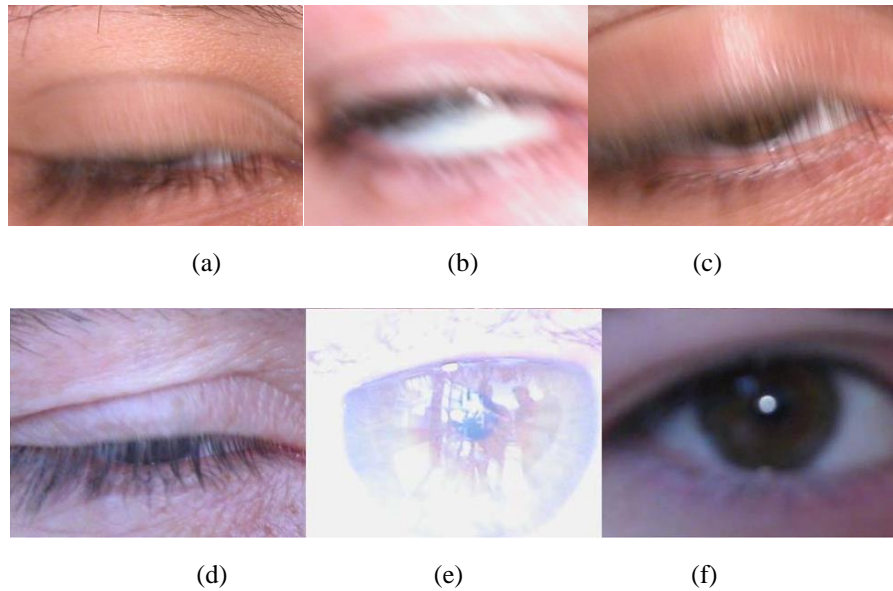
Figure 3.21: Example of closed and blurred eyes. (a), (b) and (c) are of session 1 and (d),(e) and (f) are of session 2.

In the experiments, all the images of sessions 1 and 2 are considered. Single sessions, as well as multi-session experiments, were performed both for sclera and iris image separately, followed by iris and sclera fusion experiment in the image level, score level and as well as in the feature level. For the single session experiments, sessions 1 and 2 are considered separately, with 3 images from each class of each session randomly chosen and utilised for training and the remaining 2 images for testing performance. For multisession experiments, 5 images from session 1 are considered for training, and 5 images from session 2 for testing and vice versa.

For single session experiment 241*2 scores for FRR and 242*241*2 score for FAR statistics for session 1 and 135*2 scores for FRR and 136*135*2 score for FAR statistics for session 1. For multisession experiment 135*2 scores for FRR and 242*135*2 score for FAR statistics.

3.7.2. MASD

This dataset was developed as a part of the thesis. In this dataset, a new multi-angled iris and sclera database that contains images in the visible spectrum were taken at a distance are presented. This is in contrast with existing databases that do not contain multi-angled images.

A tool was proposed here for the development of robust iris or sclera or combined recognition algorithms for biometric purposes. During the image capture, session noise factors were minimised, especially those relative to reflections, luminosity and contrast,

having installed a framework. A diagrammatic representation of the framework of the image capturing technique is given below in Figure 3.22.
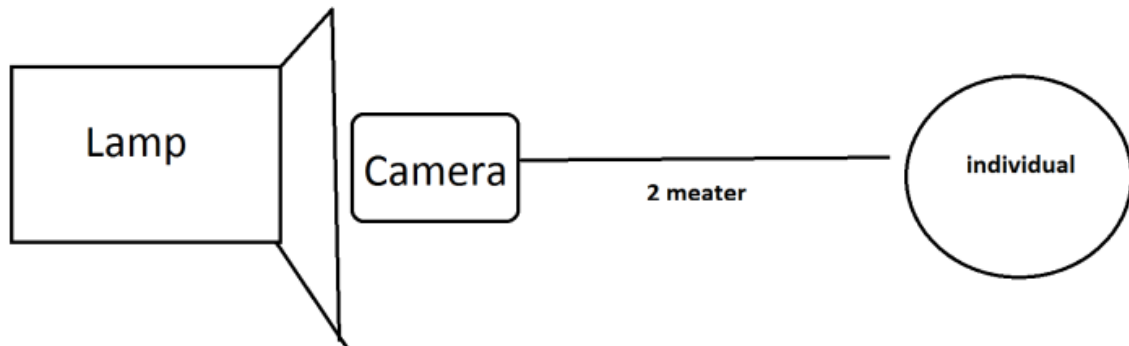
Figure 3.22: A framework of the image capturing technique [266].

The images are acquired by a digital camera in the visible spectrum at a distance of about 2 meters from the individual as shown in Figure 3.23.

Figure 3.23: Image captured at distance [266].

At first, the image is divided vertically into two halves as shown in Figure 3.24.

(a)   (b)
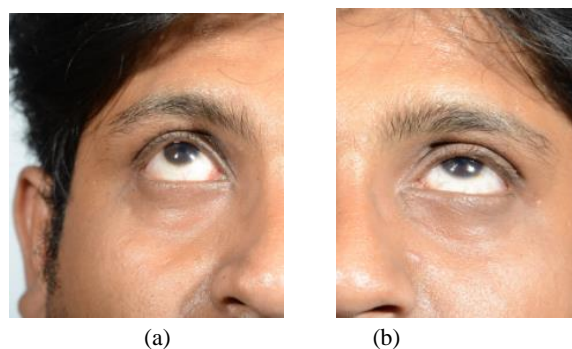
Figure 3.24: Two halves of the face image [266].

The eyes are detected in each half of the face image that is captured, by locating the eyeball through a circular Hough transform as shown in Figure 3.25 below.

Figure 3.25: Hough Circle detected the eyeball

The images are cropped automatically by calculating the radius of the eyeball as shown in the Figure 3.26. Each individual during registration as well as during validation was asked to look straight and move their eyeball towards up, left and right while keeping their face straight to incorporate liveliness of the data. The images of one individual are given in Figure 3.27.
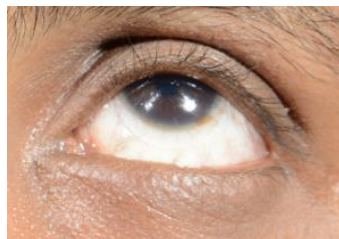
Figure 3.26: An automatically cropped image [266].

(a)   (b)

(c)   (d)
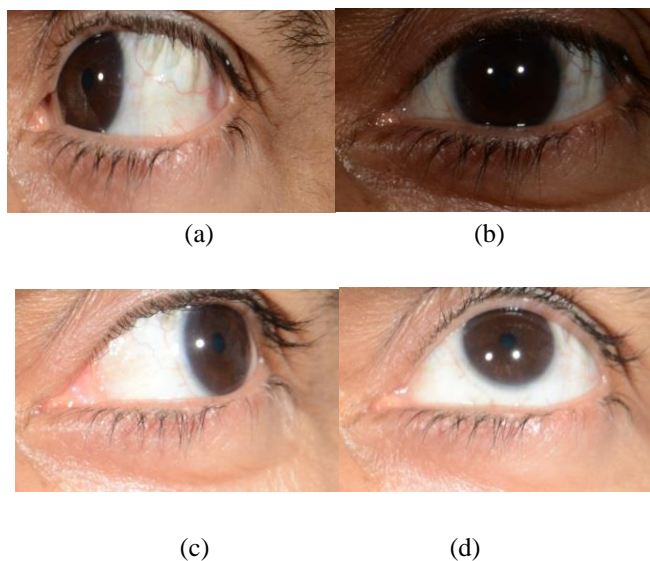
Figure 3.27: Images at different angles [266]

Few samples of images from the proposed dataset are given below in Figure 3.28.

Figure 3.28: Few samples of images from the proposed dataset [266].

The proposed multi-angled dataset consists of 5248 RGB images taken in one session from 82 individuals where each channel of RGB colour space is represented in grey-scale. The individuals were comprised of both male and female, with different ages and different colours were considered, a few of them were wearing contact lenses and images were taken at the different time of day. The database contains images with occluded eyes, closed eyes and blurred eye images, images with high resolution are provided in the database. All images are in JPEG format. Here for each individual image in four multi-angle were considered. For each angle, eight images were acquired. For each individual both left and right eye was captured. Different lighting conditions were considered during the image accusing. A NIKON D 800 camera and 28300 lenses were used for image acquisition. Different quality images were used here and some of the sample images are shown below in Figure 3.29.

(a)   (b)   (c)   (d)
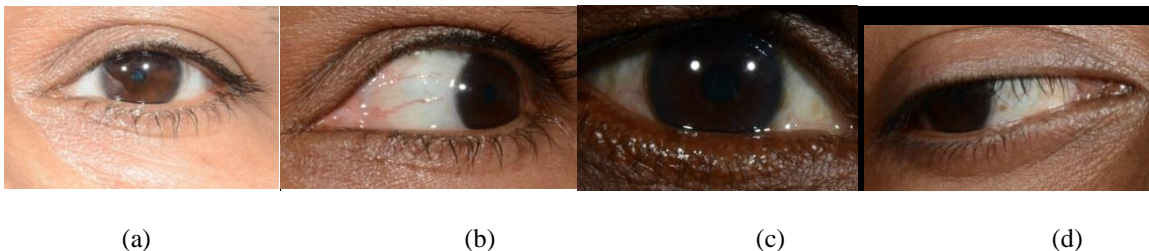
Figure 3.29: Different quality of eye images used in the experiments [266].

Some of them are not occluded having a good quality of sclera regions visible, some of them are of medium quality and the third type was of poor quality with respect to sclera region visibility. In the experiments some closed eye images were also used, examples of such images are provided below in Figure 3.30. The images were captured in an indoor lighting

condition so noise factors such as reflection, luminosity, and contrast were minimised. The database contains blurred images and images with blinking eyes as shown in Figure 3.30. In the experiments, all the images were considered for experimentation. For the experiment, 4 images from each angle, each class are randomly chosen and utilised for training and the remaining 4 set images for testing performance. So the FRR statistics is 164*16 and FAR of 164* 163 * 16. In order to analyse the effectiveness of the automatic segmentation techniques, ground truth or the manually segmented images of the dataset were designed. Here for each angle for each individual, 4 images were used for the ground truth preparation out of the 8 images for each angle present in the dataset. Few sample images of the manual segmentation are given in Figure 3.31. A set of protocols that were followed during the data collection procedure is as follows.

(a)   (b)

(a)   (e)

(e)   (f)
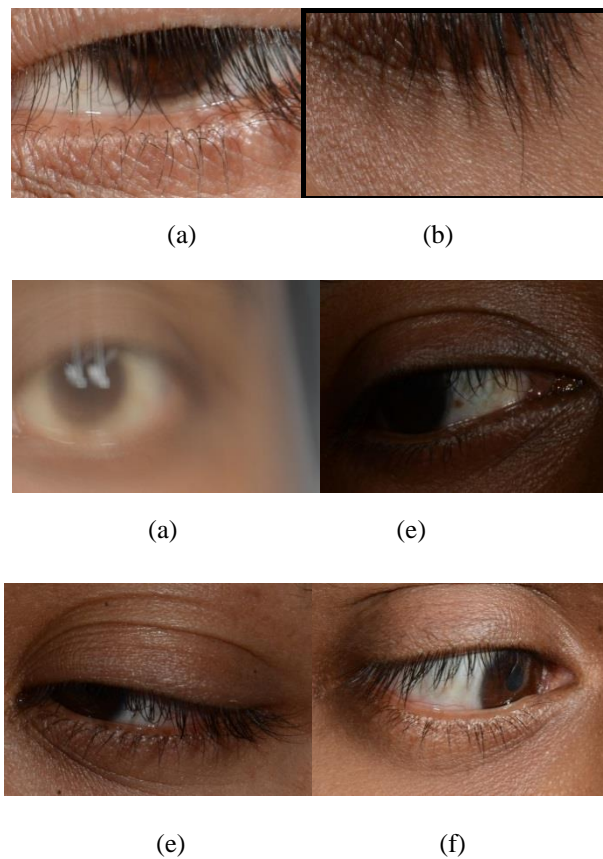
Figure 3.30: Examples of closed and blurred eyes [266].

- The images were acquired in the visible wavelength.

- Multi-angled (each individual looking left, right up, down and straight keeping their face towards the camera) eye images were captured, for each angle 8 instances were acquired.
- People were sitting in front of the camera while the images were captured.

- Between each camera sort, people walked for 2 to 3 meters and came back for next sort. The manual shot was taken for each image.

- The dataset was prepared from all ages, sexes, no glasses, no lenses, with lenses and also people with possible eye illness. All images were captured in an indoor session in room light (tungsten lights).

- The images were captured at different times of day early in the day and late in the day.

- A quality estimation program in Matlab was delivered in order to guarantee similar images from all the locations.

- Camera height position was fixed to 1m above the floor. Both left and right eye images of each individual were captured.

(a)   (b)

(c)   (d)

(e)   (f)
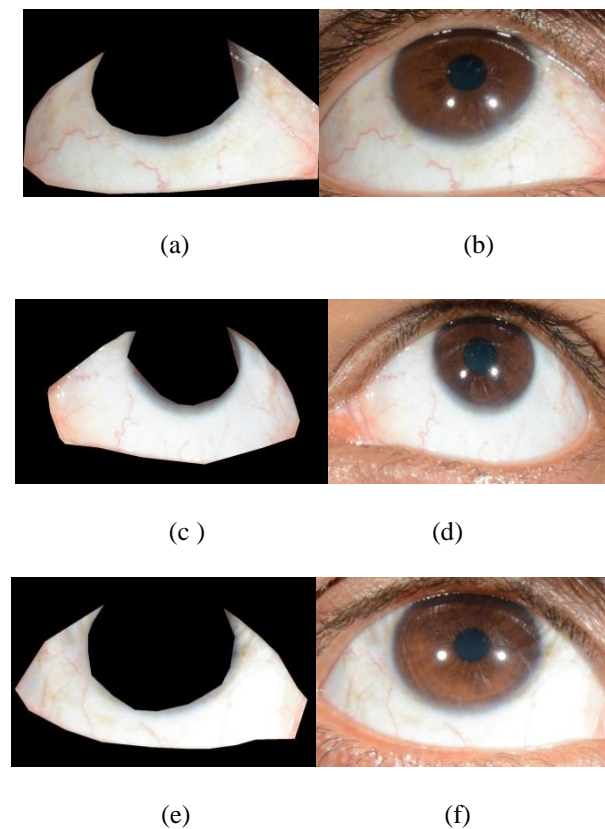
Figure 3.31: Different quality of ground truth and the original images.

3.8. Results

The results of proposed methodology on described datasets are discussed in this subsection.

3.8.1. Sclera Enhancement

In the experiments, it has been found that in the green channel of the images, the sclera vessel patterns are most prominent it can be found in the Figure 3.11. Although it can be dataset depended particular cause for it needs to be investigated. After that, adaptive histogram equalisation was performed with a tiled window size of 42 x42 at a clip limit of 0.01, with a full range and distribution exponential to get the best result.

Further, a bank of Haar wavelet was used to enhance the vessel patterns. High pass decomposition with a cut off range of -0.7, 0.65, and 0.55 was used with a window size of 3x3. In another process of sclera enhancement, the Discrete Meyer wavelet was used to enhance the vessel patterns. Low pass reconstruction with a cut-off value of $-0.9 * e^{10}$ and a window size of 3x3. Next, the same adaptive histogram equalisation with a tiled window size of 42x42 at a clip limit of 0.01, with full range and distribution exponential was imposed on the filtered image.

3.8.2. Iris Enhancement
In the experiments, it has been found that in the red channel of the images, the iris patterns are most prominent, it can be found in the Figure 3.11. Although it can be dataset depended particular cause for it needs to be investigated. After that, adaptive histogram equalisation was performed with a tiled window size of 2x2 at a clip limit of 0.01, with a full range and distribution exponential to get the best result. Further Haar filer was employed as investigated in [289], but it did not worked well.

3.8.3. Feature Extraction Experiment
The results of various feature extraction techniques used are discussed in this subsection.

3.8.3.1. Sclera Feature Extraction Experiment
The various experimental data related to sclera feature extraction are highlighted in the following sub-subsection below.

SIFT- Here a subset of UBIRIS version 1 is used, first 41 users from dataset from session one was employed here. So the FRR statistics is 41*2 and FAR of 41* 40* 2. The first experiments involved the study of the performance of the interior and exterior sclera pattern. The evaluation includes both manual and automatic segmentation of the sclera based on

SIFT features extracted from the equalised image, as shown in Table 3.1. We can find the effect of wrong segmentation on performance as also addressed in [288].

Table 3.1. EERs (%) obtained using SIFT over sclera and iris patterns.

	Segmentation	
	Manual	Automatic
Sclera Exterior	10.1%	17.5%
Sclera Interior	8.37%	22.1%

The interior sclera outperforms the exterior, and the gap between automatic and manual segmentation is significant. The difference between the interior and exterior sclera can be justified due to the higher presence of vein pattern in the former. In fact, some users do not show any vein pattern on the exterior sclera region.

In terms, if the performance of the sclera pattern it is important to emphasise the impact of the segmentation on the performance. The experiments performed show a gap of around 7% -10% of EER between manual and automatic segmentation. The influence of segmentation in the performance was evident. Moreover, an incorrect segmentation can involve not only in reducing the pattern available but also it can introduce other patterns such as eyelashes and eyelids (see Figure. 3.32).

| (a) | (b) | (c) |
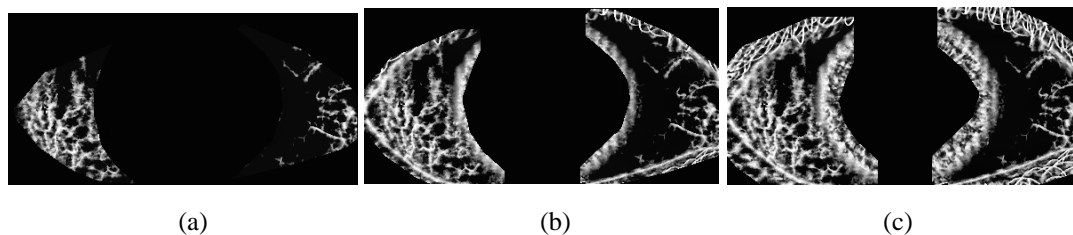
Figure. 3.32. (a) Mask applied without dilatation, mask applied with dilatation using a structural element of 50×50 (b) and 100×100 pixels (c).

The next Table shows the performance of the sclera when morphological dilatation is applied to the binary mask obtained during the segmentation.

Table 3.2. EERs (%) performance for different segmentation masks

	Segmentation			
	Manual		Automatic	
Dilatation	50×50	100×100	50×50	100×100
Sclera Exterior	2.29%	1.56%	5.69%	1.82%
Sclera Interior	4.82%	2.02%	10.4%	7.55%

The Table shows an important improvement (EER less than 2%) on the performance when dilatation was applied to the segmentation masks. The dilatation includes features obtained from patterns such as eyelashes and eyelids.

OLBP-Here a subset of UBIRIS version 1 is used: first 241 users from the dataset from session one was employed here. So the FRR statistics is 241*2 and FAR of 241* 240* 2. Among this, 54 images were discarded because of failures during acquiring. The experiments have been conducted to work out the sclera identification capability of the proposed feature and classifier. As it is a classical identification or verification problem, the results will be given in terms of Cumulative Matching Curves (CMC) and Equal Error Rate (EER) curve. The CMC & EER curve is displayed in Figure 3.33. Along the X-axis is the rank of the CMC and along the Y- axis the identification rate. Based on the interpretation of the graph it can be noted that faithful accuracy was achieved. Along the X-axis is the matching score and along the Y- axis the density.
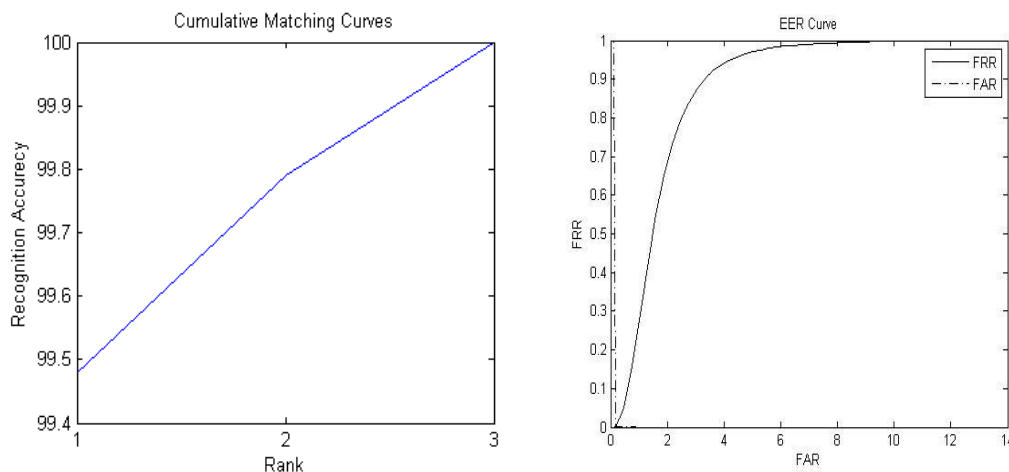
Figure 3.33.CMC curve for recognition & EER curve for recognition for MASD

The closed and occluded eye images were discarded in this experiments for both UBIRIS version 1 and MASD database. Table 3.3 provides the numerical data of Equal Error Rate and the Cumulative Matching Curves of the verification experiment.

Table 3.3: Equal Error Rate and the Cumulative Matching of the verification

Dataset	EER (%)	Cumulative Matching
UBIRIS version 1	0.52	99.48%
MASD	1.78	89.3%

Patch-Based Local Descriptors and PPDD- In this experiment, all the images from the UBIRIS dataset were used. For feature extraction, a few local features such as Dense SIFT (Scale Invariant Feature Transform), Dense LBP (Local Binary Pattern), and dense LDP (Local Directional Pattern) and PPDD are employed. The results in Table 3.4 reflect that PPDD produces the best results. As these four features produced better results, so also tested them for all multisession and single session experiments and further for fusion level experiments. Multisession 2_1 signifies images session 2 as testing and images from session 1 as testing. Multisession 1_2 signifies images session 1 as testing and images from session 2 as testing. The EER achieved in multisession experiments were somewhat higher than for the single session experiment. The reason behind the fact may be the change in the illumination and other acquiring artefacts. It can also be observed that result of Multisession 1_2 results is better than for Multisession 2_1, the reason might be due to acquiring artefact (session 1 acquired in a controlled environment, session 2 acquired in an uncontrolled environment) and another reason might be the availability of the trait acquired.

Table 3.4: Result of sclera feature extraction with different descriptors

	Feature	Equal Error Rate (%)			
		Multisession 2_1	*Multisession 1_2*	*Single session 1*	*Single session 2*
UBIRIS version 1	Dense SIFT	5.63	4.05	0.66	0.71
	Dense LBP	6.02	5.05	0.71	0.83
	Dense LDP	4.34	3.95	0.42	0.51
	PPDD	3.29	2.01	0.33	0.41
MASD	Dense SIFT	NA	NA	1.66	NA
	Dense LBP	NA	NA	1.50	NA
	Dense LDP	NA	NA	1.49	NA
	PPDD	NA	NA	1.23	NA

3.8.3.2. Iris Feature Extraction Experiment

For iris recognition also various features have been used, the result of the recognition and verification are explained below.

SIFT-The recognition performance of segmented iris based on SIFT features extracted from the equalised image was 0.24% of EER. In the experiment a subset of UBIRIS version 1 is used, the first 41 users from the dataset from session one were employed here.

Patch-Based Local Descriptors and PPDD- For iris feature extraction, a few local features such as Dense SIFT, Denes LBP, Dense LDP and PPDD are employed. The results in Table 3.5 reflect that PPDD produces the best results. In UBIRIS version 1 the in general iris trait attended better accuracy, however in MASD performance was lower. The rest of the pattern of the results remain the same as in Table 3.4.

Table 3.5: Result of iris feature extraction with different descriptors

	Feature	Equal Error Rate (%)			
		Multisession 2_1	*Multisession 1_2*	*Single session 1*	*Single session 2*
UBIRIS version 1	Dense SIFT	2..50	2.42	0.41	0.71
	Dense LBP	1.79	1.16	0.39	0.63
	Dense LDP	1.67	1.09	0.36	0.43
	PPDD	1.21	1.05	0.31	0.37
MASD	Dense SIFT	NA	NA	1.78	NA
	Dense LBP	NA	NA	1.55	NA
	Dense LDP	NA	NA	1.59	NA
	PPDD	NA	NA	1.48	NA

3.8.3.3. Iris and Sclera fusion feature selection experiment

Image Level Fusion- The superior performance of the iris is well known, so the next experiment intends to ascertain the potential of the sclera biometric to further improve the iris approach. The different nature of the iris and sclera patterns advises exploring different combination schemes. Table 3.6 shows the performance with a combination at the image level. The combination is done extracting the SIFT descriptors from each region (sclera or iris) and matching every descriptor regardless of which region it belongs to.

Table 3.6. EERs (%) obtained using SIFT and a combination at image level of sclera and iris patterns.

Image Combination	Segmentation EER (%)	
	Manual	Automatic
Sclera Ext. + Int.	5.38%	13.84%
Sclera Ext. + Iris	0.26%	0.27%
Sclera Int. + Iris	0.06%	0.27%
Sclera Ext. + Int. + Iris	0.11%	0.04%

The combination sclera with iris was effective and the EER is reduced 80% (from 0.24% to 0.04%).The combination of both sclera regions outperforms the individual results, but performances are far from those obtained with iris. However, only first 41 users of the 1st session from the UBIRIS version 1 were employed in this experiment. In the next experiment with patched based descriptors, the total dataset of UBIRIS version 1 has been used. For image label fusion extraction, a few local features such as Dense SIFT, Dense LBP, Dense LDP and PPDD were used. The results in Table 3.7 reflect that PPDD produces the best results in the image level fusion. It can also be observed that the employed fusion and featuring technique have achieved significant improvement in performance accuracy in every scenario (~0.05% in single session experiment, ~0.5% for a multisession experiment for UBIRIS version 1 and ~0.5% for MASD). The rest of the pattern of the experiments remain the same to previous experiments on sclera and iris.

Table 3.7: Result of image level fusion with different descriptors

	Feature	Equal Error Rate (%)			
		Multisession 2_1	*Multisession 1_2*	*Single session 1*	*Single session 2*
UBIRIS version 1	Dense SIFT	1.92	1.72	0.37	0.40
	Dense LBP	1.82	1.06	0.49	0.39
	Dense LDP	1.75	0.91	0.35	0.36
	PPDD	1.01	0.85	0.27	0.30
MASD	Dense SIFT	NA	NA	1.05	NA
	Dense LBP	NA	NA	1.10	NA
	Dense LDP	NA	NA	1.01	NA
	PPDD	NA	NA	0.92	NA

Score Level Fusion- Table 3.8 shows the performance when the combination is done at score level with SIFT feature for the first 41 users of the session from UBIRIS version 1. In this combination scheme, each region is classified separately and the classification scores (number of matches) are combined using a weighted sum as $score_{comb} = w_1 score_A + w_2 score_B + w_3 score_C$. The combination at score level confirms the effectiveness of the sclera pattern to further improve the iris approach. In a combined scheme, the segmentation of the iris seems to be less crucial and therefore competitive performances are obtained with both automatic and manual segmentations.

Table 3.8. EERs (%) obtained using SIFT and a combination at score level of sclera and iris patterns.

Score Combination	Weighting factors			Segmentation	
	w_1	w_2	w_3	Manual	Automatic
Sclera Ext. + Int.	0.4	0.5	0	10.1%	16.6%
Sclera Ext. + Iris	0.4	0.9	0	0.13%	0.14%
Sclera Int. + Iris	0.2	0.8	0	0.16%	0.18%
Sclera Ext. + Int. + Iris	0.2	0.1	0.9	0.15%	0.17%

The result of score level fusion with different descriptors like Dense LBP, Dense LDP. Dense SIFT and PPDD are in Table 3.9. It is apparent from the result that the result achieved is less accurate than that of image level fusion.

Table 3.9: Result of the score level fusion using different descriptor

	Feature	Equal Error Rate (%)			
		Multisession 2_1	*Multisession 1_2*	*Single session 1*	*Single session 2*
UBIRIS version 1	Dense SIFT	2.19	1.81	0.48	0.52
	Dense LBP	1.96	1.50	0.45	0.41
	Dense LDP	1.26	1.21	0.39	0.40
	PPDD	1.21	1.02	0.35	0.37
MASD	Dense SIFT	NA	NA	1.21	NA
	Dense LBP	NA	NA	1.32	NA
	Dense LDP	NA	NA	1.15	NA
	PPDD	NA	NA	1.11	NA

Feature Level Fusion-Result of score level fusion with different descriptors like Dense LBP, Dense LDP. Dense SIFT and PPDD are in Table 3.10. It can be apparent from the result that the result achieved is less accurate than that of image level fusion. Here a weighted feature fusion of 0.75 for iris and 0.25 for sclera was used.

Table 3.10: Result of feature level fusion with different descriptors

	Feature	Equal Error Rate (%)			
		Multisession 2_1	*Multisession 1_2*	*Single session 1*	*Single session 2*
UBIRIS version 1	Dense SIFT	2.19	1.81	0.48	0.52
	Dense LBP	1.96	1.50	0.45	0.41
	Dense LDP	1.26	1.21	0.39	0.40
	PPDD	1.21	1.02	0.35	0.37
MASD	Dense SIFT	NA	NA	1.21	NA
	Dense LBP	NA	NA	1.32	NA
	Dense LDP	NA	NA	1.15	NA
	PPDD	NA	NA	1.11	NA

It is clear from the result that the result achieved is less accurate than that of image level fusion, although rest of the pattern of the experiment remained the same.

3.9. Overall Experimental Results

It can be inferred from the above Tables that for session 1 as training, and session 2 as testing produces the best result for the multi-session experimental environment. For the single session experiments, session 1 produces the best results. It can also be concluded from the above Table that the result for the multisession experiments has deteriorated somewhat. The possible cause can be the different lighting condition, image properties and the presence of some eyelids and eyelashes in the feature computed area. It can also be due to the quality of the traits available in the sessions. The performance of iris was better in all scenario for UBIRIS 1, whereas results for the sclera was better in MASD. A possible reason can be the presence of more off-angle images in the dataset. Overall, better accuracy has been achieved in all the levels of fusion than the individual traits.

3.10. Comparison with the State-of-the-art

The results of the proposed work are analysed with respect to the state-of-the-art by comparing it with the most similar work tested on UBIRIS version 1 that can be found in the literature. The Table 4.14 reflects a state-of-the-art comparative analysis of the most similar work on UBIRIS version 1 dataset. From the Table it can be reflected that the proposed system 2 produces a better result than the method proposed by Zhou et al. [5] in and they have also used manual sclera segmentation for few images, as their automatic segmentation failed on that occasion, and the very poor quality (e.g., blur, blink, or no sclera-area image) images were also discarded from the experimentation.
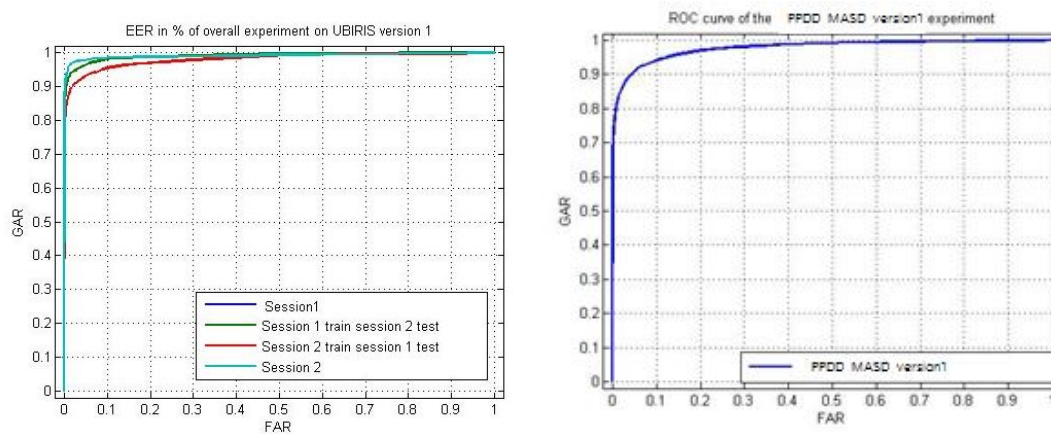
Figure 3.34. ROC curves of the overall experiments of UBIRIS version 1 and MASD with PPDD

In Oh and Toh [10], manual points were used for marking and connecting 333 images, even the experiment that they reported was not a multisession experiment, and the proposed system 2 outperforms their result. Whereas, in Oh et al. [226] proposed a multimodal biometric using sclera and peri-ocular and displayed results on single session experiments. Gottemukkul-a et al. [224] also achieved significant results on single session experiments. The results reported in the Zhou et al. [4, 6] were multimodal but not multisession and even the proposed methodology outperformed their result. Alkassar et al [223] and Tankasala et al.[225] achieved significant accuracy on both multisession and single session experiments. The proposed schemes are the most realistic one since it did not discard any images from the dataset used, multi-modal, the segmentation was fully automatic and the experiments were also performed with multisession data, where the sessions have variation in change in environmental condition, population, data accruing technique and time span gap. Another significant novelty of this work is the use of statistical classifier like SVM in contrast to the other related work, where template matching was used for classification. Among all the proposed method PPDD achieved the best accuracy among all the work proposed.

3.11. Results on Competition Conducted on MASD

To fill this gap and to raise the popularity of sclera biometrics [269], the 1st Sclera Segmentation Benchmarking Competition (SSBC 2015) in Das et al. [270] was organized in the context of the IEEE Seventh International Conference on Biometrics: Theory, Applications and Systems BTAS 2015 and the 1st Sclera Segmentation and Recognition Benchmarking Competition (SSRBC 2016) in Das et al. [272] was organized in the context of the 9th IAPR International Conference on Biometrics: ICB 2016. The proposed MASD dataset was employed in this context. The four algorithms submitted by the four participants of SSBC 2015 and three algorithms from SSRBC 2016 are as below in Table 3.12. The segmentation algorithms proposed in SSBC 2015 and SSERBC 2016 reached significant accuracy in segmentation (95.05% of precision and recall of 94.56% on the proposed SSBC 2015 on MASD dataset, but segmentation techniques are highly affected by the change in illuminations and the image quality. Especially for low-quality images, the proposed segmentation techniques are not very successful. Four scenarios were identified where the algorithms failed to successfully obtain a fair mask, as followings:

- Variation in illumination for one part of the eye – (Figure 3.35a)

- Variation in illumination at the part of the sclera and the other parts of the eye – (Figure 3.35 b & c).

- Variation in illumination for the total eye image –   (Figure 3.35 d and e)

- Variation in illumination due to the light source – (Figure 3.35 f & g)
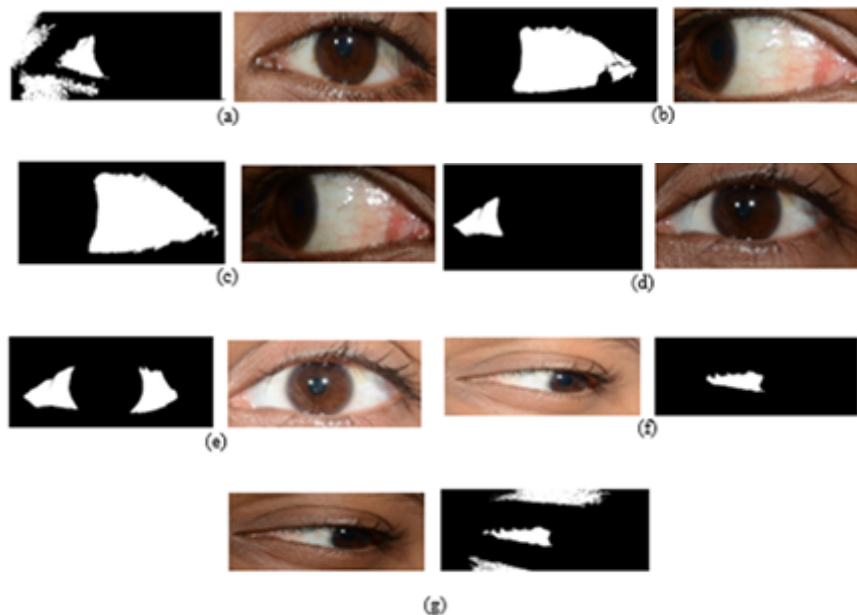
Figure 3.35: Four scenarios where algorithms failed to successfully obtain a fair mask [270]

Table 3.11: A state of the art compares of the other pieces of work on UBIRIS version 1

Work	Segme-ntation	Enhan-cement	Feature	Classifier	Accuracy in %/EER S1/S2/S12/S21
Daugman [16]^	Integro-differential operator		TM		3.72
Proenca et al. [277]^	Segmented and normalized iris image into six regions		Independent feature selection		2.38
Zhou et al. [4]*	Otsu and HSV	Gabor & thinning	Score	TM (Template Matching)	2.73/-/-/-
Zhou et al. [3]					1.34/-/-/-
Zhou et al. [6] *					96.42FAR(0.1)/94.92(0.01)/-/-/-
Zhou et al. [5]			Linde descriptor		3.38/-/-/-
Oh and Toh [10]	HSV,	CLAHE,	LBP		0.47/-/-/-
Oh et al. [226]+					3.62/3.26/-/-
Proposed methodology Das et al.[263]	Region growing	CLAHE and Haar	OLBP		0.52/-/-/-
Proposed methodology Das et al.[264]			D-SIFT	SVM	0.66/-/-/-
Proposed methodology Das et al.[267]	C-means	CLAHE, DWT	D-LDP	SVM	0.42/0.51/3.95/4.34
Proposed methodology Das et al.[265]			D-LBP		0.8/0.83/4.31/4.87
Proposed methodology			PPDD	Residual value	0.35/0.37/1.02/1.21
Tankasala et al.[225] *	K-means	CLAHE	GLCM	LDA	0.4/ 0.5 /2.4 /3.2
Gottemukkul-a et al. [224]	Eye contour and thresholding	CLAHE	Two stage	Score match	0.82,99.17/-/-/-
Alkassar et al [223]	Active contour	CLAHE	Harris corner	TM	2.19/2.67/3.68/4.11

* Multimodal sclera fusion with iris   + Multimodal sclera fusion with peri-ocular, ^ As reported in [5]

S1= UBIRIS version 1 session 1 images as training and testing, S2= UBIRIS version 1 session 2 images as training and testing, S12= UBIRIS version 1 session 1 images as training and session 2 images as testing, S12= UBIRIS version 1 session 2 images as training and session 1 images as testing

Table 3.12: Algorithms and results of SSBC 2015 and SSRBC 2016.

Participating teams	Method	Precision in %	Recall in%
The university of Reading, UK	A two-stage classifier : the first stage, a set of simple classifiers was employed, while at the second stage, a neural network classifier	95.05	94.56
Università-degli studi di Napoli Federico II, Italy	*Pre-processing:* 5x5 downsampling, 9x9 median filtering on each colour band. *Marker extraction:* Morphological closure (square structuring element 10x10), morphological opening (square structuring element 30x30), K-means clustering (k=5) on green and blue bands. *Modulus of the gradient*: Watershed and upsampling [Vincent and Soille 1991] [Puhan et al. 2011].	90.51	86.03
ATVS Biometric Recognition Group, Spain	*Pre-processing:* The red channel eye image is segmented into three clusters using the k-means algorithm. *1st stage of segmentation:* K-means clustering (k=3) applied on the pre-processed image. *2nd stage of segmentation:* Kissing ellipse around the eyelids is worked out with the vertical minor axes equal to the iris diameter and the horizontal major axes equal to the image width	90.49	80.02
Birla Institute of Technology, Mesra, Ranchi, India	*Pre-processing:* The image is pre-processed by shifting the histogram of the image towards the darker side of the image to get a greater contrast between the sclera and the background region. *Segmentation:* Otsu's binarization method was applied on the pre-processed image. Morphological filling operation was used to fill the small unmasked spaces left after the binarization due to presence of specular reflection and other noises	87.34	79.02
SJCE, Mysusru, India	Segmentation method based on Fuzzy C-Means was used. Robust Spatial Kernel FCM (RSKFCM) method was proposed to segment sclera. Gaussian kernel was used to calculate the distance between the centre of the cluster and the data point	85.21	80.21
Griffith University, Australia	Peaks are found from the gray-level histogram of Fuzzy C-Means. The number of clusters is perceived as the number of peaks (± low threshold) of that histogram Big holes found in the segmented sclera region are filled in and small holes found are filtered out as noise	75.09	70.10
	Two clusters (histogram of Fuzzy C-Means) having the highest and the next-to-highest cluster is considered. On these two clusters, Otsu's binarization is performed, followed by similar pre-processing as in the previous method to obtain better segmentation mask.	74.01	73.20

The basic faults that appear on the segmented mask due to these conditions:

- In the first scenario (Figure 3.35 a), the lighter part of the sclera is segmented partially correctly (some non-sclera parts are misclassified) but the darker part is not segmented correctly.

- In the second scenario, some parts of the sclera mainly the vessels patterns, were misclassified (Figure 3.35b and Figure 3.35c are eye images of the same individual, in Figure 3.35b sclera part are misclassified).

- In the third scenario, the lighter part of the sclera is segmented correctly, but the darker part is not segmented (Figure 3.35d and Figure 3.35e are eye images of the same individual; in Figure 3.35d sclera part is misclassified due to less illumination).

- In the fourth scenario in the darker images that is images where less illumination was applied, the skin region around the eye was also misclassified as sclera region (Figure 3.35f and Figure 3.35g are eye images of the same individual, in Figure 3.35f the non-sclera part is misclassified due to less illumination).

Similar to segmentation task a recognition competition was organised in the context of the 9th IAPR International Conference on Biometrics: ICB 2016. Histogram of Oriented Gradient and Gabor feature were used for feature extraction by the two participants of the competition.

For classification the K-nearest neighbour classifier was used by both participants. A satisfactory recognition accuracy was achieved by the systems on MASD dataset.

3.12. Summary

Considering the recent popularity and ongoing research on sclera biometric, and multimodal ocular biometric using iris and sclera, this chapter discuss the advancement proposed in this subject of research.

As identified in chapter 2 that this area of biometric needs substantial attention, therefore in this chapter we proposed and discussed various segmentation, pattern enhancement, feature extraction, classification and information fusion technique to characterise the sclera, iris, and sclera and iris-based multimodal ocular biometrics.

Two datasets namely UBIRIS version 1 and MASD were used for experimentation. MASD was proposed as a part of the thesis and it incorporates a larger number of off-angle images in the different gaze of an eye. The result achieved in the experiment depicts that

traits were best fused at the sensor level. Few initiative for benchmarking sclera segmentation and recognition is also discussed.

4

Proposed Methodologies for Liveness Detection

Traditional multimodal ocular biometric authentication systems are not equipped to discriminate between genuine users and those who illegally duplicate genuine traits and take the privileges to access a system as a genuine user. Therefore, in order to enhance the security and reliability of these biometric systems, liveness detection is a necessary step to prevent threats from intruders. This chapter of the thesis will concentrate on design software- based liveliness multimodal eye biometric systems. Software-based liveness can be established by measuring image quality features, body movement features, motion features, and physical properties. Two methods for liveness detection is proposed in the chapter described in the next to section. The first method employed a body movement feature and the second method uses a few image quality features to realise liveness.

Major parts of the chapter have been published in the articles Das et al. [266, 275].

4.1. Liveliness Detection by Multi-angle Sequence of the Eye

The liveliness of the data will be detected by the motion of the eye. During enrolment, the user will be asked to look straight, up, left and right angle keeping the face straight towards the camera. Combinations of the sequence produced considering each of the views is stored in the training model. During enrolment, the user will be asked to perform any of the random

sequence (left, right, straight and up, or up, right, straight and left, so on). A framework for the proposed technique is in Figure 4.1.

```
┌─────────────────┐
│   Test or Train │
│  Image Sequence │
└─────────────────┘
         │
         ▼
┌─────────────────┐
│     Sclera      │
│  Segmentation   │
└─────────────────┘
         │
         ▼
┌─────────────────┐
│ Sclera Enhancement │
└─────────────────┘
         │
         ▼
┌─────────────────┐
│    Feature      │
│   Extraction    │
└─────────────────┘
  Training │
         ▼
   ┌──────────────┐
   │   Training   │
   │  Knowledge   │      Testing
   │    base      │
   └──────────────┘
         │
         ▼
┌─────────────────┐
│ Classification  │◄───
│  and liveliness │
│    detection    │
└─────────────────┘
```
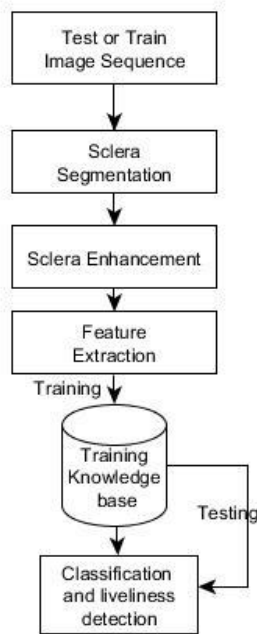
Figure 4.1. A framework of the liveliness system using a multi-angle sequence of an eye [266].

An experiment was carried out with the MASD in the visible spectrum to reflect the usefulness of the concepts. Here experiments were performed by using 4 images set for each angle from each class are randomly chosen and utilised for training and the remaining 4 set images for testing performance for each angle. Here segmentation was performed by C-means, enhancement by Haar filter, feature extraction by Dense LDP and classification by SVM. First, the ability of the multi-angle scheme to verify the user identity was checked. Table 4.1 shows the Equal Error Rate (EER) of the device using different angles.

Table 4.1: EER of the different angle

Different Angle	EER (%)
Looking up	0.9
Looking Left	1.1
Looking right	1.41
Looking straight	1.05

It can be seen that the best angle is looking up although all of them get competitive results compared to the classical strategy of looking straight. A possible reason for getting better

EER in up angle is due to the visibility of more exposed sclera vessels pattern. The EER for the right and the left angle is less due to presence more amount of specular reflection on the sclera region as compared to other two angles. The results with forgeries are obtained supposing that a high-resolution picture is presented at the system with a wrong eye orientation. In this case, the ability of the system to reject such an input is given in Table 4.2.

Table 4.2: The results with forgeries obtained if the user is looking at a different angle for that of which the system have asked for

		Training			
	Looking	Up	Left	Right	Straight
Testing	Up	0.9	20.12	17.88	19.56
	Left	19.75	1.1	21.99	14.66
	Right	15.99	22.03	1.41	19.18
	Straight	19.55	15.01	19.08	1.05

It can be reflected from the above Table of each and every forgery angel the EER is high. Hence it can be concluded that authentication with different angles of sclera pattern highly affects the efficiency of the system. In the second phase of the experiment, one image from each angle was combined in image level and feature level, to determine the effect of the combination of multi-angle on the efficiency of the system. An example of the image label fusion is given as below. The results of the different fusion levels are reflected in Table 4.3.
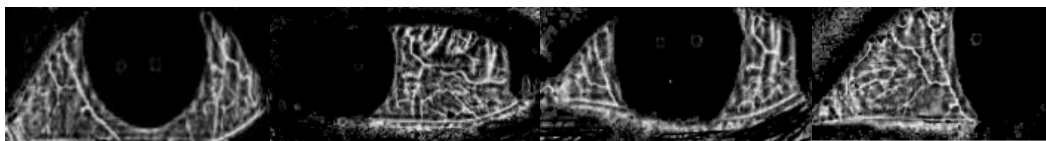
Figure 4.2.Image label fusion of different angles [266].

Table 4.3. EER of the different level of fusion

Different level of fusion	EER (%)
Image Level	0.52
Feature level	0.75

It can be inferred from the above Table that image label fusion produces the best results and even the fusion of the different angle helps to increase the efficiency of the system. Next to experiment the effect of a sequence of the orientation when an individual is asked to look in a sequence: for instance straight, up, left and right but the individual looks in some other sequence, then what is the performance of the system.

Table 4.4. The results with forgeries obtained if the user is looking at a different sequence of angles from that which the system has asked for by image level fusion

	Testing Sequence of orientation	EER in %
	Straight, up, left and right	0.52
	Straight, up, right and left	19.90
	Straight, left, up and right	17.01
	Straight, left, right and up	23.05
	Straight, right, left and up	24.01
	Straight, right, up and left	22.09
	Right, left, up and straight	24.35
	Right, left, straight and up	22.01
	Right, up, left and straight	23.44
	Right, up, straight and left	23.01
	Right, straight, up and left	22.44
Training by sequence of looking straight, up, left and right	Right, straight, left and up	19.01
	Up, straight, left and right	19.90
	Up, straight, right and left	21.77
	Up, left, straight and right	17.10
	Up, left, right and straight	23.33
	Up, straight, left, and right	24.44
	Up, straight, right and left	21.13
	Left, right, up and straight	11.90
	Left, right, straight and up	23.4
	Left, up, right, and straight	19.08
	Left, up, straight and right,	22.01
	Left, straight, up and right,	19.01
	Left, straight, right and up,	23.02

Table 4.5. The results with forgeries obtained if the user is looking at a different sequence of angles from that which the system has asked for, by feature level fusion

	Testing Sequence of orientation	EER in %
	Straight, up, left and right	0.75
	Straight, up, right and left	19.99
	Straight, left, up and right	19.09
	Straight, left, right and up	23.95
	Straight, right, left and up	24.81
	Straight, right, up and left	22.39
	Right, left, up and straight	24.05
	Right, left, straight and up	22.81
	Right, up, left and straight	23.94
	Right, up, straight and left	23.81
Training by sequence of looking straight, up, left and right	Right, straight, up and left	22.49
	Right, straight, left and up	19.01
	Up, straight, left and right	19.99
	Up, straight, right and left	21.8
	Up, left, straight and right	17.90
	Up, left, right and straight	23.77
	Up, straight, left, and right	24.66
	Up, straight, right and left	22.03
	Left, right, up and straight	12.0
	Left, right, straight and up	23.87
	Left, up, right, and straight	19.99
	Left, up, straight and right,	22.65
	Left, straight, up and right,	19.88
	Left, straight, right and up,	23.74

It can be reflected from the above Table of each and every forgery angle sequence the EER is high. Hence it can be concluded that this sequence of eye movement can work as a good form for the liveliness of detection. The experiment is extended by training with image sequences from the dataset and testing them with a set of images captured by images of the eye of the same set of individuals from a mobile or portable screen (to stimulate a practical life scenario when the eye image can be scanned for spoofing in front of a sensor by high-resolution image). Examples of such images are given below in Figure 4.3.

(a)   (b)

(c)   (d)
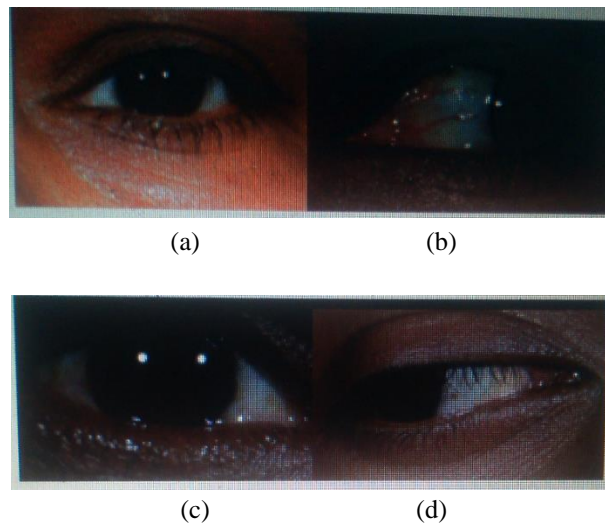
Figure 4.3: Examples of images taken by displaying eye images from mobile [266].

The EER obtained in the result of the above-mentioned experiment was 10.05. This signifies the robustness of the system to spoofing by portable devices. Although a significant result is achieved in the experiments but trade-off of adaptability and liveness is not addressed. Therefore, further research is conducted which is summarised in the next section.

Table 4.6. Equal Error Rate of the different level of fusion by testing the mobile images

Different level of fusion	EER (%)
Image level	10.05
Feature level	10.79

4.2. Image Quality-Based Liveness Framework

In this section, a new framework for software-based liveness detection exploring image quality features for ocular biometric in the visible spectrum is proposed. The specific contributions of the proposed liveness detection scheme are as followings [275]:

1. A new framework for liveness detection, as shown in Figure 1(b) is proposed at the intra-class level, which makes the quality feature more useful than the other previous liveness framework.

2. A set of quality parameters is proposed for liveness detection in ocular biometrics in the visible spectrum. These measures are based on transformed domain, geometrical relation and contrast measures.

3. As liveness is detected at the intra-class level (intra-class level and inter-class level is emitted in Figure 4.4 (a and b)), adaptiveness of such system is also high (as the classification is done per user so obtain different thresholds are used per user and hence adaptation is required in user level).

4. In order to demonstrate the proposed framework different spoofing techniques are explored (here images are taken from the portable screen as well as from printed).

5. Moreover, this experiment was performed on the low-end image acquired from the mobile camera in a regular room environment, which reflects potentiality to work in real life environment.

4.2.1. Proposed Liveness Framework

It can be referred from the literature, that the biometric liveness detection problem is a two class classifier problem i.e. it classifies the input image into two classes, either a real sample or a fake sample category. It indicates that either the scanned image is from a real live body or it is acquired from a non-live body, by processing it by image processing and computer vision based and signals processing based quality assessment.

Various liveness framework proposed in the literature have been designed at the inter-class level. In the contrast to the existing frame work, the proposed framework deals with the liveness problem as two class classifier problems at the intra-class level (fake and real classification at each user level. A block diagram of the intra-class and inter-class level is provided in Figure 4.4 (a and b).

In a real-life scenario liveness detection is required to be ensured if the data is recognised correctly. So, the liveness detection problem can be clearly reduced to a two class classifier problem at the intra-class level rather than the inter-class level. This new adaptation of framework not only reduce the complexity of the schema, but also makes the quality features more useful to classify the real and fake data. Moreover, as each class has individual represented by a threshold of quality feature score (build a classifier per user, different

threshold per user is obtained, so adapt the quality parameter threshold to the user) so adaptability of the system will be higher than the dataset level framework that was proposed previously.

The proposed liveness framework for each class is as follows: At the enrolling step real and fake representations of the user, the eye is obtained. For enrolling the real data individual collaboration is required, while for the fake sample is acquired in a user transparent way, i.e. do not require the individual collaboration and it is done automatically as shown in Figure 4.4 (c). The images acquired from each user in the enrolment phase can be displayed on a portable screen in front of a camera to produce fake images as shown in Figure 4.4 (b).

At the identification step, the individual is required to be identified correctly and then the liveness is detected by comparing the various quality parameters with the real and fake representation of the recognised class. A framework of the above mention framework for liveness detection and the framework of the image scanning system is given below in Figure 4.4 (c).

The various existing and new quality-based features employed to detect the liveness can be categorised into three main categories namely transformed domain (focus)-related quality feature, aspect-related feature and contrast-related feature. These features are described below in the following sub-sections.

4.2.1.1. Transform Domain or Focus-related Quality Feature

Various types of direct attack that can be used for spoofing in ocular biometrics in the visible spectrum are scanning a high resolution printed image or a high-resolution image or high definition video from a portable screen such as a mobile or notepad etc. However in the entire scenarios, as the spoofing is committed by scanning images which are 2D objects, it is expected that there will be a focus different with the images captured from live data which are 3D objects. So, various transformed domain (focus) related feature is explored here as an image quality assessment tool such as in.

- **Power Spectrum (QF1):** The power spectrum of an image is a unique feature to discriminate between the real and fake image. The power spectrum splits a signal or an image into frequency bins, where the maximum frequency which can be observed is the Nyquist frequency or half of the sampling frequency.

(a)

(b)

(c)
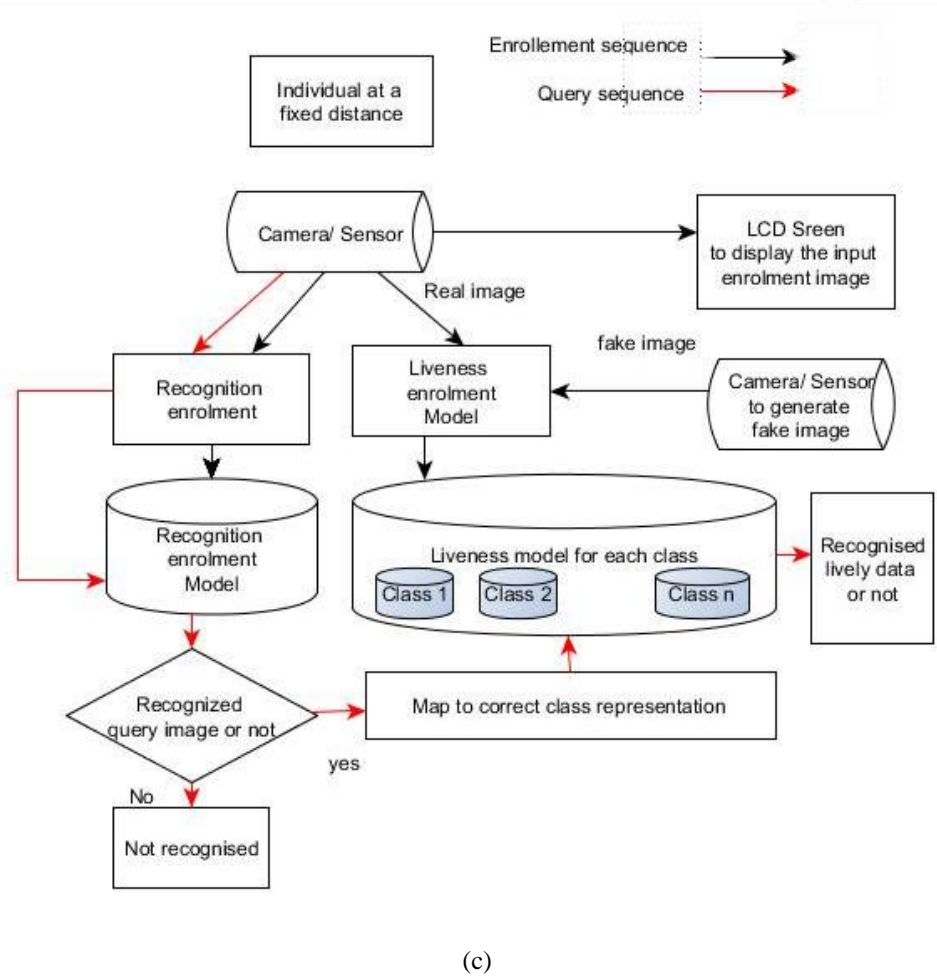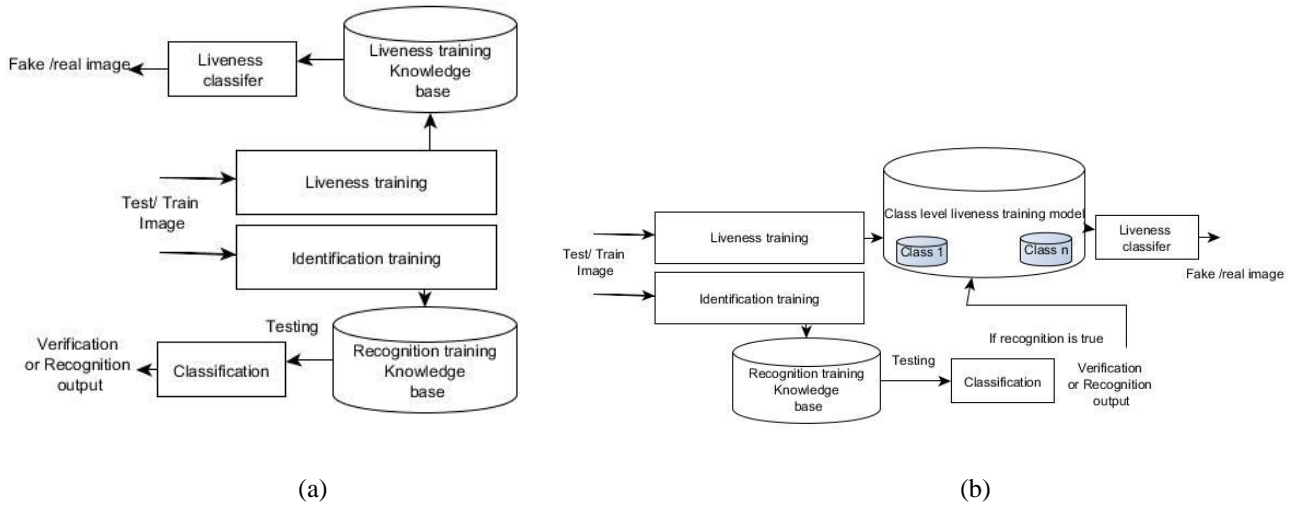
Figure 4.4: (a) Inter-class level or dataset level liveness framework, (b) intra-class / class level liveness framework(c) A pictorial representation of the above mention framework for liveness detection [275].
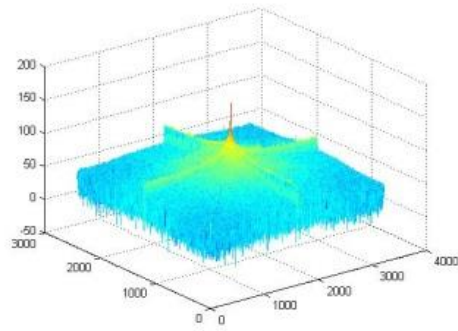
(a)
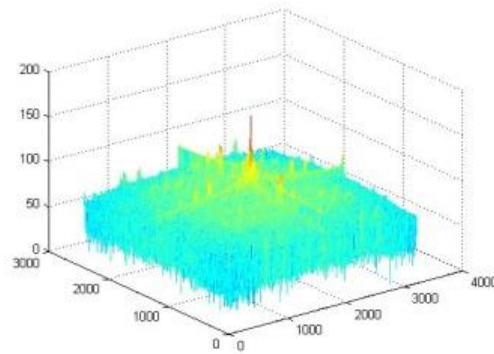
(b)

(c)   (d)

Figure 4.5: (a) Power spectrum of the real image, (b) Power spectrum of the fake image, (c) real image and (d) fake image [275].

- **Discrete approximation of the Laplacian (QF2):** The discrete Laplace operator is an analogue of the continuous Laplace operator, it provides an accurate *approximation of the Laplacian* operator of digital signals passing through this filter.
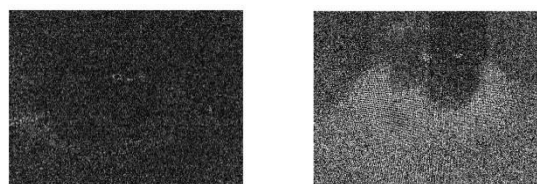
Figure 4.6: (a) Laplacian of the real image of 4.5(c), (b) Laplacian of the fake image of 4.5(d) [275].

- **High-frequency 2D filter (QF3):** The filter response from a high-frequency 2D filter is also a signal processing tool to detect the quality of an image. Here Discrete Meyer decomposition filter was employed for the implementation of high-frequency filters.
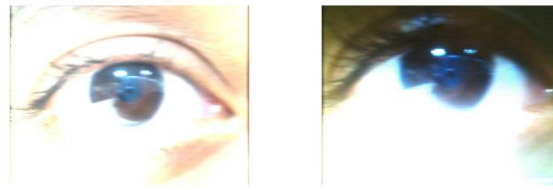
Figure 4.7: (a) High-frequency filter response of the real image of 4.5(c), (b) High-frequency filter response of the fake image of 4.5(d) [275].

4.2.1.2. Aspect-related Feature

Like the focus related features, aspect ratio-based features can also play an important role in aliveness detection in the visible spectrum. The reason because the images scanned for a system has a unique camera specification even this constraint is quite similar to cross sensor system scenario and they will produce a sound difference in aspect ratios between the real and fake image, which also reflected in the literature. Hence the various aspect ratio-based features should work well to discriminate between the real and fake image. A set of aspect related feature is proposed and explored here for the proposed liveness system.

- **The ratio of the pupil and the iris radius (QF4):** The first aspect related feature proposed here is the ratio of the pupil and the iris radius. The ratios were calculated by the integrodifferential operator proposed in [17].

- **The ratio of the iris radius and image length (QF5):** The aspect of the ratio of iris radius and image length is also expected to be different for a genuine image and a fake image. As because the original dimension of the real and fake eye image are different.

- **The ratio of the iris radius and image width (QF6):** The aspect of the ratio of iris radius and image length is expected to be similar to a genuine image even if the image is scanned from a small varying distance.

- **The ratio of the pupil radius and image width (QF7):** Similar to the previous quality feature QF6, an aspect ratio of the pupil radius and the image with it can play an important role as an aspect based quality feature. This explored quality feature is assumed to be different for real and fake images, as the papillary dilation changes for 2D (printed images or video use to spoof) and 3D objects (real human eye) will always be different.

- **The ratio of the pupil radius and image length (QF8):** Similar to the previous aspect feature based on the ratio of pupil radius and the image width, in this feature image length is introduced which is also expected to be enough capable of discriminating a live and fake image.

- **The ratio of the sclera length and image width (QF9):** In this aspect ratio based quality feature the ratio of sclera length and the image width is employed. The sclera length is estimated by calculating the length difference between the two corners of the eyes. At first, the sclera is segmented by the Time-Adaptive Region growing algorithm as proposed in [5]. Then the two corners are estimated by finding the first column of the binary segmented mask image having a white pixel and the corresponding last column having a white pixel as shown in Figure 4.8.

- **The ratio of the sclera length and image length (QF10):** As similar to QF9, sclera length is estimated by calculating the length difference between the two corners of the eyes from the sclera segmented image and then the ratio of the sclera length and image length is calculated.

- **The ratio of the sclera length and iris radius (QF11):** The ratio of the sclera length and the iris radius is one another quality feature that can be used for liveness detection. The sclera length is calculated in a similar way as in QF9.

Figure 4.8: Sclera length estimation technique adopted by calculating the two corners from the segmented mask [275].

- **The ratio of the sclera length and pupil radius (QF12):** The ratio of the sclera length and pupil radius is also a unique aspect for liveness detection, which is employed in this quality feature.

- **The ratio of the sclera segmented image and a binary image (QF13):** The ratio of the count of the white pixel of the segmented mask and the binary image achieved by applying Otsu's binarization method is quite different for the real and fake image because of the intensity distribution difference present in both category of image. This aspect related feature of the two binarization method is employed for liveness detection.

4.2.1.3. Contrast Related Feature

It can be easily visualised looking at the fake and the real images that there is a huge difference in the contrast distribution between both the category of image. As a reason, the contrast-related quality feature can be a key attribute to distinguish the fake and the real image correctly. So, the following contrast based quality features are proposed in this work.

- **Global contrast (QF14):** The global construct is the first contrast related quality feature employed in this work. The global construct of the image is calculated for each image as a quality feature, by the following equation.

$$\text{Contrast} = \text{Value of highest intensity - average intensity} \qquad (4.1)$$

   The global contrast of the fake image and the real image varies in a huge difference which is reflected from the images, so this feature plays an impotent role in this framework.

- **Local construct (QF15):** It is also evident from the fake and the real images that there is a good discriminable difference in local contrast in between them. So, the images are divided into10X10 patches and the contrast of each patch is summed to get the final representation. Similar to the global contrast, this feature also plays an impotent role in detecting liveness for this framework.

- **Local construct (QF16) at the channel level:** A new image channel based contrast related quality feature is proposed in this work for liveness detection. The images are divided into10X10 patches at each channel level (red, green and blue channel) and the contrast of each patch of subsequent channel representations are added to get the channel level local feature. Finally, the three channel level representations are added to get the final representation of this proposed feature.

- **Image red channel contrast (QF17):** Among the contrast related feature few channel based global feature is also proposed. In this feature, the red channel global contrast of the image is calculated by the following equation.

$$RcC = RcHi - \ RcAi \qquad (4.2)$$

Where   RcC= Red channel Contrunst.   RcHi= Value of highest intensity in the red channel of an image.

RcAi= Average intensity in red channel of an image;

- **Image green channel contrast (QF18):** In this feature, the green channel contrast of the image is calculated, similarly by equation 2 only by replacing the red channel attribute by green channel attribute. This was a most effective feature among other contrast feature.

- **Image blue channel contrast (QF19):** Similar to .red and green channel the blue channel contrast is proposed and calculated by the same equation employing the .blue channel contrast attributes. This quality based feature was also quite efficient at detecting liveness.

The result of the liveness detection after employing the above-mentioned set of the proposed quality feature is reported in the next section.

4.2.2. Experimentation Result

To justify practical effectiveness the proposed framework an experimental setup was designed, the detailed result of the experiment and the dataset used to implement the experiment is explained in the following sub-section.

4.2.2.1. Dataset

In order to implement the proposed aliveness framework and to assess the effectiveness of the proposed quality features an in-house dataset was prepared. This database consists of 200 real RGB images from both eyes of 25 identities (so 50 different eyes), 4 samples for each eye were captured. The database contains blurred images and images with blinking eyes. The high-resolution images (3200 × 2400) and 72 dpi are provided in the database. All the images are in JPEG format. The individual comprises of both male and female (14 male and 11 female), of different age and different skin colours were considered, 2 of them were wearing contact lens and the images were taken at the different time of the day. Have used different quality images and some of the sample images are shown in Figure 4.9. The images were captured using a Micromax mobile camera doodle version with an 8 megapixel rear camera.

Figure 4.9: Different real images of different quality in the dataset [275].

In order to emit the forge attack experiment, the fake images for enrolment were prepared automatically by displaying original the acquired images during real image enrolment, in a digital screen and then generate the fake image by, capturing the displayed image by a camera stalled in front of the screen. Varying type of display screen was used to emit the

real life scenario and the same standard sensor is used to acquire them. The 100 fake images were prepared by the above methodology for enrolment, 2 fake images for each eye. For testing, 100 fake images were prepared i.e. 2 images for each eye.

They were prepared either by scanning a high quality image captured from the same camera or a NIKON D 800 camera and 28300 lenses (as imposter can use very sophisticated camera to acquire the original biometric trait) or an low quality image capture by camera having same specification as the sensor and scanned from a portable screen like mobile notepad, etc. Even spoof images were also prepared from printed images printed from laser colour printer, employing the above mention the high and low-quality images and then scanned in front of the sensor. Examples of such few fake images are given in Figure 4.10.

(a)   (b)

(c)   (d)
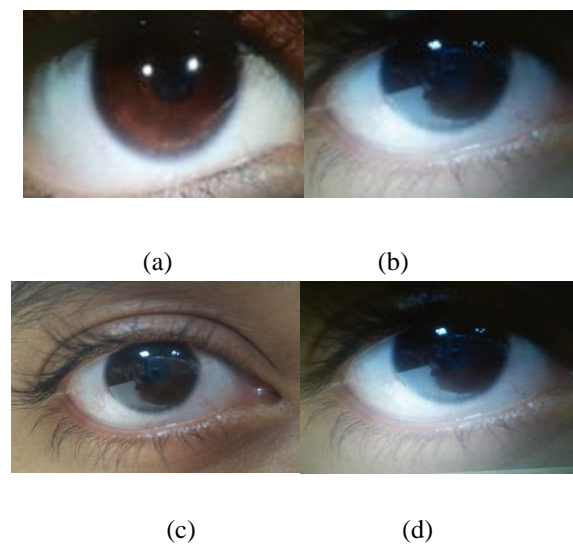
Figure 4.10: (a) Fake image capture from screen where the original image was captured by NIKON camera, (b) fake image capture from screen where the original image was captured by Micromax mobile camera, (c) fake image capture from printed image where the original image was captured by NIKON camera, and (d) fake image capture from printed eye where the original image was captured by Micromax camera [275]..

4.2.2.2. Classifier Used and Feature Selection and Optimization Technique

As liveness classification is a two-class classification problem and the dimension of the feature used are not large, so various pair-wise classifier such as a Euclidean distance, city block distance, Chebyshev distance, cosine distance, spearman distance, Hamming distance and Jaccard distance which are available in the literature are exploited here. Among them, the Jaccard distance produced the best result. For feature selection first found the performance of the individual features and then the feature producing the best result is combined with the second best result and so on.

4.2.2.3. Experimental Result Details

The liveness experimental results with various quality-based features are explained in this subsection. For training, five samples from each class from the fake and the genuine categories are used to produce the training model (the feature values are averaged to get the feature representation of each class) and the remaining five samples from each class of fake and genuine images were used for testing. The performances of the above-mentioned features individually and in combination are presented in Table 4.7.

The table illustrates the satisfactory performance of the proposed quality feature for both aspects of liveness detection (i.e. ability to classify genuine and fake samples correctly). It can be seen from the above Table that the focus-related features worked for detecting liveness. Aspect-related features worked better than the focus-related feature. Among the aspect-related features, the performance of the QF4 (i.e. the ratio of iris and pupil radius) was the best. Furthermore, the group of contrast-related features produced the best results. Among them, QF 18 i.e. the green channel contrast, outperformed the other quality features introduced here. As mentioned previously, a combination of this feature is also used to analyse the performance. Fused the features according to the performance rank so, combined the 1st rank feature with 2nd and so on. It can be concluded from Table 4.7 that the combination of the contrast-based features and the aspect-based features produced the best result.

Moreover, it will be also quite interesting to observe the correlations between the features. It can be seen from the results that the accuracy of the features is quite close. But the features are significant because when they are combined, they boost the accuracy as opposed to when they are applied individually.

Although the contrast-related features have worked exceptionally well in the proposed schema, unfortunately, such features can be attacked by intruders at the software level by using photometric normalisation. However, for such scenarios of attack, the intruder will be required to have technical details about the inner functionality and a clear architecture of the liveness system for tonal correction of the fake images. Moreover, they need to attack at the software level rather the sensor level, which is more difficult than a direct attack.

The feature distributions of the best discriminative features, such as the pupil and the iris radius QF4 and contrast quality features QF19, are shown in Figure 4.12 and the contrast quality features (QF14, QF17, and QF18) are shown in Figure 4.11. Although the cumulative frequency or the probability distributions, i.e. the score of the feature normalised at each class level, would have been a better measure, for better discernibility of the feature, this feature distribution is used. Moreover, the feature distribution is also a better measure to reflect the effectiveness of the feature at the class level and the database level. In each graph, the quality feature score distribution of the entire genuine sample is represented by a green line and the fake sample by a blue line. Along the X-axis is the

Table 4.7: Liveness detection performance of the various individual and combinations of image quality-based features.

	Feature	Test averaged accuracy in % achieved for	
		Fake samples	Genuine samples
Focus	QF1	81	79
	QF2	70	83
	QF3	76	80
Aspect features	QF4	95	94
	QF5	86	82
	QF6	87	84
	QF7	84	86
	QF8	87	84
	QF9	85	78
	QF10	84	70
	QF11	80	70
	QF12	78	78
	QF13	85	86
Contrast measures	QF14	96	96
	QF15	88	89
	QF16	89	90
	QF17	96	95
	QF18	98	97
	QF19	95	94
Combination	QF14+QF18	98	98
	QF14+QF17+QF18	98	99
	QF14+QF17+QF18+QF19	99	99
	QF4+QF14+QF17+QF18+QF19	100	100

sample and along the Y-axis is the feature value. In each of the lines in the graph, the first ten feature values represent the feature value of the ten fake/genuine samples of the first

class, the next ten from the second class and so on. It is clear from the graphs that the feature values of the fake and genuine samples have a discernible difference within each class. Whereas, if database-level feature distribution is considered, then this feature value would have a certain overlapping region. Therefore that creates confusion in the classification of 'alive' and fake data at the database level.

(a)

(b)

(c)
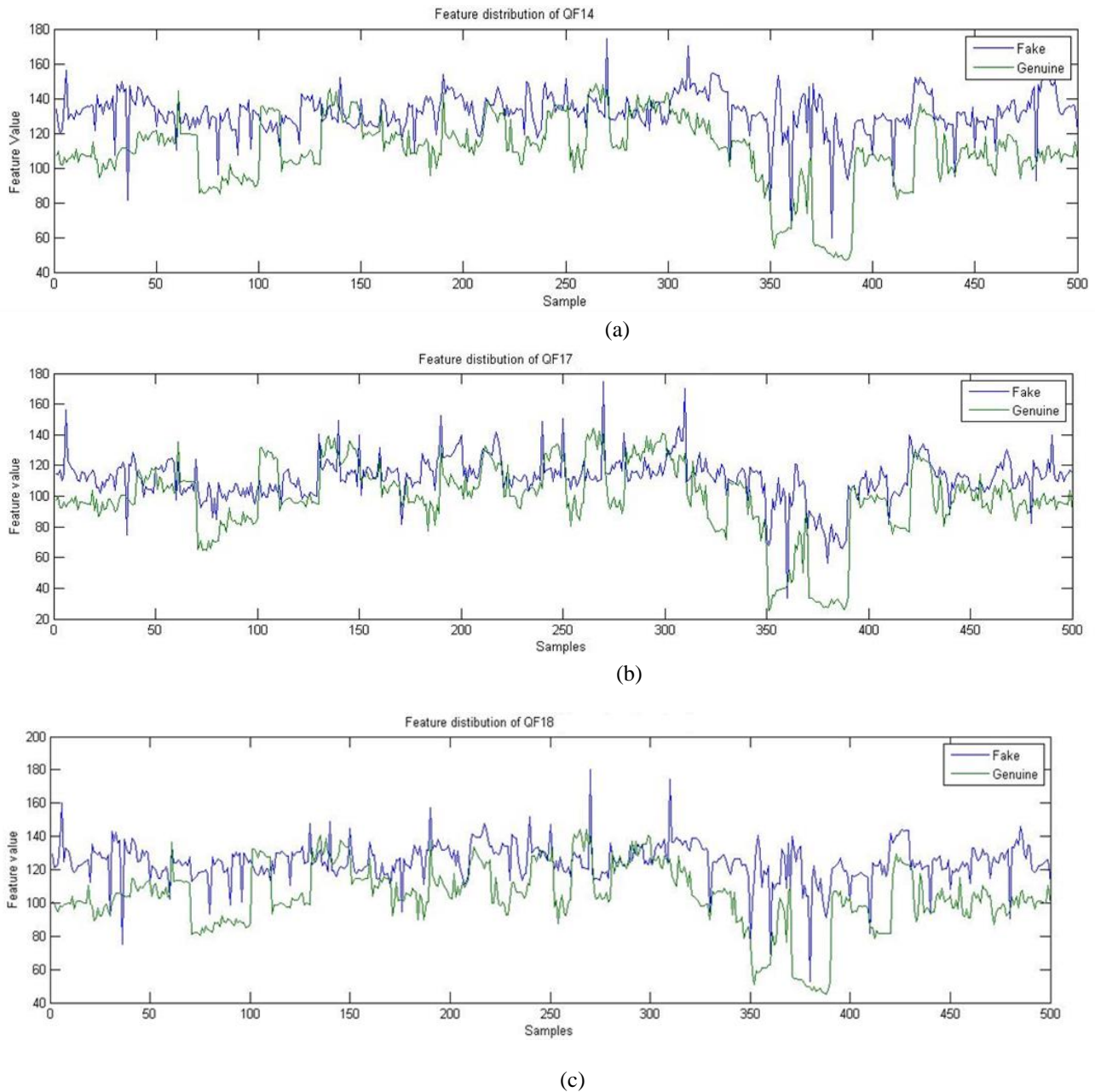
Figure 4.11. Feature distributions of the best discriminative quality features for the genuine and fake samples of each class (a) Global contrast QF14, (b) Red channel contrast QF17, and (c) Green channel contrast QF18 [275].

(a)

(b)
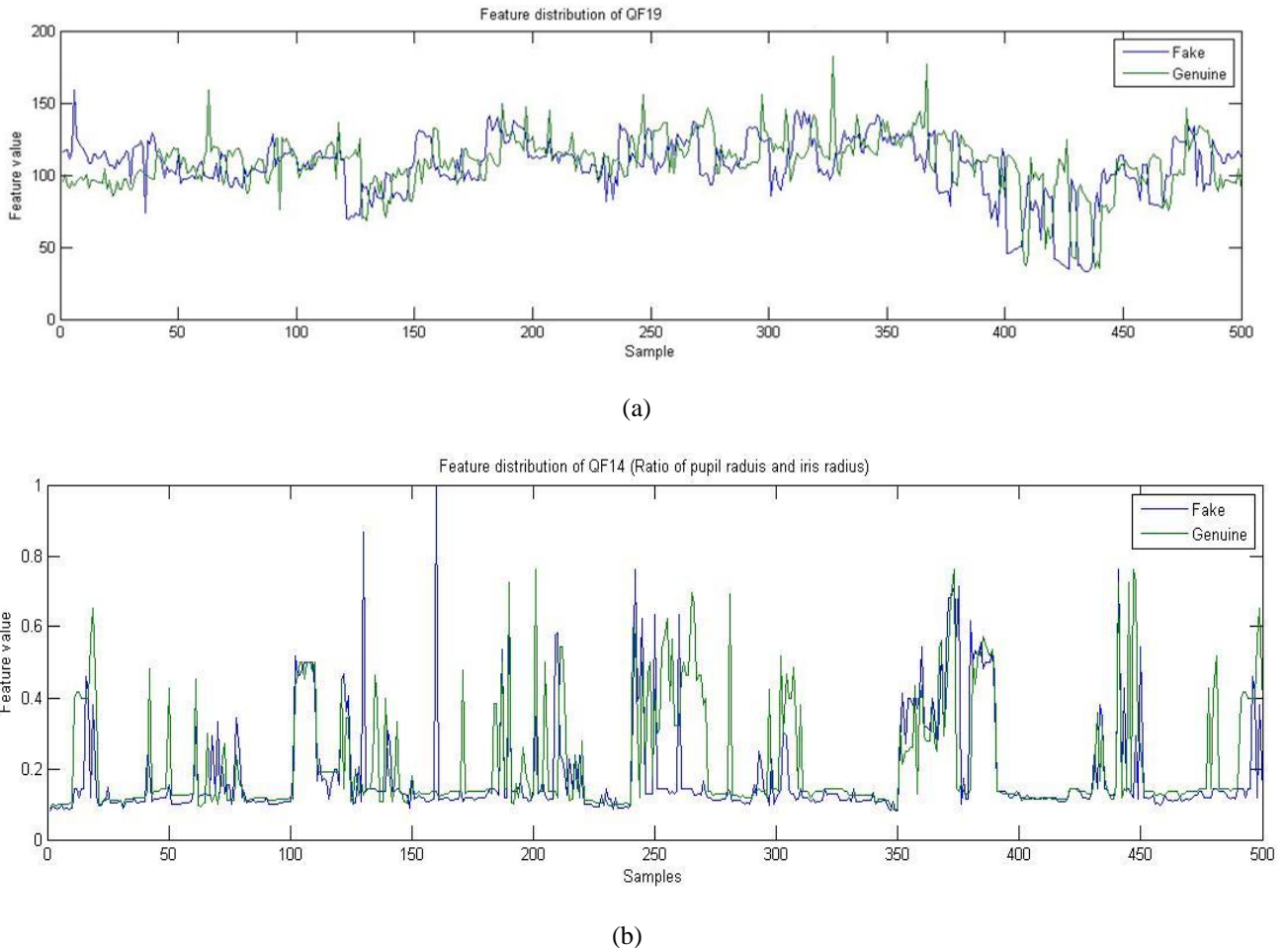
Figure 4.12: Feature distributions of (a) Blue channel contrast QF18, (b) QF4 (is the ratio of the pupil and the iris radius) [275].

4.2.2.4 Comparison with the State-of-the-art Methods

The performance of the above-mentioned framework is compared with the most relevant previously proposed liveness framework in Galbally et al., [102] using the proposed set of quality features, feature selection process and classification technique. The results producing the better performance were on the basis of the newly proposed liveness framework. The detailed comparison of the results of the two frameworks is given in Table 4.8. It can be seen from Table 4.8 that the focus-related feature worked averagely for detecting liveness in the previous framework of Galbally et al., [102]. Whereas the aspect-related feature worked less accurately than the focus-related feature. Furthermore, the group of contrast-related features produced the best result. Similar to the results of Table 1, here also the QF18, i.e. the green channel contrast, outperformed every other quality feature introduced here. The combination of the features was also performed, and the improvement in results was noticeable.

Table 4.8: The detailed performance-based comparison of results between the proposed framework and the framework presented in Galbally et al., [102] using the proposed set of quality features.

	Feature	Test averaged accuracy in % achieved for	
		Proposed framework	Framework Galbally et al., [102]
Focus	QF1	80	70
	QF2	77	73
	QF3	79	74
	QF4	95	86
Aspect features	QF5	84	83
	QF6	85	80
	QF7	85	80
	QF8	85	78
	QF9	81	75
	QF10	77	74
	QF11	75	74
	QF12	78	70
	QF13	86	80
	QF14	96	89
	QF15	88	84
Contrast measures	QF16	90	82
	QF17	96	88
	QF18	97	100
	QF19	95	87
Combination	QF14+QF18	98	91
	QF14+QF17+QF18	99	93
	QF14+QF17+QF18+QF19	99	94
	QF4+QF14+QF17+QF18+QF19	100	94
	All	100	94

Although the proposed aspect-related features worked for the previous framework in Galbally et al., [102], it is clear from the above Table that the concept of class-level liveness classification has outperformed the database-level liveness detection/classification by an appreciable margin. These results and comparisons demonstrate the effectiveness of the proposed framework in contrast to the previous framework.

For further analysis and comparisons, the best quality feature combinations in Galbally et al., [102] i.e. the combination of occlusion (pupillary dilation), global contrast and local construct are applied in the database, both using the class-level liveness classification and database-level classification. In the database level classification, these features were able to discriminate 94% of the genuine and 89% of the fake images. Whereas, in the inter-class level liveness framework, these same features were able to correctly discriminate only 95% of the genuine and 93% of the fake images.

From the above analysis, it is again demonstrated that the class-level classification is more efficient than the database-level liveness classification framework. Moreover, it is also clear that the best quality feature combination of Galbally et al., [102] in the class-level classification could not outperform the result of the proposed quality-related feature.

Another comparison was performed with a very recent and most efficient work on ocular liveness detection proposed in Sequeira et al., [122]. The liveness algorithm of the above-mentioned research was employed using the framework and the proposed database to perform the analysis. On the basis of the experiments performed it is clear from the results that it can only efficiently classify 89% of the fake images and 94% of the real images.

Whereas, employing their algorithm at the database-level liveness framework and using the database, the result was less effective. Thus, similar to the previous analysis, this analysis also demonstrates the superior effectiveness of the proposed framework and the feature set.

So, from the above analysis, the effectiveness and applicability of the proposed framework in a real-life scenario are demonstrated. Moreover, the effectiveness of the quality features is also justified on the basis of the above comparison.

4.3. Summary

This chapter proposes a new liveness detection approach for multimodal ocular biometrics in the visible spectrum based on multi-angle eye images and image quality features. Both methods seem to achieve potential results. The novel framework proposes inter-class/class level liveness detection based on the combination of domain transforms, geometrical ratios and contrast measures.

Furthermore, this framework and the new quality features proposed can also be used to explore liveness detection of multimodal biometric traits across the visible spectrum, in a more realistic and accurate way compared to previous liveness detection schemas. The success of the proposed framework and the proposed set of quality features of liveness are evident from the experimental results. Moreover, a new database is proposed for liveness detection, consisting of fake images that were developed with more versatile forging technology that can be used by intruders. Moreover, the images in the database also contain sufficient accurate biometric information for the aforementioned ocular traits.

5

Proposed Methodologies for Adaptive Biometrics

In this chapter, we address the potential incremental learning techniques which can be applied in the biometric domain to create an adaptive learning system. The motivation to create an adaptive learning system for biometrics is explained below. In real-world scenarios, where we use machine learning algorithms, we often have to deal with cases where the input data changes its nature with time. In order to maintain the accuracy of the learning algorithm, we frequently have to retrain the learning system, thereby making the system inconvenient and unreliable. This problem can be solved by using learning algorithms which can learn continuously with time (incremental/online learning). In contrast, offline learning works fine in an ideal scenario where there is no change in the underlying distribution of the input with time. However, for various reasons, this does not often hold in real time problems that are intended to address (i.e. of the robust biometric system) using machine learning.

In contrast to offline learning, ideally, incremental/online learning can be simultaneously trained and tested. Precisely, it need not stop performing its task (i.e. prediction or classification) if the learner has to update its learning parameters. Learning parameters can be updated as soon as the new training data is available. This leads to the creation of a never-ending learning process which can adjust itself even if the environment changes and can perform learning while performing the task.

The critical assumption on which most of the incremental learning algorithms are based upon is that previous data is completely or partially accessible. Based on this assumption, to handle streaming data they apply the time windowing technique of either fixed or variable size [146, 143 and 146]. Others have handled streaming data by weighting models in the ensemble [144, 147 and 148] or by weighting the data [149] or by retaining only the relevant subset of previous data [143 and 144]. It is assumed for experimentation that there is no access to the previous data, thus making the algorithm capable of handling the scenario where old data is inaccessible. Despite these above-highlighted advantages, a lot of limitations is also associated with the existing online to the employee for adaptive biometric systems.

The main challenge is feeding substantial amount of samples for such systems, for which need to acquire a large number of samples which is a quite time consuming and complex process. If an adopted self-updating system captures only limited amount samples during enrollment, a large number informative and significant variations remain unenrolled and as a result, it can achieve limited performance gain or even loss over the performance of baseline system.

To overcome this in the next section framework is proposed and discuss some potential methods which can be used to make an adaptive biometric system. Next, the experimental details and that were produced are exploded. Major parts of the chapter have been published in the articles Das et al. [274].

5.1. Proposed Framework for Adaptive Biometrics

In a biometric system requires 1 to 1 or 1 to n match as its intended to verify or recognise the claimers identity by matching the presented biometric property with the enrolled biometric knowledge base. This scenario can be mathematically formulated by:

Let f be a mathematical representation of the biometric property or feature vector extracted from the presented biometric image and e be the enrolled representation feature vector stored for the claimed identity I.

The task is to determine if the pair (I, f) belongs to class I which is to accept (genuine) the user or class else which is to reject (imposter) the user.

Let S(f, e) denote the distance matching score computed by matching e and f and T denotes the threshold determined at the learning stage. Then the verification/ recognition is defined as:

$$(l, f) \in \frac{I, \text{if } S(f,e) \qquad < T}{class\ else, \qquad otherwise} \qquad (5.1)$$

Unfortunately, in real verification or recognition applications, it is usually difficult to design a classifier that satisfies the above assumption of classification and minimise errors. As a reason, various types of classifiers are assembled to build a more reliable classifier. The same disadvantage is true for the base classifier and the online version of the base classifier. The base classifier lacks in performance in long run. Whereas, the main challenge that is faced in the online learning is the substantial number of sample to train the classifier. In contrast, the number of samples to train a non-online or the base classifier needs less amount of training samples. If we compare their performance, the base classifier will give a respectable accuracy in the initial query samples, whereas the online learner will perform better in long run. Therefore, it can be assumed that a combination of these two can be a solution if we can adjust them and utilise them in their point of best performance. Therefore, this work proposed the below framework blending both the classifier, via cascade classifier method.
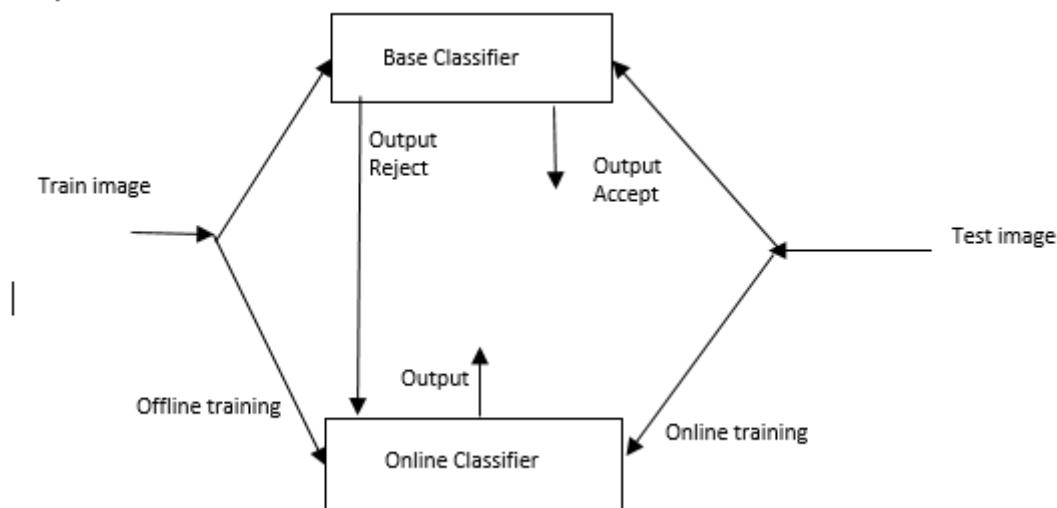
Figure 5.1: Proposed Adaptive biometric framework using cascade based classifier selection.

In the above framework, the base classifier and the online classifier version of the base classifier are cascades in a framework. As shown in the Figure the training images are both utilised by the base classifier for training and offline training for the online classifier. Whereas the test images are used for testing in base classifiers and in the online version, it is also used for online training. The base classifier cascades the online version of it. If the output of the base classifier is rejected with low confidence score less than *t,* then classification decision of online version of the base classifier is considered as the output, otherwise, the decision of the base classifier is considered as the output. Although must be mentioned that the framework can face a risk of FAR but ensure better FRR. The online classifiers used for the proposed framework are described in the next sections.

5.2. Ensemble of Classifiers

Since the inception of ensemble-based classification, it has been one of the most studied classification methods [151, 152]. Ensemble-based classifiers have often been used in past for performing incremental/online learning [144, 146, 147, 150, 152, 153]. The principle behind the ensemble decision is that the individual predictions combined appropriately should have better overall accuracy, on average, than any individual ensemble member [152]. There are various reasons why an ensemble-based classification is chosen over a single classifier, a few are listed below.

1. No free lunch theorem states that in the absence of prior knowledge about a problem, no one classifier is universally better than any other classifier [154], this also includes random guessing.

2. In the case of extremely high dimensional data, a single classifier's complexity may scale with the dimensionality of the data thus making the generation of a reliable single classifier infeasible. Instead of a single classifier, generate multiple classifiers on different subsets of features thus reducing the complexity of each classifier trained on the subset.

3. Single classifiers may not work well with data that are too little or too large in size. To work around this problem, ensembles can generate classifiers on multiple bootstrap datasets.

4. Reduces bias towards majority class (a class that is well represented by training samples). And generating single strong classifier may be infeasible due to computational costs.

The success of ensemble learning algorithms is believed to depend both on the accuracy and on the diversity among the base learners [155] and some empirical studies revealed that there is a positive correlation between accuracy of the ensemble and diversity among its members [156, 157]. Breiman [69] also shows that random forests with lower generalisation error have a lower correlation among base learners and higher base learners' strength. Besides, he derives an upper bound for the generalisation error of random forests which depends on both correlation and strength of the base learners.

Literature suggests that there is a trade-off between base learner's accuracy and diversity, meaning that lower accuracy may indicate higher diversity. However, a study in [158] shows that relationship between accuracy and diversity is not straightforward and lower accuracy may not essentially mean higher diversity. A recent study in Freund et al, [159, 160] discusses that when, how and why ensembles of learning machines can help to handle concept drift in online learning, through a diversity study in the presence of concept drift. This work presents an analysis of low and high diversity ensembles combined with

different strategies to deal with concept drift and proposes a new approach "Diversity for Dealing with Drifts" (DDD) to handle drifts. DDD maintains ensembles with different diversity levels, exploiting the advantages of diversity to handle drifts and using information from the old concept to aid the learning of the new concept. The authors claim that DDD is accurate both in the presence and in the absence of drifts.

In a recent study in Kunwar et al, [161] has reiterated the efficacy of ensemble-based learning to create an adaptive/online learning system for handwritten character recognition, have used that method to make an adaptive biometric system which learns using one sample at a time. The system as presented in Kunwar et al, [161] is briefly described below.

The block diagram is shown in the Figure.5.2 shows the overall picture of the online learning method proposed in Kunwar et al, [161]. The method proposed in the work is to conduct both online supervised as well as online semi-supervised learning. In general, to conduct semi-supervised learning abundant unlabeled data is required but unfortunately, we have very limited number of samples/class in the biometric learning problem. Therefore, only online supervised learning can be conducted but with the availability of more data in future, semi-supervised online learning as well can be used. Technical details are given below:

Let us introduce some notation to describe the data. Training dataset $\chi = \{(X^1, Y^1) \dots (Y^N, Y^N)\}$ where $X^i = x_1^i \dots x_D^i$, $X^i \epsilon R^D$, are the samples in a D dimensional feature space and $Y \epsilon \{1, \dots K\}$ are the corresponding labels for a K-class classification problem.

Using Bayes rule and conditional independence among the feature given the class label (assumption used to formulate Naïve Bayes classifier), can write the posterior probability as:

$$P(Y = y_k | x_1 \dots x_D) = \frac{P(Y=y_k) \prod_i P(x_i|Y=y_k)}{\sum_j P(Y=y_j) P(x_1 \dots x_D|Y=y_j)} \tag{5.2}$$

So to train classifier can fit a Gaussian $\mathcal{N}\left(x_i; \widehat{\mu_{lk}}, \widehat{\sigma_{lk}^2}\right)$ to each $P(x_i|Y = y_k)$, and estimate mean and variance for the same using the training data. Next, perform Maximum Likelihood Estimation (MLE) to find the mean $\widehat{\mu_{lk}}$ and variance $\widehat{\sigma_{lk}^2}$ of $P(x_i|Y = y_k)$ for each feature x_i, which is just equal to sample mean and sample variance respectively. And the classification rule for a new sample $X^{new} = <x_1 \dots x_D>$ can be written as

$$Y^{new} = \arg max_{y_k} P(Y = y_k) \prod_i P(x_i|Y = y_k) \tag{5.3}$$

$$^{new} = \arg max_{y_k} \pi_k \prod_i \mathcal{N}\left(x_i^{new}; \widehat{\mu_{lk}}, \widehat{\sigma_{lk}^2}\right) \tag{5.4}$$

In order to make an ensemble of B classifiers, repeat the following steps B times: Randomly select F features from the pool of D features. Estimate the learning parameters for the classifier.
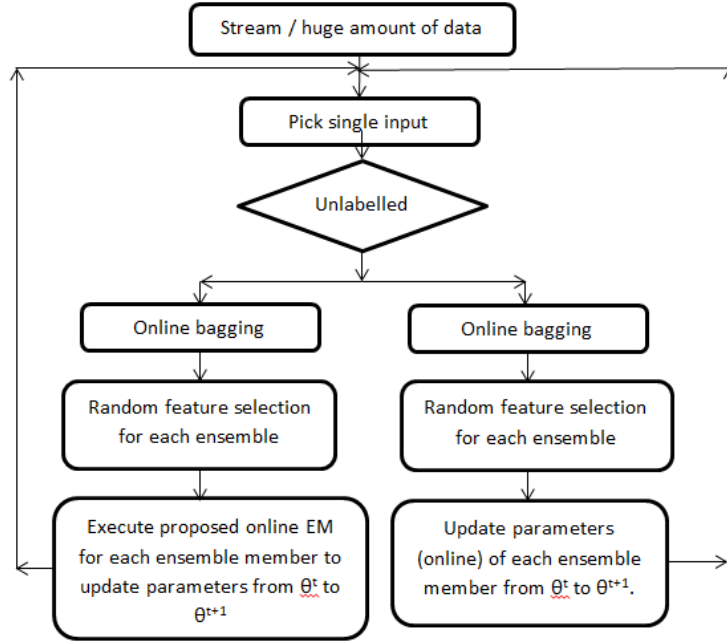
Figure. 5.2: Block diagram representing the batch learning (MLE) of Augmented Naive Bayes network [274].

A test sample will be classified by each classifier in the ensemble and the class which gets the majority vote by the ensemble will get assigned to the test sample. In an above-explained way an ensemble of B classifiers is trained as an initialization step, by just 1 samples/class. Beyond this with time, as we get more samples of a class, we can update its respective learning parameter as shown below in an online (on the fly) manner using 1 sample at a time. This enables the system to adapt to the changes in the underlying distribution of input samples. Initialization (by just one labelled training sample):

$$\widehat{\mu_{ik}} = x_{ik}^1 \; ; \; \widehat{\sigma_{ik}^2} = \sigma_0 \; ; \; \pi_k = \frac{1}{no. \, of \, classes} \; ; \; c_k = 1 \; ; \; \alpha = \alpha_0$$

Where $c_k = no. \, of \, samples \, used \, so \, far \, for \, training,$

$\alpha = decides \, the \, length \, of \, memory \, of \, the \, classifier \, (\alpha < 1)$

Repeat steps below for all the incoming labelled training samples for any class k:

$$c_k = c_k + 1 \; ; \; \eta_k = \left(\frac{1-\alpha}{c_k} + \alpha \right) \qquad (5.5)$$

where η_k is learning rate for class k

$$\mu_{ik}(t) = (1 - \eta_k)\mu_{ik}(t-1) + \eta_k x_i^j \delta\big(Y^j = y_k\big) \qquad (5.6)$$

$$\sigma_{ik}^2(t) = (1 - \eta_k)\sigma_{ik}^2(t-1) + \eta_k \left(x_i^j - \mu_{ik}(t)\right)^2 \delta\big(Y^j = y_k\big) \qquad (5.7)$$

In the same paper of Kunwar et al.[161], another method has been suggested to conduct online learning in a semi-supervised manner. The only difference between supervised online learning and semi-supervised online learning lies in the definition of learning rate. Learning rate definition for semi-supervised learning is:

$$\eta_k = q_k \left(\frac{1-\alpha}{c_k} + \alpha\right)\lambda \, ; \; (\alpha < 1) \qquad (5.8)$$

Where λ = weight factor applied to moderate the contribution of unlabelled data in the parameter estimation step.

If an incoming new sample is unlabelled then the trained classifier is used to produce the posterior $q_k = P(Y^j = y_k | X)$ corresponding to all k (class). This posterior will be used to calculate the learning rate corresponding to all the classes and subsequently this learning rate will be used to update learning parameters of all the classes as is done in case of the supervised online learning.

In Kunwar et al, [161] the authors have upgraded the Naive Bayes network structure and have suggested a method to conduct an online learning for that upgraded network. The network structure was upgraded to get rid of the Naïve Bayes unrealistic assumption of conditional independence between different features given the class label. The structure was upgraded with a restriction that all the features will have at most two parents (earlier each had just one) Figure 5.3. The improved structure was proved to be working much better in the concerned application. The technical detail is briefly explained below.
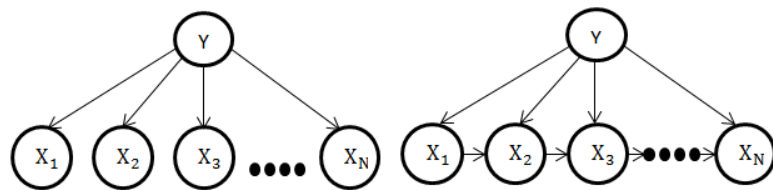
Figure 5.3: Left: Bayes net for Naive Bayes. Right: Bayes net for Augmented Naive Bayes [274].

$P(X_i | X_{i-1}, Y)$ can be parameterized by the following Gaussian distribution: $P(X_i | X_{i-1}, Y) = N(\beta_0 + \beta_1 X_{i-1}, \sigma^2)$

The author in Kunwar et al, [161] performs MLE estimation to evaluate the learning parameters $\beta_0, \beta_1 \; and \; \sigma^2$ for supervised learning

$$\beta_1 = \frac{E_D[X_i X_{i-1}] - E_D[X_i] E_D[X_{i-1}]}{E_D[X_{i-1} X_{i-1}] - (E_D[X_{i-1}])^2} = \Sigma_{X_{i-1} X_{i-1}}^{-1} \Sigma_{X_i X_{i-1}} \tag{5.9}$$

$$\beta_0 = \mu_{X_i} - \Sigma_{X_{i-1} X_{i-1}}^{-1} \Sigma_{X_i X_{i-1}} \mu_{X_{i-1}} \tag{5.10}$$

$$\sigma^2 = \Sigma_{X_i X_i} - \Sigma_{X_i X_{i-1}} \Sigma_{X_{i-1} X_{i-1}}^{-1} \Sigma_{X_i X_{i-1}} \tag{5.11}$$

The authors further propose to update $E_D[X_i]$, $E_D[X_{i-1}]$, $E_D[X_{i-1} X_{i-1}]$,

$E_D[X_i X_{i-1}]$ in an online manner in order to update $\beta_0, \beta_1 \text{ and } \sigma^2$ because they are the building block which is obvious from their definition. Hence, it can be written as:

$$E_D[X_i](t) = (1 - \eta_k) E_D[X_i](t - 1) + \eta_k X_i \tag{5.12}$$

$$E_D[X_{i-1}](t) = (1 - \eta_k) E_D[X_{i-1}](t - 1) + \eta_k X_{i-1} \tag{5.13}$$

$$\sigma_{X_{i-1}}^2(t) = (1 - \eta_k) \sigma_{X_{i-1}}^2(t - 1) + \eta_k \left(X_{i-1} - E_D[X_{i-1}](t)\right)^2 \tag{5.14}$$

Covariance between two RVs, A and B is given by:

$$\sigma_{A,B} = E[AB] - E[A] E[B] \tag{5.15}$$

Therefore: $E_D[X_{i-1} X_{i-1}](t) = \sigma_{X_{i-1}}^2(t) + \{E_D[X_{i-1}](t)\}^2$

Similarly: $\sigma_{X_i X_{i-1}}(t) = (1 - \eta_k) \sigma_{X_i X_{i-1}}(t - 1) + \eta_k \left(X_i - E_D[X_i](t)\right)\left(X_{i-1} - E_D[X_{i-1}](t)\right)$

Using the above equations:

$$E_D[X_i X_{i-1}](t) = \sigma_{X_i X_{i-1}}(t) + E_D[X_i](t) E_D[X_{i-1}](t) \tag{5.16}$$

In the equations above, η_k refers to learning rate and its definition is same as in case of Naïve Bayes online learning case. And along similar lines, online semi-supervised learning was proposed with a changed definition of learning rate. It has been shown that the upgraded network performs much more accurately as it captures the relationship between different features and accordingly learns. Details can be found in Kunwar et al, [161].

5.3. Incremental/Adaptive Support Vector Machines (SVMs)

SVM is based on a kernel method; however unlike suboptimal kernel methods, as in the case of a kernel method based on clustering, kernel methods for SVMs are optimal, with the optimality being rooted in convex optimisation. Realising the theoretical strength of SVMs, researchers have developed incremental versions of them. And considering the fact that incremental SVMs have never been explored in the biometric domain, it becomes

imperative to discuss SVMs and their incremental versions in the context of adaptive biometrics.

Classification and regression methods based on SVMs in Vladimir and Vapnik [162] are very powerful, which generalise well even in the case of very sparse and high dimensional data. SVM is based on Vapnik's structural risk minimization induction principle which carries out searching over hypothesis classes of varying capacity with best generalisation performance.

A two-class classifier based on SVM can be represented as $f(X) = w.\varphi(X) + b$ are learned from the data $\chi = \{(X^1, Y^1) ... (Y^N, Y^N)\}$ where $X^i = x_1^i ... x_D^i, X^i \epsilon R^D$ and $Y^i \epsilon \{-1,1\}$ by minimizing

$$\min_{w,b,\xi} \frac{1}{2}||w||^2 + C \sum_{i=1}^{N} \xi_i^p \tag{5.17}$$

For $p \in \{1,2\}$ subject to the constraints (soft margin)

$$Y^i\left(w.\varphi\left(X^i\right) + b\right) \geq 1 - \xi_i^p, \; \xi_i^p > 0 \; \forall \; i \; \in \; \{1, ..., N\} \tag{5.18}$$

A set of slack variables are introduced for the system to allow few samples to be on the wrong side of the margin (to handle overlapping class distributions) but impose penalty of $\xi_i^p = |Y^i - f(X^i)|^p$ over the objective cost for the samples to be on the wrong side of the margin boundary. Value of $\xi_i^p = 0$ for being on the correct side of the margin boundary. p = 1 is what generally preferred in practice because of the robustness to outliers that hinge loss offers as compared to the quadratic loss which corresponds to p = 2. The goal is to minimize above the objective function while softly penalizing the points that lie on the wrong side of the margin boundary. Parameter C > 0 controls the trade-off between the slack variable penalty and the margin. Above minimization can be done using quadratic programming but to simplify and take advantage of the kernel trick the above minimization problem is expressed in its dual form

$$\min_{0 \leq \alpha^i \leq C} W = \frac{1}{2}\sum_{i,j=1}^{N} \alpha^i Q^{ij} \alpha^j - \sum_{i=1}^{N} \alpha^i + b \sum_{i=1}^{N} Y^i \alpha^i \tag{5.19}$$

With the Lagrange multiplier (and offset) b and $Q^{ij} = Y^i Y^j \varphi(X^i). \varphi(X^j)$. The above dual form of the original minimization problem must satisfy the famous Karush-Kuhn-Tucker (KKT) condition. The KKT conditions generally involves the Primal constrains, dual constrains and complementary slackness. Therefore the above dual form along with the KKT condition gives rise to a linearly constrained quadratic programming problem. And there are standard solvers available to solve them. The resulting dual form of the SVM is then $f(X) = \sum_{i=1}^{N} y^i \alpha^i \; \varphi(X^i)\varphi(X) + b$. Point to be noted here is that the transformed sample now only appear in dot product. Therefore one can employ a positive definite kernel

function to implicitly project the input samples into some high dimensional (which can be infinite) space and calculate the dot product to perform classification or regression in that space.

In the mid-90's Support Vector Machines (SVMs) emerged and subsequently researcher's interest in its online version arose. Early work on this subject by [163] suggests that for each new batch of data, a Support Vector Machine is trained on the new data and the Support Vectors from the previous learning step. And the logic behind this approach is that the decision function of an SVM depends only on its Support Vectors, i.e. training an SVM on the Support Vectors alone results in the same decision function as training on the whole data set. Because of this, one can expect to get an incremental result that is equal to the non-incremental result, if the last training set contains all examples that are Support Vectors in the non-incremental case. However, the shortcoming of this approach is that as there are typically only very few Support Vectors, their influence on the decision function in the next incremental learning step may be very small if the new data is distributed differently. Note: Support Vectors are a sufficient description of the decision boundary between the examples, but not of the examples themselves.

The above problem was addressed in [164] by making a clever change in the objective function to be optimised, and i.e. by making the error on old Support Vectors (which represent the old learning set) more costly than an error on a new example. Details can be found on the concerned paper. At the same time [165] exploits the locality of the RBF kernel to build online SVM. The authors do not use all the previous support vectors (as done in [67, 68]), instead, it only uses the support candidates in the neighbourhood of the new incoming sample. Though deciding the neighbourhood is critical, the method would be fast. However above three approaches and methods proposed by [166]; provide an only approximate solution and may require many passes through the dataset to reach a reasonable level of convergence.

An exact solution to the problem of online SVM learning has been found by [167]. Their incremental algorithm updates an optimal solution of an SVM training problem after one training example is added (or removed). In this, the authors construct the solution recursively one point at a time such that the KKT condition is satisfied over all the data are already seen as well as the new incoming samples.

The first order condition on W reduces to KKT condition:

$$g^i = \frac{\partial W}{\partial \alpha^i} = \sum_{j=1}^{N} Q^{ij}\alpha^j + Y^i b - 1 = Y^i f(X^i) - 1 \qquad (5.20)$$

$$g^i = \begin{cases} \geq 0 & \alpha^i = 0 \\ = 0 & 0 < \alpha^i < C \\ \leq 0 & \alpha^i = C \end{cases}$$

$$\frac{\partial W}{\partial b} = \sum_{j=1}^{N} y^j \alpha^j = 0$$

This partitions the data into three categories:

A) $x^i \in S \subset \chi$ where S is a set of margin support vectors, strictly on the margin (i.e. $Y^i f(X^i) = 1$).

B) $\in O \subset \chi$, where O is the set of other vectors for which $Y^i f(X^i) > 1$ i.e. the sample is on the correct side of the margin boundary (correctly classified).

C) $x^i \in E \subset \chi$ where E is a set of error vectors $Y^i f(X^i) < 1$, sample is on the wrong side of the margin boundary but not necessarily misclassified.

The set $R = \{O \cup E\}$ is a set of reserve vectors. Lowercase letters s, e, o and r will be used to refer to such kind of partitions.

By writing the KKT conditions before and after an update $\Delta\alpha$ obtain the following conditions that must be satisfied after an update [167]:

$$\begin{bmatrix} \Delta g^c \\ \Delta g^s \\ \Delta g^r \\ 0 \end{bmatrix} = \begin{bmatrix} Y^c & Q^{cs} \\ Y^s & Q^{ss} \\ Y^r & Q^{rs} \\ 0 & Y^{sT} \end{bmatrix} \begin{bmatrix} \Delta b \\ \Delta\alpha^s \end{bmatrix} + \Delta\alpha^c \begin{bmatrix} Q^{ccT} \\ Q^{csT} \\ Q^{crT} \\ Y^c \end{bmatrix} \tag{5.21}$$

It is easy to see that $\Delta\alpha^c$ is in equilibrium with $\Delta\alpha^s$ and Δb in order for the above condition to hold. Considering the fact that $\Delta g^s = 0$, from line 2 and 4 of the above equation can be written:

$$\begin{bmatrix} 0 \\ 0 \end{bmatrix} = \begin{bmatrix} 0 & Y^{sT} \\ Y^s & Q^{ss} \end{bmatrix} \Delta s + \begin{bmatrix} Y^c \\ Q^{csT} \end{bmatrix}; where \ \Delta s = \begin{bmatrix} \Delta b \\ \Delta\alpha^s \end{bmatrix} \tag{5.22}$$

Above linear equation can be solved for Δs

$$\Delta s = \beta \Delta\alpha^c$$

Where

$$\beta = - \begin{bmatrix} 0 & Y^{sT} \\ Y^s & Q^{ss} \end{bmatrix}^{-1} \begin{bmatrix} Y^c \\ Q^{csT} \end{bmatrix} \tag{5.23}$$

is the gradient of the manifold of optimal solutions parameterized by α^c

Similarly from line 1 and 3

$$\begin{bmatrix} \Delta g^c \\ \Delta g^r \end{bmatrix} = \gamma \Delta \alpha^c \qquad (5.24)$$

Where

$$\gamma = \begin{bmatrix} Y^c & Q^{cs} \\ Y^r & Q^{rs} \end{bmatrix} \beta + \begin{bmatrix} Q^{ccT} \\ Q^{crT} \end{bmatrix} \qquad (5.25)$$

is the gradient of the manifold of gradient g^r at an optimal solution parameterized by α^c. These refined set of equations shows that that update process is controlled by very simple sensitivity relation: $\Delta s = \beta \Delta \alpha^c$ and $[\Delta g^c \quad \Delta g^r]^T = \gamma \Delta \alpha^c$, where β is the sensitivity of Δs with respect to $\Delta \alpha^c$ and γ is the sensitivity of Δg^c *and* Δg^r with respect to $\Delta \alpha^c$.

At this stage to carry out the parameter update process, the key is to find out the largest possible increment of $\Delta \alpha^c$ and subsequently Δs and Δg is updated. Authors of Cauwenberghs and Poggio [167] have very exhaustively addressed all the cases by which one can determine the largest value of $\Delta \alpha^c$. And once the step is determined, one can follow the steps of algorithm 1 given in Laskov et al, [168] to carry out online learning.

Finding an absence of a well-accepted implementation of the work by [167]; [168] proposed a new design of storage and numerical operation which speeds up the incremental SVM training by a factor of 5 to 20. On the similar line, [169] have applied the accumulated knowledge of optimisation to the computational problem presented by the SVM to propose a very efficient way of training SVM in an incremental fashion.

5.4. Incremental/Adaptive Neural Network

Neural Networks is one of the oldest methods of machine learning, it is very obvious that umpteen amount of work has been done on that domain and many of them deal with incremental and adaptive learning. Following is the list of few Neural Network which can be useful to create an adaptive biometric system.

Fuzzy ARTMAP: This is a neural network based structure and it is one of the earliest methods used in incremental learning. The fuzzy ARTMAP has two fuzzy ART modules that are linked via an inter-art module known as "map field". The map field is used to form predictive categories for learning class association. Fuzzy ARTMAP will generate new decision clusters in response to new input patterns that are sufficiently different from previously seen instances. The 'sufficiently different' patterns are controlled using a free parameter of ARTMAP known as the vigilance parameter. ARTMAP is sensitive to the vigilance parameter especially in presence of significant noise in the training data. Using stability and match tracks, fuzzy ARTMAP automatically constructs as many categories as are needed to learn any static training set to 100%. Thus, fuzzy ARTMAP may over-fit, leading to poor generalisation.

Learn ++: This is one of the most notable families of the incremental learning algorithm, which was first introduced by Polikar et al. in [170] and later upgraded by few other authors for e.g. [171]. It creates multiple classifiers to each data chunk presented to the system. Inspired by AdaBoost [172, 173] for each chunk, the training set for each base learner is created by sampling examples according to a distribution of probability. Like AdaBoost, Learn++ maintains a distribution of instance weights; however, Learn++ does not update the weights in the same manner as performed with AdaBoost. In AdaBoost, the distribution of probability is built to give higher priority to instances misclassified by the last previously created classifier whereas Learn++ uses the ensemble decision, rather than the decision of the latest classifier. When a new dataset arrives, the distribution is re-initialized by evaluating the entire ensemble and initializing the distribution. Pros: Learn++ does not have to access the previous data chunks and it demonstrates considerable improvement at generalisation when compared with fuzzy ARTMAP on common databases. *Cons:* Problem is that a new set of classifiers is created for each new data chunk. So, the ensemble size can become extremely large considering lifelong learning.

Self-Organized Incremental Neural Network (SOINN): This is an unsupervised incremental learning method which was proposed in [178] for topology learning and classification to handle noisy unlabelled data. This method is essentially a combination of the self-organizing map [180] and competitive Hebbian learning [181, 182] which can be used to learn the topology of the input data stream. The proposed algorithm makes a two-layered neural network Figure 5.4. The first layer which represents a reasonable topological structure of unlabelled data gives a reasonable number of clusters and gives a typical prototype pattern of every cluster. Prior knowledge regarding the number of classes or codebook is not required.

The first layer learns the density distribution of the input pattern. Subsequently, the output of the first layer serves as the input of the second layer, where the different clusters are separated by detecting the low-density overlap area. The method uses similarity threshold and a locally accumulated error-based insertion criterion for growing the system incrementally and accommodating the input patterns of online non-stationary data distribution. It also uses an online criterion to delete nodes from the low probability regions and this enables the system to separate the cluster and simultaneously eliminate the noise noisy samples from the input data. Authors use "error radius" as the utility parameters to control the growth of a number of nodes in the network and check successful node insertion. Though the method has been successfully applied to some real-time problems, it has several limitations for e.g. a) in case of high-density overlap it is difficult for the method to separate the clusters b) several important parameters value need to be decided by the users which increase the chances that the system getting used sub-optimally. On the similar lines, authors have further modified the SOINN to make a semi-supervised incremental active learning

system [179] which is very promising and claims have been made that this method can be very useful to create a never-ending learning system.
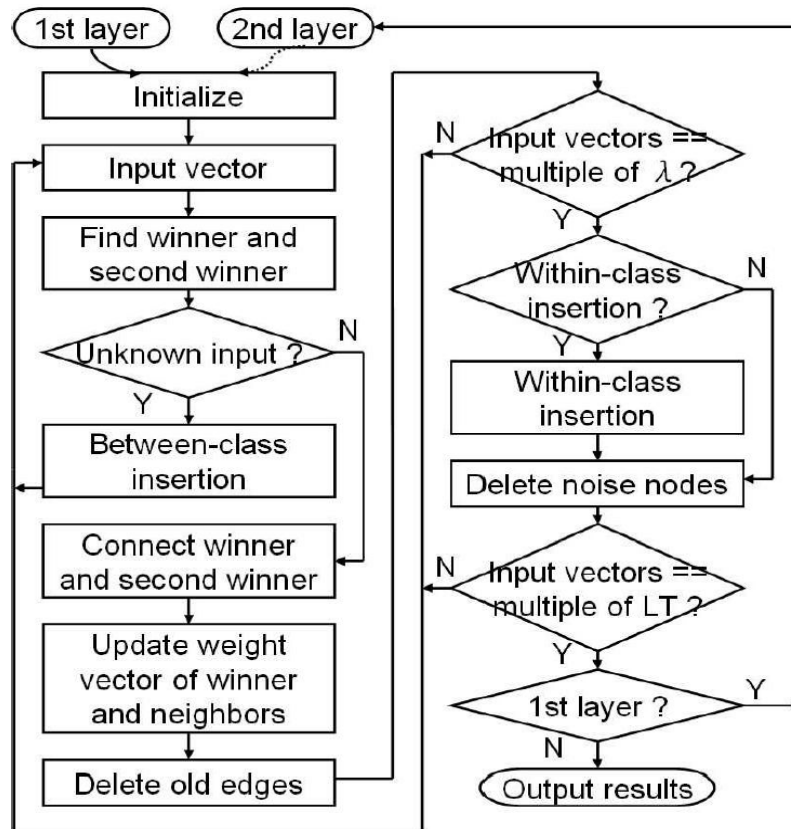
Figure 5.4: Flowchart of SOINN, shows the basic overflow of the proposed algorithm. This Figure has been taken from [180, 274].

5.5. Experimental details and results

Two set of experiment was performed for AB, They are summarised in the next subsections.

5.5.1. Experiment on the UBIRIS Version 1

In order to evaluate the effectiveness of the discussed incremental learning algorithms a part of UBIRS version 1 was employed. One of the discussed methods is used to develop an adaptive sclera biometric system. Similar sclera pre-processing as proposed in Chapter 3 was performed. Fuzzy C-means clustering was used to segment the sclera. A histogram equalisation on the green channel, followed by a bank of the filter based on Discrete Meyer wavelet was used to enhance the vessel patterns. Sclera feature extraction based on the D-LDP was performed. The irises were segmented along the radius by calculating the centre and the radius by the integrodifferential operator and further enhanced using an adaptive

histogram equalisation technique. The red channel of the colour image was used for iris image enhancement. Image level fusion was performed using iris and sclera, and subsequently, the patterns were classified using the developed features.

It was observed that the number of participants in the two sessions was not the same which produced a very uneven number of samples corresponding to different individuals. Even the number of the population was different for the two sessions. The first session consisted of 241 users and in the second session, there were 135 users. Experiments have used 50 out of 241 total classes present because many classes did not have data from both sessions which makes the number of samples too few to apply the learning algorithm over them. Experiments did not use a few classes because the iris and sclera region of the participants were too occluded to be used for learning. For experiment as a learner, incremental Naive Bayes classifier as proposed in [164] was used. The number of features used for each class was 30480. The total number of classes used was 50. For each feature, a single Gaussian of the form $P(x_i|Y = y_k)$ corresponding to each class was fitted. Where i and k refer to i[th] feature and k[th] class, respectively. The classifier is initially trained offline with few numbers of samples using maximum likelihood estimation. Subsequently, updated the learning parameters of each Gaussian corresponding to each class in the online fashion as discussed in Section 1.3.1 and in [161]. The value of constant α was empirically decided to be 0.55 for the experiments. The work did not concentrated on creating ensemble of classifiers and semi-supervised learning as the iris no enough data per class to create different classifiers. But creating an ensemble using a randomization technique is a powerful technique to create a boost in accuracy of the classifier.

Few parameters used in the learning method employed are as follows:

A) c_k which keeps track of the number of samples that have been used for each class for online training.

B) α it is a constant which decides the length of the memory of the classifier, it influences the value of η_k which decides how much weight must be given (in general and when the convergence (when $c_k \to \infty$) is achieved) to the new incoming samples in the learning parameter estimation step.

C) η_k is the learning rate parameter whose value depends on the value of count of samples and the value of α and the value of c_k. The detailed discussion over the role of these parameters in learning process is given in [161].

The results table shows the accuracy of the applied method under different settings of the experiments. Considering the fact that Naive Bayes is a classifier which is based on a very

strong assumption of conditional independence among the features given the class, it is performing reasonably well. Therefore it can be assumed that the stronger version of incremental learning algorithms could perform even better. This experimental process shows that larger accuracies can be achieved using incremental learning in the biometric domain by more experimentation with other adaptive learning techniques available in the machine learning literature.

Table 5.1. Results show that adaptive/online Naïve Bayes classifier is more accurate (fusing sclera and iris at image level fusion). Adaptive classifiers are initially trained with a few samples in batch/offline mode and later learn in an online/adaptive manner i.e. using one sample at a time. For example row 2:- classifier was initially trained with 5 samples per class, subsequently it was adaptively trained with 2 samples per class and later tested with 3 samples per class.

Classifier Name	Training/Testing	Accuracy (%)
Naive Bayes (NB)	7 offline/3	60
Online/adaptive NB	5 offline + 2 online/3	72
Online/adaptive NB	5 offline + 3 online/2	86
Online/adaptive NB	5 offline + 4 online/1	88

5.5.2 Experiments on Proposed Dataset

To overcome the drawback of the above-mentioned experiment and justify the proposed framework, a new dataset was developed. It consists of images from 37 individual, for each individual 200 samples eye images were collected. The images were captured from the camera of Lenovo K3 note mobile. The users were asked to look at random angles, while the images were captured. The base classifier was trained by first 50 samples, rest of the images were used for testing. For online classifier initiation was done by 10 samples and 140 samples for online training, rest of the images were used for testing. A high variation in a trait due to the change in gaze angle of the eye is reflected from the sample images in Figure 5.5.

Figure 5.5. Example of images from the proposed dataset for AB with a large sample.

For segmentation, at first the corner of the eye was detected and the image is cropped along the boundary of the eye, to minimise the effect of illusion on segmentation algorithm used (C-means as proposed in Chapter 3). For sclera enhancement, an adaptive histogram equalisation (as used in earlier work) was applied on the green channel of the image. Followed by second derivatives, using the Hessian matrix used in [1] is employed to get the

final enhanced image. The pre-processing technique proposed for iris in chapter 3 was used for iris segmentation and enhancement. For feature extraction, D-LDP descriptors were used. An information fusion of sclera and iris was performed in the sensor/image level after pre-processing them individually. A base classifier and online classifier of SVM, NN (online version used was Fuzzy ARTMAP) and NB were used. From the Table 5.2, the validity of the prosed framework can be perceived.

Table 5.2: Result of the different classifiers used in the framework and their individual performances in EER %.

Type of Classifier	Base Classifier	Online Classifier	Framework
NB	31.55	55.25	65.76
SVM	40.69	63.45	70.33
NN	50.98	68.59	76.22

Significant improvement is achieved in the result of the framework in comparison to the base and online classifier, still, more experiment is required performed to attend the better performance.

5.6 Summary

This chapter discusses many potential existing adaptive learning methods, which can be applied in the biometric domain to create a robust adaptive biometric system. A framework coupling online and the base version of the classier is proposed. To demonstrate this one existing learning method to create an adaptive multimodal ocular approach using iris and sclera was applied. It is evident from the experiments that the adaptive/incremental system applied outperforms the base classifier performance. It is also evident from the results that when the numbers of samples are increased, the adaptability also improves. Due to lack of availability of a large number of samples, other theories like online semi-supervised learning methods were not tested.

Further, to explore all the promising adaptive techniques in the biometric domain, to justify the framework and build a reliable never-ending learning biometric system a dataset is developed. A significant improvement in the accuracy is achieved applying the framework. Future work should involve in developing the framework to attend the higher performance.

6

Contribution to Other Fields of Pattern Recognition

This chapter addresses and summarises the contribution of the thesis to other closely connect topic of the thesis in the field of biometrics and pattern recognition. The contributions are discussed in the next three sub-sections. Major parts of the chapter have been published in the articles Das et al. [268, 276].

6.1. Multi-Script Signature Verification

Most law enforcement agencies, governments of various countries, financial institutions, or forensic units use the signature as identity proof in their daily activities[3]. Usually, signature verification involves a manual procedure carried out by Forensic Handwriting Experts (FHEs), where individual characteristics of the signature are observed, such as inclination, slant, hooks, the relationship between letters, and so on, using a common set of protocols and methods. This analysis is time-consuming and moreover, its performance depends on many factors such as expertise of the observer, availability of data and sample quality. To mitigate these drawbacks, ASV (Automatic Signature Verification) has been proposed. Computer vision and pattern recognition frameworks have been employed to build such systems, in which the signatures are mathematically modelled, and further, a quantitative similarity called the likelihood is calculated to identify the query signature. Such systems are nowadays becoming accepted for law enforcement agencies, governments of various

---

[3] http://legal-dictionary.thefreedictionary.com/signature

countries, financial institutions and courts. As a result, various commercial ASV systems have become available[4].

Signature verification schemes are usually focused on a single-script environment *(Here by script means the set of letters or characters i.e. different symbols, used for writing a particular language).* The multi-script signature scenario is also a very practical situation, which can be encountered in international security or forensic paradigms, where aggregation of a variety of script signatures coming from different geographical areas can be encountered. The performance of multi-script based ASV scenarios has hardly been studied [183] in the literature. The multi-script scenario is usually studied by merging several single-script databases to build a multi-script database and comparing their performance [2] are compared with the single-script databases. Furthermore, the literature implies that the performance Automatic Signature Verifier (ASV) reduces when applied to a multi-script dataset [184]. The reason behind poorer results reported in the multi-script ASV scenario in construct to the single-script database possibly could be due to the larger number of users. However, to the best of the knowledge, no studies have focused on the database merging procedure or proposing a statistical measure for a fair comparison of multi-script verses single-script scenarios.

Therefore, in order to investigate the aforementioned gap in the literature, the present work is conceived. This work proposes a statistical measure, as well as a merging procedure for a fair comparison between single-script and multi-script databases. This study includes extracting features from the signatures by various well-known techniques, and subsequently perform an analysis of the different single-script and multi-script databases. Thereafter, a statistical measure is also employed for a fair comparison of the multi-script vs. single-script scenarios. Before explaining the proposed approach, the databases used, as well as the off-line ASV feature extraction techniques, are briefly described.

6.1.1. Background

Automatic Signature Verification has been considered an active problem in the scientific research community since the 1980's. The majority of initiatives have produced several contributions to the field over the years [185-190]. However, some issues have not yet been fully identified due to their recent emergence [190]. One such active aspect is multi-script signature processing.

Western signatures are most commonly dealt with in regards ASV scenario in the research community. These kinds of signatures have two different parts: the text and the flourish.

---

[4] http://www.biometricupdate.com/service-directory/signature-verification

The text has a more regular kinematic per signer. Conversely, the variation in the flourish is unpredictable according to its lexical morphology [191]. In addition, the mean velocities in both parts are very different: the flourish average velocity is not nearly as high as the text velocity average. However, these features cannot be directly estimated from image-based signatures. Whereas, Indian, Chinese and Japanese signatures consist of mainly short and rapid strokes. This way, each pen-down is far smaller than the pen-downs of Western signatures.

A large number of approaches proposed in the literature on non-Latin signature have considered script-based text recognition and static signature recognition over the years without dependence on the number of scripts or their combination [190]. In [192], the authors evaluated three different signature scripts - Bengali, Devanagari and Roman – throughout automatic signature systems. They found that the majority of system errors were due to the misclassification of Bengali and Devanagari signatures. The same authors also used a modified gradient feature and an SVM classifier for identification and verification purposes in [193]. They concluded that the verification rates were more competitive for off-line Hindi signature scripts than for English (the achieved False Acceptance Rate (FAR) was more than twice for the latter). In the following work of [194], at first the identification of the script are considered and then verifier method is applied accordingly to the detected signature script (Hindi or English). In this work, the average error rate was significantly reduced to 4.81%, mainly due to the first stage of script identification. For Bengali and English off-line signature verification, in [195] the authors propose a combination of gradient features and chain code features as templates for signature verification. They were able to obtain similar high accuracies of 99.41%, 98.45%, and 97.75% using the respective feature extraction techniques. In the case of English and Chinese static signature scripts, in [196] the authors proposed a script identification approach on the basis of a foreground and background technique. Their contribution for multi-script verification relied on script identification before employing the verification process, which reached an accuracy 97.70% during the identification stage.

This combination opens up some relevant questions to the currently used technology. On the one hand, the accuracy of single-script systems can be progressed by the combination of scripts. However, the system achieves a competitive performance with a Roman script or Bengali script-based signature when considered separately, but similar accuracy is not obtained when these scripts are combined. This way, we wonder about the real influence of low accuracy in the multi-script ASV.

Therefore, although substantial research has previously been undertaken in the area of signature verification, particularly involving single-script signatures, multi-script ASV needs further attention. Moreover, a multi-lingual country like India has many different

scripts that are used for writing as well as for signing purposes, based on different locations or regions. In India, a single official transaction sometimes needs signatures using more than one script. Thus, the consideration of signatures dealing with more than one or two scripts is important mainly for multi-lingual and multi-script countries. Moreover, the development of a general multi-script signature verification system is very complicated. This is where the present research concentrates on investigating the real cause of the lower performance of multi-script ASVs and proposes a fair method to analyse their performance.

6.1.2. Databases

To look into the cause of the lower performance in the multi-script scenario, eight different databases have been used for the experimental study of this work. Some of them contain western signatures, to follow up the single-script merging dataset case, whereas the others include different scripts such as Devanagari, Bengali, Chinese and Arabic. The datasets are described as follows:

1. The GPDS100 contains the first 100 signatures of the GPDS960 signature database [197], which was recorded in Spain in Roman script. The signers used their own pen to sign on a piece of paper. For each signer, it consists of 24 genuine signatures and 30 forgeries. The 24 genuine specimens of each signer were collected in a single day writing sessions. The forgeries were produced from the static image of the genuine signature. Each forger was allowed to practice the signature for as long as they required to produce the forgery. Each forger imitated 3 signatures of 5 signers each day. The genuine signatures shown to each forger are chosen randomly from the 24 genuine ones.

2. The MCYT100 contains the first 100 signatures of the MCYT online database from Spain [16] in Roman script. This was recorded on a WACOM Tablet. Each user produces 25 genuine signatures, and 25 skilled forgeries are also captured for each user. These skilled forgeries are produced by the 5 subsequent users by observing the static images of the signature to imitate and to attempt to copy.

3. The SUSIG Visual [199] contains Roman script signatures of 94 users acquired in two sessions. They were recorded in Turkey on an LCT touch device. Each signer supplied 20 samples of his/her signature in two different sessions, supplying 10 signatures at each session. There was approximately a one-week time period in between the two signing sessions. A total of 10 skilled forgeries (5 skilled and 5 highly-skilled) were collected for each person. Skilled forgers watched an animation of the signature to be falsified and practised as long as they required. Once they felt sufficiently skilled, they proceeded to write the forged specimen.

4. The NISDCC [200] was used for a signature competition during ICDAR 2009. It was collected by the Netherlands Forensic Institute. This corpus comprises off-line Roman script signatures of 79 users. Only 19 users of this database include forgeries. Each forger copied the genuine signature as fluently as possible, focusing on mimicking the shape of the specimen.

5. The SVC2004 [201] online database was collected in Hong Kong. It contains Chinese and Roman script signatures of 80 users. This dataset was obtained from the SVC-2004 competition held in conjunction with the First International Conference on Biometric Authentication (ICBA 2004). Each set of signers contains 20 genuine signatures and 20 skilled forgeries from five other contributors. To collect the forgeries, each contributor saw the writing order in which the signature was written. Then, after practising, they decided when to reproduce it.

6. The off-line Bengali [202] signature database was recorded in India with 100 signers using paper as the medium for capturing the writing. From each individual, 24 genuine signatures were collected. A total number of 2400 genuine signatures from 100 individuals were collected. For each contributor, all genuine specimens were collected in a single day's writing session. In addition, only skilled forged signatures were collected for this proposed work. In order to produce the forgeries, the imitators were allowed to practice their forgeries as long as they wished with static images of genuine specimens. A total number of 3000 forged signatures were collected from the writers.

7. The off-line Hindi dataset [202] was recorded in the same conditions as with the Bengali one. From each individual, 24 genuine signatures were collected. A total number of 2400 genuine signatures from 100 individuals were collected. A total number of 3000 (10 per signer) forged signatures were also collected from the writers.

8. Finally, the offline Arabic database [203] was recorded in Egypt and it contains 22 signers. A set of signature data consisting of 220 true samples and 110 forged samples was used. Every signer was asked to sign 10 times using common types of pens (fountain pen or ballpoint pen). For forgery signatures, 5 samples were collected; since it was very difficult to source professional forgers volunteers were asked to simulate the true samples of all persons. They were allowed to practice many times and correct their mistakes in the final version of the forgery samples.

In the online corpuses, the off-line version was obtained by 8-connecting the on-line samples through Bresenham's lines algorithm and applying the ink deposition model [204, 206, 207]. This procedure allowed an increase in the number of off-line databases in the experiments. The off-line resolution was adjusted to 600 dpi for all the databases through a bi-cubic

interpolation obtained as a weighted average of pixels in the nearest 4×4 neighbourhood and using the original resolution in which the signatures were collected. A few sample images from the above-mentioned databases are shown in Figure 6.1. Finally, relevant information for the datasets considered is summarised in Table 6.1. Apart from SVC2004 and SUSIG Visual where writers are supposed to modify their original signature, the rest of the databases included real signatures used daily by the signers.

Table 6.1: Main information of the considered datasets with genuine and the fake sample statistics

Name of the Database	No of Users	Genuine per user	Forgeries per user	Year of development	Country where database was developed
GPDS100	100	24	30	2012	Spain
MCYT100	100	25	25	2003	Spain
SUSIG Visual	94	20	10	2009	Turkey
NISDCC	100	12	6 from 19 user	2009	Netherlands
SVC2004	80 (40 Western and 40 Chinese)	20	20	2004	Hong Kong
Bengali	100	24	30	2014	India
Hindi	100	24	30	2014	India
Arabic	22	10	5	2000	Egypt

6.1.3. Merging of Databases

This section presents the signature database merging technique. The first condition to compare the performance combination of several databases with the dataset individually is that all of them contain a very similar number of users. Let $\{N_r\}_{r=1}^{R}$ be the number of users of R databases to be merged. Then, the number of users of each individual database to be selected should be $\{L_r\}_{r=1}^{R}$, holding that $L_r \approx N_r/R$ and $\sum_{r=1}^{R} N_r/R \approx \sum_{r=1}^{R} L_r$.

To avoid bias due to user selection, the L_r users of a database to be merged with the other databases are selected as follows: Let $\{EER_i\}_{i=1}^{N_r}$ be the sequence of each signer's EER for database r. Those values are sorted in ascending order, i.e. from lower to greater EER per signer as:

$$j(i) \leftarrow i \mid EER_{j(i)} < EER_{j(i+1)}, i \in \{1, \dots, N_r - 1\} \qquad (6.1)$$

Then, select the users to be merged by the equidistant sampling of L_r users in the j index, in other words, the selected users are those with indices $j(\lceil kN_r/L_r \rceil)$, $k \in \{0, \dots, L_r - 1\}$. This procedure guarantees that the selected users have a similar EER distribution as the original database for a fairer merging approach and performance comparison between the merged and non-merged databases. This procedure is illustrated in Figure 6.2.
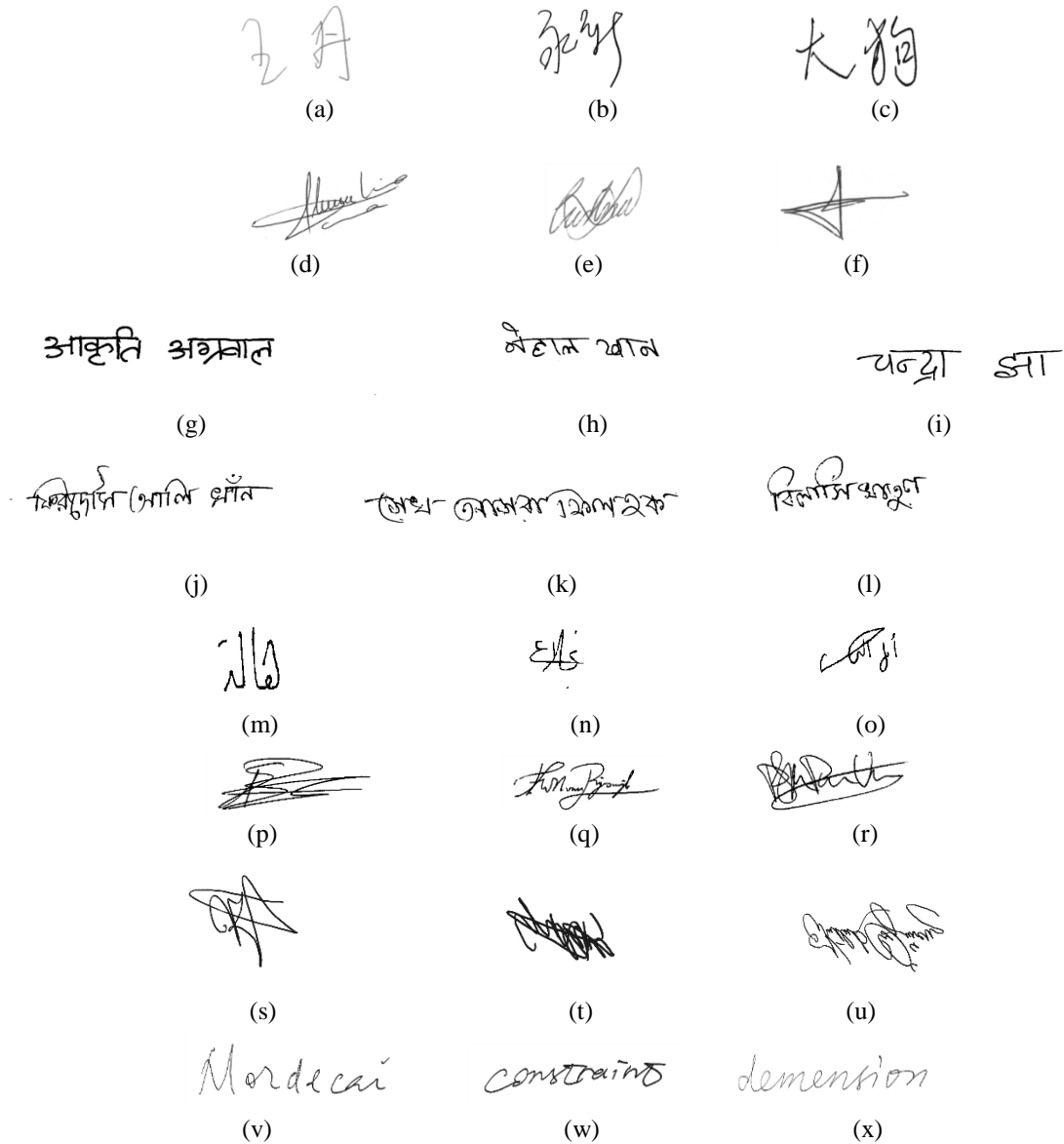
Figure 6.1: Sample signature images from different databases: (a-c) SVC 2004, (d-f) GPDS and MCYT, (g-i) Hindi signature, (j-l) Bengali signature, (m-o) Arab script dataset. (p-r) NFI, (s-u) SUSIG VISUAL, (v-x) SVC2004 western [276].

guarantees that the selected users have a similar EER distribution as the original database for a fairer merging approach and performance comparison between the merged and non-merged databases. This procedure is illustrated in Figure 6.2.
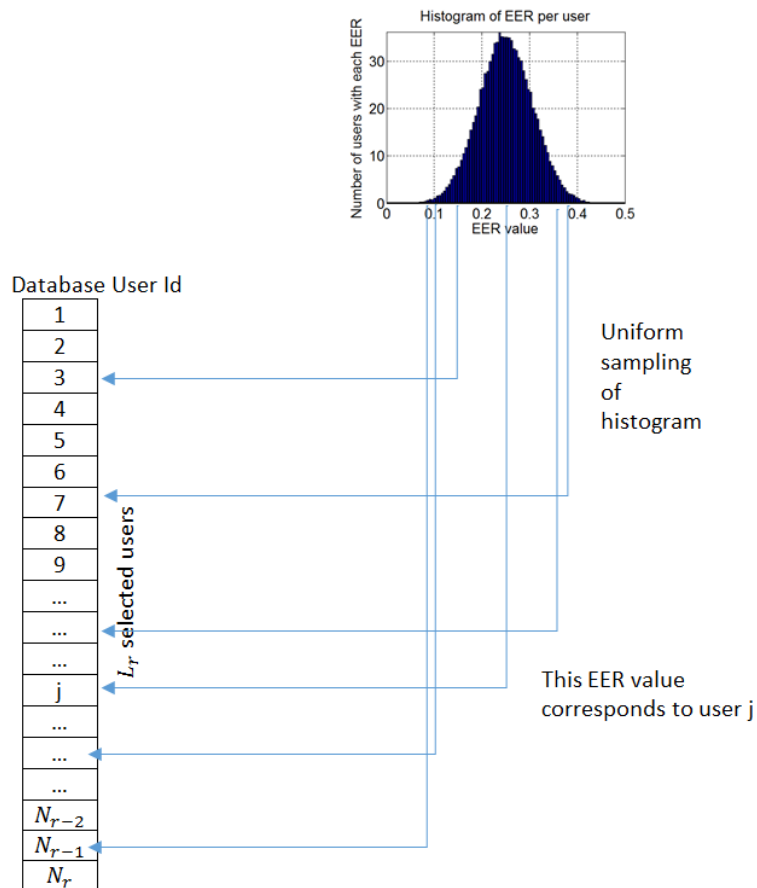
Figure 6.2. Similar EER distribution procedure for user selection when merging databases [276]

6.1.4. Feature and Performance Analysis

Different types of feature extraction techniques that can be found in the pattern recognition literature can be classified into three categories: shape features (feature extraction based on the geometry of the object), colour-based and texture-based features. Among them, shape-based and the texture-based features are prominent for use with signatures, so they are used in the different automatic signature verifiers that can be found in the literature. The shape features aim to extract the discernible information from the signature by the ridges, blob, edges and corners present in them. Whereas, texture features give information about the spatial arrangement of colour or intensities in an image or a selected region of an image locally. The texture-based features explore repetitive pattern and intensity distributions in the signature. These shape and texture features are both applicable for multi-script signatures as well. Therefore, several geometric and texture-based feature extraction techniques are employed in this study.

The use of several features and classifiers allowed a comparison of the performance of databases and parameters to form a conclusion about the performance analysis of single-script and multi-script ASV. Here, the following published ASVs have been considered for the experimental study.

1. A Hidden Markov Model (HMM) classifier with geometrical features used in [205] is employed in the work. The signature is parameterized in Cartesian and polar coordinates. Both features are combined at the score level. The Cartesian parameters consist of equidistant samples of the height and length of the signature envelope plus the number of times the vertical and horizontal line cuts the signature stroke. In polar coordinates, the parameters are equidistant samples of the envelope radius plus the stroke area in each sector. A multi-observation discrete left-to-right HMM is chosen to model each signer's features. The classification (evaluation), decoding, and training problems are solved with the Forward-Backward algorithm, the Viterbi algorithm, and the Baum-Welch algorithm.

2. A Euclidean distance between Zernike moments used in [196] is also employed in this analysis. Zernike polynomials are an orthogonal set of complex-valued polynomials: Zernike moments have mathematical properties and make them ideal image features to be used as shape descriptors in shape classification problems. They have rotational invariant properties and could be made to be scale and translation-invariant as well. These properties are quite adequate for ASVs, therefore they are widely used in the ASV literature. Inspired by previous work.

3. Texture-based features, as Local Binary Patterns (LBP) and a Support Vector Machine (SVM) [198], are employed. In this case, the LBP operator has been used for static signature parameterization. The grey-level image is transformed into a code matrix that is divided into 4 equal vertical blocks and 3 equal horizontal blocks, which overlap by 60%. From each block, calculate the 255-bin histograms and the features are obtained concatenating them. A Least Square Support Vector Machine (LS-SVM) with an RBF kernel has been used as the classifier.

The three verifiers are trained with the first 5 genuine signatures of each signer in the database for repeatability of the experiments. The remaining genuine signatures are used for testing the false rejection rate. The false acceptance rate for the random forgeries has been obtained with the genuine test samples from all the remaining users, while the false acceptance rate for the skilled forgery experiments has been worked out with all the forgery samples of each signer.

The three verifiers are trained with the first 5 genuine signatures of each signer in the database. This procedure is chosen instead of training with 5 randomly selected samples several times and providing the averaged performance for the sake of repeatability of the experiments. It is worth mentioning the fact that the procedure introduces a certain amount of bias but this is always the same, therefore the comparison between results is fair.

Setting aside the 5 training samples, the remaining genuine signatures are used for testing the false rejection rate. The false acceptance rate for the random forgeries has been obtained

with the genuine test samples from all the remaining users, while the false acceptance rate for the skilled forgery experiments has been worked out with all the forgery samples of each signer. For the sake of repeatability, Tables 6.2 and 6.3 show the exact number of training and testing samples for each experiment.

The results are given in both (EER) and Bhattacharyya distance for both the random and skilled forgeries. The EER measures the error point when the false acceptance and false rejection are equal, obtaining the overlap of both the distributions. On the other hand, the Bhattacharyya distance is a divergence-type measure between distributions; in this case, the false acceptance and false rejection score distributions called $p(x)$ and $q(x)$ respectively, are obtained as:

$$D_B(p, q) = -\ln(BC(p, q)) \qquad (6.2)$$

being $BC(p, q)$ the Bhattacharyya coefficient defined as:

$$BC(p, q) = \int \sqrt{p(x)q(x)}dx \qquad (6.3)$$

In statistics, the Bhattacharyya distance measures the similarity of two discrete or continuous probability distributions. It is a measure of the amount of overlap between two statistical samples or distributions. Therefore, the relative closeness of the two samples or distributions are being considered. It is used to measure the separability of classes in a classification problem. In single-script vs. multi-script signatures, the ASV scenario is similar. In this scenario, it is needed to measure the overlap between the two distributions rather than the accuracy of the system which can get affected also due to increase in the database size.

6.1.5 Experimental Setup, Results and Discussion

The following experimental setups were followed in the proposed set of experiments.

6.1.5.1. Single-script Scenario

In the case of the single-script scenario, two experiments were conducted to study the effect of merging databases. The first experiment (E1) studied three individual databases: GPDS100, MCYT100 and SUSIG Visual. They were selected because of the similarity in their number of users. The first two databases were recorded under similar conditions while the third one is different in both methodology and geographical location.

Table 6.2: FAR and FRR statistics for each dataset used in multi-script experiments.

Name of the Database	Training samples per user	Test samples for random forgery experiments per user	Test samples for skilled forgery experiments per user
GPDS100	Positive: 5 Negative: 99*5	FRR experiment: (24-5) FAR experiment: (24-5)*99	FRR experiment: 30 FAR experiment: 30*99
MCYT100	Positive: 5 Negative: 99*5	FRR experiment: (25-5) FAR experiment: (25-5)*99	FRR experiment: 30 FAR experiment: 25*99
SUSIG Visual	Positive: 5 Negative: 93*5	FRR experiment: (20-5) FAR experiment: (20-5)*93	FRR experiment: 10 FAR experiment: 10*93
E2-Comb1 Users per database GPDS: 34 MCYT: 33 SUSIG: 33 Total: 100 users	Positive: 5: Negative: 99*5	FRR experiment: if GPDS user: (24-5) if MCYT user: (25-5) if SUSIG user: (20-5) FAR experiment: (24-5)*A+(25-5)*B+ (20-5)*C	FAR experiment If GPDS user: 30 If MCYT user: 25 If SUSIG user: 10 FRR experiment: 30*A+25*B+10*C
		if GPDS user: A=33,B=33,C=33 if MCYT user: A=34,B=32,C=33 if SUSIG user: A=34,B=33,C=32	
E2-comb2 Users per database GPDS: 20 MCYT: 20 SUSIG: 20 SVC: 21 NISDC: 19 Total: 100 users	Positive: 5: Negative: 99*5	FRR experiment: if GPDS user: (24-5) if MCYT user: (25-5) if SUSIG user (20-5) if SVC user: (20-5) if NSDCC user: (12-5) FAR experiment: (24-5)*A+(25-5)*B+(20-5)*C +(20-5)*D+(12-5)*E	FAR experiment if GPDS user: 30 if MCYT user: 25 if SUSIG user: 10 if SVC user: 20 if NSDCC user: 6 FRR experiment: 30*A+25*B+10*C+ 20*D+6*E
		if GPDS user: A=19, B=20,C=20,D=21,E=19 if MCYT user: A=20, B=19,C=20,D=21,E=19 if SUSIG user: A=20, B=20,C=19,D=21,E=19 if SVC user: A=20, B=20,C=20,D=20,E=19 if NSDCC user: A=20, B=20,C=20,D=21,E=18	
E2-comb3 Users per database GPDS: 100 MCYT: 100 SUSIG: 94 SVC: 40 (western) NISDC: 19 Total: 353 users	Positive: 5: Negative: 99*5	FRR experiment: if GPDS user: (24-5) if MCYT user: (25-5) if SUSIG user (20-5) if SVC user: (20-5) if NSDCC user: (12-5) FAR experiment: (24-5)*A+(25-5)*B+(20-5)*C +(20-5)*D+(12-5)*E	FAR experiment if GPDS user: 30 if MCYT user: 25 if SUSIG user: 10 if SVC user: 20 if NSDCC user: 6 FRR experiment 30*A+25*B+10*C+ 20*D+6*E
		if GPDS user: A=99, B=100,C=94,D=40,E=19 if MCYT user: A=100, B=99,C=94,D=40,E=19 if SUSIG user: A=100, B=100,C=93,D=40,E=19 if SVC user: A=100, B=100,C=94,D=39,E=19 if NSDCC user: A=100, B=100,C=94,D=40,E=18	

Table 6.3: FAR and FRR statistics for each dataset used in single script experiments.

Name of the Database	Training samples per user	Test samples for random forgery experiments per user	Test samples for skilled forgery experiments per user
GPDS100	Positive: 5 Negative: 99*5	FRR experiment: (24-5) FAR experiment: (24-5)*99	FRR experiment: 30 FAR experiment: 30*99
Hindi100	Positive: 5 Negative: 99*5	FRR experiment: (24-5) FAR experiment: (24-5)*99	FRR experiment: 30 FAR experiment: 30*99
Bengali	Positive: 5 Negative: 93*5	FRR experiment: (24-5) FAR experiment: (24-5)*99	FRR experiment: 30 FAR experiment: 30*99
E2-Comb1 Users per database GPDS: 34 Hindi: 33 Bengali: 33 Total: 100 users	Positive: 5: Negative: 99*5	FRR experiment: (24-5) FAR experiment: (24-5)*99	FRR experiment: 30 FAR experiment: 30*99
E2-comb2 Users per database GPDS: 20 Hindi: 20 Bengali: 20 SVC: 20 Chinese Arabic: 20 Total: 100 users	Positive: 5: Negative: 99*5	FRR experiment: if GPDS, user: (24-5) if Hindi user: (24-5) if Bengali user (24-5) if SVC user: (20-5) if Arabic user: (10-5) FAR experiment: (24-5)*A+(24-5)*B+(24-5)*C +(20-5)*D+(10-5)*E	FAR experiment If GPDS user: 30 If Hindi user: 30 If Bengali user: 30 if SVC user: 20 if Arabic user: 5 FRR experiment 30*A+30*B+30*C+ 20*D+5*E
		if GPDS user: A=19, B=20,C=20,D=20,E=20 if Hindi user: A=20, B=19,C=20,D=20,E=20 if Bengali user: A=20, B=20,C=19,D=20,E=20 if SVC user: A=20, B=20,C=20,D=19,E=20 if Arabic user: A=20, B=20,C=20,D=20,E=19	
E2-comb3 Users per database GPDS: 100 Hindi: 100 Bengali: 100 SVC: 40 Chinese Arabic: 22 Total: 362 users	Positive: 5: Negative: 99*5	FRR experiment: if GPDS, user: (24-5) if Hindi user: (24-5) if Bengali user (24-5) if SVC user: (20-5) if Arabic user: (10-5) FAR experiment: (24-5)*A+(24-5)*B+(24-5)*C +(20-5)*D+(10-5)*E	FAR experiment If GPDS user: 30 If Hindi user: 30 If Bengali user: 30 if SVC user: 20 if Arabic user: 5 FRR experiment 30*A+30*B+30*C+ 20*D+5*E
		if GPDS user: A=99, B=100,C=100,D=40,E=22 if MCYT user: A=100, B=99,C=100,D=40,E=22 if SUSIG user: A=100, B=100,C=99,D=40,E=22 if SVC user: A=100, B=100,C=100,D=39,E=22 if NSDCC user: A=100, B=100,C=100,D=40,E=21	

The second experiment is divided into two protocols. The first one (E2-comb1), merges equally from the three above databases. This way, 34, 33 and 33 users from each database were selected respectively by the *similar EER distribution* criterion to obtain a 100-user database. The second one (E2-comb2) merges 20 users from each of the three databases

mentioned above, which are selected with a *similar EER distribution* criterion and the first 21 English signatures from the SVC2004 database as well as 19 users from the NSDCC database that includes forgeries. The two last databases were recorded under different conditions from the first three.

The next experiment (E2-comb3) compares the performance of the *Similar EER distribution* with respect to aggregate databases. This experiment sums all the aforementioned databases: GPDS100, MCYT100, SUSIG, SVC2004 and NSDCC and measures its performance.

6.1.5.2. Multi-Script Scenario

To study the effects of the multi-script scenario in off-line automatic signature verification, two experiments have been carried out again. As above, the first experiment (E1) studies individually the GPDS100, Hindi and Bengali databases which contain 100 users in each of them. Note that the Hindi and Bengali databases were recorded under similar conditions whilst the GPDS100 was recorded differently. Again, the second experiment was performed in two steps. The first one (E2-comb1), merges 34, 33 and 33 users of the above databases selected by the *similar EER distribution* criterion. Finally, the second one (E2-comb2), merges 20 users selected from the above three databases with the first 20 users of the Arabic database and the first 20 Chinese signatures of the SVC2004 database. Again these two databases were recorded under different conditions compared to the first three. Therefore, the comparison between single-script and multi-script results is expected to be statistically fair. In E2-comb3, to compare the performance of similar EER distributions with respect to aggregate databases, this experiment adds all the aforementioned databases and measures their performance.

6.1.6. Results and Discussion

The EERs-based results are given in Table 6.4 and 6.5 for single and multi-script experiments, whereas the Bhattacharyya distances are given in Tables 6.6 and 6.7, respectively. A DET curve of the multi-script and singe-script signature environments for both random and skilled forgeries are shown in Figures 6.3 and 6.4. Analysing the single script random forgery experiment results, (Table 6.4), it can be seen that aggregating all the databases (E2-comb3) worsens the performance significantly with respect to the single script database. It is mainly due to the increment of users. Instead, mixing the databases using the similar EER distribution procedure (E2-comb1) keeps a similar performance as compared to the single database scenario (E1-GPDS, E1-MCYT and E1-SUSIG). The small decrease in performance is due to the fact that each database contains a watermark that can help the classifier to decide on borderline signatures. This reduction is much clearer when adding 5 databases using the similar EER distribution mixing of the databases (E2-comb2).

Given that the last two databases added (SVC2004 and NSDCC) were very different to the three first ones (GPDS, MCYT and SUSIG), the watermark of the database undoubtedly helps the classifier to decide.

In the random forgery multi-script scenario, (i.e. Table 6.5), noted similar findings. To aggregate, the different scripts provide a significantly worse result (E3-comb2) as opposed to blending the different scripts properly, i.e. using the EER similar distribution procedure. In this case, the mixing of different scripts barely decreases the performance (E2-comb1 and E2-comb 2) with respect to the single script database (E1-GPDS, E1-Hindi and E1-Bengali) in Geometric and Zernike-based classifiers. This fact, in comparison to the result in the single script case, is surprising since the different scripts should spread the parameters helping the classifiers to improve their performance. Instead, the performance is improved significantly with the Texture-based classifier. This result contributes to the recommendation that texture-based classifiers should be used in multi-script environments. Tables 6.6 and 6.7 confirm the results of Table 6.4 and 6.5. Usually, when the EER increases, the Bhattacharyya distance decreases. Found some exceptions in the doubtful cases, helping to make the conclusion clearer. For instance, Table 6.4, Geometric case in Random Forgeries. It can be stated that E2-comb1 and EER-comb2 are barely better than E1-SUSIG because the EER is similar but the Bhattacharyya distances are greater for all cases.

In skilled forgeries, the results are not as clear as the above. The EER does not display a clear tendency. This fact is given due to the different skills of the forgers along with the different databases. Despite the similarity of the EER distributions, the skilled forgeries of the GPDS dataset are mixed with those of the MCYT dataset, which are less skilful and so on. Thus, the result of blending the skilled forgeries is more affected by the skill of the individual databases than by the mixing procedure. Looking over the DET curves, they highlight the effect of the similar EER distribution procedure. It is easy to realise that in all the curves there is one odd curve which corresponds to the E2-comb3 experiments. It is due to both the difference in performance and the mixing of different distributions that distort the DET curve. For instance, this fact is clearly seen in the two cases of the texture-based classifier for random forgeries.

Table 6.4. Single-script results for random and skilled forgeries in terms of EER in (%)

Experiment	Random Forgeries			Skilled Forgeries		
	Geometric	Zernike	Texture	Geometric	Zernike	Texture
E1- GPDS	4.72	25.07	2.05	22.50	35.16	18.80
E1-MCYT	4.21	23.06	1.78	19.98	35.51	16.07
E1-SUSIG	3.44	23.07	1.47	31.95	44.73	28.81
E2-comb1	4.10	21.27	1.02	24.84	42.19	21.23
E2-comb2	3.15	20.09	1.09	23.59	41.48	17.30
E2-comb3	7.78	30.41	2.55	38.76	54.16	34.64

Table 6.5. Multi-script results for random and skilled forgeries in terms of EER in (%)

	Random Forgeries			Skilled Forgeries		
Experiment.	Geometric	Zernike	Texture	Geometric	Zernike	Texture
E1-GPDS	4.72	25.07	2.05	22.50	35.16	18.80
E1-Hindi	3.85	17.71	1.22	16.83	20.83	12.16
E1- Bengali	3.35	15.28	1.52	20.97	21.35	12.82
E2-comb1	4.73	25.17	1.20	21.25	32.58	15.62
E2-comb2	5.43	27.04	0.94	24.54	32.55	24.24
E2-comb3	7.89	32.61	2.55	29.56	43.56	29.23

Table 6.6. Bhattacharyya distance between the densities of genuine and forgery scores for the single-script experiment

	Random Forgeries			Skilled Forgeries		
Experiment	Geometric	Zernike	Texture	Geometric	Zernike	Texture
E1- GPDS	1.21	0.24	2,18	0.26	0.06	0.40
E1-MCYT	1.19	0.22	2,31	0.34	0.03	0.51
E1-Susig	1.32	0.24	2,45	0.11	0.01	0.14
E2-comb1	1.38	0.25	3,20	0.22	0.01	0.30
E2-comb2	1.47	0.29	3,14	0.24	0.01	0.47
E2-comb3	0.98	0.25	1.69	0.16	0.01	0.21

Table 6.7. Bhattacharyya distance between the densities of genuine and forgery scores for the multi-script experiment

	Random Forgeries			Skilled Forgeries		
Experiment	Geometric	Zernike	Texture	Geometric	Zernike	Texture
E1- GPDS	1.21	0.24	2.18	0.26	0.06	0.40
E1-Hindi	1.29	0.48	2.47	0.31	0.28	0.63
E1- Bengali	1.29	0.42	2.68	0.41	0.31	0.65
E2-comb1	1.32	0.34	2.70	0.30	0.05	0.51
E2-comb2	1.31	0.37	2.86	0.19	0.06	0.23
E2-comb3	0.63	0.35	1.43	0.11	0.02	0.17

Analysing the DET curves in detail, similar conclusions are drawn. By observing and comparing individual curves of experiments of E1 with the experiments of aggregating databases E2-com3, it seems that the multi-script database performs less accurately. Whereas comparing the E1 experiment with the merged datasets using similar EER distribution i.e. the experiments of E2-comb1 and E2-comb2, the performance seems to be very similar or better. Therefore the problem is not merging the signatures from different scripts but merging datasets or increasing the population. This fact is also clear from the Bhattacharyya distances of the E1, E2-comb1, E2-comb2 and E2-comb3, whereby the different Bhattacharyya distances of this experimental pair is less than the EER differences that this combination poses. It can be found in the random forgeries that merging of databases implies a reduction of the EER and an increment of the Bhattacharyya distance in both scenarios except for Zernike
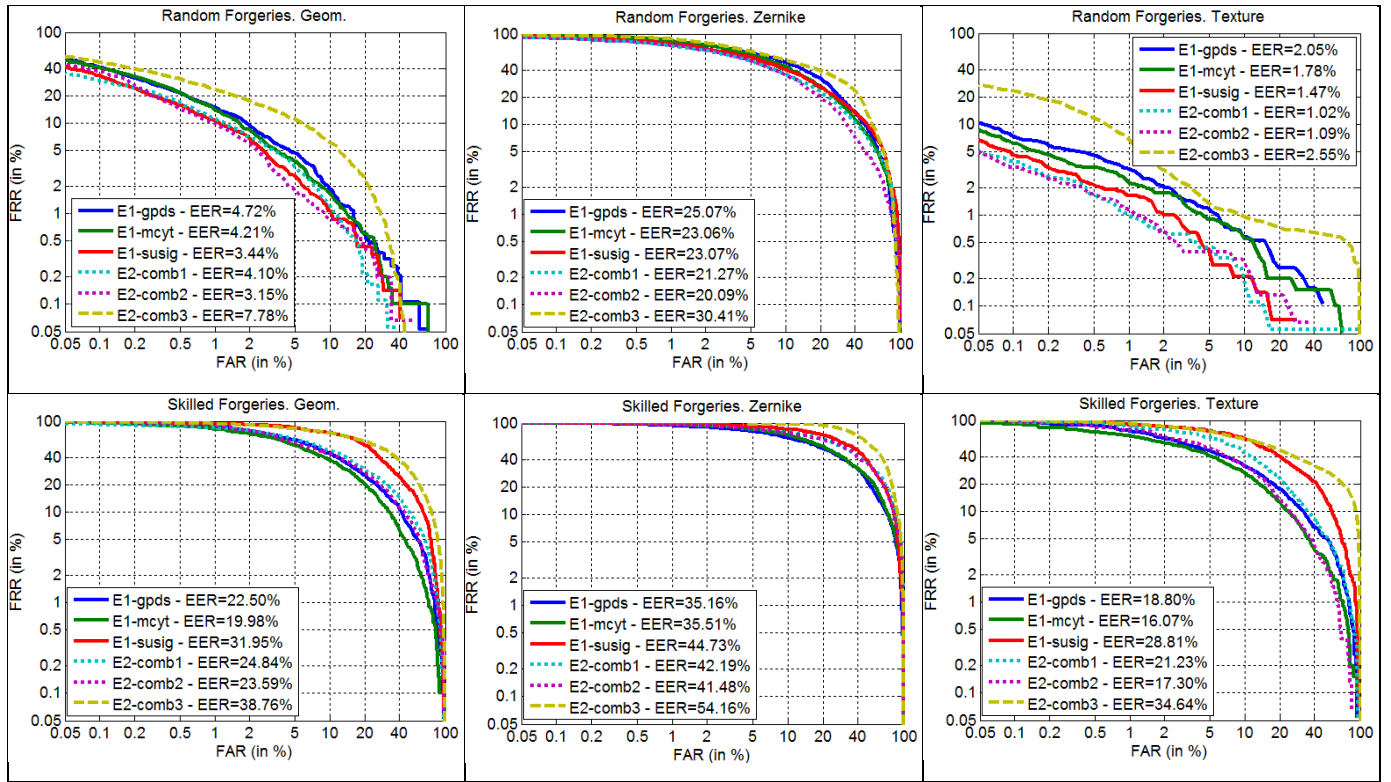
Figure 6.3: DET curves of the multi-script and single script signature environments for random forgeries.
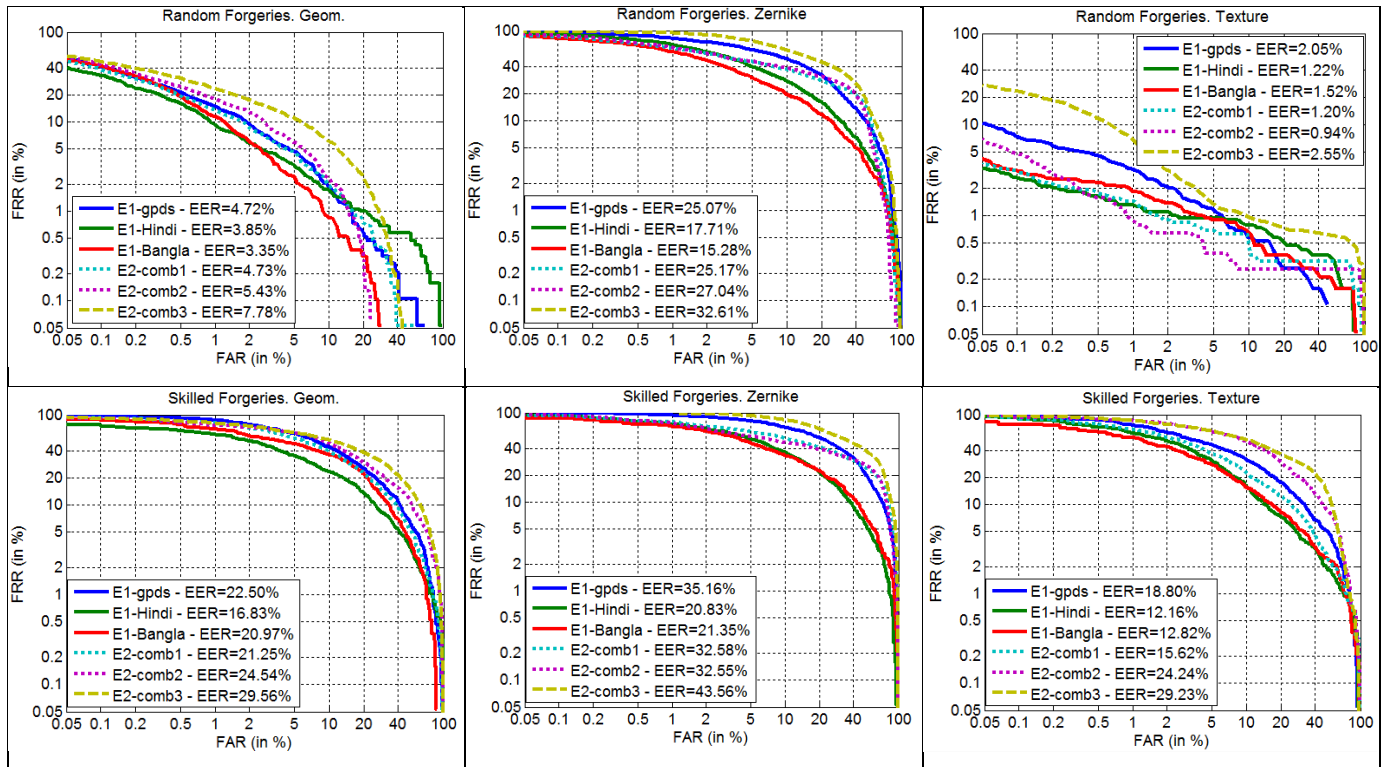
Figure 6.4: DET curves of the multi-script and single script signature environment for skilled forgeries [276].

Bhattacharyya distances of the E1, E2-comb1, E2-comb2 and E2-comb3, whereby the different Bhattacharyya distances of this experimental pair is less than the EER differences that this combination poses.

It can be found in the random forgeries that merging of databases implies a reduction of the EER and an increment of the Bhattacharyya distance in both scenarios except for Zernike features in the multi-script case. So it shows that the score distributions are less overlapping and there is more distinction between them. It is supposed to be due to the features of the different databases, which are statistically different for each database reducing the confusion among signatures, and this is regardless of the single or multi-script properties of the database.

In the case of Zernike features, experiments show that these features are oriented to Hindi and Bengali scripts because of:

1) The EER obtained with Hindi and Bengali are similar between them,

2) The achieved EER with Latin, Arabic and Chinese are similar between them, and

3) The EERs with Hindi and Bengali are significantly lower than the EERs with Latin, Arabic and Chinese.

Therefore, if we properly merge just the Bengali and Hindi datasets, i.e. merging by means of the similar EER distribution procedure, the error of the merged database is lower. Similar observations are made when the Latin, Arabic and Chinese datasets are merged. Therefore it can be concluded that the merged databases have to display similar performance if they are fairly compared with their merged versions.

6.1.7. Thai and Roman Bi-script Signature Verification

Inspired by the significant result of the multi-script signature verification proposed earlier in this section, this work is conceived. In Thailand, Thai people generally sign their names using the Thai alphabet, however, some of them sign their names in Roman or mixture of Roman and Thai scripts (i.e. bi-script nature). The Thai language is the official language of Thailand; however, people also use the English language, hence, they choose to sign their names in Roman script. From one of the authors' own experience, some Thai people even use different signatures on different occasions (official vs. non-official). Furthermore, one person may have some Roman script-based signatures (or English-like signatures) as well as Thai signatures. It must be noted that their signatures will be consistent if signing a formal document (i.e. banking or government-related business), the language selected to sign can be Thai, Roman or using Thai and Roman alphabets to form their signatures. To solve the

above mention challenge this work is undertaken. The contribution of the study is in three-fold.

1) To explore the characteristics of the signatures of Thai people, which can be signed in Thai, English, or English-like alphabets. Also to baseline their performance using available baseline features.

2) To investigate the influence in the multi-script environment (Thai vs. Roman/English script).

3) Development of a Thai signature dataset which will be available publicly.

Although a couple of Thai signature recognition studies are found in the literature [5], [6], they have only focused on recognition rather than verification, even if the dataset was lacking in skilled and random forged signatures. It only contained genuine signatures. Conversely, the proposed dataset, employed in the present experiments, contained most of the necessary types of signature samples, being genuine, skilled forged, and random forged signatures, which made the dataset suitable for signature verification. Moreover, the dataset employed in the literature [208], [209] considered a very small number of individuals, as there were 600 (10 signers' × 60 samples) samples in the dataset.

6.1.7.1 Proposed Thai Dataset

The Thai signatures, both genuine and forged, were obtained from 100 volunteers, whose ages were between 15-40, included both males and females. Each volunteer was asked to write their signature 30 times, using the motion time interval technique, on white paper in the given space; they were asked to sign their signatures as they normally do. They were asked to write ten signatures at a time, and then take a rest. After a short moment of rest, they were asked to repeat the process two more times. In total, there were 3,000 (100 signers × 30 times) genuine signatures obtained. For each of the genuine signatures, 12 skilled forged and 12 random forged signatures were produced; therefore, there were 24 forged signatures per each genuine signature. In total, there were 1,200 (100 signers × 12 times) skilled forged, and 1,200 (100 signers × 12 times) random forged signatures. Altogether there were 5,400 signatures in this collection. It was found that 36 volunteers signed their name in English, whereas the other 64 signed their signature in Thai. Among 100 signers 5 signers used both scripts. Since, the volunteers were asked to sign as they normally do, signing their Thai names in English (or English-like) can be expected. Examples of each type (based on its characteristic) of the signatures are displayed in Table 6.8. All signatures were scanned at 300 dpi resolution and stored in a grey-level format, and then were transformed into Portable Network Graphics (PNG) format. It was observed that many of

the random signatures were signed in Thai language-like rather than English-language-like signatures.

The existing studies of [208], [209] relied on global features which concerned shapes of Thai signatures and grid features involving the overall signature appearance information. For global features, such as the signature area, net width, net height, ratio of the signature image, base-line shift, horizontal centre, vertical centre, maximum number of black pixels in each column (vertical), largest value of the number of black pixels of all columns, maximum number of black pixels in each row (horizontal), and the largest value of the number of black pixels of all rows were used. The grid feature was employed for signature image density. Local features such as blob, strokes, and textures can also be important features that need to be considered for Thai signatures as they are found prominently in the literature and are also visually prominent in the collected data.

Table 6.8. Example of Thai Signature

Characteristic	Actual Name	Signature Reading	Genuine	Skilled	Random
Thai language-like	อาทิมา	อันทิมา			
	สุชานาภ	ส			
English (alike) language	วันวิสา	Fah			
English and Thai	ธารทรายทอง	Chenเชอรรี่			
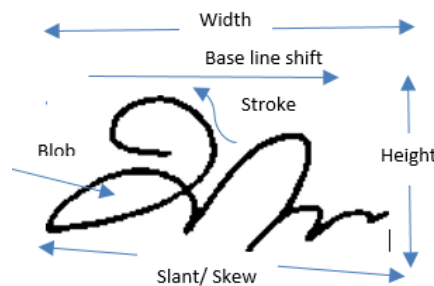
Figure 6.5: A Thai signature image labelled with the local and global features.
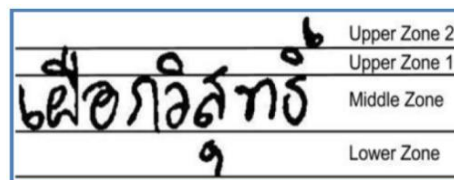
Figure 6.6. Thai People Signatures structure and their zones

The same set of features, classification and performance analysis as used in previous multi-

script experiments were used here. An extra feature LBP+LDP combined was used here. The LBP and LDP were merged together in order to extract features.

6.1.7.2. Experimental Details and Discussions

To investigate the influence of the script dependency on this ASV scenario, the proposed database is divided into the following components. The database was divided into three datasets for the experiments; the details are described as follows:

Dataset I: dataset I contains 50% Thai signatures and 50% English-like Thai signatures. There were 1,080 (36 writers) genuine signatures, 432 skilled forged signatures, and 432 random forged signatures. In total there were 1,944 signatures in this dataset. The samples were ordered by the characteristic of each of the signatures. Thai signatures start from $1 - 18$ and English-like Thai signatures start from $19 - 36$.

Dataset II: dataset II contains 50% Thai signatures and 50% English-like Thai signatures. There were 2,160 (72 writers) genuine signatures, 864 skilled forged signatures, and 864 random forged signatures. In total there were 3,888 signatures in this dataset. The samples were ordered by the characteristic of each of the signatures. Thai signatures start from $1 - 36$ and English-like Thai signatures start from $37 - 72$.

Dataset III (the full proposed database): dataset III contains 64% Thai signature and 36% English-like Thai signatures. There were 3,000 (100 writers) genuine signatures, 1,200 skilled forged signatures, and 1,200 random forged signatures. In total there were 5,400 signatures in this dataset. The samples were ordered by the characteristic of each of the signatures. Thai signatures start from $1 - 64$ and English-like Thai signatures start from $65 - 100$.

The verifiers are trained with the first 10 genuine signatures of each signer in the database for repeatability of the experiments. The remainder of the 20 genuine signatures and 12 skilled and 12 random forged signatures of each signer were used for testing. The EER is obtained by getting the genuine score from the genuine samples and the forgery from the skilled or random forgery samples. The FAR and FRR statistics of each of the database I, II, and III, and for each script scenario (Thai, Roman and their combination) are summarised in Table 6.9.

The results obtained by the above-mentioned protocols are shown in Table 6.10 and 6.11. The results and analysis of Table 6.10 and 6.11 are described as follows:

Table 6.9. FAR and FRR statistics of the experiments

Database	Training samples per user	Test samples for random forgery experiments per user	Test samples for skilled forgery experiments per user
Database I-Thai	Positive: 10 Negative: 17*10	FRR experiment: (30-10) FAR experiment: (30-10)*17	FRR experiment: 12 FAR experiment: 12*17
Database I-Roman	Positive: 10 Negative: 17*10	FRR experiment: (30-10) FAR experiment: (30-10)*17	FRR experiment: 12 FAR experiment: 12*17
Database I-All	Positive: 10 Negative: 35*10	FRR experiment: (30-10) FAR experiment: (30-10)*35	FRR experiment: 12 FAR experiment: 12*35
Database II-Thai	Positive: 10 Negative: 35*10	FRR experiment: (30-10) FAR experiment: (30-10)*35	FRR experiment: 12 FAR experiment: 12*35
Database II-Roman	Positive: 10 Negative: 35*10	FRR experiment: (30-10) FAR experiment: (30-10)*35	FRR experiment: 12 FAR experiment: 12*35
Database II-All	Positive: 10 Negative: 71*10	FRR experiment: (30-10) FAR experiment: (30-10)*71	FRR experiment: 12 FAR experiment: 12*71
Database III-Thai	Positive: 10 Negative: 35*10	FRR experiment: (30-10) FAR experiment: (30-10)*35	FRR experiment: 12 FAR experiment: 12*35
Database III-Roman	Positive: 10 Negative: 63*10	FRR experiment: (30-10) FAR experiment: (30-10)*63	FRR experiment: 12 FAR experiment: 12*63
Database III-All	Positive: 10 Negative: 99*10	FRR experiment: (30-10) FAR experiment: (30-10)*99	FRR experiment: 12 FAR experiment: 12*99

Table 6.10. EER in % for the proposed experimental setup

		Database 36 (Dataset I)			Database 72(Dataset II)			Database 100 (Dataset III)		
		Thai	Roman	All	Thai	Roman	All	Thai	Roman	All
HMM	Random	0.87	0.87	0.94	1.35	2.08	1.48	1.99	2.08	1.95
	Skilled	4.53	8.56	6.15	4.94	10.74	8.46	9.42	8.84	9.41
LBP	Random	0.87	1.38	1.57	1.64	1.82	1.60	1.70	1.82	1.84
	Skilled	5.60	11.95	9.46	8.63	10.07	9.76	9.16	10.39	9.40
LDP	Random	1.38	2.26	1.57	1.27	2.08	1.70	1.81	2.08	1.81
	Skilled	6.43	11.16	9.31	7.03	11.50	8.77	8.64	11.48	8.98
LBP+ LDP	Random	1.01	0.87	0.87	1.20	1.64	1.29	1.41	1.64	1.34
	Skilled	4.95	11.01	8.03	6.57	10.34	8.42	7.92	10.20	8.64

Table 6.11. Bhattacharyya Distance for the proposed experimental setup

		Database 36 (Dataset I)			Database 72 (Dataset II)			Database 100 (Dataset III)		
		Thai	Roman	All	Thai	Roman	All	Thai	Roman	All
HMM	Random	2.07	1.87	2.01	2.03	1.51	1.77	1.85	1.62	1.77
	Skilled	1.27	0.94	1.01	1.09	0.68	0.86	0.86	0.77	0.81
LBP	Random	4.99	3.02	3.65	3.85	3.01	3.32	3.39	3.04	3.08
	Skilled	1.47	0.72	0.99	1.08	0.85	0.95	1.09	0.86	0.98
LDP	Random	4.62	2.82	3.79	3.78	2.94	3.31	3.46	2.95	3.15
	Skilled	1.52	0.74	1.09	1.18	0.77	0.97	1.13	0.78	0.99
LBP+ LDP	Random	5.35	3.29	4.18	4.22	3.32	3.68	3.76	3.32	3.43
	Skilled	1.65	0.80	1.14	1.23	0.88	1.04	1.20	0.89	1.06

We can conclude from Table 6.10 that HMMs and LBP+LDP performed better than the other features extraction techniques employed. Precisely, the combination of LBP+LDP was better in a maximum number of scenarios (in the scenario of database II and III). It can be noted that although the combination of LBP+LDP achieved better EERs in most cases, for dataset I, however, it failed to obtain the same in the case of skilled forge scenario. An EER of ~0.9% was achieved for Random Forged Signature (RFS) experiments, whereas for Skilled Forged Signature (SFS) experiments, the EERs of ~5% to ~11% were achieved for Database I. With the SFS and RFS experiments with Thai and Roman Scripts, the EERs attained were similar for HMM and LBP+LDP. The EERs slightly increased when the two scripts are combined, as compared to the EER for Roman signatures, and decreases w.r.t to EERs obtained for Thai signatures.

It can be noted that the EERs had increased in RFSs experiments with Dataset II and III. With regards to dataset II, from Table 6.10, it can be seen that the LBP+LDP feature extraction technique was able to attain the best EER rates for RFS of all script types. The range of EERs was ~1.20% to ~1.65%. It can also be seen that the resulting EERs having less than ~0.20%, were obtained when LBP was employed to the dataset. For SFS, it was observed that for Thai scripts, HMMs were able to attain the best EER of 4.94%, whereas LBP+LDP was able to achieve the best EER for the Roman script. When both scripts were combined, the best EER of 8.42% was attained when LBP+LDP was utilised. However, the remaining patterns of the results remained the same for dataset I. For Dataset III, the best EER rates of ~1.4% to ~1.6% were attained when the LBP+LDP feature extraction

technique was employed on RFS of each type of scripts. However, when compared to Dataset I and II, the rates were slightly increased. Also, very similar to dataset II, similar results (EERs less than 0.5%) were obtained when LBP was applied to the dataset. With SFS, it was observed that for Thai scripts, LBP+LDP was able to attain the best EER of 7.92%, whereas HMMs were able to achieve the best EER of 8.84% for the Roman script. However, when both scripts were combined, the best EER of 8.64% was attained when LDP was utilised.

For the skilled signatures EERs fluctuated when results are compared to each scenario from Dataset I to II to III, and in most of the cases, they increased. Other patterns of the SFS's experiments remained similar to the RFS's experiments on dataset I. The EER are found to increase slightly or decrease slightly when the signature of two scripts are combined, which signifies that these increase or decrease depend on number of users and nature of the database and signature verification can be performed in a script-independent way in a Thai signature verification system regardless of the challenges addressed in section I. These observations also imply that the usefulness of texture features for bi-script ASV.

When observing the Bhattacharyya Distance (BD) in Table 6.11, for Dataset I the experiments employing Roman script best BD was attained utilising LBP+LDP. Overall, the BDs for Roman SFS is in the range of 0.72% − 3.29%. It was further observed that the results obtained when Thai script was employed are less that of attained when Roman SFS was employed. The Thai script BDs were in a range of 1.27% − 5.35%. Thai BDs were lower than Roman script BDs, in the combined scripts experiments the BDs were also lower than the Roman script experiments. It can be seen in Table 6.11 that the BDs of the bi-script were more than the Thai script but yielded less score when compared to Roman script. The bi-script BDs were in a range of 0.99% − 4.18%. For Dataset II and III, as can be seen in Table 6.11, the results were similar to the BDs attained when each type of the scripts were used in the experiments of database I. It was observed that for all experiments, the BDs attained when the SFS of any type of script was employed, were less compared to the RSF. For Dataset II, BDs of the Roman SFS were in a range of 0.68% − 3.32%, whereas for Dataset III, the range was 0.77% − 3.33%. Also, similarly for Dataset I, it was observed that the results obtained when Thai script was employed were less score than the results attained when the Roman script was employed. For Dataset II, the Thai script BDs were in a range of 1.08% − 4.22% and for Dataset III, the range was between 0.86% − 3.76%. And once again the Thai BDs were lower than Roman BDs when the combined scripts were used in the experiment, the BDs were also lower than the Roman script experiments but higher than Thai script. The BDs of the bi-script were more than the Thai script but yielded lower performance when compared to Roman script. For Dataset II, the bi-script BDs were in a range of 0.86% − 3.68%, and when Dataset III was employed, the range was between 0.81%

– 4.43%. The BD found to be decreasing from the dataset I to II to III for all scenarios.

The Bhattacharyya distance measures the similarity of two discrete or continuous probability distributions. Higher the distance it is less overlapping and therefore higher the chance of distributions not to be similar. So, the above observation of the BD implies similar implication that was made from EER observations. The DET curves of the multi-script and single script signature performance, employing Thai and Roman signatures, can be seen in Fig. 6.7.

6.1.8 Summary of Multi-script Signature Verification

This work has designed and implemented a novel method to merge individual databases according to the statistical similarities in the user-performance distribution. Also, we proposed a statistical performance analysis method namely the Bhattacharyya distance for a fair comparison between single and multi-script scenarios. It can conclude that the performance of the merged databases is slightly better than or quite similar to the individual ones if the individual databases

1) have a similar performance, i

2) are merged keeping the same number of users, and

iii) if the users are selected on the basis of similar EER.

This analysis advocates that the lower performance of the multi-script signatures that was reported in the literature in contrast to the single script scenario is not due to the presence of multi-script signatures. Rather it is due to the increase in the number of classes while merging the databases. Furthermore, this finding is independent of the single-script or multi-script properties of the merged databases. Therefore, the multi-script automatic signature verifier can be seen as an interoperability problem from the system point of view or a generalisation problem from the pattern recognition perspective. This research opens the door for applying generalisation and interoperable techniques to the multi-script signature problem.

Inspired by the result, extended the work for Thai and Roman based Bi-script ASV. The motivation of this research was to comprehensively study signature verification on off-line Thai signatures. As described in previous sections, Thai signatures have unique characteristics due to their bilingual nature (Thai and English/Roman) as well as for a single language (Thai or English/Roman). The novelty of this research includes the custom Thai signature collection, which contains genuine signatures as well as skilled and random forged signatures. Also, this is the first time that Thai signature verification has been investigated. General challenges for Thai signature verification are also discussed.

Experiments were performed on the dataset using features employed in previous ASVs. It can be concluded from all the experimental results that the best EER of 0.87% was achieved when either HMMs or LBP+LDP were employed on Thai, Roman, and bi-script RFS of Dataset I (see Table III). However, for BD, the best result of 5.35% was attained when Thai RFS of Dataset I was employed, using HMMs (see Table IV). It can be noted that for both EER and BD, the best results were attained when RFS were employed on Roman Script. It can also be concluded from the overall experiments that textural features have proven that Thai ASVs is a script identification independent problem.

It was difficult to compare the results attained in this study with others in the literature, as to the best of the knowledge, to date no studies have been conducted on Thai signature verification. However, Thai signature recognition was reported in [208], [209] and accuracy rate of ~90% on the dataset size of 600 samples from 10 signers was achieved.

Overall, the experiments suggest the script independency of Thai signatures. As this work aims to baseline the dataset, more feature extraction techniques will need to be investigated in the future to identify its importance. Future research needs to be undertaken for improvements and to enhance the performance of the proposed Thai signature verification system. Techniques such as deep learning may be investigated on the datasets. Larger and supplementary databases will also be created, so a more detailed study can be performed. The proposed dataset can be also used for Thai signature recognition purposes.

The future plan is to conduct a scientific analysis of this dataset to enrich its usefulness, by conduction completion and challenges on the dataset. Initially, requests may be sent for a part of the dataset, which will be available for academic research purposes. The full dataset will also be made publicly available in due course.

6.2 Wrist Biometrics

One possible and promising upcoming biometrics is the wrist vein pattern, which can be easily combined with fingerprint or palm print biometrics to make it more universal.

In the literature, few works on the wrist can be found [208- 215]. The authors of [216] come up with the proposal that the wrist vein can be utilized for biometric authentication.

In [215] the authors proposed a dataset of wrist vein in the infra-red band of 30 individual and proposed a prototype of for image capturing of wrist vein images by quality measurement. The first work on the wrist vein biometrics system can be found in [208], where a large dataset is used to report the result. The low-quality PUT vein images were
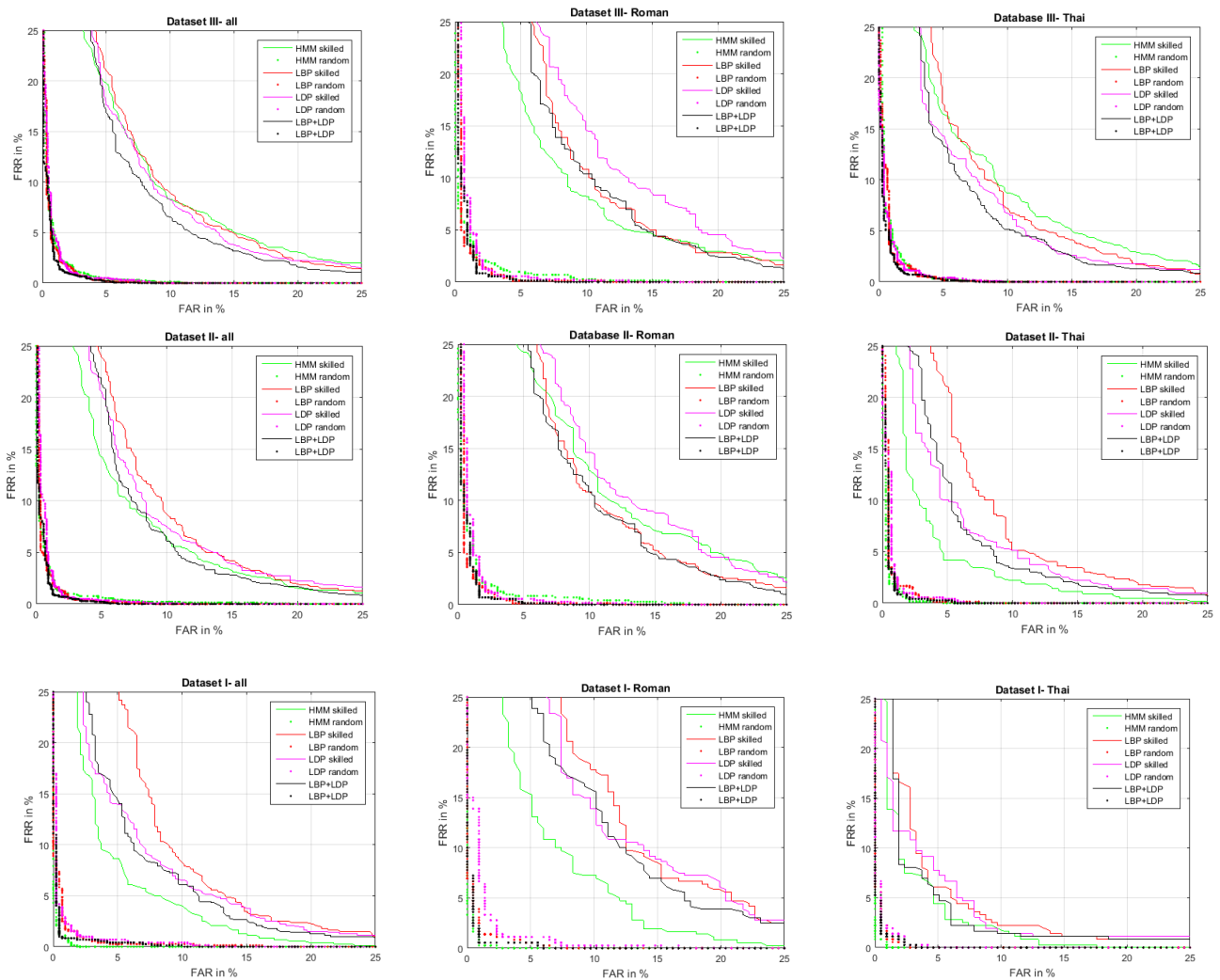
Figure 6.7. DET the multi-script and single script signature performed employing Thai and Roman signature.

used for biometrics. Binarization was used for enhancement further followed by correlation for recognition.

In [209] an analysis of the different segmentation technique is performed. For the segmentation analysis, purpose enhancement was performed by Discrete Fourier Transformation (DCT) and classification by correlation. In [210] benchmarking of the PUT dataset was reported. For enhancement Gaussian filter was used.

In [206] minutia feature based wrist vein recognition system was proposed. Whereas in [204] chain code based fusion is used for wrist vein recognition. In this work different level of skeleton, fusion is used followed by chain code. In [211] spectral minutia based feature extraction was used to represent the wrist vein pattern after pre-processing the vein images. An approach to extract the vein minutiae and to transform them into a fixed-length,

translation and scale invariant representation where rotations can be easily compensated is presented in [213].

To date, this biometric has not been prominently studied and very little is known about its usefulness. Because of this, in this work, we concentrate to explore this biometric trait.

6.2.1. Proposed Wrist Vein Biometric System

This present work proposes a whole biometric system for personal identification based on wrist veins. Here wrist vein segmentation was not required. A new pre-processing approach for vein highlighting is proposed here by the Adaptive Histogram Equalisation and Discrete Meyer wavelet. Wrist feature extraction based on the Dense Local Binary Pattern (D-LBP) was used. Support Vector Machines (SVMs) are used for classification.

(a)   (b)
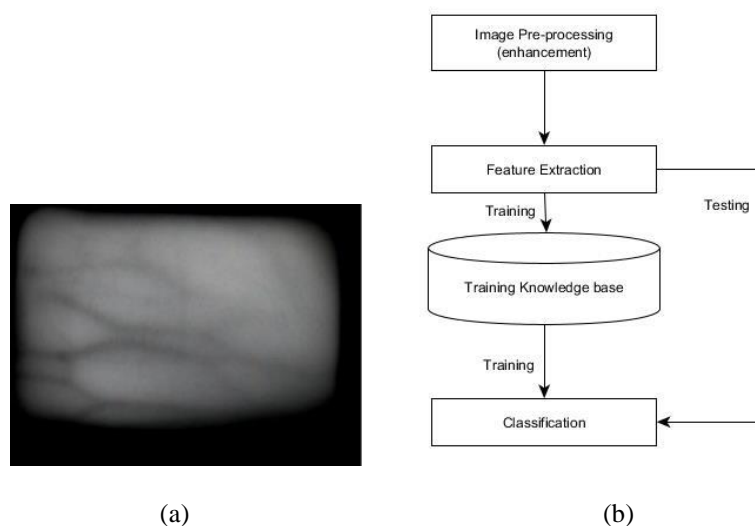
Figure 6.8: (a) A wrist vein image. (b) A system design of the proposed system [268].

In order to make the vein pattern clearly visible, image enhancement was performed. Adaptive histogram equalisation was performed with a window size of 14x14 (the window value was selected by analysis, window value that produces the best result was used for experimentation) was performed on the image to make the vein structure more prominent as shown in Figure 6.9.
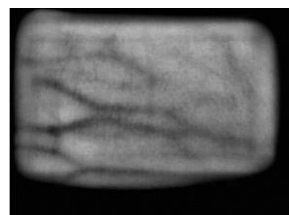
Figure 6.9: Image after adaptive histogram equalisation [268]

Further, the Discrete Meyer wavelet was used to enhance the vein patterns. A low pass reconstruction of the above-mentioned filter was used to enhance the image. Figure 6.10 shows the vein enhanced image after applying the filter.
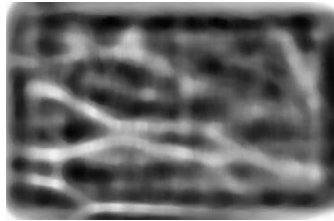
Figure 6.10: The final vein enhanced image [268].

For feature extraction, a local descriptor method was applied in this work for the wrist vein feature. Feature extraction based on the Dense Local Binary Pattern (D-LBP) was performed. D-LBP patch descriptors of each training image are used to form a bag of features, to produce the training model. Next, a K-means clustering technique was applied on the patches on the training set for the generation of a codebook. The vocabulary size for the experiment was 1024. Descriptors from each training image are used with the codebook to form a bag of features, further which was used to produce the training model.

Support Vector Machines (SVMs) are used for classification in this work. SVMs are a popular supervised machine learning technique, which performs an implicit mapping into a higher dimensional feature space. After the mapping is performed, it finds a linear separating hyperplane with maximal margins to separate data from this higher dimensional space.

The Library for Support Vector Machines (LIBSVM) was used here for the SVM implementation. Though various new kernels are being proposed, the most frequently used kernel functions are linear, polynomial, and Radial Basis Function (RBF). This work uses the RBF kernel.

6.2.2. Experimental Results

The experimental setup and the results of the proposed work are explained in this section.

6.2.2.1. Dataset

In order to evaluate the performance of the proposed method, the PUT wrist Vein database [217] was utilised for the experiments. A framework of the image capturing technique is given in Figure 6.11 (g). This database consists of 1200 RGB images taken in three distinct sessions (400 images in each session) from 50 identities (both left and right hand) where each channel of RGB colour space is represented in grey-scale. In each session 4 images of each individual wrist vein are captured. This database also consists of 1200 RGB palm vein images taken in three distinct sessions (400 images in each session) from 50 identities (both

left and right hand) where each channel of RGB colour space is represented in grey-scale. In each session, 4 images of individual palm veins are captured. The database contains blurred images also. High-resolution images (1024 x 768) are provided in the database. All the images are acquired in the Infra-red spectrum. All the images are in BMP format.

Different quality wrist vein images were used and some of the sample images are shown below in Figure 6.11(a-f). The dataset also consists of palm vein images they are not used in the experiment. Examples of such images is in Figure 6.11(h-m).

(a) (b) (c) (d)

(e) (f) (g)

(h) (i) (j) (k)

(l) (m)
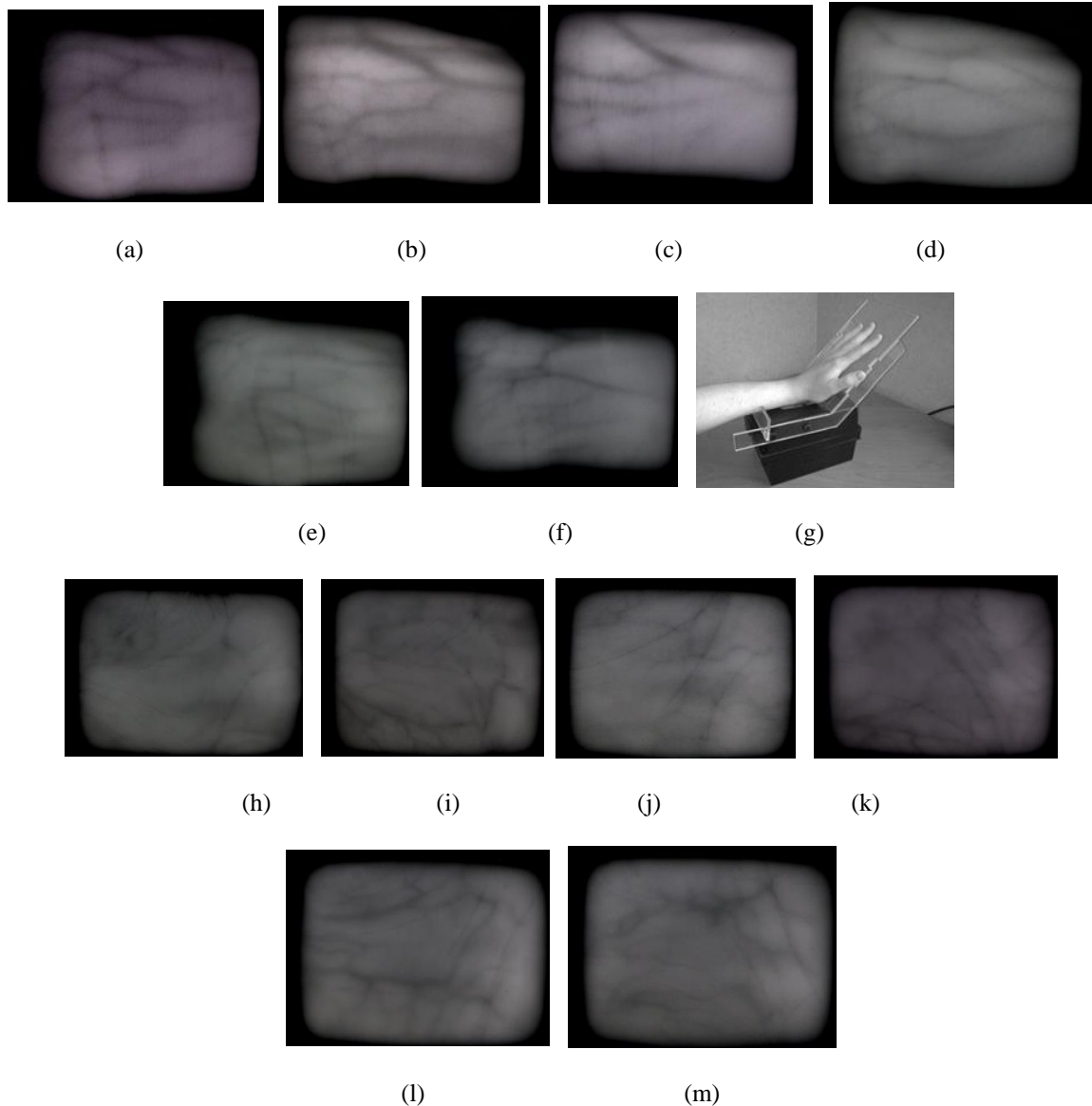
Figure 6.11:(a)- (f) Different quality of wrist vein images used in the experiments, (g) A framework of the image capturing technique[9].(h)-(m)Images of low resolution palm print from the mention dataset [268].

Only the wrist vein images are utilised in this experiment. Some of the wrist vein images are having good quality of vein regions visibility, some of them are of medium quality and the third type was of poor quality with respect to vein visibility. In the experiments, all the images of sessions 1, 2 and 3 were considered.

Here single sessions, as well as multi-session experiments were performed. For the single session experiments, sessions 1, 2 and 3were considered separately, 2 images from each class of each session randomly chosen and utilised for training and the remaining 2 images for testing the performance.

For multisession experiment 4 images from one session were considered for training, and images from a other session for testing and vice versa. Also tested by two sessions and trained by one session, and testing by one session and training by other. For single session experiments 100*2 (100 as because 50 individual left and right hand both and for each individual left and right hand pattern varies) scores for FRR and 100*99 score for FAR statistics.

For multisession with two sessions and 100*4 scores for FRR and 100*99 score for FAR statistics for multisession experiment between two sessions. For multisession experiment between three session, when two for testing and one for training 100*8 scores for FRR and 100*99 score for FAR statistics are achieved. For multisession experiment between three session, when one for testing and two for training 100*4 scores for FRR and 100*99 score for FAR statistics are achieved.

All the simulation experiments performed here were developed in Matlab 2013a on the Windows 7 platform, core I5 processor having 4 GB of RAM.

6.2.2.2. Results

First adaptive histogram equalisation was performed with a tiled window size of 14x14 at a clip limit of 0.01, with a full range and distribution exponential to get the best result. Further, the Discrete Meyer wavelet was used to enhance the vessel patterns more prominently. Low pass reconstruction with a cut off range of -0.9 * e^{10} and a window size of 3x3. Next, the adaptive histogram equalization with a tiled window size of 14x14 at a clip limit of 0.01is used again, with full range and distribution exponential is applied to the filtered image. The result obtained from the different multisession and single session experiments performed are in the Table 6.12. It can be observed from the above experiment that result did not varied between the experiments carried out with Single session and multisession experiment with two training session and one testing session. This signifies the robustness of the system with variation in time duration and other acquiring conditions is achieved. Whereas the result for the multisession experiment with one session for training and two sessions for testing have deteriorated a bit, possible reason can be the ratio of number of training and testing images.

Table 6.12: EER in % of the single and multi-session experiments

Type of experiment	EER in %
Single session using session 1	0.8
Single session using session 2	0.83
Single session using session 3	0.75
Multi-session using session 1 as test 2 as train	0.91
Multi-session using session 2 as test 1 as train	0.89
Multi-session using session 1 as test 3 as train	0.88
Multi-session using session 3 as test 1 as train	0.89
Multi-session using session 2 as test 3 as train	0.81
Multi-session using session 3 as test 2 as train	0.84
Multi-session using session 1 as test 2 and 3 as train	0.81
Multi-session using session 2 as test 1 and 3 as train	0.8
Multi-session using session 3 as test 2 and 3 as train	0.79
Multi-session using session 1 and 2 as test and 3 as train	1.31
Multi-session using session 1 and 3 as test and 2as train	1.42
Multi-session using session 3 and 2 as test and 1as train	1,23

Multisession experiment for session 1and 2 for training and session 3 as testing produces the best result for the multi-session experimental environment. For the single session experiments, session 3 produces the best results. It can also be concluded from the above Table that the results for the multisession experiments have deteriorated somewhat. The possible cause can be the presence of some lighting and other conditions changes in between the sessions.

6.2.2.3. Comparison with the State-of-the-art

The results of the proposed work are analysed with respect to the state-of-the-art by comparing it with the most similar work on the PUT hand vein dataset that could be found in the literature. Table 6.13 reflects a state-of-the-art comparative analysis of the most similar work on the PUT hand vein dataset.

Table 6.13. A state of the art comparison with the proposed work.

Work	Equal Error Rate (in %)
Kabaciński et al. [208]	3.51
Kabaciński et al. [209]	2.19
Kabaciński et al. [210]	3.8
Proposed System	0.79 (multisession experiment with all the images)

The proposed technique outperformed the other previous techniques in terms of recognition and validation which is reflected in the Table 6.14. The result reported in the previous works was not reported with multisession experiment.

Table 6.14. A state of the art comparison of different methods employed in various stages with the proposed work.

Work	Enhancement technique	Feature extraction technique	Classification technique
Kabaciński et al. [208]	Binarization	Correlation Matching	
Kabaciński et al. [209]	Discrete Fourier Transformation	Correlation Matching	
Kabaciński et al. et al. [210]	Gauss filters	Correlation Matching	
Proposed System	Adaptive histogram equalization and a low pass Discrete Meyer Wavelet	Dense LBP	SVM

Hence the proposed scheme is the most realistic one, since it did not discarded any images from the dataset used, and the experiments were also performed with multisession data, where the sessions have variation in change in environmental condition, population, data accruing technique and time span gap.

Another significant novelty of this work is the usage of statistical classifier like SVM in contrast to the other related work, where correlation matching was used for classification. In order make a state of art compares with the most similar work that can be found in the literature on PUT dataset are compares with the different enhancement, feature extraction and classification used in the previous work with contrast the proposed in the Table 6.14.

6.2.3. Summary of Wrist Biometrics

This work has proposed a novel method of wrist vein recognition. Adaptive histogram equalisation was used for wrist vein pre-processing and a low pass Discrete Meyer Wavelet reconstruction filter for establishing appropriate features was employed. Dense LBP is used here for feature extraction, which provides information about the different pattern structures followed by clustering by K-means. Identification is achieved by SVM classification. The proposed approach has achieved high recognition accuracy employing the PUT hand vein dataset. The future scope will include exploring the multimodal biometric system using all biometric trait present in hand.

6.3. Script Identification

With the increasing demand for creating a digital world, many Optical Character Recognition (OCR) algorithms have been developed over the years. The scripts can be defined in the graphical form of the writing system, which is used to write statements all around the world. Designing a universal OCR considering all the script, is a challenging task as the featuring character usually depends on the structural script properties and the amount of possible classes or characters. Moreover, the size of such classes would be huge. Therefore, most OCR systems are script dependent.

An option for handling documents in a multiscript environment is a two-step scheme: first the script identification of the document, in block, line or word level and in the second phase the appropriate OCR is used. This approach requires a script identifier and a bank of OCR, one per script. Many Script Identification algorithms have been proposed over the last years. A survey published in 2010, with a taxonomy of the script identification system can be found in 0. The script identification can be done offline from the scanned document or online if the writing sequence is available. The problem can also be divided into printed or handwritten document. Challenge for handwritten it is more challenging. The script identification can be performed at different levels, namely: page or document, paragraph, block, line, word and character level.

The script identification problem depends on the number of possible scripts that can be found in the document. Bi-script is the most usual problem although tri-scripts scenario are also found in 0. The presence of more than three scripts in a document is less common. Other relevant variable for the script identification is the scripts to be identified. The

challenge of script identification is not the same for a different combination of script, for example, the challenge to discriminate between Bengali and Devanagari, than Latin and Japanese is quite different. The features of script identification methodologies can be divided into Structure-Based and Appearance-Based Script Recognition. Structure-based method extracts connected components and analyse their shapes and structures so as to reveal the intrinsic morphological characteristics of the script. So, usual features are the script upward or downward concavities, curvatures, etc. Whereas appearance based features analyse the script by their shape, without analysing character by character. Therefore, usual parameters are height distribution, bottom and upper line profiles, horizontal and vertical projection profiles, image texture based on Gabor filtering and so on.

Recently, an approach based on local patterns has been proposed 0. Histograms of local patterns are used as features describing both the stroke directions distribution and global appearance. Most of the works claim for identification rates over 92%, but each work uses different datasets with different scripts. Therefore it is difficult to compare the different approaches. The databases include usually two to four scripts. A few works include more than four up to thirteen. Most popular scripts are Latin, Indian Scripts plus Japanese and Chinese. Also Greek, Russian a Hebrew is found 0. A common database for algorithms comparison would be desirable. Years ago, it was really costly to build a dataset. Nowadays it becomes simpler and easier. For instance, documents in different scripts can be generated using Google translator application as in 0 but their font and size would be unique. To alleviate this drawback, this work is aimed to offer as a resource for researchers a wide range database for script identification along with a benchmarking of it with local patterns features. The dataset has been obtained from different local newspaper and magazines, containing in this way different fonts, sizes, cursive, bold, etc. A benchmark is given using local pattern texture based features with a Support Vector Machines as a classifier. Next, to the traditional Local Binary Pattern and Local Directional Pattern, other features are here suggested, such as Oriented Local Binary Patterns, Local Derivative Patterns and Dense Multi-Block Local Binary Patterns, the last ones used for the first time in this work for script identification.

6.3.1. Database

The database has been recorded from a wide range of local newspapers and magazines so that the contents are as realistic as possible. The newspapers were collected mainly from India, which is one of the richest countries in a variety of scripts, Thailand, Japan, UAE and Europe. It includes 12 different scripts: Arab, Bengali, Gujarati, Gurmukhi, Hindi, Japanese, Kannada, Malayalam, Oriya, Latin, Telugu and Thai.

The newspapers were scanned at 300dpi resolution. Paragraphs with only one script were selected for the database. As paragraph, it means the headline and text. In this way, different text sizes, fonts, cursive, bold, etc. for each script are included in the database. All

the text lines are horizontal. The images were saved in TIFF format. The files were named as *script_xxx.tif,* being s*cript* an acronym for each script and *xxx* the file number starting at 000 for every script. The *script* and the number of documents for every script can be found in table 6.15.

6.3.2. Preprocessing

The benchmarking of the database has been performed at three levels: block, line and word. The next subsections describe the segmentation procedure to obtain the blocks, lines and words.

6.3.2.1. Block Segmentation

The document images were cropped and divided into blocks of 128x128 pixels overlapped 15%. An example of the results is given in Figure 6.12. These images are not provided with the database due to the easiness of the procedure.

Figure 6.12. Block segmented documents

Table 6.15. Details about the proposed database

Script	Notation	Documents	lines	Words
Arabic	*Arab*	51	1105	8141
Bengali	*bang*	54	472	2674
Gujarati	*gujr*	56	398	2365
Gurmukhi	*gurm*	120	1075	11021
Devanagari	*hind*	67	401	3233
Japanese	*japa*	80	565	2619
Kannada	*kana*	67	597	2357
Malayalam	*mala*	70	730	5502
Oriya	*oriy*	44	560	2401
Latin	*roma*	56	972	8143
Telugu	*telu*	67	494	2209
Thai	*thai*	64	467	4034
	Total:	796	7836	54704

6.3.2.2 Text Line segmentation

To segment the line, they are required to be horizontal. If it is not the case, a skew correction algorithm should be used. The lines have been segmented as follows: each connected object of the image has been labelled and its convex hull worked out. The result is dilated horizontally in order to connect the objects belonging to the same line table 6.15.

Then the horizontal histogram is obtained and the line located at the maximums point of the histogram is located. In each line, a horizontal line is drawn in order to connect distant object of the same line. The next step is to extract line by line which has been done as follows:

1. Select the top object of the dilated lines and work out its horizontal histogram

2. If its histogram has a single maximum, it is supposed a single line and the dilated object it is used as a mask to segment the line.

3. If the object has several peaks, it is supposed that several lines have been mixed in the object. To separate them, by the next steps:

    a. The object is horizontally eroded until the top object contains single peak.

    b. The new top object is dilated to recover the original shape and it is used as mask to segment the top line

4. The top line is deleted and goes to step 1 until finishing.
The segmentation results were reviewed and the lines wrongly segmented were manually fixed. The lines were saved and the files named as *script_xxx_yyy.tif* being *yyy* the line number of the document *script_xxx*. Examples of segmented lines are shown in Figure 6.14.These images are saved in grayscale. The number of lines per script can be found in table 6.15.
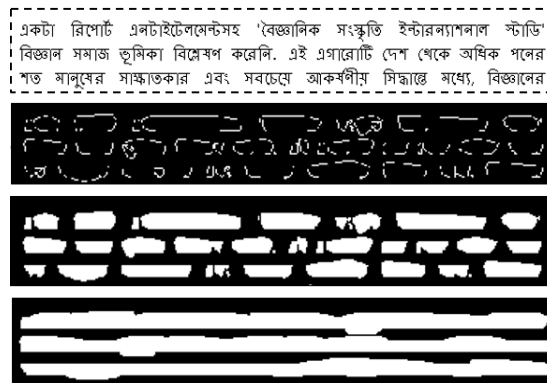
Figure 6.13: Line detection procedure
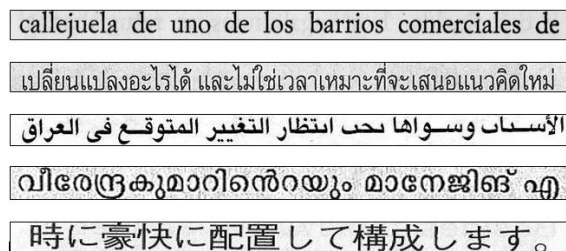
Figure 6.14. Examples of segmented lines in Latin, Thai, Arab, Malayalam and Japanese, respectively.

6.3.2.3.Word Segmentation

The words were segmented line by line in two steps. The first one was automatic. The lines were converted to black and white, and the gaps were identified as vertical histogram equal to zero. The gaps wider than one-third of the line height were labelled as words separations.

In the second step, words for which segmentation failures occurred were manually corrected. Every word was saved individually in black and white. The files were named as *script_xxx_yyy_zzz.tif* being *zzz* the word number of the line *script_xxx_yyy*. For instance, the file named *roma_004_012_0*04.tif contains the image in black and white of the fourth word in the line 12th of the 4th document in Latin script. An example of the segmentation result can be seen in figure 6.15. The number of words per script can be found in table 6.15.

In Thai and Japanese words segmentation is heuristic. The Thai and Japanese lines consist of two or three long sequences of characters separated by a greater space as can be seen in Figure 6.15. Each sequence contains several words, the separation or the blank spaces depends on the meaning. Therefore, they have been pseudo segmented as follows. For each sequence of characters, the two first characters are the first pseudo word. The third to the fifth character is the second pseudo-word, the sixth to the ninth character are the third pseudoword and son up to the end of the sequence.
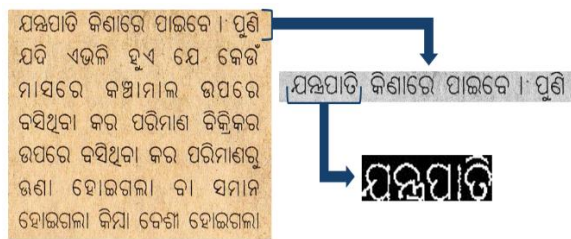
Figure 6.15. Word Segmentation example.

6.3.3. Script Identification Features

For benchmarking the database few script identifiers are employed. Several sets of local patterns for script featuring is used. Local patterns can be seen as a unifying approach to the traditional appearance and structural approaches for texture analysis. Applied to black and white images, local patterns can be considered as the concatenation of the binary gradient directions. The histogram of these micro-patterns contains information of the distribution of the edges, spots, and other local shapes in the script image which can be used as features for script detection. Local patterns used for featuring are LBP, OLBP, LDP, Local Derivative Patterns (LDerP) and DLBP. LDerP is variations of LDPs which are sensitive to random noise. Zhang et al. [271] investigated the effectiveness of using high-order local patterns in which the $(n-1)^{th}$ order derivative direction variations are coded based on binary coding function. Concisely, the first order derivatives along $\alpha = 0^o, 45^o, 90^o \; or \; 135^o$ are calculated as follows:

$$I'_0(Z_c) = I(Z_c) - I(Z_3)$$
$$I'_{45}(Z_c) = I(Z_c) - I(Z_2)$$
$$I'_{90}(Z_c) = I(Z_c) - I(Z_1)$$

$$I'_{135}(Z_c) = I(Z_c) - I(Z_0)$$

The local derivative pattern is defined as:

$$LDP'(Z_c) = \{LDP'_\alpha(Z_c)|\ \alpha = 0^o, 45^o, 90^o, 135^o\} \qquad (6.4)$$

being $LDP_\alpha'(Z_c)$ the local derivative pattern in α direction:

$$LDP_\alpha'(Z_c) = \{s(I'_\alpha(Z_i) \cdot I'_\alpha(Z_c))|\ i = 0,1,\dots.,7\} \qquad (6.5)$$

The above definition can be generalised to $(n-1)^{th}$ order derivate.

Block features-The blocks were transformed to $LBP(Z)$, $OLBP(Z)$, $LDP(Z)$ and $LDerivP(Z)$ code matrixes. Each code matrix contains information about the structure to which the pixel belongs: the stroke edge, stroke corners, stroke ends, inside the character or background, etc. It is supposed that the distribution of these structures define the script. Therefore, the block features are calculated as the histogram of the $LBP(Z)$, $OLBP(Z)$, $LDP(Z)$ and $LDerivP(Z)$ code matrixes which are named as h_{LBP}, h_{OLBP}, h_{LDP} and $h_{LDerivP\alpha}$ with $\alpha = 0^o, 45^o, 90^o, 135^o$. The histogram of $LBP(Z)$ contains 255 bins which are the 255 components of the LBP feature. The $LDerivP$ feature is obtained concatenating the four 255 bins histogram being 255X4=1012 long. In the same way, the $OLBP$ and LDP featurs contains 20 and 56 components respectively. Take into account that the bin corresponding to the code of the background has not been considered.

Line and word features- In this case, the script line or word image is transformed to $LBP(Z)$, $OLBP(Z)$, $LDP(Z)$ and $LDerivP(Z)$ code matrixes. As at line and word level the characteristic of the top, bottom and central area of the lines are different and distinctive of the each script. Therefore it is possible to model the spatial distribution of local pattern by dividing the line into a number of adjacent regions, calculating the histogram in each region and concatenating them. After conducting several experiments, testing a range of smaller and greater region sizes, the best performance was obtained when dividing the image into 4 equal horizontal regions which overlapped by 30%. For each region, calculate the histograms $\{h^i_{LBP}\}_{i=1}^4$, $\{h^i_{LDP}\}_{i=1}^4$ and $\{h^i_{LDerivP\alpha}\}_{i=1}^4$ with $\alpha = 0^o, 45^o, 90^o, 135^o$. The feature is obtained concatenating the histograms of all 4 regions in order to do not loss the spatial information obtaining the next vectors (nevertheless, experiments accumulating the histograms have been also done with discouraging results): The LBP feature of dimension

1020, the *OLBP* of dimension 80, the *LDP* feature with a dimension equal to 224 and the LDerP feature of dimension 4080.

In order to obtain scale invariance, the feature vectors are normalised to an area equal to one. An example of this procedure for *LBP* feature vector calculation is shown in Figure .16.
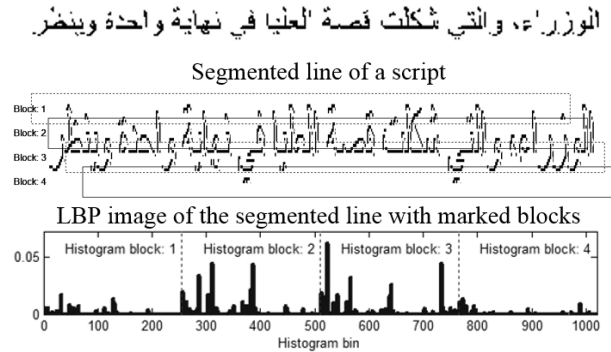
Figure 6.16. Example of LBP feature vector

A Support Vector Machine (SVM) has been used as classifier due to the large dimension of the feature vectors. SVM is a popular supervised machine learning technique which performs an implicit mapping into a higher dimensional feature space. This is the so-called kernel trick. After the mapping is completed it finds a linear separating hyperplane with maximal margin to separate data from this higher dimensional space. Least Squares Support Vector Machines (LS-SVM) are reformulations to standard SVMs which solve the indefinite linear systems generated within them. Robustness, sparseness and weightings can be imposed to LS-SVMs where needed and a Bayesian framework with three levels of inference is then applied. Though new kernels are being proposed, the most frequently used kernel functions are linear, polynomial, and Radial Basis Function (RBF). This study uses the RBF kernel for LBP, OLBP, LDP and LDerP and a linear kernel for Dense LBP. SVM or LS-SVM makes binary decision and multi-class classification for script identification has been made in this study by adopting the one-against-all techniques. Carried out grid-search on the hyper-parameters in the 10-fold cross-validation for selecting the parameters of the training sequence.

6.3.4. Experimental Results

The script database benchmarking is given in bi-script experiments in three levels: block, line and word. The scripts pair compared have been Latin with Indian languages and Devanagari with Indian languages, which are common cases. The training sequences consist of 30% of each script samples while the remainder 70% is used for testing. The released dataset includes the training and testing sequences. When a cropped block, line or word image contain less than the 10% of pixels belonging to strokes the image is discarded.

The benchmark results are given in Table 6.16, for block, line and word levels. In average, the results at block level are worse than at line level. But it doesn't stand for all the experiments, for instance in the experiment Devanagari vs. Malayalam. The result from line to word level, when comparing with Latin the results in average get worse, but comparing with Devanagari, the results in average improves. In general, there are not clear tendencies in the results. Therefore, this problem seems a case to case problem and the results are very dependent on the script to discriminate and the level: block, line, word.

Table 6.16. Benchmark: Hit ratio in % at Block, Line and Word level for different texture features

	Scripts	Block Level					Line Level					Word Level				
		LBP	OLPB	LDP	LDerP	DLBP	LBP	OLPB	LDP	LDerP	DLBP	LBP	OLPB	LDP	LDerP	DLBP
Latin	Arab	94.22	96,60	97,67	94,18	94,74	92,25	92,38	92,31	92,31	99,10	99,67	99,53	99,48	99,54	96,90
	Bengali	99,44	99,61	98,88	99,49	89,80	98,94	100,00	100,00	100,00	98,90	99,62	99,43	99,32	99,55	99,70
	Gujarati	95,54	96,99	97,92	95,87	89,00	96,39	99,90	99,36	99,18	96,20	97,89	97,68	98,56	97,82	94,20
	Gurmukhi	59,79	63,98	63,86	59,33	96,90	92,59	92,86	92,86	92,79	93,40	80,69	80,73	80,60	80,80	87,90
	Devanagari	99,52	97,54	98,22	99,52	89,80	99,72	100,00	100,00	100,00	98,60	99,64	99,21	99,26	99,50	99,80
	Japanese	99,28	99,77	98,82	99,18	92,70	98,84	99,65	99,95	99,82	98,30	98,04	97,54	96,05	96,02	98,80
	Kannada	98,32	98,59	98,82	98,49	93,90	99,49	100,00	98,72	99,70	97,70	98,69	98,62	98,70	98,97	99,50
	Malayalam	97,29	91,42	95,19	97,26	81,60	97,48	97,97	96,72	96,06	99,10	91,24	91,41	90,54	92,22	99,70
	Oriya	94,18	94,79	93,57	94,51	88,30	98,88	99,82	99,68	99,91	96,20	97,23	98,53	97,58	97,28	99,50
	Telugu	97,29	97,15	97,70	97,41	97,90	99,12	100,00	99,29	99,29	99,00	98,85	98,54	98,29	98,53	99,20
	Thai	99,13	98,48	98,91	99,02	82,50	98,76	99,64	99,64	100,00	97,00	98,46	96,70	97,14	96,12	91,30
Devanagari	Bengali	94,41	82,77	86,00	94,65	77,30	87,88	88,19	85,12	88,34	96,70	95,57	95,86	96,19	97,63	99,10
	Gujarati	69,32	70,31	73,23	70,95	75,30	92,67	98,71	99,81	97,52	92,40	97,59	98,88	99,09	98,50	99,40
	Gurmukhi	51,05	53,02	53,77	50,89	71,50	55,43	55,43	55,43	55,43	81,90	50,00	50,00	50,00	50,00	82,60
	Kannada	69,15	83,00	78,40	67,60	96,90	76,41	77,15	77,15	76,53	100,00	98,02	98,46	98,54	97,15	99,80
	Malayalam	97,03	99,36	97,88	97,03	100,00	68,23	68,23	68,23	68,23	100,00	70,50	70,39	70,47	70,50	99,90
	Oriya	84,37	75,89	77,04	86,82	96,00	80,00	80,00	80,00	80,00	99,90	99,80	99,17	99,53	99,67	99,90
	Telugu	85,73	97,39	89,59	82,21	95,70	86,53	86,98	86,83	86,83	99,10	95,12	99,29	98,37	98,30	99,60

The script identification rate between Devanagari and Gurmukhi is around 50% in all the experiments. At first, it was considered as a lack of training for Gurmukhi. Therefore the number of Gurmukhi documents in the dataset were increased which yielded a greater

training sequence. Still the results remained the same. Analysing in detail both in scripts, they display a very similar structure in their characters. The similar number of horizontal, vertical and curved components in both scripts seems to be the origin of the confusion for texture-based features. Although lesser extent, it also happens with Gujarati. So they need another descriptor to be distinguished. The Dense LBP works much better than LBP, OLBP, LDP and LDerP. It can be due to their multi-scale property and greater spatial resolution.

6.3.5. Summary of Script Identification

A new printed multiscript dataset for free distribution has been introduced in this work. It contains realistic samples obtained from local newspaper and magazines. Different fonts, size, cursive, bold texts are considered in the dataset. The dataset includes scanned documents at 300dpi, the segmented lines and words along with the training and testing sequences for fair algorithms comparison.

The benchmarking is provided at the block, line and word level with different texture based features, which are the well-known LBP, OLBP, LDP and LDerP. Additionally, a set of parameters never used for script identification called Dense-LBP is proposed in this work with excellent results due to their multi-scale and denser spatial description.

Just to pint out there is not a clear tendency in the results, so this problem seems a case to case problem, i.e. there is not a universal solution but the optimal solution for each script identification problem is different.

7

Conclusions and Future Scope

This chapter concludes the thesis by summarising the research contributions, limitations and suggests some areas for future work. The recent popularity of biometric systems in trusted involuntary security zones, adhere the biometric system to be more reliable in relation to a spoofing attack. To overcome the spoofing attack several liveness detection methods are proposed in the literature. However, adaptability of the trait with respect to different changes and liveness detection is found to be a trade-off. This thesis has made an attempt to solve the trade-off. The thesis also contributes to advance the multimodal ocular biometric using the sclera and iris. In addition, the thesis also contributes to other field of pattern recognition: wrist biometrics, multi-script signature verification and script identification. A summary of the contribution is listed in the next section.

7.1. Contributions

In Chapter 2, the existing state-of-the-art methods published in the various research areas within sclera, iris, and multimodal ocular biometrics using sclera and iris are reviewed. After reviewing iris literature, it was found that the recent trend of research in iris biometrics is iris recognition in non-ideal conditions. To increase the applicability multimodal iris biometrics is proposed. Among iris multimodal biometrics, iris combination with sclera is most popular. The state-of-the-art of sclera biometrics is still not well explored. Therefore, different challenges in processing sclera trait are discussed followed by a review of its literature. Specifically, the published methods on the sclera and iris segmentation enhancement, feature extraction, classification, and information fusion are reviewed. It was found that multimodal ocular biometrics-based on iris and sclera is a very upcoming

research area and has a promising literature. The methodology used on sclera segmentation can be classified into two categories: intensity based and shape based. Further, sclera feature can be broadly grouped into two categories: shape based and texture based. Different databases available and performance on them are discussed. Pros and cons of each of these approaches are discussed and potential research scope is identified. Followed by a way forward of research on this subject of research. In the next part of the chapter, 2 literature review on liveness detection and adaptive biometrics are discussed. Various shortcomings and open research areas were identified based on the review. The main shortcoming identified is the trade-off between adaptability and liveness. The problem description and scope for the current research described in this thesis were finalised based on the identified open research areas.

In Chapter 3, various segmentations, pattern enhancement, featuring, classification and information fusion techniques are employed to advance the iris and sclera-based multimodal biometrics. Intensity-based segmentation techniques were found to be more successful to produce better sclera segmentation. Wavelet-based bank of filters was found to give best enhancement for both the sclera and iris pattern. A dictionary based learning feature extraction was found to best model the traits at the sensor level of information fusion. Two datasets were employed namely UBIRIS version 1 and MASD. MASD database was developed as a part of the contribution of the thesis. From the experiments conducted the effect of gaze angle and acquiring artefacts on the identification performance of the trait is identified. A state-of-the-art comparison of the proposed advancement is performed, which inferred effective research contribution. A method for artificial synthesis of sclera pattern is also proposed. Further, results of the biometric competition organised is analysed and open research areas are discussed in details.

In Chapter 4, a couple of liveness detection methods were proposed and their results are discussed. The first liveness detection method an anti-spoofing method using eye gaze angle sequence was proposed. Next, a framework for liveness detection based on image quality features is proposed. The framework performs user-level liveness detection is a contrast to the previous framework proposed in the literature. To conduct the experiment a database was proposed. The state-of-the-art comparison of the framework is also found to be very effective in comparison to the previous frameworks. Some limitation and future work of the proposed framework are also discussed.

In Chapter 5, the online-based classifier was proposed for adaptiveness of biometric trait with respect to change in position, acquiring artefacts and ageing. Further, a framework employing the base and the online classier was proposed to curtail the limitation of each of this classier in AB and proposed a best optimal solution, A dataset was proposed with a

large sample and multi-angle eye images to experiment the effectiveness of the proposed framework.

In Chapter 6, contributions to various other fields of pattern recognition are discussed. In the first contribution, the influence of script on multi-script signature verification is investigated. It was found that the multi-script signature verification is a script independent problem. Several statistical measures, feature extraction techniques and signature databases from different scripts were employed in the study. In the next study, the wrist vein biometric was investigated. A whole wrist vein biometric system was proposed and its results were found to be effective in comparison to the previous works in the literature. The last contribution of the chapter was on script identification of printed documents. A realistic dataset was proposed in the work. Three level of script identification was investigated: document level, line level and word level. Among them, word level was found to be most effective using the Dense-LBP feature.

7.2. Future Work

A variety of research areas in the field of sclera and iris multimodal ocular biometric and few other pattern recognition research domains were investigated in this thesis with the objective of creating a robust and reliable recognition systems. Several research areas and scope for improvement were identified for future research. Possible future research work can be summarised as follows:

- Various open research areas are identified at the different stages of the sclera biometrics and a whole set of way forward is also discussed in the thesis which can be considered for future research.

- Liveness detection-based on the fusion of image quality feature, bodily response and the voluntary signal from individuals can be employed to design more robust anti-spoofing technique.

- Dataset for liveness detection considering larger population size is also required to be developed.

- Different online learning-based classifiers are required to be investigated for finding the capability of online learning for adaptive biometrics.

- Dataset for experimenting adaptive biometrics considering larger population size and different change in acquiring condition is also required to be developed.

- The influence of script on multi-script ASV for other scripts is required to be investigate.

- Literature of the wrist biometric is very limited, therefore intense research on this field of biometrics is highly anticipated.

- Script identification for handwritten documents can be highly challenging and very limited research has been conducted. Therefore, intense research on this subject is required.

7. 3. Criticism of the proposed work

Some limitations of the present work are also identified and critics of this work are addresses and how they can be solve are summarised as following:

- The sclera segmentation are performed by clustering-based and intensity-based shape techniques. Miss-classification was found in these techniques due to changes in intensity etc. These challenges can be resolved-based on CNN-based segmentation techniques, some initial investigations found from the algorithms submitted from the participants of SSBC 2015 and SSERBC 2017.

- The sclera segmentation enhancement techniques proposed were found not perfectly robust with changes in lighting, illumination, etc. Therefore, more advance image enhancement techniques like grey scale grouping, Tabu search, etc. can be used.

- The performance quality-based features proposed for liveness detection of ocular biometrics in visible spectrum can fluctuate due to change in illumination. More robust texture-based feature and signal to action response can also be employed.

- The performance of the adaptive biometric in the proposed framework in chapter 5 found to achieve limited performance accuracy. A very initial ground of this subject of research was founded in the thesis. A wide spectrum of advancement including designing larger dataset, betterment of the performance can be done by fine tuning the classifiers.

- The experiments conducted on the script recognition were performed on the printed script, whereas handwritten script recognition can be more challenging in the sense due to their huge intra-class and inter-class variance.

- The experiment conducted for the wrist vain recognition is on a very limited population size, so a potential research is required to outperform the limitation and push the boundary of this research.

- The vain enactment techniques employed for the wrist biometrics found to not perform adaptively with respect to change in light and illumination resulting in noise inclusion in the images. A potential research should be performed to uplift the present research work conducted.

- The wrist vain was also experimented without segmentation, so potentiating non-wrist information was also included

References:

[1] R. Derakhshani, A. Ross, and S. Crihalmeanu. A new biometric modality based on conjunctival vasculature. Proceedings of Artificial Neural Networks in Engineering: 1-8, 2006.

[2] R. Derakhshani and A. Ross. A texture-based neural network classifier for biometric identification using ocular surface vasculature. Proceedings of International Joint Conference on Neural Networks: 2982–2987, 2007.

[3] Z. Zhou, Y. Du, N. L. Thomas, and E. J. Delp. Multi angled sclera recognition. IEEE Workshop on Computational Intelligence in Biometrics and Identity Management: 103 – 108, 2011.

[4] Z. Zhou, Y. Du, N. L. Thomas, and E. J. Delp. Multimodal eye recognition. Proceedings of the International Society for Optical Engineering, 7708(770806):1-10, 2010.

[5] Z. Zhou, Y. Du, N. L. Thomas, and E. J. Delp. A new biometric sclera recognition. IEEE transaction on System, Man and Cybernatics –PART A: System and Human, 42(3): 571-583, 2012.

[6] Z. Zhou, Y. Du, N. L. Thomas, and E. J. Delp, Quality Fusion Based Multimodal Eye Recognition, IEEE International Conference on Systems, Man, and Cybernetics: 1297-1302, 2012.

[7] M. H. Khosravi and R. Safabakhsh, Human eye sclera detection and tracking using a modified time-adaptive self-organizing map, Pattern Recognition, 41: 2571 – 2593, 2008.

[8] S. Crihalmeanu and A. Ross, Multispectral sclera patterns for ocular biometric recognition, Pattern Recognition Letters, 33: 1860–1869, 2012.

[9] S. PavanTankasala, P. Doynov, R. R. Derakhshani, A. Ross and S. Crihalmeanu, Biometric Recognition of Conjunctival Vasculature using GLCM Features, International Conference on Image Information Processing : 1-6, 2011.

[10] K. Oh and K.Toh, Extracting Sclera Features for Cancelable Identity Verification, 5th IAPR International Conference on Biometric: 245-250, 2012.

[11] V. Gottemukkula, S. K. Saripalle, S. P. Tankasala, R. Derakhshani, R. Pasula and A. Ross, Fusing Iris and Conjunctival Vasculature: Ocular Biometrics in the Visible Spectrum, IEEE Conference on Technologies for Homeland Security: 150-155, 2012.

[12] U. Park, A. Ross, and A. K. Jain, Periocular Biometrics in the Visible Spectrum: A Feasibility Study, IEEE 3rd International Conference on Biometrics: Theory, Applications, and Systems: 1-6, 2009.

[13] Z. Zhou, E. Y. Du, and N. L. Thomas, A Comprehensive Sclera Image Quality Measure, 11th International Conference on Control, Automation, Robotics and Vision: 638-643, 2010.

[14] S. Crihalmeanu, A. Ross , and R. Derakhshani, Enhancement and Registration Schemes for Matching Conjunctival Vasculature, Appeared in Procceding of the 3rd IAPR/IEEE International Conference on Biometrics :1247–1256, 2009

[15] T. F. Chan, and L. A. Vese, Active Contours Without Edges, IEEE Transaction On Image Proccessing 10(2): 266-277, 2001

[16] J. G. Daugman. High confidence visual recognition of persons by a test of statistical independence. IEEE Transactions on Pattern Analysis and Machine Intelligence, 15(11):1148–1161, 1993.

[17] H. Shah-Hosseini and R. Safabakhsh, TASOM: a new time adaptive self-organizing map, IEEE Trans. Syst. Man Cybern. Part B, vol. 33, no. 2, pp. 271-282, 2003.

[18] H. Shah-Hosseini and R. Safabakhsh, A TASOM-based algorithm for active contour modelling, Pattern Recognition Letter, vol. 24, no. 9, pp. 1361-1373 2003.

[19] Z. Zhou, E. Y. Du, and N. L. Thomas, A Comprehensive Sclera Image Quality Measure, 11th International Conference on Control, Automation, Robotics and Vision, pp. 638-643, 2010.

[20] S. Lazebnik, C. Schmid, and J. Ponce: Beyond bags of features: Spatial pyramid matching for recognizing natural scene categories, In Proc. Computer Vision and Pattern Recognition (CVPR), 2, 2169–2178.

[21] Hugo Proença and, Luís A.Alexandre, UBIRIS: A noisy iris image database, Proceed. of ICIAP 2005 - Intern. Confer. on Image Analysis and Processing, 1, 970-977,2005.

[22] S. Crihalmeanu and A. Ross, On the use of multispectral conjunctival vasculature as a soft biometric. In: Proc. IEEE Workshop on Applications of Computer Vision (WACV), pp. 204-211, 2011.

[23] Ko Nishino and Shree K. Nayar. Eyes for relighting. ACM Trans. Graph., vol 23, no. 3, pages 704–711, 2004.

[24] J. Canny. A computational approach to edge detection. IEEE Transactions on Pattern Analysis and Machine Intelligence, vol. 8, pages 679–698, 1986.

[25] D. Martin-Roche, C. Sanchez-Avila, and R.Sanchez-Reillo. Iris recognition for biometric identification using dyadic wavelet transform zero-crossing. IEEE Aerospace and Electronic Systems Magazine, Mag. 17, no. 10, pages 3–6, 2002.

[26] A. Bertillon, "La couleur de Piris".Revue scientifique, vol. 36, no. 3, pp. 65-73, 1885.

[27] J. Daugman, "High confidence personal identification by rapid video analysis of iris Texture", Proc. IEEE International Carnaha conf. on security technology, 1992.

[28] J. Daugman,"High confidence visual recognition of persons by a test of statistical independence,", IEEE Trans. on Pattern Analysis and Machine Intelligence, vol.15, no. 11, pp. 1148-1161, 1993.

[29] J. Daugman, "How iris recognition works," Circuits and Systems for Video Technology," IEEE Trans. , Vol. 14, no. 1, pp. 21-30, 2004.

[30] J. Daugman," New Methods in Iris Recognition," Proc. IEEE Trans. on the system, man and cybernetics-part B, vol. 37, no 5, pp. 1167-1175, 2007.

[31] S. Mallat, "A theory for multiresolution signal decomposition: the wavelet representation," IEEE Pattern Anal. and Machine Intell., vol. 11, no. 7, pp. 674–693. 1989.

[32] J. B. MacQueen,. "Some Methods for classification and Analysis of Multivariate Observations". Proceedings of 5th Berkeley Symposium on Mathematical Statistics and Probability, University of California Press. pp. 281–297. MR 0214227. Zbl 0214.46201. Retrieved 2009-04-07, 1967.

[33] J. C. Dunn : "A Fuzzy Relative of the ISODATA Process and Its Use in Detecting Compact Well-Separated Clusters", Journal of Cybernetics 3: 32-57, 1973.

[34] J. C. Bezdek : "Pattern Recognition with Fuzzy Objective Function Algoritms", Plenum Press, New York, 1981.

[35] B.N. Li, C.K. Chui, S. Chang, and S.H. Ong, Integrating spatial fuzzy clustering with level set methods for automated medical image segmentation. Computers in Biology and Medicine 41(1) 1-10, 2011.

[36] S. M. Pizer, E. P. Amburn, J. D. Austin: Adaptive Histogram Equalization and Its Variations. Computer Vision, Graphics, and Image Processing 39 (1987) 355-368.

[37] I. Daubechies, Ten lectures on wavelets, CBMS-NSF conference series in applied mathematics, SIAM Ed., pp. 117–119, 1992.

[38] H. William; A. Saul; T. William; B. P. Flannery,. "Section 16.5. Support Vector Machines". Numerical Recipes: The Art of Scientific Computing (3rd ed.). New York: Cambridge University Press. ISBN 978-0-521-88068-8,2

[39] A. Das and R. Parekh "Iris Recognition using a Scalar based Template in Eigen-space", International Journal of Computer Science and Telecommunication, vol.3, no.5, pp 74-79., May 2012.

[40] A. Das and R. Parekh "Iris Recognition in 2D Eigen-space", International Journal of Computer Applications, vol .52,no.19, pp 1-6, August 2012.

[41] K. Oh, B.-S. Oh, K.-A. Toh, H.-L.Eng and W.-Y.Yau, "Combining Sclera and Periocular Features for Multi-modal Identity Verification", Neurocomputing, vol. 128, pp. 185-198, 2014.

[42] A. Das, Face Recognition in reduced Eigen plane", International Conference on Communications, Devices and Intelligent Systems , 620- 623, 2012.

[43] D. Sheet, H. Garud, A. Suveer, J. Chatterjee and M. Mahadevappa, Brightness Preserving Dynamic Fuzzy Histogram Equalization, IEEE Trans., Consumer Electronics, 6(4), 2475 - 2480, Nov. 2010.

[44] T. Mäenpää, M. Pietikäinen, Texture Analysis with local binary Patterns, in C.H. Chen, P.S.P. Wang (eds.): Handbook of Pattern Recognition and Computer Vision, 3rd edn. World Scientific, pp. 197-216, 2005.

[45] W. Bu., X. Wub, E. Gaob: Hand Vein Recognition Based on Orientation of LBP. Proc. of SPIE, Vol. 8371(83711), pp. 1-12 (2012).

[46] D. G. Lowe, 'Distinctive image features from scale-invariant keypoints', Proceedings of IJCV 2004, 2, (60), pp. 91-110. 2004.

[47] A. Morales, M. A. Ferrer and A. Kumar. "Toward Contactless Palmprint Authentication". IET Computer Vision 2011, Volume 5, Issue 6, pp. 407-416.

[48] F. Alonso-Fernandez, P. Tome-Gonzalez, V. Ruiz-Albacete, and J. Ortega-Garcia: Iris recognition based on sift features. In: Int'l Conf. on Biometrics, Ident. and Sec (BIdS), pp. 1–8 (2009).

[49] Md. H. Kabir, T. Jabid and O. Chae, "A Local Directional Pattern Variance (LDPv) based Face Descriptor for Human Facial Expression Recognition", in Proceedings of the IEEE Advanced Video and Signal Based Surveillance (AVSS), pp. 526–532, August 2010

[50] R. P. Wildes. Iris recognition: an emerging biometric technology. In Proceedings of the IEEE, vol. 85, no.9, pages 1348–1363, U.S.A., September 1997.

[51] J. Huang, Y. Wang, T. Tan, and J. Cui. A new iris segmentation method for recognition. In Proceedings of the 17th International Conference on Pattern Recognition (ICPR04), vol. 3, pages 23–26, 2004.

[52] W. K Kong and D. Zhang. Accurate iris segmentation method based on novel reflection and eyelash detection model. In Proceedings of the 2001 International Symposium on Inteligent Multimedia, Video and Speech Processing, pages 263–266, Hong Kong, May 2001.

[53] W. K Kong and D. Zhang. Accurate iris segmentation method based on novel reflection and eyelash detection model. In Proceedings of the 2001 International Symposium on Inteligent Multimedia, Video and Speech Processing, pages 263–266, Hong Kong, May 2001.

[54] L. Ma, Y. Wang, and T. Tan. Iris recognition using circular symmetric filters. In Proceedings of the 25th International Conference on Pattern Recognition (ICPR02), vol. 2, pages 414–417, Quebec, August 2002.

[55] L. Ma, T. Tan, Y. Wang, and D. Zhang. Personal identification based on iris texture analysis. IEEE Transactions on Pattern Analysis and Machin Intelligence, vol. 25, no. 12, pages 2519–2533, December 2003.

[56] L. Ma, Y. Wang, and D. Zhang. Efficient iris recognition by characterizing key local variations. IEEE Transactions on Image Processing, vol. 13, no. 6, pages 739–750, June 2004.

[57] Y. Du, R. Ives, D. Etter, T. Welch, and C. Chang. A new approach to iris pattern recognition. In Proceedings of the SPIE European Symposium on Optics/Photonics in Defence and Security, vol. 5612, pages 104–116, October 2004.

[58] J. Mira and J. Mayer. Image feature extraction for application of biometric identification of iris - a morphological approach. In Proceedings of the 16th Brazilian Symposium on Computer Graphics and Image Processing (SIBGRAPI 2003), pages 391–398, Brazil, October 2003.

[59] J. Kim, S. Cho, and J. Choi. Iris recognition using wavelet features. Kluwer Academic Publishers, Journal of VLSI Signal Processing, no. 38, pages 147– 256, November 2004.

[60] W. W. Boles and B. Boashash. A human identification technique using images of the iris and wavelet transform. IEEE Transactions on Signal Processing, vol. 46, no. 4, pages 1185–1188, April 1998.

[61] D. Martin-Roche, C. Sanchez-Avila, and R.Sanchez-Reillo. Iris recognition for biometric identification using dyadic wavelet transform zero-crossing. IEEE Aerospace and Electronic Systems Magazine, Mag. 17, no. 10, pages 3–6, 2002.

[62] R. P. Wildes. Iris recognition: an emerging biometric technology. In Proceedings of the IEEE, vol. 85, no.9, pages 1348–1363, U.S.A., September 1997.

[63] J. Ali and A. Hassanien. An iris recognition system to enhance e-security environment based on wavelet theory. AMO - Advanced Modeling and Optimization, vol. 5, no. 2, pages 93–104, 2003.

[64 S. Lim, K. Lee, O. Byeon, and T. Kim. Efficient iris recognition through the improvement of feature vector and classifier. ETRI Journal,
vol. 23, no. 2, pages 61–70, June 2001.

[65] A. Muron, P. Kois, and J. Pospisil. Identification of persons by means of the Fourier spectra of the optical transmission binary models of the human irises. Elsevier Science, Optics Communications, no. 192, pages 161–167, June 2001.

[66] K. Nam, K. Yoon, J. Bark, and W. Yang. A feature extraction method for binary iris code construction. In Proceedings of the 2nd International Conference on Information Technology for Application, pages 284–288, China, January 2004.

[67] C. Tissue, L. Martin, L. Torres, and M. Robert. Person identification technique using human iris recognition. In Proceedings of the 25th International Conference on Vision Interface, pages 294–299, Calgary, July 2002.

[68] Y. Huang, S. Luo, and E. Chen. An efficient iris recognition system. In Proceedings of the First International Conference on Machine Learning and Cybernetics, pages 450–454, China, November 2002.

[69] Y. Zhu, T. Tan, and Y. Wang. Biometric personal identification based on iris patterns. In Proceedings of the 13th International Conference on Pattern Recognition (ICPR00), pages 2801–2804, Barcelona, September 2000.

[70] L. Ma, T. Tan, D. Zhang, and Y. Wang. Local intensity variation analysis for iris recognition. Pattern Recognition, vol. 37, no. 6, pages 1287–1298, 2004.

[71] Y. Du, B. Bonney, R. Ives, D. Etter, and R. Schultz. Analysis of partial iris recognition using a 1-d approach. In Proceedings of the IEEE International Conference on Acoustics, Speech and Signal Processing (ICASSP'05), pages 961–964, U.S.A., March 2005.

[72] V. Dorairaj, N. Schmid, and G. Fahmy. Performance evaluation of non-ideal iris based recognition system implementing global ICA encoding. In Proceedings of the IEEE International Conference on Image Processing (ICIP 2005), pages 285–288, Italy, September 2005.

[73] E. Sung, X. Chen, and J. Yang. Towards non-cooperative iris recognition systems. In Proceedings of the Seventh International Conference on Control, Automation, Robotics and Vision (ICARV'02), pages 990–995, Singapore, December 2002.

[74] C. Fancourt, L. Bogoni, K. Hanna, Y. Guo, R. Wildes, N. Takahashi, and U. Jain. Iris recognition at a distance. In Proceedings of the 2005 IAPR Conference on Audio and Video-Based Biometric Person Authentication, pages 1–13, U.S.A., July 2005.

[75] Y. Du, B. Bonney, R. Ives, D. Etter, and R. Schultz. Analysis of partial iris recognition using a 1-d approach. In Proceedings of the IEEE International Conference on Acoustics, Speech and Signal Processing (ICASSP'05), pages 961–964, U.S.A., March 2005.

[76] D. Ort, H. David, "Development of the Eye". Retrieved 22 April 2015

[77] the University of Bath. University of Bath iris image database, 2004. http://www. bath.ac.uk/elec-eng/pages/sipg/.

[78] Institute of Automation, Chinese Academy of Sciences. CASIA iris image database, 2004. http://www.sinobiometrics.com.

[79] National Institute of Standards and Technology. Iris challenge evaluation, 2006. http://iris.nist.gov/ICE/.

[80] Multimedia University. MMU iris image database, 2004. http://pesona.mmu. edu.my/centre.

[81] M. Dobes and L. Machala. UPOL iris image database, 2004. http:// phoenix.inf.upol.cz/iris/.

[82] A. Ross, S. Crihalmeanu, L. Hornak, and S. Schuckers. A centralized web-enabled multimodal biometric database. In Proceedings of the 2004 Biometric Consortium Conference (BCC), U.S.A, September 2004

[85] A. M. Joussen, Vascular plasticity - the role of the angiopoietins in modulating ocular angiogenesis, Graefe's Archive for Clinical and Experimental Ophthalmology, vol. 239, no 12, pp. 972 - 975, 2001.

[86] H. Kobayashi and S. Kohshima, Unique morphology of the human eye, Nature, vol. 387, no. 6635, pp. 767-768, 1997.

[87] D. Ort, H. David, "Development of the Eye". Retrieved 22 April 2015'

[88] T.W. Sadler, Langman's medical embryology (6th ed.). Williams and Wilkins. ISBN 0683074938. (1990)

[89] A. M. V. Keller, "Embryonic Development of the Eye". Retrieved 22 April 2015.

[90] S. Fuhrmann, E. M. Levine, T. A. Reh, "Extraocular mesenchyme patterns the optic vesicle during early eye development in the embryonic chick". Development 127, 4599-4609. 2000.

[91] A. Eiraku, "Self-organizing optic-cup morphogenesis in three-dimensional cell culture", Nature 472, 51–56 (07 April 2011)

[92] K. Trier, Advances in organ biology. The Sclera. The Biology of the Eye, vol. 10. Elsevier Inc., pp. 353–373, 2006.

[93] J. J. Kanski, Clinical Ophthalmology: A Systematic Approach. Elsevier Science Limited. 2003.

[94] G. Heath, The episclera, sclera and conjunctiva, Optometry today. Different. Diagnosis Ocular Dis. 9 (2), 36–42, 2006.

[95] C.G. Owen, R.S.B. Newsom, A.R. Rudnicka, T.J. Ellis, and E.G. Woodward, Vascular response of the bulbar conjunctiva to diabetes and elevated blood pressure. Ophthalmology 112 (10), 1801–1808. 2005.

[96] C.G. Owen, R.S.B. Newsom, A.R. Rudnicka, T.J. Ellis, and E.G. Woodward, Diabetes and the tortuosity of vessels of the bulbar conjunctiva. Ophthalmology 115 (6), e27–e32, 2008

[97] A. Ross and A. K. Jain, Multimodal biometrics: an overview, Appeared in Proc. of 12th European Signal Processing Conference (EUSIPCO), (Vienna, Austria), pp. 1221-1224, September 2004.

[98] S, U. Uludag, A. Mink, M. Indovina, A. K. Jain, Large-scale evaluation of multimodal biometric authentication using state-of-the-art systems, IEEE Transactions On Pattern Analysis And Machine Intelligence, 450-455, 27(3), MARCH 2005

[99] Md. El-Abed1, C. Charrier , C. Rosenberger, Quality assessment of image-based biometric information, EURASIP Journal on Image and Video Processing (2015) 2015: 1-15

[100] Ratha, N., Connell, J., Bolle, R., 2001. An analysis of minutiae matching strength. Proc. AVBPA, International Conference on Audio- and Video-Based Biometric Person Authentication III, 223-228.

[101] B. Toth, Biometric Liveness Detection, Information Security Bulletin, 10: 291-297, 2005.

[102] J. Galbally, J. Ortiz-Lopez, J. Fierrez, J. Ortega-Garcia, a. Iris liveness detection based on quality related features, in Proc. Intl. Conf. on Biometrics, ICB, India, pp. 271-276, 2012.

[103] A. Rattani, B. Freni, G. L. Marcialis, F. Roli, Template update methods in adaptive biometric systems: A critical review'. Proc. Third Int. Conf. Biometrics, Sardinia, Alghero: 847–856, 2009.

[104] N. Poh, A. Rattani and F. Roli, Critical Analysis of Adaptive Biometric Systems, IET Biometrics, 1(4): 179 - 187, 2012.

[105] A. Rattani, G. L. Marcialis, E. Granger, F. Roli, A Dual-staged Classification-Selection Approach for Automated Update of Biometric Templates, Intl Conf. on Pattern Recognition (ICPR), Japan: 2972 - 2975, 2012.

[106]. A. Rattani, Adaptive biometric system based on template update procedures. PhD thesis, University of Cagliari, Italy, 2010

[107]. A. Rattani, B. Freni, G. L. Marcialis, F. Roli: Template update methods in adaptive biometric systems: A critical review. Proc. Third Int. Conf. Biometrics, Sardinia, Alghero, 2009, pp. 847–856

[108]. N. Poh, J. Kittler, S. Marcel, D. Matrouf, J. F. Bonastre.: Model and score adaptation for biometric systems: coping with device interoperability and changing acquisition conditions. Proc. Int. Conf.on Pattern Recognition, Istambul, Turkey, 1229–1232, 2010.

[109]. U. Uludag, A. Ross, A. Jain: Biometric template selection and update: A case study in fingerprints, Pattern Recognition., 37, (7): 1533–1542, 2004.

[110]. X. Jiang, W. Ser: 'Online fingerprint template improvement', IEEE Trans. Pattern Anal. Mach. Intell., 24, (8), .1121–1126, 2008.

[111]. C. Ryu, K. Hakil, A. K. Jain: 'Template adaptation based fingerprint verification'. Proc. 18th Int. Conf. on Pattern Recognition, HongKong, 582–585, 2006.

[112]. X. Liu, T. Chen, S. M. Thornton: Eigenspace updating for nonstationary process and its application to face recognition', PatternRecognit., 36, (9), 1945–1959, 2003.

[113] F, Roli, L. Didaci, G. L. Marcialis: Template co-update in multimodal biometric systems. Proc. IEEE/IAPR Int. Conf. on Biometrics, Seoul, Korea, 1194–1202, 2007.

[114] F. Roli, G. L. Marcialis: Semi-supervised PCA-based face recognition using self-training. Proc. Joint IAPR Int. Workshop on S+SSPR06, HongKong, China, 560–568, 2006.

[115] A. Rattani, G. L. Marcialis, F. Roli: Biometric template update using the graph min-cut: a case study in face verification. Proc. Sixth IEEEBiometric Symp., Tampa, USA, 23–28, 2008.

[116] M. Une, Y. Tamura, Liveness detection techniques. IPSJ Magazine, 47(6), 605–608. 2006.

[117] E. Lee, K. Park, J. Kim, Fake iris detection by using purkinje image, in Advances in Biometrics, ser. Lecture Notes in Computer Science. Springer Berlin / Heidelberg, vol. 3832, pp. 397–403. 2005.

[118] J. Fierrez, J. Ortega-Garcia, T. Toledano, J. Gonzalez-Rodriguez, Biosec baseline corpus: A multimodal biometric database, Pattern Recognition,40(4), 1389–1392. 2007.

[119] A., C., S. Schuckers, K. Bowyer, D Yambay, Liveness Detection - Iris Competition 2013, 2013, http://people.clarkson.edu/projects/biosal/iris/. 2013,

[120] J. Doyle, and K. W. Bowyer, Notre Dame image dataset for contact lens detection in iris recognition, 2004.

[121] A. Czajka, Database of Iris Printouts and its Application: Development of Liveness Detection Method for Iris Recognition, Methods and Models in Automation and Robotics (MMAR), pp. 28-33, 2013.

[122] A. F. Sequeira, J. Murari, J.S. Cardoso. Iris liveness detection methods in mobile applications, International Conference on Computer Vision Theory and Applications (VISAPP), 2014.

[123] F. Alonso-Fernandez, J. Fierrez, J. Ortega-Garcia, J. G. Rodriguez, H. Fronthaler, K. Kollreider, J. Bigun. A comparative study of fingerprint image quality estimation methods. IEEE Trans. on Information Forensics and Security, 2(4):734–743, 2008.

[124] K. Kollreider, H. Fronthaler, M. Faraj. J. Bigun, Real-time face detection and motion analysis with application in liveness assessment. IEEE Trans. on Information Forensics and Security, 2(3-2):548-558, 2007,

[125] M. Kanematsu, H. Takano, K. Nakamura, Highly reliable liveness detection method for iris recognition, in SICE, Annual Conference. IEEE, pp. 361–364. 2007.

[126] A. Abhyankar, S. Schuckers, Iris quality assessment and biorthogonal wavelet-based encoding for recognition, Pattern Recognition, 42(9), 1878 – 1894, 2009.,

[127] X. He, S. An, P. Shi, Statistical texture analysis-based approach for fake iris detection using support vector machines, in Advances in Biometrics. Springer, pp. 540–546. 2007.

[128] L. Ma, T. Tan, Y. Wang, D. Zhang, Personal identification based on iris texture analysis, IEEE Transactions on Pattern Analysis and Machine Intelligence, 25(12), 1519–1533. 2003.

[129] A.F. Sequeira, J. Murari, J.S. Cardoso, Iris liveness detection methods in the mobile biometrics scenario, International Joint Conference on Neural Networks, pp. 3002-300, 2004.

[130] A K Jain, A Ross, S Prabhakar, An introduction to biometric recognition IEEE Transactions on circuits and systems for video technology 14 (1), 4-20

[131] J. Wright, A.Y. Yang, A. Ganesh, S. S. Sastry, Y. Ma, Robust face recognition via sparse representation, IEEE Trans. PAMI, 31(2), 210–227, 2009.

[132] J. Mairal, F. Bach, J. Ponce, Task-driven dictionary learning, IEEE Trans PAMI, 34(4), 791–804, 2012

[133] Z. Jiang, Z. Lin, L. Davis, Label consistent k-svd: learning a discriminative dictionary for recognition, IEEE Trans. PAMI 35(11), 2651–2664, 2013

[134] M. Aharon, M. Elad, A. Bruckstein, K-svd: An algorithm for designing overcomplete dictionaries for sparse representation, IEEE Trans. on Signal Processing, 54(11), 4311–4322, 2006

[135] J. Mairal, F. Bach, J. Ponce, G. Sapiro, A. Zisserman, "Supervised dictionary learning," In NIPS., 1033-1040, 2008

[136] I. Ramirez, P. Sprechmann, G. Sapiro, Classification and clustering via dictionary learning with structured incoherence and shared features, In CVPR, 3501-3508, 2010

[137] M. Yang, L. Zhang, X. Feng, D. Zhang, Fisher discrimination dictionary learning for sparse representation, In ICCV, 543-550, 2011

[138] Z. Wang, J. Yang, N. Nasrabadi, T. Huang, A max-margin perspective on sparse representation-based classification, In ICCV., 1217-1224, 2013

[139] M. Soltanolkotabi, E. Elhamifar, E. Candes, Robust subspace clustering, The Annals of Statistics, 42(2), 669-699, 2014.

[140] A. Coates, A.Y. Ng, The importance of encoding versus training with sparse coding and vector quantization, In ICML. 921-928, 2011

[141] L. Zhang, M. Yang, X. Feng, Sparse representation or collaborative representation: Which helps face recognition?, In ICCV., 471-478, 2011

[142] S.Gu, L. Zhang, W. Zuo, X. Feng., Projective dictionary pair learning for pattern classification., In NIPS 2014, 1-9, 2014.

[143] M. Scholz, R Klinkenberg, Boosting classifiers for drifting concepts, IDA − Special Issue on Knowledge Discovery from Data Streams 11 (1): 3–28, 2007.

[144] G. Widmer, M. Kubat, Learning in the Presence of Concept Drift and Hidden Contexts, Machine Learning, 23, 69–101, 1996.

[145] P. P. Rodrigues, J. A. Gama, J. A. Araújo, L. Lopes, L2GClust: local-to-global clustering of stream sources, in Proceedings of the 2011 ACM Symposium on Applied Computing, 1006–1011, ACM, 2011.

[146] J. Z. Kolter, M. A. Maloof, Dynamic Weighted Majority: An Ensemble Method for Drifting Concepts, J. Mach. Learn. Res., 8, 2755–2790, December 2007.

[147] N. W. Street, Y. Kim, A streaming ensemble algorithm (SEA) for large-scale classification, in KDD '01: Proceedings of the seventh ACM SIGKDD international conference on Knowledge discovery and data mining, 377–382, ACM, 2001.

[148] R. Klinkenberg, Learning drifting concepts: Example selection vs. example weighting, Intelligent Data Analysis, 8, 281–300, 2004.

[149] A. Fern, R Givan, Online ensemble learning: An empirical study, Machine Learning 53: 71–109, 2003.

[150] R. Polikar, Bootstrap inspired techniques in computational intelligence, IEEE Signal Processing Magazine, 24, 57–72, 2007.

[151] L. I. Kuncheva, Combining Pattern Classifiers: Methods and Algorithms. John Wiley & Sons, Inc., 2004.

[152] G. Brown, Ensemble learning, Encyclopedia of Machine Learning, 1-9, 2010.

[153] D. H. Wolpert, W. G. Macready, No free lunch theorems for optimization, IEEE Transactions on Evolutionary Computation, 1(1), 67–82, 1997.

[154] T. G. Dietterich, Machine learning research: Four current directions, Artificial Intelligence 18(4): 97–136, 1997.

[155] T. G. Dietterich, An experimental comparison of three methods for constructing ensembles of decision trees: Bagging, boosting, and randomization, Machine Learning 40(2): 139–157, 2000.

[156] L. I. Kuncheva, C. J. Whitaker, Measures of diversity in classifier ensembles and their relationship with the ensemble accuracy, Machine Learning 51: 181–207, 2003.

[157] L. Breiman, Random Forests, Machine Learning 45: 5–32, 2001.

[158] L. L.Minku, A. White, X. Yao, The impact of diversity on on-line ensemble learning in the presence of concept drift, IEEE Transactions on Knowledge and Data Engineering (TKDE) 22: 730–742, 2010.

[159] T.M. Martinetz, S.G. Berkovich, K. J. Schulten, Neural-Gas Network for Vector Quantization and its Application to Time-Series Rrediction, IEEE Trans. Neural Networks, 4(4), 558-569, 1993.

[160] Y. Freund, R. E. Schapire, Experiments with a new boosting algorithm, Proceedings of the Thirteenth International Conference on Machine Learning (ICML'96), Morgan Kaufmann, Bari, Italy, 148–156, 1996.

[161] R. Kunwar, U. Pal and M. Blumenstein. Semi-Supervised Online Learning of Handwritten Characters Using a Bayesian Classifier. Second IAPR Asian Conference on Pattern Recognition, Okinawa, Japan, 2013.

[162] V. Vladimir, V.Vapnik. Statistical Learning Theory. Springer-Verlag New York, 1998

[163] N. A. Syed, H. Liu, and K. K. Sung. Incremental learning with support vector machines. In SVM workshop, IJCAI, 1999.

[164] S. Ruping. Incremental learning with support vector machines. Technical Re ¨ port TR-18, Universitat Dortmund, SFB475, 2002.

[165] L. Ralaivola, F. d'Alche Buc. Incremental support vector machine learning: A local approach. Lecture Notes in Computer Science, 2130:322–329, 2001.

[166] J. Kivinen, A. J. Smola, R. C. Williamson. Online learning with kernels., Advances in Neural Inf. Proc. Systems (NIPS 01), 785–792, 2001.

[167] G. Cauwenberghs and T. Poggio. Incremental and decremental support vector machine learning. Advances in Neural Information Processing Systems,13, 409–415. MIT Press, 2001.

[168] P. Laskov, C. Gehl, S. Kruger, K.R. Muller. Incremental Support Vector Learning: Analysis, Implementation and Applications. Journal of Machine Learning Research, 1909–1936, 2006.

[169] A. Shilton, M. Palaniswami, D. Ralph, A. C. Tsol, Incremental Training of Support Vector Machines, IEEE Transactions on Neural Networks, 16(1), 114-131, 2005.

[170] M. Muhlbaier, A. Topalis, R. Polikar, Learn++.NC: Combining Ensemble of Classifiers Combined with Dynamically Weighted Consult-and-Vote for Efficient Incremental Learning of New Classes," IEEE Transactions on Neural Networks, 20(1), 152–168, 2009.

[171] T.M. Martinetz, S.G. Berkovich, K. J. Schulten, Neural-Gas Network for Vector Quantization and its Application to Time-Series Rrediction, IEEE Trans. Neural Networks, 4(4), 558-569, 1993.

[178] Y. Freund, R. E. Schapire, Experiments with a new boosting algorithm, Proceedings of the Thirteenth International Conference on Machine Learning (ICML'96), Morgan Kaufmann, Bari, Italy, 148–156, 1996.

[179] A. Shilton, M. Palaniswami, D. Ralph, A. C. Tsol, Incremental Training of Support Vector Machines, IEEE Transactions on Neural Networks, 16(1), 114-131, 2005.

[180] F. Shen and O. Hasegawa, An Incremental Network for Online Unsupervised Classification and Topology Learning, Neural Networks, 19(1), 90-106, 2006.

[181]F. Shen, K. Sakurai, Y. Kamiya, O. Hasegawa: An Online Semi-supervised Active Learning Algorithm with Self-organizing Incremental Neural Network, International Joint Conference on Neural Network (IJCNN), 2007.

[182] T. Kohonen, Self-organized Formation of Topologically Correct Feature Maps, Biol. Cybern, 43(1), 59-69, 1982.

[183] S. Pal, M. Blumenstein, U. Pal: 'Non- English and Non-Latin Signature Verification Systems: A Survey', Proceedings of the 1st International Workshop on Automated Forensic Handwriting Analysis, pp. 1-5, Beijing, China, September 2011.

[184] S. Pal, U. Pal, M. Blumenstein: 'Multi-script Off-line Signature Verification: A Two-Stage Approach', Proceedings of the 2nd International Workshop on Automated Forensic Handwriting Analysis, pp. 31-35, Washington D.C., USA, September 201

[185] R. Plamondon, G. Lorette: Automatic signature verification and writer identification—the state of the art, Pattern Recognition. No. 22 pp 107–131, 1989.

[186] F. Leclerc, R. Plamondon, Automatic signature verification: the state of the art, 1989–1993, Int. J. Pattern Recognit. Artif. Intell. Vol. 8, pp. 643–660, 1993.

[187] M. Fairhurst, Signature verification revisited: promoting the practical exploitation of biometric technology, Electronics. Communication. Eng. J. vol. 9, 273–280, 1997.

[188] R. Plamondon, S.N.,Srihari: On-line and off-line handwriting recognition: a comprehensive survey, IEEE. Trans. Pattern Anal. Mach. Intell. Vol 22, pp. 63–84, 2000.

[189] D. Impedovo, G. Pirlo, Automatic signature verification: the state of the art, IEEE Trans. Syst. Man Cybern. Part C: Appl. Rev. vol. 38 no. 5, pp. 609–635, 2008.

[190] M. Diaz-Cabrera, A. Morales, M. A., Ferrer: Emerging Issues for Static Handwritten Signature Biometric, (Eds.), Advances in Digital Handwritten Signature Processing. A Human Artefact for e-Society, World Scientific, pp. 111-122, 2014.

[191] M. Diaz-Cabrera, M. A. Ferrer, A. Morales, "Modeling the Lexical Morphology of Western Handwritten Signatures", PLoS ONE 10(4): e0123254, April 2015.

[192] S. Pal, A. Alireza, U. Pal, M. Blumenstein, Multi-script off-line signature identification", 12th Int. Conf. on Hybrid Intelligent Systems, Pune, India, pp. 236–240 2012.

[193] S. Pal, U. Pal, M. Blumenstein, ' Hindi and English Off-line Signature Identification and Verification", Proceedings of International Conference on Advances in Computing. Advances in Intelligent Systems and Computing Ed, vol 174, pp 905-910. 2012.

[194] S. Pal, U. Pal, M. Blumenstein, 'A Two-Stage Approach for English and Hindi Off-line Signature Verification', International Workshop on Emerging Aspects in Handwritten Signature Processing, Naples, Italy, September 9-10, 2013.

[195] S. Pal, A. Alireza, U. Pal, M. Blumenstein, "Off-line Signature Identification Using Background and Foreground Information," in Digital Image Computing Techniques and Applications (DICTA), 2011 International Conference on, pp.672-677, 6-8 Dec. 2011.

[196] S. Pal, U. Pal, M. Blumenstein,., 'Off-line English and Chinese signature identification using foreground and background features, Proceedings of the 2012 International Joint Conference on Neural Networks, pp.1,7, Brisbane, Australia, June 2012.

[197] M. Ferrer, F. Vargas, A. Morales, A. Ordoñez: 'Robustness of Off-line Signature Verification Based on Grey Level Features', in IEEE Transactions on Information Forensics and Security, vol. 7, no. 3, pp. 966-977, June 2012.

[198] J. Ortega-Garcia, J. Fierrez-Aguilar, D. Simon, J. Gonzalez, M. Faundez, V. Espinosa, A. Satue, I. Hernaez, J. Igarza, C. Vivaracho, D. Escudero, Q. Moro: 'MCYT baseline corpus: A bimodal biometric database', in IEE Proceedings Vision, Image and Signal Processing, Special Issue on Biometrics on the Internet, vol. 150, no. 6, pp. 395-401, December 2003.

[199] A. Kholmatov, B. Yanikoglu, "SUSIG: an online signature database, associated protocols and benchmark results", in Pattern Analysis and Applications, vol. 12, pp. 227-236, 2009.

[200] V. Blankers, C. Heuvel, K. Franke, L. Vuurpijl: 'Signature verification competition', in 10th International Conference on Document Analysis and Recognition, pp. 1403-1407, Barcelona, Spain, 2009.

[201] D. Yeung, H. Chang, Y. Xiong, S. George, R. Kashi: 'SVC2004: First international signature verification competition', in Lecture Notes in Computer Science: Biometric Authentication, Ed. by D. Zhang and A. Jain, vol. 3072, pp. 16-22, Springer, Berlin Heidelberg, 2004.

[202] S. Pal: "Multi-Script Off-line Signature verification", PhD. Dissertation, Griffith University, October 2014.

[203] M. Ismail, S. Gad : 'Off-line Arabic signature recognition and verification', in Pattern Recognition, vol. 33, pp. 1727-1740, 2000.

[204] M. Ferrer, M. Diaz, A. Morales, "Static Signature Synthesis: A Neuromotor Inspired Approach for Biometrics," in Proceedings of IEEE Transactions on Pattern Analysis and Machine Intelligence, vol. 37, no.3, pp.667-680, March 2015.

[205] M., Ferrer, J. Alonso, C Travieso: 'Offline geometric parameters for automatic signature verification using fixed-point arithmetic', in IEEE Transactions on pattern analysis and machine intelligence, vol. 27, no. 6, pp 993-997, June 2005.

[206] M. A. Ferrer, M. Diaz-Cabrera, A. Morales, J. Galbally, M. Gomez-Barrero, "Realistic Synthetic Off-Line Signature Generation Based on Synthetic On-Line Data", 47th IEEE International Carnahan Conference on Security Technology, Medellin, pp. 116-121, 8-11 October 2013.

[207] M. A. Ferrer, M. Diaz-Cabrera, A. Morales, A., "Synthetic Off-Line Signature Image Generation", 6th IAPR International Conference on Biometrics, Madrid, pp. $1 - 7$, 4-7 June 2013.

[208] R. Kabaciński and M. Kowalski. Human vein pattern segmentation from low-quality images a comparison of methods. Image Processing and Communications Challenges 2, 84 of Advances in Intelligent and Soft Computing, 105-112, 2010.

[209] R. Kabaciński and M. Kowalski.Human vein pattern correlation - a comparison of segmentation methods.Computer Recognition Systems 4, 95 of Advances in Intelligent and

[210] R. Kabaciński and M. Kowalski.Vein pattern database and benchmark results. Electronics Letters, 47(20), 1127-1128, 2011.

[211]] D. Hartung, M. A. Olsen, H. Xu, and C. Busch, Spectral minutiae for vein pattern recognition. In Biometrics (IJCB), 2011 International Joint Conference on, 1 −7, 2011.

[212] D. Hartung, A. Pflug, and C. Busch, Vein pattern recognition using chain codes spatial information and skeleton fusing.In Sicherheit , 245–256, 2012.

[213] D. Hartung, M. A. Olsen, H. Xu, H. T. Nguyen and C. Busch, Comprehensive analysis of spectral minutiae for vein pattern recognition. In IET Biometrics (1), 25–36, 2012.

[214] J. Uriarte-Antonio, D. Hartung, J. Pascual and R. Sanchez-Reillo, Vascular biometrics based on a minutiae extraction approach. In Security Technology (ICCST), IEEE International Carnahan Conference on , 1 −7, 2011.

[215] M. Akhloufi . and A. Bendada, Capturing Hand or Wrist Vein Images for Biometric Authentication Using Low-Cost Devices, Sixth International Conference on Intelligent Information Hiding and Multimedia Signal Processing (IIH-MSP), 318 − 322, 2010

[216] J.E. Suarez Pascual, J. Uriarte-Antonio, R. Sanchez-Reillo, M.G. Lorenz, Hand and Wrist Physiological Features Extraction for near Infrared Biometrics, Canadian Conference on Computer and Robot Vision, CRV '08. 341 − 344, 2008.

[217] PUT vein dataset available at http://biometrics.put.poznan.pl/home/new-news-page/

[218] D. Ghosh, T. Dube, A. P. Shivaprasad, Script Recognition—A Review, IEEE Transactions on Pattern Analysis And Machine Intelligence, vol. 32, no. 12, December 2010.

[219] U. Pal, B.B. Chaudhuri, Indian script character recognition: a survey, Pattern Recognition, vol 37, no. 9, Pages 1887-1899. September 2004,

[220] M. A. Ferrer, A. Morales, U. Pal, LBP Based Line-wise Script Identification, Proceedings of the twelfth IAPR International Conference on Document Analysis and Recognition, Washington DC, USA, August 23-29th, 2013.

[221] M. A. Ferrer, A. Morales, N. Rodríguz, U. Pal, Multiple Training − One Test methodology for Handwritten Word Script Identification, 14th International Conference on Frontiers in Handwriting Recognition, pp. 750-759, Crete, Greece, 1-4 September, 2014.

[222] N. Sharma, U. Pal, M. Blumenstein, A study on word-level multi-script identification from video frames, 2014 International Joint Conference on Neural Networks, pages 1827-1833, 6-11 July 2014.

[223] S. Alkassar, W. L. Woo, S. S. Daly, J. A. Chambers, Robust Sclera Recognition System With Novel Sclera Segmentation and Validation Techniques, IEEE Transaction SMC 1, 47 (3), 474 – 486, 2015

[224] V. Gottemukkula, S. Saripalle, S. P. Tankasala, R. Derakhshani, Method for using visible ocular vasculature for mobile biometrics, IET Biometrics, Volume: 5, Issue: 1, pp. 3-12, 2016.

[225] S.P.Tankasala, P.Doynov, R. Derakhshani: Visible spectrum, bi-modal ocular biometrics. Proc. of ICCCS, pp. 564–573, 2012.

[226] K.Oh, B. Oh, K.Toh, W.Yau, H. Eng, Combining sclera and periocular features for multi-modal identity verification, Neurocomputing, Volume 128, pp 185-198, March 2014

[227] H. Proenc̦ Towards Non-Cooperative Biometric Iris Recognition, Thesis submitted to University of Beira Interior, October 2006.

[228] T. Tan, Z. He, Z. Sun, Efficient and robust segmentation of noisy iris images for non-cooperative iris recognition, Image Vis. Comput. 28 (2), 223–230, 2010.

[229] X. Zhang, Z. Sun, T. Tan, Texture removal for adaptive level set based iris segmentation, in 17th IEEE International Conference on Image Processing, pp. 1729–1732, 2010.

[230] K. Roy, C. Suen, P. Bhattacharya, Segmentation of Unideal Iris Images Using Game Theory, in 20th International Conference on Pattern Recognition, 2010, pp. 2844–2847. 2010,

[231] S. Pundlik, D. Woodard, S. Birchfield, Iris segmentation in non-ideal images using graph cuts, Image Vis. Comput. 28 (12) (2010) 1671–1681. 2010,

[232] J. Zuo, N. Schmid, On a methodology for robust segmentation of nonideal iris images, IEEE Trans. Syst. Man Cybern. Part B: Cybern. 40 (3) (2010) 703–718. 2010,

[233] M. De Marsico, M. Nappi, R. Daniel, ISIS: Iris Segmentation for Identification Systems, in 20th International Conference on Pattern Recognition, 2010, pp. 2857–2860. 2010,

[234] H. Proença, Iris recognition: on the segmentation of degraded images acquired in the visible wavelength, IEEE Trans. Pattern Anal. Mach. Intell.32 (8) (2010) 1502–1516. 2010,

[235] J. Koh, V. Govindaraju, V. Chaudhary, A robust iris localization method using an active contour model and Hough transform, in 20th International Conference on Pattern Recognition, 2010, pp. 2852–2856. 2010,

[236] C.-W. Tan, A. Kumar, Automated segmentation of iris images using visible wavelength face images, in IEEE Computer Society Conference on Computer Vision and Pattern Recognition Workshops, 2011, pp. 9–14. 2011.

[237] C.-W. Tan, A. Kumar, a Unified framework for automated iris segmentation using distantly acquired face images, IEEE Trans. Image Process. 21 (9) (2012) 4068–4079. 2012.

[238] G. Sutra, S. Garcia-Salicetti, B. Dorizzi, The Viterbi algorithm at different resolutions for enhanced iris segmentation, in 5th IAPR International Conference on Biometrics, 2012, pp. 310–316. 2012.

[239] H. Li, Z. Sun, T. Tan, Robust iris segmentation based on learned boundary detectors, in 5th IAPR International Conference on Biometrics, 2012, pp. 317–322. 2012

[240] C.-W. Tan, A. Kumar, Efficient iris segmentation using Grow-Cut algorithm for remotely acquired iris images, in Fifth IEEE International Conference on Biometrics: Theory, Applications and Systems, 2012, pp. 99–104. 2012.

[241] A. Uhl, P. Wild, Weighted adaptive Hough and ellipsopolar transforms for real-time iris segmentation, in 5th IAPR International Conference on Biometrics, 2012, pp. 283–290. 2012.

[242] H. Li, Z. Sun, T. Tan, Accurate iris localization using contour segments, in 21st International Conference on Pattern Recognition, 2012, pp. 3398–3401. 2012

[243] F. Alonso-Fernandez, J. Bigun, Iris boundaries segmentation using the generalized structure tensor. A study on the effects of image degradation, in Fifth International Conference on Biometrics: Theory, Applications and Systems, 2012, pp. 426–431. 2012

[244] C.-W. Tan, A. Kumar, Towards online iris and periocular recognition under relaxed imaging constraints, IEEE Trans. Image Process. 22 (10) (2013) 3751–3765. 2013.

[245] Y. Hu, K. Sirlantzis, G. Howells, A robust algorithm for colour iris segmentation based on l1-norm regression, in: IEEE International Joint Conference on Biometrics, 2014, pp. 1–8. 2014

[246] Y. Zhou, A. Kumar, Personal identification from iris images using localized radon transform, in: 20th International Conference on Pattern Recognition, 2010, pp. 2840–2843. 2010,

[247] K. Roy, P. Bhattacharya, C. Suen, J. You, Recognition of unideal iris images using region-based active contour model and game theory, in: 17th IEEE International Conference on Image Processing, 2010, pp. 1705–1708. 2010,

[248] M. Zhang, Z. Sun, T. Tan, Deformable DAISY Matcher for robust iris recognition, in: 18th IEEE International Conference on Image Processing, 2011, pp. 3189–3192.2011.

[249] A. Bastys, J. Kranauskas, V. Krger, Iris recognition by fusing different representations of multi-scale Taylor expansion, Comput. Vis. Image Underst. 115 (6) (2011) 804–816. 2011.

[250] H. Proença, G. Santos, Fusing color and shape descriptors in the recognition of degraded iris images acquired at visible wavelengths, Comput. Vis. Image Underst. 116 (2) (2012) 167–178. 2012.

[251] A. Kumar, T.-S. Chan, C.-W. Tan, Human identification from at-a-distance face images using sparse representation of local iris features, in: 5th IAPR International Conference on Biometrics, 2012, pp. 303–309. 2012,

[252] P. Li, G. Wu, Iris recognition using ordinal encoding of log-euclidean covariance matrices, in: 21st International Conference on Pattern Recognition, 2012, pp. 2420–2423. 2012,

[253] A. Rahulkar, R. Holambe, Half-iris feature extraction and recognition using a new class of biorthogonal triplet half-band filter bank and flexible k-out-of-n: a post-classifier, IEEE Trans. Inf. Forensics Secur. 7 (1) (2012) 230–240. 2012,

[254] M. Zhang, Z. Sun, T. Tan, Perturbation-enhanced feature correlation filter for robust iris recognition, IET Biometrics 1 (1) (2012) 37–45. 2012,

[255] X. Liu, P. Li, Tensor decomposition of SIFT descriptors for person identification, in: 5th IAPR International Conference on Biometrics, 2012,pp. 265–270. 2012,

[256] A. Kumar, T.-S. Chan, Iris recognition using quaternionic sparse orientation code (QSOC), in: IEEE Computer Society Conference on Computer Vision and Pattern Recognition Workshops, 2012, pp. 59–64. 2012,

[257] H. Zhang, Z. Sun, T. Tan, J. Wang, Iris image classification based on colour information, in 21st International Conference on Pattern Recognition, 2012, pp. 3427–3430.

[258] L. Wang, Z. Sun, T. Tan, Robust regularized feature selection for iris recognition via linear programming, in 21st International Conference on Pattern Recognition, 2012, pp. 3358–3361. 2012,

[259] Z. Sun, H. Zhang, T. Tan, J. Wang, Iris image classification based on a hierarchical visual codebook, IEEE Trans. Pattern Anal. Mach. Intell. 36 (6)(2014) 1120–1133. 2014

[260] Z. Sun, L. Wang, T. Tan, Ordinal feature selection for iris and palmprint recognition, IEEE Trans. Image Process. 23 (9) (2014) 3922–3934. 2014

[261] C.W. Tan, A. Kumar, Accurate Iris Recognition at a Distance Using Stabilized Iris Encoding and Zernike Moments Phase Features, IEEE Transactions on Image Processing 23 (9) (2014) 3962–3974. 2014

[262] C.-W. Tan, A. Kumar, Efficient and Accurate At-a-Distance Iris Recognition Using Geometric Key-Based Iris Encoding, IEEE Transactions on Information Forensics and Security 9 (9) (2014) 1518–1526, 2014.

[263] A. Das, U. Pal, M. A. Ferrer, M. Blumenstein, A New Method for Sclera Vessel Recognition using OLBP, appeared in International Conference Chinese Conference on Biometric Recognition , LNCS 8232, pp. 370–377,2013.

[264] A. Das, U. Pal, M. A. Ferrer, M. Blumenstein, Sclera Recognition Using D-SIFT, Appeared In 13th International Conference on Intelligent Systems Design and Applications pp.74-79, 2013.

[265] A. Das, U. Pal, M. A. Ferrer, M. Blumenstein, Fuzey Logic based Sclera Recognition, pp. 561-568, In IEEE World Congress on Computational Intelligence - IEEE International Conference on Fuzzy Systems 2014.

[266] A. Das, U. Pal, M. A. Ferrer, M. Blumenstein, Multi-angle Based Lively Sclera Biometrics at a Distance'. pp. 22-29, IEEE Symposium Series on Computational Intelligence, December 9-12, 2014, Orlando, USA.

[267] A. Das, U. Pal, M. A. Ferrer, M. Blumenstein, A New Efficient and Adaptive Sclera Recognition System", pp.1-6, IEEE Symposium Series on Computational Intelligence, December 9-12, 2014, Orlando, USA.

[268] A. Das, U. Pal, M. A. Ferrer, M. Blumenstein, A New Wrist Vein Biometric System, pp. 68-75, IEEE Symposium Series on Computational Intelligence, December 9-12, 2014, Orlando, USA.

[269] A. Das, U. Pal, M. A. Ferrer, M. Blumenstein, Sclera Recognition - A Survey. in Recent Advancement in Computer Vision and Pattern Recognition, pp. 917 -921, 2013.

[270] A. Das, U. Pal, M. A. Ferrer, M. Blumenstein, SSBC 2015: Sclera Segmentation Benchmarking Competition, pp. 1-6, at International Conference Biometrics Theory, Applications and Systems (BTAS), 2015.

[271] A. Das, P. Mondol, U. Pal, M. Blumenstein, M. A. Ferrer, Sclera Pattern Synthesis Based on Non-parametric Texture Synthesis Technique, at Computer Vision and Image Processing (CVIP-2016).

[272] A. Das, U. Pal, M. A. Ferrer, M. Blumenstein, SSRBC 2015: Sclera Segmentation and Recognition Benchmarking Competition. at International Conference on Biometrics, 2016.

[273] A. Das, P. Mondol, U. Pal, M. Blumenstein, M. A. Ferrer, Fast and Efficient Multimodal Eye Biometrics using Projective Dictionary Pair Learning, IEEE World Congress on Computational Intelligence- IEEE CEC 2016.

[274] A. Das, R. Kunwar, U. Pal, M. A. Ferrer, M. Blumenstein, Book chapter entitled, An online learning technique for the adaptive biometric system, pp. 73-96, in the book of Adaptive Biometric Systems to be published by Springer.

[275] A. Das, U. Pal, M. A. Ferrer, M. Blumenstein, A Framework for Liveness Detection for Direct Attack in Visible Spectrum for Multimodal Ocular Biometrics. Pattern Recognition Letter, ISSN: 0167-8655, 2015.

[276] A. Das, M. A. Ferrer, U. Pal, S. Pal, M. Diaz and M. Blumenstein, Multi-script vs single-script scenarios in automatic off-line signature verification. IET biometrics.

[277] H. Proenca and L. A. Alexandre, "Toward noncooperative iris recognition: A classification approach using multiple signatures," IEEE Trans. Pattern Anal. Mach. Intell., vol. 29, no. 4, pp. 607–612, Apr. 2007.

[288] Z. Zhao and A. Kumar An Accurate Iris Segmentation Framework Under Relaxed Imaging Constraints Using Total Variation Model, ICCV 2015.

[289] A. Kumar and A. Passi, Comparison and the combination of iris matchers for reliable personal authentication,' Pattern Recognition, vol. 43, pp. 1016-1026, 2010.